Heterogeneous catalytic conversion of carbon dioxide to chloromethyl ethylene carbonate and styrene carbonate using a novel Zr/ZIF-8 catalyst

by

Bisi Ajayi Olaniyan

A Doctoral thesis submitted in partial fulfilment of

the requirements for the award of

Doctor of Philosophy in Chemical, Process and Energy Engineering

School of Engineering

London South Bank University

March 2020

Declaration

I hereby declare that except where specific reference is made to the work of others, the contents of this thesis are original and have been composed by myself with the support of my supervisor. The thesis is submitted for examination in consideration of the award of a degree of Doctor of Philosophy in Chemical, Process and Energy Engineering. I would like to emphasise that it is my personal effort and that the work has not been submitted for any other degree or professional qualification. Furthermore, I took reasonable care to ensure that the work is original and to the best of my knowledge, does not breach copyright law and has not been taken from other sources except where such work has been cited and acknowledged within the text.

Dedication

I would like to dedicate this PhD thesis and all its hard work to my beautiful wife, Mrs Grace Olubukola Olaniyan.

…… I love you more than words can ever express.

Acknowledgements

…… Now unto him, that is able to do exceeding abundantly above all that we ask or think, according to the power that worketh in us……..

Ephesians 3:20

First and foremost, I want to give thanks to the Almighty God for making this dream a reality. I want to sincerely express my deepest gratitude to my supervisor, Professor Basu Saha for his guidance and support throughout my PhD degree. His wide knowledge, constructive criticism, patience and experience have contributed significantly to the success of this research work. I express a very big thank you to the London South Bank University, School of Engineering for funding this research study.

I would like to acknowledge the efforts of Dr Adegboyega Adeleye for the foundation he laid in this area of research. I would not forget to thank Dr Victor Onyenkeadi and Dr Omar Aboelazayem for their inestimable supports during this research work. I want to thank Mr Charles and Mr William (Technicians) for their wonderful support. And to all my other colleagues in the Basu research group; Yusuf, Zarah, Ferishsten, Alamgir, Shahenda, Joshua and Rana, you are all wonderful people.

It is a great privilege for me to say a massive thank you to my wife, Grace Olaniyan, who supported my decision to make a radical turn in my life to embark on PhD studies in order to fulfil my career goals, despite the significant changes it involves in our lives. She has endured many long hours waiting for me to come home from the lab and has provided stability to our family by taking charge of our home and our children's education. I thank my daughters; Temiloluwa, Temitope, Temilade and my beautiful son Temidayo, for their understanding and encouragement throughout this

lonely journey. You are all my jewels and the wheel force to complete my PhD degree. Daddy loves you all!

A special thank you goes to Dr and Mrs Adefila in Houston, Texas, U.S.A for their selfless and moral supports all the way through this doctoral journey. You are a destiny helper; I am glad my paths cross your paths. I owe you more than I can ever payback. My unfailing thanks also go to my fathers in the Lord, Pastor Kunle Anifowose and Pastor Fidelis Akinbogun for their supports and prayers through the lonely path of my doctoral study. Obviously, words and space may have failed me in expressing my deep-held appreciation to many who should be on this page, but in my heart, that which words cannot say is written here.

Thank you all!

……..I am eternally grateful to my Almighty God……..

Abstract

In the last two decades, several attempts have been made to develop new catalytic systems for the chemical fixation of CO_2, both homogeneous and heterogeneous catalysis. However, these attempts have failed to yield satisfactory results as most of these catalysts requires high temperature and/or pressure (usually around 453 K and pressure higher than 8 atm), further separation and purification steps, many of these catalysts deactivate after few recycle experiments and worse of all, low product yield. Hence, this research is focused on the use of metal-organic frameworks (MOFs) catalysts as a relatively new and promising candidate that addresses these aforementioned shortfalls.

The development of a novel Zr/ZIF-8 catalyst *via* a simple low-cost solvothermal method, easy separation by centrifugation, and its excellent recyclability properties have demonstrated that the catalyst could be viable for large-scale industrial applications. The heterogeneity of the catalyst has been proven by recovering and reusing the catalyst for up seven times without any significant loss in catalytic activity. The powder x-ray diffraction (XRD), fourier transform infrared (FTIR) spectroscopy and thermogravimetric analysis (TGA) of the recycled catalyst shows that its framework is quite stable after reusability performance.

Furthermore, the catalyst shows high substrates tolerance towards different epoxides including epichlorohydrin (ECH), styrene oxide (SO) and butylene oxide (BO). The reaction has been carried out under solvent-free and co-catalyst conditions. The catalytic properties of the novel catalyst have been satisfactorily consistent with pristine ZIF-8 catalyst using multiple physicochemical characterisation techniques. We believe that this work

could provide a new direction for designing more sustainable, non-toxic catalysts for the transformation of CO_2 and other substrates.

The comparison of catalytic activity of both the pristine ZIF-8 and the novel Zr/ZIF-8 catalysts have been drawn based on the effect of various reaction conditions such as reaction temperature, CO_2 pressure, catalyst loading, reaction time, stirring speed and reusability studies. Zr/ZIF-8 catalyst has been assessed as a suitable heterogeneous catalyst outperforming the catalytic activity of pristine ZIF-8 catalyst with respect to the conversion of epoxide, selectivity and yield of the desired carbonates.

In addition, experimental design, modelling and optimisation techniques *via* response surface methodology (RSM) have also been implemented for different process responses. The experimental results have been employed to design and simulate chloromethyl ethylene carbonate (CMEC) and styrene carbonate (SC) using batch experimental studies. The adequacy of the models has been validated by the correlation between the experimental and predicted values of the responses using an Analysis of Variance (ANOVA) method. Therefore, statistical modelling using RSM can be used as a reliable prediction tool for system optimisation for greener synthesis of both chloromethyl ethylene carbonate and styrene carbonate.

In conclusions, the catalyst has displayed high epoxide conversion and high carbonate selectivity. The optimum experimental conditions and results for the synthesis of chloromethyl ethylene carbonate were found to be 353 K, 8 bar of CO_2 pressure and 8 h using fresh 10% (w/w) Zr/ZIF-8 catalyst loading for a 93% ECH conversion, 86% and 76% of CMEC selectivity and yield, respectively. While the optimum experimental conditions and results for the synthesis of styrene carbonate were found to be 353 K, 6 bar of CO_2

pressure and 8 h using fresh 6% (w/w) Zr/ZIF-8 catalyst loading for a 98% SO conversion, 72% and 68% of SC selectivity and yield, respectively. Similarly, the optimised reaction conditions and results using RSM techniques for the synthesis of chloromethyl ethylene carbonate were found at 353 K, 11 Bar of CO_2 pressure 12 h using 12% (w/w) fresh catalyst loading for a 96% ECH conversion and 68% CMEC yield while 353 K, 6.1 Bar of CO_2 pressure and 8.2 h using fresh 6% (w/w) Zr/ZIF-8 catalyst loading for 98% SO conversion and 68% SC yield for the synthesis of styrene carbonate.

Table of contents

List of figures

List of tables

List of Abbreviations

Al_2O_3	Aluminium oxide
$AlCl_3$	Aluminium chloride
AlO_4	Tetrahedra of alumina
ANOVA	Analysis of variance
BBD	Box-Behneken Design
BC	1,2-Butylene carbonate
BET	Brunauer-Emmett-Teller
BO	Butylene oxide
CaO	Calcium oxide
CH_2O	Formaldehyde
CH_3OH	Methanol
CO	Carbon monoxide
CO_2	Carbon dioxide
$COCl_2$	Phosgene
DMAP	Dimethylformamide
DMC	Dimethyl carbonate
DME	Dimethyl ether
DMF	N,N-dimethylformamide
Et4NBr	Ethyl-ammonium bromide
FID	Flame ionisation detector
FT-IR	Fourier transform infrared spectroscopy
GC	Gas chromatography

GO	Graphene oxide
Gt/y	Gigatonne per year
H	Hour
H_2	Hydrogen
H_2O	Water
H_2O_2	Hydrogen peroxide
H_2SO_4	Sulphuric acid
H_3PO_4	Phosphoric acid
HCl	Hydrochloric acid
HPLC	High performance liquid chromatography
K	Kelvin
MCM-41	Molecular sieve
MeOH	Methanol
MgO	Magnesium oxide
Mg-Al oxide	Magnesium- aluminium mixed oxide
MOF	Metal-Organic Framework
Mt/y	Megatonne per year
$NaNO_3$	Sodium nitrate
Nb	Niobium
Nb_2O_5	Niobium pentoxide
n-Bu_4NBr	Tetra-*n*-butyl ammonium bromide
NGP	Natural graphite powder
$NiCl_2$	Nickel chloride

O_2	Oxygen
OFAT	One-factor at a time analysis
OH	Hydroxide ion
PC	Propylene carbonate
PO	Propylene oxide
ppm	Parts per million
ppmv	Parts per million by volume
PVC	Polyvinyl chloride
RS	Raman spectroscopy
RSM	Response Surface Methodology
SBA-15	Mesoporous silica
SC	Styrene carbonate
$scCO_2$	Supercritical CO_2
SEM	Scanning electron microscopy
SiO_2	Silica
SmOCl	Samarium oxychloride
SO	Styrene oxide
TBAB	Tetra-n-butyl ammonium bromide
TEM	Transmission electron microscopy
TiO_2	Titanium oxide
V_2O_5	Vanadium oxide
XPS	X-ray photoelectron spectroscopy
XRD	Powdered X-ray diffraction

Zn	Zinc
$ZnCl_2$	Zinc chloride
ZnO	Zinc oxide
Zr–O	Zirconium oxide
ZIF-8	Zeolitic imidazole framework
Zr/ZIF-8	Zirconium/ Zeolitic imidazole framework
$ZrO(NO_3)_2.6H_2O$	Zirconium (IV) oxynitrate hydrate
ZrO_2	Zirconium oxide

Publications

Journal publications

Olaniyan, B. Saha, B. (2020) Comparison of catalytic activity of ZIF-8 and Zr/ZIF-8 for greener synthesis of chloromethyl ethylene carbonate by CO_2 utilization'', *Energies*,158 (2), pp. 405 -19. doi:10.3390/j.energies13030521.

Olaniyan, B. Saha, B. (2020) Multiobjective optimization for the greener synthesis of chloromethyl ethylene carbonate by CO_2 and epichlorohydrin *via* response surface methodology,'' *Energies*, 162 (4) pp. 408–20. doi:10.1016/j.energies.2067.07.194

Olaniyan, B., Kanmodi, J., Onyenkeadi, V., B. Saha. ''A greener approach and system optimisation of styrene carbonate synthesis *via* CO_2 utilisation,'' *Energy*, **under review**.

Olaniyan, B., Onyenkeadi, V., Adeleye, I., Saada R., Saha, B. ''Recent progress in heterogeneous catalytic conversion of carbon dioxide (CO_2) to organic carbonates using metal oxide and metal-organic frameworks (MOFs) catalysts,''. **In preparation**, to be submitted to *Reaction Chemistry & Engineering.*

Conference publications

Olaniyan, B. Saha, B. ''Greener synthesis of chloromethyl ethylene carbonate by CO_2 utilisation using a novel Zr/ZIF-8 catalyst'', 17th International Conference on Carbon Dioxide Utilisation - ICCDU 2019. Aachen, Germany, 23-27 June 2019.

Olaniyan, B. Saha, B. ''Multiobjective optimisation for the greener synthesis of chloromethyl ethylene carbonate by carbon dioxide (CO_2) and epichlorohydrin (ECH) *via* response surface methodology (RSM),'' 5th

European congress of applied biotechnology. Florence, Italy, 15-19 November 2019.

Olaniyan, B. Saha, B. ‘’Heterogeneous catalytic synthesis of chloromethyl ethylene carbonate from carbon dioxide and epichlorohydrin using a novel Zr/ZIF-8 catalyst,’’ CHISA 2020, 24th international congress of chemical and process engineering, 23-27 August 2020, accepted.

Olaniyan, B., Kanmodi, J., Onyenkeadi, V., B. Saha. ‘’A novel heterogeneous catalytic process for styrene carbonate synthesis *via* co_2 utilisation,’’. IEX2020- A Vision for the Future, Cambridge, United Kingdom, 8 July 2020 -10 July 2020, accepted

Chapter 1

Introduction

Outline of the chapter

This chapter gives a background to the research work, its aims and objectives, contribution to knowledge and provides an outline of the thesis.

The chapter is organised as follows:

1.1. Background

1.2. Motivation

1.3. Carbon dioxide chemistry

1.4. Source of CO_2 emission

1.5. Reactivity of CO_2

1.6. Supercritical CO_2

1.7. Utilisation of CO_2

1.8. Sustainability

1.9. The principle of green chemistry

1.10. Carbon capture sequestration and utilisation

1.11. Barriers to further development of CO_2 conversion and utilisation

1.12. Research aims and objectives

1.13. Contribution to knowledge

1.14. Thesis structure

1 Introduction

1.1 Background

The current level and accumulation of carbon dioxide (CO_2) in the atmosphere is high and requires urgent attention (Saada *et al.*, 2018). However, regardless of any environmental regulations and discharge limits placed on greenhouse gases (GHGs) emitted into the atmosphere, CO_2 is still believed to be environmentally benign, abundant, non-toxic, non-flammable and readily available C1 source for the synthesis of organic carbonates. In this regard, the development of efficient catalytic systems for chemical fixation of CO_2 has been a subject of immense research in academia and industry today. This is evidenced by the rising number of research grants and publications in all areas of CO_2 management (Liu *et al.*, 2015a). Although, CO_2 fixation is unlikely to consume significant quantities of CO_2 in the atmosphere, however, this measure can be regarded as a significant strategy for the development of sustainable and safe processes (Xie *et al.*, 2013).

The trade-off between the increase in the world energy demand and the considerable efforts to reduce its harmful CO_2 emissions and other greenhouse gases (GHGs) have been in the spotlight of international and environmental controversy. From a political standpoint, the toughening regulation of CO_2 emissions by ratifying Kyoto protocol has not been upheld by many countries today including the U.S, UK, China, India and other developed countries (Song, 2002a). As a result of this noncompliance, the net anthropogenic increase of 13,000 million tons of carbon dioxide is estimated to be added to the atmosphere annually as opposed to 110 million tons of CO_2 been utilised for fuels and other valuable chemicals such as urea (75 million tons of CO_2), salicylic acid, cyclic carbonates, and polycarbonates (Van Meerendonk, 2005).

1.2 Motivation

The effective transformation and utilisation of CO_2 have compelled the modern science to device sustainable technologies to convert CO_2 into valuable chemicals and fuels in order to achieve an anthropogenic and a sustainable carbon cycle. One of the most promising reaction schemes of CO_2 currently being researched is the synthesis of cyclic carbonates *via* cycloaddition reaction of CO_2 and epoxides. This process has been found to be 100% atom efficient reaction, used in the synthesis of both cyclic carbonates and polycarbonates. With the intriguing applications of organic carbonates, the use of CO_2 as a raw material to synthesise cyclic organic carbonates has gained extensive attention in chemical industry. Cyclic organic carbonates such as propylene carbonate (PC), styrene carbonate (SO) and chloromethyl ethylene carbonate (CMEC) are an attractive family of compounds with broad applications; used as polar aprotic solvents with low odour and toxicity (Shi *et al.*, 2013), as intermediates in the synthesis of fine chemicals (Stewart, 2015), as starting materials for the production of polymers (Liu *et al.*, 2015b) and as electrolytes for lithium-ion batteries (Zhao *et al.*, 2016).

1.3 Carbon dioxide chemistry

Carbon dioxide is a chemical compound of two elements: carbon and oxygen, in the ratio of 1:2. It has a slightly irritating odour, colourless and is denser than air. At atmospheric pressure, CO_2 is about 1.5 times as heavy as air and maybe liquefied by compressing to 2 MPa and cooling to 255 K CO_2, or by compressing to higher pressure of 5.78 MPa at 294 K (Wu *et al.*, 2017). If liquid CO_2 is cooled further to 216.4 K, the pressure drops to 0.518 MPa, solid CO_2 is formed, which co-exists with liquid and gaseous CO_2 - this is known as the triple point. The solid CO_2 can sublimate directly into a gas (without going through the liquid phase) upon absorbing heat, and this it is called dry ice. CO_2 cannot exist as a liquid below the triple point. If the pressure on dry ice is reduced to atmospheric pressure, the temperature of dry ice drops to 194.5 K. CO_2 cannot be liquefied

above 304 K, the critical temperature (Jessop, 2004). It exists as a supercritical fluid when the temperature and pressure are above 304 K (T_c) and 7.38 MPa (P_c), respectively (Taherimehr *et al.*, 2012). Table 1.1 shows the physical and chemical properties of CO_2.

Carbon dioxide is a linear molecule with a double bond between the carbon and oxygen atoms (0=C=0), the oxygen atoms are weak Lewis (and Brønsted) bases and the carbon is electrophilic. Reactions of CO_2 are dominated by nucleophilic attacks at the carbon, which result in bending of the O—C—O angle to about 393 K (de Falco *et al.*, 2013).

Table 1. 1. Physical and chemical properties of CO_2 (Source: Bazzanella, 2014)

Properties of CO_2	
Molar Mass	44 g mol^{-1}
Heat of formation at 298 K	-393.5 kJ mol^{-1}
Entropy of formation at 298 K	213.6 JK^{-1} mol^{-1}
Gibbs free energy at 298 K	-394.3 kJ mol^{-1}
Sublimation point at 1 atm	194.7 K
Melting point at 1 atm	216.6 K
Critical temperature	304 K
Critical pressure	73.9 bar
Critical density	0.468 g cm^{-3}
Gas density	1.976 kg m^{-3}
Liquid density	770 kg m^{-3}
Solid density	1560 kg m^{-3}
Specific volume	0.546 m3 kg^{-1}
Latent heat of vaporisation K	231.3 J g^{-1}
Latent heat of vaporisation at 194.5 K	353.4 J g^{-1}
Viscosity at 194.5 K and 1 atm	0.07 cP
Solubility in water at K	0.3346 g L^{-1}
Solubility in water at 298 K	0.1449 g L^{-1}

1.4 Source of CO_2 emissions

The sources of CO_2 emissions may include stationary, mobile, and natural sources. The anthropogenic emissions include those from energy utilisation in stationary and mobile sources but exclude natural sources (Wilhelm *et al.*, 2015). There are various sources of CO_2 emissions, which are dominated by combustion of liquid, solid, and gaseous fuels (Song, 2002b). Indeed, coal has a higher emission of CO_2 (Sankaranarayanan and Srinivasan, 2012) (950 g of CO_2 per kWh) compared to natural gas and oil, and therefore such a situation resulted in growing world production of CO_2. The quantity of CO_2 consumption for the synthesis of organic chemicals is relatively small compared to the amount of CO_2 emitted from fossil fuel combustion (An *et al.*, 2016). However, CO_2 conversion and utilisation should be an integral part of carbon management. Proper use of CO_2 for chemical processing can add value to the CO_2 disposal by making industrially useful carbon-based products. Studies on CO_2 conversion into carbon-based chemicals and materials are important for sustainable development. CO_2 conversion and utilisation could also be positioned as a step for CO_2 recycling and resource conservation. Within the industrial sector, there are two principal routes of CO_2 formation, manufacturing of industrial products where CO_2 is a by-product from the process (such as the processes for production of cement, limestone, hydrogen, and ethylene oxide), and from energy supply (either as process heat or as electricity) by combustion of fossil fuels, which produces CO_2 (Pérez-Fortes *et al.*, 2016).

The global coal emissions grew the most of any fuel from 2005–2017 period at 2.1% yearly as shown in figure 1.1, while the natural gas-related emissions grew by 2.0% yearly, and petroleum-related emissions grew at 1.1% yearly. Further forecast for Coal-related emissions of CO_2 is expected to increase by 0.6% in 2018 and 2019. Petroleum-related emissions of CO_2 are projected to grow by

1.6% in 2018 but drop by 0.2% in 2019. Natural gas-related emissions of CO_2 are projected to grow by 0.6% in 2018 and remain even in 2019 (EIA, 2017).

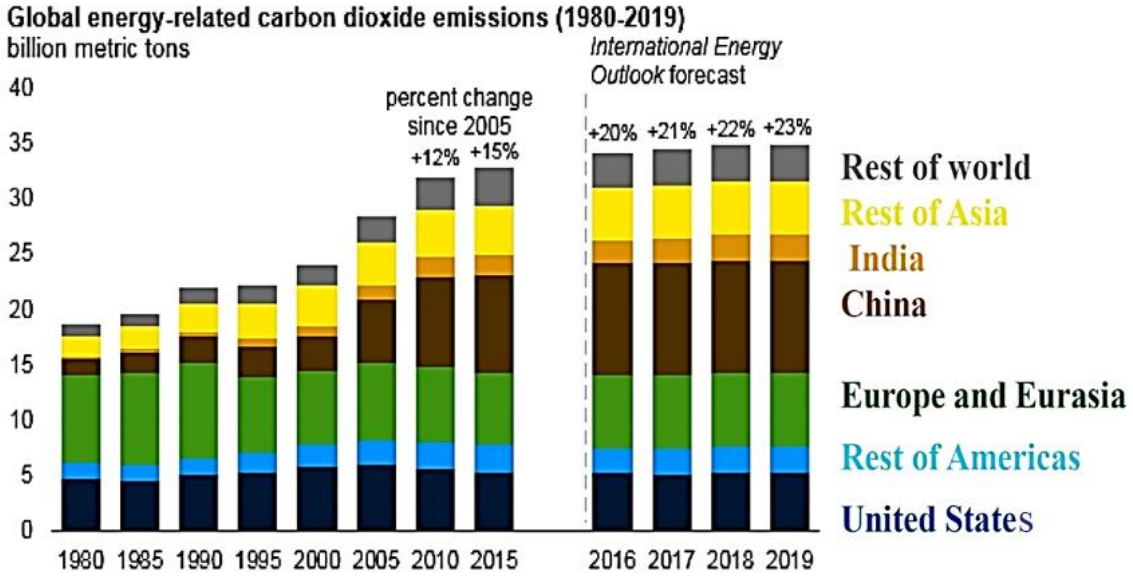

Figure 1. 1. Global emission of CO_2 from 1980 predicted to 2019. Source: U.S. Energy Information Administration, International Energy Statistics, International Energy Outlook, and Short-Term Energy Outlook (eia, 2019)

1.5 Reactivity of CO_2

Carbon dioxide is an inert gas with a very high kinetic and thermodynamic stability but lower reactivity than CO (Cheng *et al.*, 2016). This is due to the strong double bonds between the carbon and oxygen atoms (Pescarmona and Taherimehr, 2012). CO_2 is the most oxidised state of carbon and has an extremely low energy level (ΔGf°=-396 kJ/mol) (Liu *et al.*, 2015b). This is the reason why just a few processes use CO_2 as a raw material. As a result, this has slowed further development of efficient catalysts in its utilisation (Zhong *et al.*, 2014). However, this obstacle can be overcome by effective reaction conditions, active catalysts or reacting CO_2 with compounds with a relatively high free energy. Among these reactions is the synthesis of cyclic organic carbonates *via* cycloaddition of CO_2 to

epoxides (Bhanage and Arai, 2014). High temperatures, extremely reactive reagents, electricity, or the energy from photons may be exploited to carry out carbon dioxide reactions.

Carbon dioxide reactivity can be classified into two types: reductive and non-reductive. Reductive reactions involve the loss of oxygen atom(s) from CO_2 and/or addition of hydrogen to form formic acid, methanol, methane, or carbon monoxide. On the other hand, in non-reductive reactions, oxygen atoms of CO_2 are retained, and carbon dioxide is fixed to form carbon-carbon, carbon-nitrogen, or carbon-oxygen bonds; carboxylic acid and the derivatives, carbamate or urea, and carbonate are the products (Liu *et al.*, 2012). With respect to atom economy, non-reductive reactions retaining oxygen atoms are considered more advantageous for chemical utilisation of carbon dioxide (Beckman, 2004). A representative example is the copolymerisation of carbon dioxide and epoxide to form an alternating copolymer, an aliphatic polycarbonate (Ola *et al.*, 2013). CO_2 can react with basic compounds such as amines, to form carbamic salts, or with water to form carbonic acid, which dissociates further to form bicarbonate and carbonate ions, depending principally on the pH of the solution (Dai *et al.*, 2009). The solubility of CO_2 in water increases with decreasing temperature and increasing pressure. In contrast to this, carbonate salts are more soluble in water at high temperatures. CO_2 can also react with hydrogen, alcohols, acetals, epoxides and oxiranes, but normally these reactions are only successful in the presence of a catalyst (Baj *et al.*, 2014). The reactivity of CO_2 towards nucleophiles makes the incorporation of this molecule possible, leading to the formation of a carbon-element bond between the carbon atom of CO_2 and the substrate (Dai *et al.*, 2009).

1.6 Supercritical CO_2

Supercritical CO_2 ($ScCO_2$) is a fluid state of carbon dioxide where the gas is held above or equal to its critical temperature and critical pressure which causes it to go beyond liquid or gas into a phase where it acts as both simultaneously (Pérez-Fortes et al., 2016). $ScCO_2$ is inert, non-toxic, non-flammable low viscosity with a relatively low cost and has moderate critical constants (Liu et al., 2015b). It is an attractive and environmentally benign alternative to conventional solvents due to its non-toxicity (Liu et al., 2015b). $ScCO_2$ can be easily separated from reagents and products, has notable dissolving power and displays high molecular diffusivity, low viscosity and low surface tension. Because of its low critical temperature (31.17 °C) and moderate critical pressure (73.8 bar), the supercritical state of carbon dioxide is easily available.

1.6.1 Uses of supercritical CO_2

At temperatures higher than 31.1 °C and pressures above 73.9 bar (critical point), CO_2 reaches its supercritical state, where it behaves like gas but appears like a liquid, approaching or even exceeding the density of water (Jazi *et al.*, 2016). Due to its fascinating physicochemical properties and its high miscibility rates at a supercritical state, CO_2 can be used as a benign solvent for synthetic processes (Jazi *et al.*, 2016). The use of supercritical $ScCO_2$ allows contaminant-free supercritical extraction of various substances ranging from beverage materials (such as caffeine from coffee bean), foods (such as excess oil from fried potato chips), and organic and inorganic functional materials, to herbs and pharmaceuticals (Bhanage and Arai, 2014). It is also possible to use $scCO_2$ to remove pollutants such as Polyaromatic hydrocarbons (PAHs) from waste sludge and contaminated soils and toxics on activated carbon adsorbent (Kazemi, 2013). A large variety of synthetically useful reactions can be performed in $scCO_2$ with competitive results compared to those obtained in conventional organic solvents (Butterworth, 2006) as shown in figure 1.2.

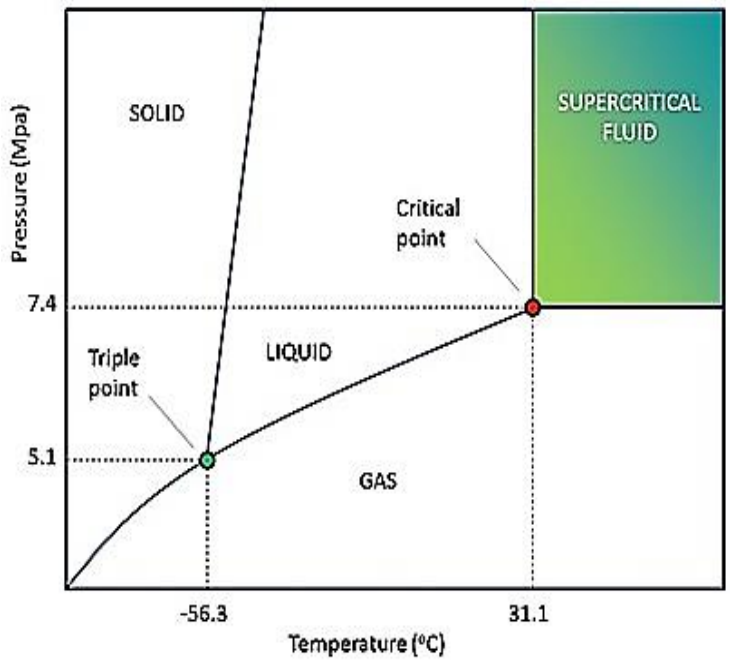

Figure 1. 2. A simplified phase diagram of CO_2 illustrating density changes from liquid to gas points 7.4 Mpa and 31.1 ^oC are the critical pressure and temperature, respectively (Source: Kazemi, 2013)

1.7 Utilisation of CO_2

Carbon dioxide as a raw material for the chemical industry is receiving growing attention due to its environmental sustainability as explained previously. The highest amount of CO_2 converted into a chemical is consumed in the production of urea (150 Mt/year) (Biotecnologia, 2016), followed by the synthesis of inorganic carbonates and pigments (30 Mt/year) (Biotecnologia, 2016). Lower quantities of CO_2 are used in the synthesis of methanol (6 Mt/year), salicylic acid (20 kt/year) and propylene carbonate (kt/year). About 18 Mt CO_2/year is used as a technological fluid, being recovered after utilisation (Biotecnologia, 2016). The followings are major industrial use of CO_2:

- Fire Extinguishers: CO_2 extinguishes fires.
- Beverage: CO_2 is used to make carbonated soft drinks and soda water.

- Solvent: Liquid CO_2 is considered as a good dissolving agent for many organic compounds; hence, it can be used to remove caffeine from coffee.
- Plants: Plants require CO_2 to execute photosynthesis, and greenhouses can promote plant growth with additional CO_2.
- Pressurised Gas: It is used as the cheapest non-combustible pressurised gas. Pressurised CO_2 are inside tins in life jackets. Compressed CO_2 gas is used in paintball markers, airguns, for ballooning bicycle tyres.
- Medicine: In medicine, up to 5% CO_2 is added to pure oxygen. This helps in provoking breathing and to stabilise the O_2/CO_2 balance in the blood.
- CO_2 Laser: The CO_2 laser, a common type of industrial gas laser uses CO_2 as a medium.
- Welding: It also finds its use as an atmosphere for welding.
- Oil Wells: Carbon dioxide is commonly injected into or next to producing oil wells to draw lost traces of crude oil.
- Chemical Industry: It is used as a raw material in the chemical process industry, especially for urea and methanol production.
- Metals Industry: It is used in the manufacture of casting influences so as to enhance their hardness.
- Fumigation: Used as a fumigant to increase shelf life and remove infestations.

Table 1.2. Shows the utilisation of CO_2 into chemicals and non-chemical. Applications range around 200 Mt/y as of 2019. The potential process that involves the use of CO_2 on an industrial scale in the coming decade providing a new carbon-based economy. The conversion of CO_2 into fuels and organic carbonates are predicted to play a major role in the management of CO_2 emission strategies. Although the conversion of CO_2 into fuel will be a huge market when compared to organic carbonates because CO_2 emissions were as a result of energy produced from fossil fuel.

Table 1. 2. Utilisation of CO_2 (Source: Gaseous carbon waste (2019)

Industry	Actual production ($MtCO_2$/y)	Usage ($MtCO_2$/y)	Future production ($MtCO_2$/y)	CO_2 needed ($MtCO_2$/y)
Urea	155	114	180	132
Methanol	50	8	60	10
Dimethyl ether (DME)	11.4	3	>20	>5
Methyl tert-butyl ether (TBME)	30	1.5	40	3
Formaldehyde (CH_2O)	21	3.5	25	5
Organic carbonates	0.2	0.005	>2	0.5
Polycarbonates	4	0.01	5	1
Inorganic carbonates	200	50	250	70
Technological	-	28		80
Algae for biodiesel production	0.005	0.010	1	2
Total		200		299

1.8 Sustainability

The concept of sustainability is a relatively new idea that was coined out in the Brundtland Report of 1987, “Our Common Future”. The report argued that a balance needs to be established between three pillars (people, planet and profit), hence the working definition of sustainability; which is defined as “meeting the needs of the present generation without compromising the needs of future generations to meet their own needs.”(Arends *et al.*, 2007). Green chemistry emphasises the efficient use (preferably renewable) raw materials, in order to eliminate waste, this avoids the use of toxic and/or hazardous solvents and reagents in the manufacture and application of chemical products. In response to the increasing pressures coming from national and international regulations, and

from society in general, corporations are gradually pushed towards the adoption of principles of both social and environmental responsibility within their strategies, structures and management systems (Saada, 2015).

This concept of sustainability dictates that not only the availability of natural resources and the capacity of the environment to cope with human activities should be taken into account, also the limitations set by the current state of technology and the future developments, therefore, are an essential part in the realisation of the concept of sustainable development. From that point of view, chemical engineering and process technology are key-disciplines at the interface of an expanding and demanding market of consumers on the one side and a concerned and suspicious society on the other (Gaudino *et al.*, 2016). This implies that both scientists and engineers should focus on the development, at the same time it satisfies and anticipates the needs of present and future generations. In that respect, the process discussed in this thesis contributes to sustainable development for three different reasons:

- The chemistry of this process allows the production of cyclic organic carbonates without requiring unfavourable chemicals such as phosgene.
- Carbon dioxide, a renewable resource that is often treated as waste, is effectively converted into a useful product.
- The suggested production process does not require solvents and, consequently, prevents the possibility of solvent losses to the environment. The contribution of this process to sustainable.

1.9 The principle of green chemistry

The term green chemistry was introduced by the Environmental Protection Agency (EPA), an agency of the US Government. A reasonable working definition of green chemistry can be formulated as follows: Green chemistry efficiently

utilises (preferably renewable) raw materials, eliminates waste and avoids the use of toxic and/or hazardous reagents and solvents in the manufacture and application of chemical products (Clark and Macquarrie, 2002). The chemical industry has faced growing concerns regarding the sustainability aspects of chemical process design during the last decade.

The followings are 12 principles of green chemistry (Source: Clark and Macquarrie, 2002)

- Waste prevention instead of remediation.
- Atom efficiency.
- Less hazardous/toxic chemicals.
- Safer products by design.
- Innocuous solvents and auxiliaries.
- Energy-efficient by design.
- Preferably renewable raw materials.
- Shorter syntheses.
- Catalytic rather than stoichiometric reagents.
- Design products for degradation.
- Analytical methodologies for pollution prevention.
- Inherently safer processes.

1.10 Carbon capture sequestration & utilisation

CO_2 capture involves chemical or physical separation of CO_2 from gas mixtures. Common methods include absorption using an agent such as monoethanolamine, physical adsorption using solid adsorbent, cryogenic separation at low temperatures, and membrane separation. CO_2 sequestration refers to the long-term storage of CO_2 in various reservoir locations with large capacities, such as geologic formations, ocean, aquifers, and forest (Choe *et al.*, 2014). The industrial separation of CO_2 from the flue gas of power plants is currently carried out by using the absorption process with monoethanolamine as

the liquid absorbent. It is usually carried out using gas mixtures that contain CO_2 in relatively high concentrations. Large-scale separations in the industry are currently based on chemical absorption of CO_2 from concentrated gas mixtures such as flue gases from power plants, from hydrogen plants or ammonia plants (Xie *et al.*, 2013a).

1.11 Barriers to further development of CO_2 conversion and utilisation

According to Ryan and Daly, (2019), the field of *Barrier Research* as a study has received very little recognition by researchers and scholars, this includes the study of barriers to CO_2 commercialisation. That explains why there is little progress in the conversion and utilisation of CO_2. In view of this negligence, there are significant barriers that have hampered the fixation and reuse of CO_2 in chemical processes. Such hurdles and possible strategies to overcome them are briefly outlined below.

1.11.1 Costs of CO_2 capture separation, purification, and transportation to user site

One of the major users of CO_2, the enhanced oil recovery (EOR) industry, typically cannot provide a solution to overcome these barriers, therefore, one of the strategies to deal with this barrier would be to identify and use concentrated CO_2 - containing gas mixtures at or near the sites of chemical conversion and utilisation (Darensbourg, 2010). Considering the separation part, better separation techniques and improved separation reaction process can lower this barrier. However, if it is beneficial and practically applicable, a new processing scheme for using CO_2 in a gas mixture without pre-separation of CO_2 would be desired. A proposed new approach is to make industrially useful synthesis gas with desired H_2/CO ratios by using CO_2 along with H_2O and O_2 in flue gas for tri-reforming of natural gas without CO_2 pre-separation (Extavour and Bunje, 2016).

1.11.2 Energy requirements of CO_2 chemical conversion

In order to effectively overcome the energy barrier in CO_2 utilisation, the corresponding strategies will be to use CO_2 as a co-reactant along with one or more compounds that have higher Gibbs free energies (Styring *et al.*, 2011). The use of a novel and effective catalyst can also play a significant role in enhancing higher conversion at comparatively lower temperatures (Ramin, 2006). CO_2 reduction by hydrogenation has been studied and reported by many research groups. For such processes, H_2 will need to be made from processes that do not co-produce CO_2 (Kleij, 2014). It should be noted that H_2 is currently produced by the reforming of hydrocarbons which is an energy-intensive process and accompanied by CO_2 formation both from the conversion process and from the combustion of the fuels which is used to provide the process heat (Agarwal *et al.*, 2016).

1.11.3 Market size limitations, and lack of investment-incentives for CO_2-based chemicals

Currently, only EOR industries hold a reasonable and promising scale for compliance purposes for coal-based utilities (Shui *et al.*, 2015). The estimated or perceived market sizes for CO_2 conversion vary for different applications. If all carbon-based synthetic chemicals and materials can be made using CO_2, then the current annual production of such chemicals and materials could provide an estimated upper limit of market demands for CO_2 for chemicals and materials (Gaudino *et al.*, 2016)

1.11.4 Lack of socio-economic and political driving forces that facilitate enhanced CO_2 utilisation

There are several ways for an industrialised society to encourage more utilisation of CO_2. If an environment-conscious society wants to promote CO_2 utilisation,

various incentives could be given to manufacturers that produce useful chemicals and materials using CO_2, or make use of CO_2 for environmentally-benign processing (such as replacement of phosgene) (Valavanidis, 2012). If the consumers and buyers in the industrialised societies recognise the need to such a level as to support CO_2 utilisation, price differential could be instituted for CO_2 utilisation which may be characterised as "carbon pricing for greenness'' (Agarwal *et al.*, 2016)

1.12 Research aims and objectives

The aim of this research work is to synthesise cyclic organic carbonates *via* an environmentally benign process from CO_2 and epoxide. To achieve this aim, the following objectives have been identified.

- Review the existing technologies for the production of cyclic organic carbonates.
- Highlight a greener and sustainable technology that could be implemented for effective fixation of CO_2.
- Design a novel and highly selective catalytic system for the efficient transformation of CO_2 to cyclic organic carbonate.
- Use multiple-physicochemical techniques to characterise both the commercial catalyst and the as-prepared catalyst.
- Compare the catalytic activity of commercial catalyst against the as-prepared novel catalyst.
- Investigate the effect of reaction conditions such as temperature, CO_2 pressure, reaction time and catalyst loading.
- Carry out catalyst reusability studies and offer a recommendation.
- Apply Response Surface Methodology (RSM) technique to model and optimise reaction process.

1.13 Contributions to knowledge

Several publications have reported the synthesis of many cyclic organic carbonates using different technologies. Some of these technologies have high cost and severe environmental implications including high temperature/pressure, longer reaction time, use of phosgene and solvent/cocatalysts (Miao *et al.*, 2008). This research work has employed the use of metal-organic frameworks (MOFs) catalyst as a novel new class of heterogeneous catalyst for the synthesis of many organic carbonates.

Recently, the stability of MOFs for large-scale industrial applications have been questioned in many published papers. This is due to their weak thermal, chemical and mechanical stability. To the best of our knowledge, Zr/ZIF-8 catalyst has never been developed or used for any catalytic reaction. However, the development of the novel catalyst will afford a stable and efficient reactive system for the synthesis of organic carbonate has proven to be a promising greener technology that offers a remarkable reinforcement to these weak functionalities, making a significant contribution to knowledge in the field of green and sustainable engineering. The activity of reused Zr/ZIF-8 catalyst showed consistent stability over seven subsequent runs.

The PXRD, FT-IR, and TGA analyses of the recycled catalyst show that the catalyst framework is quite stable after reusability performance. The high selectivity towards epichlorohydrin carbonate and styrene carbonate, simple separation of the catalyst by centrifugation, and excellent recyclability demonstrated that the catalyst is viable for large scale industrial applications. The catalytic properties of the new catalyst have been satisfactorily consistent with pristine ZIF-8 catalyst using multiple physicochemical characterisation techniques. We believe that this work could provide a new directive for designing

more sustainable, non-toxic catalysts for the transformation of CO_2 and other substrates.

1.14 Thesis structure

The structure of the thesis is as follows:

Chapter 1: Introduction

This chapter presents a general overview and the motivation for this research work. The background of CO_2, sources of CO_2, emissions of CO_2, policies of CO_2 emissions, policies of CO_2 emissions reduction, solutions for CO_2 emissions reduction and sustainability are extensively discussed. The aims and objectives of the research are also included in this section as well as the novelty of this research and the thesis structure.

Chapter 2: Literature review

This chapter gives a detailed review of the conventional and recent methodologies for the synthesis of cyclic carbonates. It discussed an overview of different organic carbonates, its applications and properties. The chapter also presents an elaborate approach of CO_2 transformation to organic carbonates such as cyclic and polycyclic carbonates. Has focused more on the use of various metal-organic frameworks (MOFs) catalysts to synthesis both chloromethyl ethylene carbonate (CMEC) and styrene carbonate (SC) than any other cyclic carbonates. Finally, it carried out a benchmark evaluation between reported ZIF based catalysts and current Zr/ZIF-8 catalytic system.

Chapter 3: Catalyst preparation and characterisation

This chapter discusses the greener synthesis and characterisation of a novel Zr/ZIF-8 catalyst as a highly efficient and stable CO_2-reduction catalyst for the synthesis of organic carbonates. An in-depth analysis of catalyst characterisation

of both commercially available ZIF-8 and as-prepared Zr/ZIF-8 catalysts using multiple physiochemical techniques have been discussed in this chapter.

Chapter 4: Comparison of catalytic activity of ZIF-8 and Zr/ZIF-8 for the greener synthesis of chloromethyl ethylene carbonate by CO_2 utilisation

This chapter provides the fundamentals on which subsequent cycloaddition of CO_2 and epoxides were built. It explains the detailed calibration process of pure samples and gas chromatographic (GC) analysis of the product sample. It compares the catalytic activity of both pristine ZIF-8 and as-prepared Zr/ZIF-8 catalysts. It examines the effect of different reaction parameters (temperature, pressure time and catalyst loading) on the conversion of epichlorohydrin (ECH), selectivity and chloromethyl ethylene carbonate (CMEC) yield. Finally, it detailed the reusability studies of both catalysts.

Chapter 5: Multiobjective optimisation for the greener synthesis of chloromethyl ethylene carbonate by CO_2 and ECH *via* response surface methodology (RSM)

This chapter provides details of the design, modelling and optimisation of chloromethyl ethylene carbonate using Box Behnken Design (BBD) to study the single and several independent reaction variables (such as temperature, pressure, time and catalyst loading). Furthermore, multiple responses optimisation and optimum conditions validation are presented.

Chapter 6: A greener approach and system optimisation of styrene carbonate synthesis *via* CO_2 utilisation

This chapter gives a detailed background for the synthesis of styrene carbonate using a novel Zr/ZIF-8 catalyst. It detailed the description of materials used, experimental methods, and method of analysis are presented. Furthermore, results and discussion that covers the reaction pathway, proposed reaction mechanism, the different heterogeneous catalysts, reaction time, catalyst

loading, reaction temperature and CO_2 pressure are discussed. The response surface methodology (RSM) modelling and optimisation of the process are explained. The batch studies for catalyst stability and reusability studies are presented.

Chapter 7: Conclusions and recommendations for future work

In this chapter, conclusions of the overall research work and recommendations for future research work are summarised and outlined respectively.

Chapter 8: References

This chapter shows all the used references from the literature, which have been cited in this research work

Chapter 2

Literature review

Outline of the chapter

This chapter gives a detailed review of the conventional and recent methodologies for the synthesis of organic carbonates. It focuses more on the use of various metal-organic frameworks (MOFs) catalysts to synthesis both chloromethyl ethylene carbonate (CMEC) and styrene carbonate (SC). Finally, it carried out a benchmark evaluation between reported ZIF-based catalysts and current Zr/ZIF-8 catalytic system.

The chapter is organised as follows:

2.1. Introduction

2.2. Organic carbonates

2.3. Catalysis

2.4. Metal-organic frameworks (MOFs) catalysts

2.5. Recent progress in the catalytic activity of MOFs for CO_2 fixation

2.6. Design of highly efficient and stable Zr/ZIF-8 catalyst for greener synthesis of organic carbonate

2.7. Conclusions

2 Literature review

2.1 Introduction

Major research efforts in the last two decades have been directed to the development of new catalytic systems for the chemical fixation of CO_2, both homogenous and heterogeneous catalysis. However, these attempts have failed to yield satisfactory results as most of these catalysts requires high temperature and/or pressure (usually around 453 K and pressure higher than 8 atm), further separation and purification steps, many of these catalysts deactivate after few recycle experiments and worse of all, low product yield. Hence this research is focused on the use of metal-organic frameworks (MOFs) catalysts as a relatively new and promising candidate that addresses these aforementioned shortfalls.

This chapter critically reviews previous research works on the use of MOFs catalysts for the conversion of carbon dioxide to organic carbonates. It examines how these prior studies directly relate to current research. It then draws a fine balance between these two reports by carrying out a benchmark evaluation between the current catalytic system of Zr/ZIF-8 and other reported ZIF based heterogeneous catalysts for coupling reaction of CO_2 and epoxides to form organic carbonates.

2.2 Organic carbonates

Organic carbonates, also known as organocarbonates or carbonic acid esters are a class of compounds with a carbonyl flanked by two alkoxy/aryloxy groups with a general structural formula of R_1OCOOR_2 (Bobadilla *et al.*, 2015b). Esterification of carbonic acid with hydroxy compounds produces a stable organic species known as organic carbonates. The carbonates formed can either be dialkyl, diaryl or substituted dialkyl diaryl carbonates depending on the nature of hydroxy groups (Srivastava *et al.*, 2005). Organic carbonates occur both naturally

and through synthetic approaches. While the natural occurrence of organic carbonates has suffered negligence over the years (Zhang *et al.*, 2014), the synthetic approaches have experienced significant research interest in the last three decades due to their wide industrial applications (Schäffner *et al.*, 2008). Although, organic carbonates may be referred to as ‘‘green solvents’’, this statement does not hold for their synthetic methodologies (Scha *et al.*, 2010) as some are produced *via* the traditional route of phosgenation. Phosgenation is one of the major industrial routes for linear carbonates such as dimethyl carbonate (DMC), while the cyclic organic carbonates are synthesised *via* cycloaddition reaction and transesterification (Saada *et al.*, 2018; Wen *et al.*, 2015). Organic carbonates are versatile compounds used as raw materials for many industrial applications including raw materials for polycarbonate and polyurethane synthesis (Sathe *et al.*, 2017b), green solvents (Liu *et al.*, 2012) gasoline (Maeda *et al.*, 2014), fuel additives (Adeleye *et al.*, 2015), electrolytes in energy storage devices (Onyenkeadi *et al.*, 2018), as fine chemical intermediates for pharmaceuticals (Miao *et al.*, 2008), automobiles (Sakakura and Kohno, 2009), electronic (Sakakura and Kohno, 2009) and alternative for fuels(Shukla and Srivastava, 2017b). Five most important organic carbonates which have attracted significant research interest in recent years include dimethyl carbonate (DMC), diethyl carbonate (DEC), glycerol carbonate (GC), propylene carbonate (PC), and ethylene carbonate (EC) as shown in figure 2.1-2.3.

Organic carbonates can be categorised as follows:

- Linear carbonates: These are open-chain structures which are either aliphatic or aromatic e.g. dimethyl carbonate (DMC), diallyl carbonate (DAC), diethyl carbonate (DEC), diphenyl carbonate (DPC).

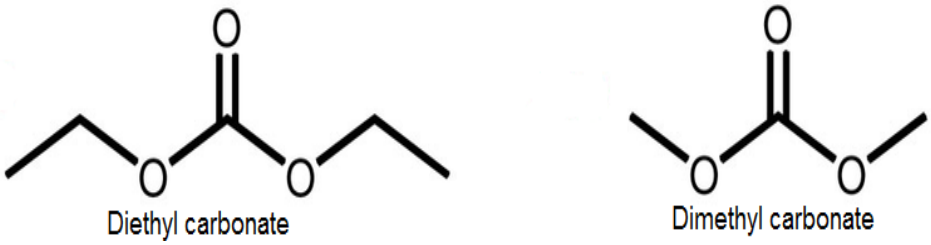

Figure 2. 1. Linear carbonates (Source: Bobadilla et al. 2015b)

- Cyclic carbonates: These are cyclic or closed chain e.g. ethylene carbonate (EC), propylene carbonate (PC), chloromethyl ethylene carbonate (CMEC) and styrene carbonate (SC).

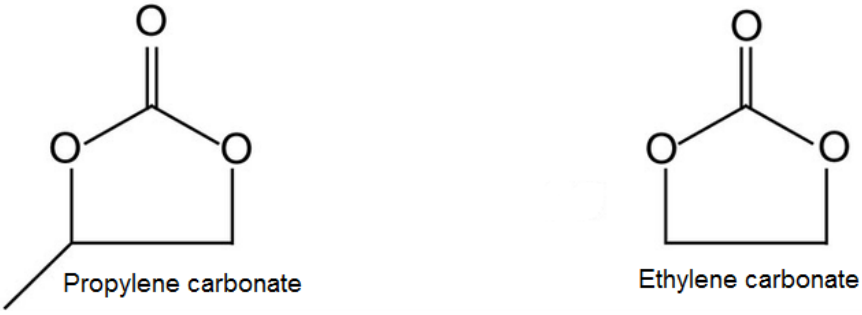

Figure 2. 2. Cyclic carbonates (Source: Wen et al. 2015)

- Polycarbonates: e.g. poly-(propylene carbonate) and bis-phenol A-polycarbonate

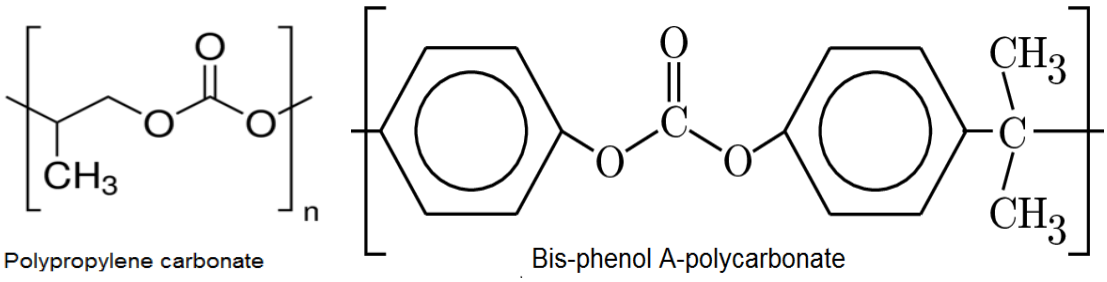

Figure 2. 3. Polymeric carbonates. (Source: Srivastava et al. 2005).

2.2.1 Market capacity for consumption of organic carbonates

The current global market potential of organic carbonates are yet to be fully exploited with dimethyl carbonate (DMC) and ethylene carbonate (EC) having the largest market share of around 100 kt/y and 96 kt/y, respectively (Vansant, 2013) as shown in figure 2.4. A large amount of these organic carbonates do not reach the market because they are used as intermediates in other processes (Wang *et al.*, 2006). For example, the current annual propylene carbonate (PC) production is close to 80 kt/y (Shukla and Srivastava, 2017a), on free-market. However, only 16-17 kt/y of these, produced by three European companies; Enichem (8 kt/y), SNPE (ca. 4tk/y) and UBE in Japan (ca. 5 kt/y), are actually available in the market (Serrano *et al.*, 2015). In 2009, the worldwide consumption of organic carbonates was about 100 000 tons (Sakakura and Kohno, 2009) with an anticipated increase of several tens of megatons each year (Shukla and Srivastava, 2017b). Today, a market of about 18 million tons per year of organic carbonates is estimated (Cucciniello and Cespi, 2018) as shown in figure 2.5. Yet, it is uncertain if the current on-stream technologies will satisfy market demand. Currently, much attention is being focused on DMC applications due to its low toxicity, high biodegradability and absence of mutagenic effect (Gminsights.com, 2019; Cucciniello and Cespi, 2018). The application is predicted to expand more than 10% due to its newfound end-use in automobile e.g. electric cars and in electronic industries (Sakakura and Kohno, 2009).

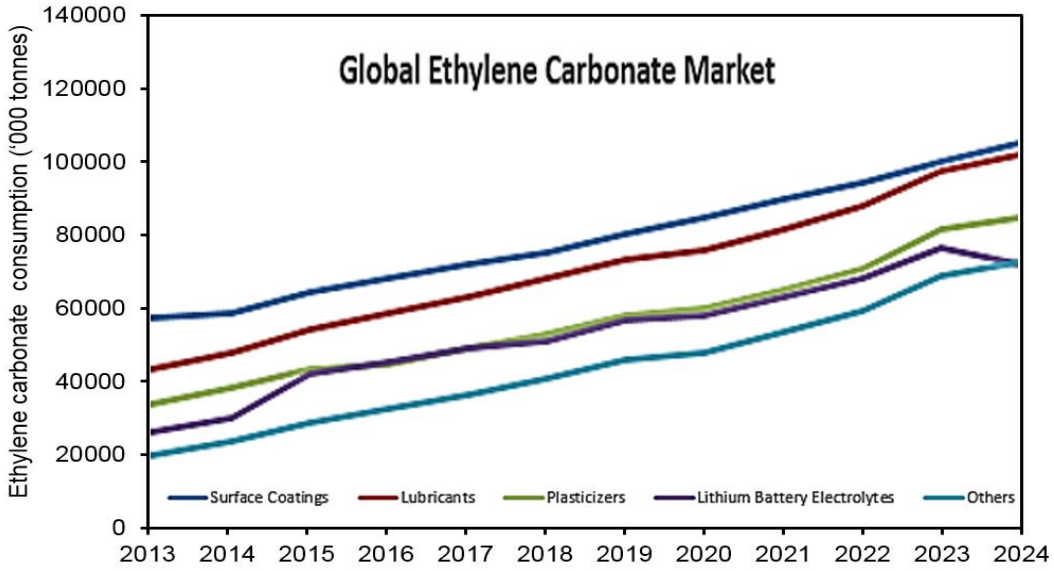

Figure 2. 4. Global Ethylene Carbonate Market Key Trends – Market Size (Source: Vansant, 2013)

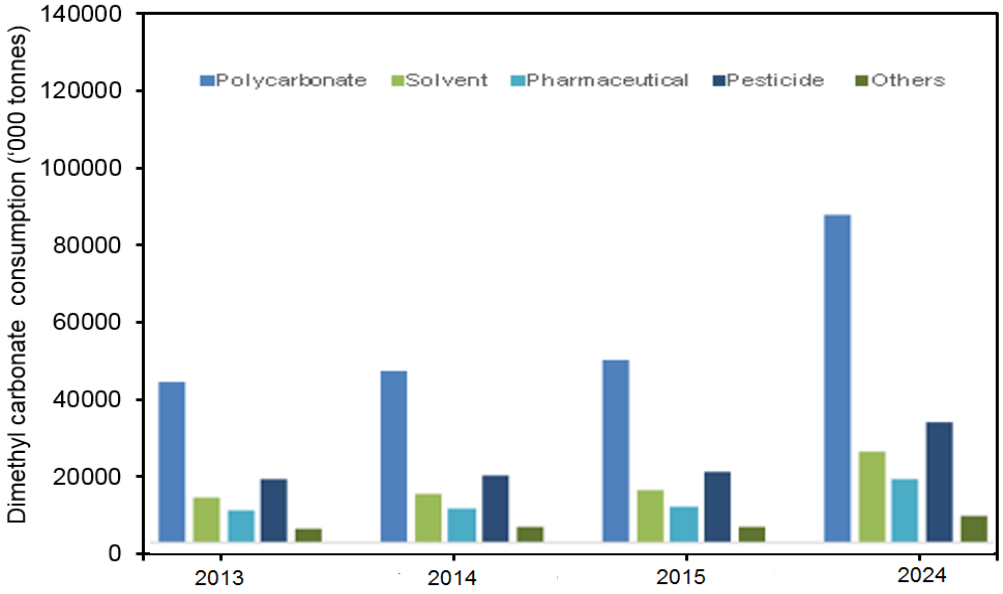

Figure 2. 5. Global dimethyl carbonate Market demand (Source: Cucciniello and Cespi, 2018)

Today, the major production platform of organic carbonates is centred on phosgene route. Although, this technology has raised several safety concerns as acutely toxic substances of phosgene ($COCl_2$) is formed (Van Meerendonk, 2005). The following section identifies some other possible phosgene-free technologies that have been tried and tested as commercially sustainable alternatives.

2.2.2 General methods of preparation of organic carbonates

Many synthesis technologies of molecular organic carbonates have been discussed and reviewed extensively in many literatures. As previously mentioned, phosgenation technique is by far the most popular method adopted by many manufacturers because of its high carbonate yield (Wu *et al.*, 2012) and huge economic gain (Shukla and Srivastava, 2017b). However, its negative effects on the environment are becoming more obvious than ever before (Hong *et al.*, 2018; Liu *et al.*, 2012). Acyclic carbonates are produced by oxidative carbonylation of alcohols or phenols, while the five-membered cyclic carbonates can be produced from diols, or epoxides and a one-carbon synthon (Sathe *et al.*, 2017b).

2.2.2.1 Phosgenation

Phosgenation of alcohol is the oldest method used for preparing organic carbonates (Shukla and Srivastava, 2017b) exploited as far back as 1970 by SNPE (Vansant, 2013). The technique as shown in figure 2.6 is mainly associated with noncyclic carbonates e.g. dimethyl carbonate (Schäffner *et al.*, 2008). In this method, organic compounds (aliphatic or aromatic) containing a single or mixture of inert, anhydrous solvent (dichloromethane, chloroform, benzene, and toluene) with excess pyridine are phosgenated at or below room temperature. Pyridine acts as an acid acceptor and reacts with phosgene, and anionic adduct is formed.

The adduct formed is more reactive than the corresponding chlorocarbons acid esters (Andraos, 2011). Pyridine is only one among the acid acceptors that may be used. Nearly all the organic carbonates (except few like ortho- and pyrocarbonate) can be prepared by this method. The main advantages of this method are higher carbonate yields compare to other methods, although the obvious drawbacks are the application of toxic chemicals like pyridine and phosgene, the neutralisation of excess used pyridine and by-products removal.

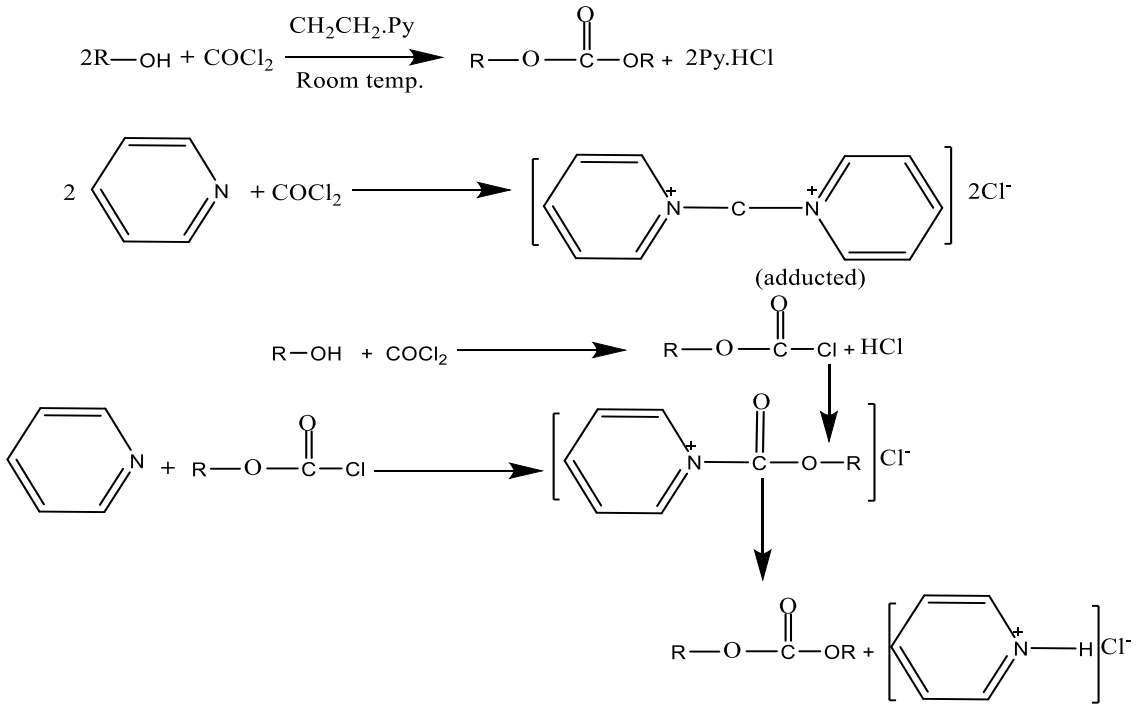

Figure 2. 6. Cyclic carbonates synthesis using phosgene in the presence of pyridine and dichloromethane solvent. (Source: Andraos, 2011)

2.2.2.2 Oxidative carbonylation of alcohols or phenols

The synthesis of dialkyl carbonates from the reaction of alcohols and carbon monoxide is enhanced by transition metal and post-transition metal compounds (Sathe *et al.*, 2017b). Palladium, mercury or copper-based catalysts were often

used. However, the reaction with Palladium and mercury is not selective and involves a reduction to the metal while copper is the only species that can be directly re-oxidised. The method as shown in figure 2.7 is suitable for alkyl carbonates, however, some of the drawbacks associated with this method include lower basicities of phenols, expensive catalysts, low yields, and low catalyst turnover efficiencies have precluded a commercial process based on oxidative carbonylation of phenols (Gaikwad and Bhanage, 2018).

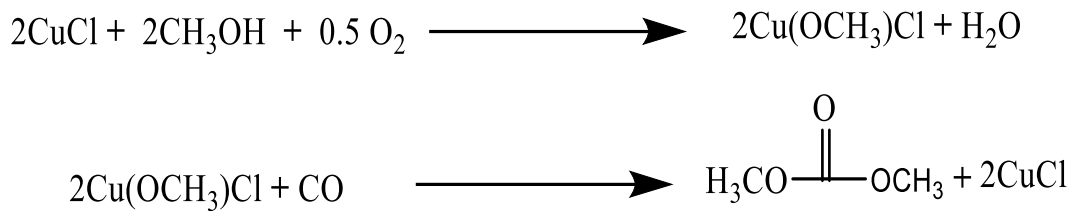

Figure 2. 7. Oxidative carbonylation of phenols catalysed by palladium (Source: Sathe et al. 2017b)

2.2.2.3 Reaction of urea with alcohols or phenols

The reaction of urea with alcohols when it is combined with metal salts like zinc acetate or lead acetate can form carbamates (Ramin, 2006). When triphenylphosphine is used as a co-catalyst during this reaction can lead to the formation of carbonates as shown in figure 2.8. The yields of carbonates are >99%. In principle, the ammonia which is discharged during the reaction can be recycled for the synthesis of urea. Primary, secondary, and low-boiling alcohols can be converted into carbonates. The carbamate that is formed as intermediate is thermally stable at the reaction condition and is transformed into dialkyl carbonate. The main by-products are isocyanuric acid and similar compounds. Adequate catalysts are dibutyl tin oxide and triphenyl tin chloride.

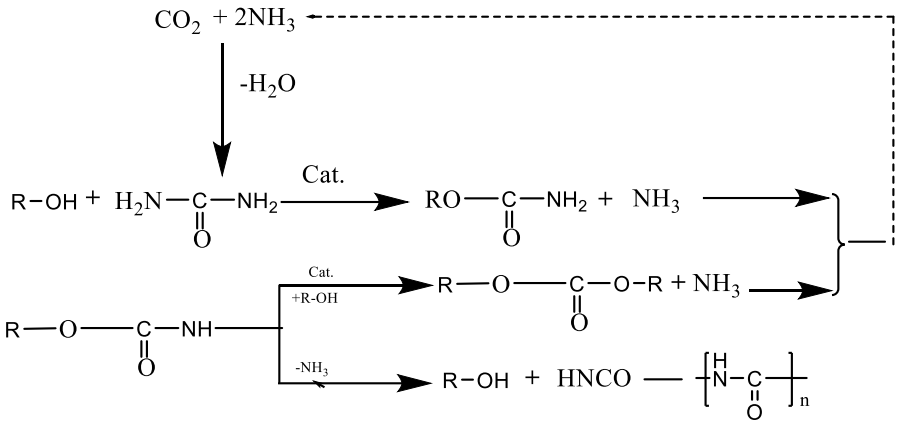

Figure 2. 8. Two stages synthesis of carbonates from urea. (Source: Ramin, 2006)

2.2.2.4 Carbonate interchange reactions

Carbonate interchange reactions also known as carbonate transesterification can be defined as a catalytic process in which one carbonate is being converted to another carbonate in the presence of sufficient amount of alcohol using a suitable catalyst. Normally, the more nucleophilic alcohol substitutes the less nucleophilic compound. If both compounds exhibit a similar nucleophilicity, the less volatile alcohol substitutes the more volatile alcohol (Wilding, 2011). Figure 2.9 shows that a broad range of different reactants and catalysts are used; the reaction conditions differ a lot, too.

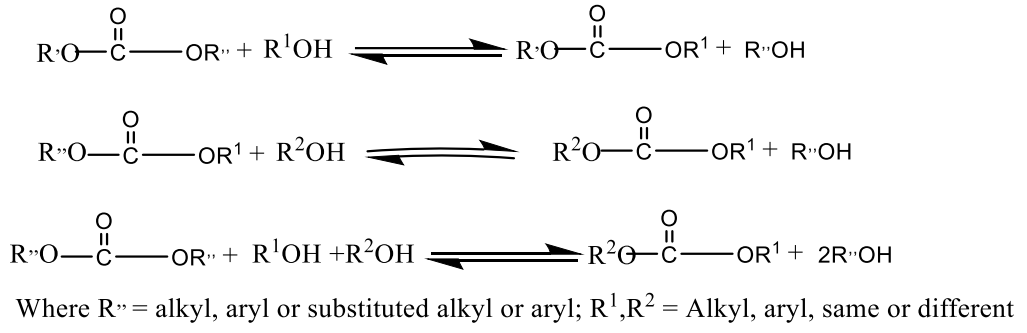

Figure 2. 9. Carbonate synthesis by carbonate interchange reaction. (Source: Wilding, 2011).

2.2.2.5 Use of metal carbonate

This is a less popular method of preparation of organic carbonate. Th e method as shown in figure 2.10 involves the transformation of inorganic (metal) carbonates to organic carbonates, except the reaction of silver carbonate with alkyl iodide. This could be as a result of the insolubilities of inorganic carbonates in aprotic organic solvents. Many carbonates ($RCH_2O)_2CO$ (R) CH_3,C_2H_5, CH_2dCH, C_3H_7, C_5H_{11}, C_6H_5) have been synthesised by this method with the corresponding halogen derivatives in the presence of activating agents such as crown ethers, polyglymes, polyamines, and triethylbenzylammonium chloride (He *et al.*, 2017).

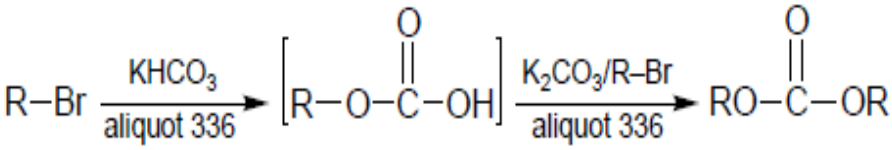

Figure 2. 10. Carbonate synthesis using metal carbonate (Source: He et al. 2017)

Some drawbacks associated with this method include: (Source: He et al. 2017)

- Reactions of inorganic carbonates with alkyl halides are sluggish even at elevated temperatures.
- This reaction requires a long time, and obtained are also low but can be improved under specific reaction conditions.
- This reaction works satisfactorily only with an alkyl bromide and K_2CO_3. It is difficult to prepare organic carbonates, using alkyl chloride and iodide with Na_2CO_3, and other group II metal carbonates.
- The solubility of most metal carbonates in nonpolar solvents is negligible, and the solubility is not appreciably better in dipolar aprotic solvents.

- This method is not applicable for the preparation of diaryl and activated dialkyl carbonates.
- In the preparation of dialkyl carbonates by this process, side products such as dialkyl ethers are produced

2.2.2.6 Reaction of epoxide with carbon dioxide

The coupling of carbon dioxide (CO_2) and epoxides to synthesise of cyclic carbonates is a highly attractive and 100% atom efficient process (Upare *et al.*, 2012). It represents a greener and safer alternative to the conventional ways of synthesising organic carbonates as described above. Figure 2.11 represent the reaction between CO_2 and epoxides. The reaction does not occur rapidly but requires the use of some catalysts, co-catalysts, and/or solvents to promote the reaction. These reactions are mostly carried out at high pressure, which may not be economically suitable and also pose safety concerns. The challenge is to develop efficient catalysts that are capable of activating CO_2 under low pressure (preferably at 1 atm), and thus incorporating CO_2 into organic molecules catalytically.

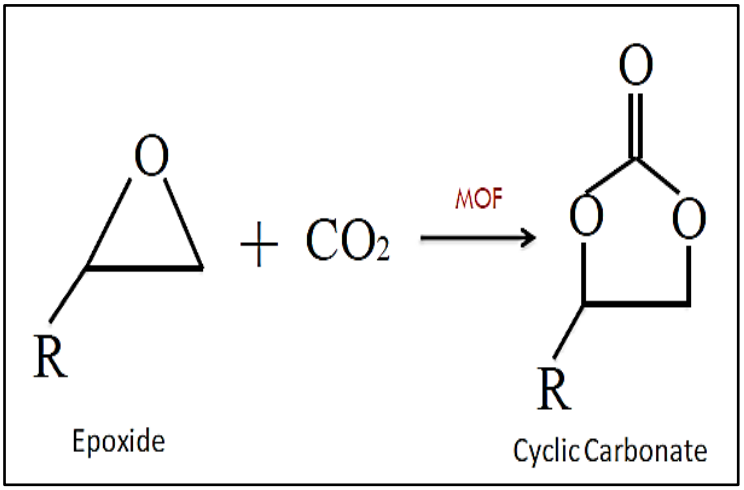

Figure 2. 11. Reaction of CO_2 and epoxide (Source: Upare et al. 2012).

2.3 Catalysis

Adeleye et al. (2015) defined catalyst as a substance which increases the rate of a chemical reaction without itself undergoing a permanent chemical change. During the last two decades, a variety of catalysts have been synthesised for the cycloaddition reaction of CO_2 and epoxides. These include metal oxides, organic bases or onium salts, metal complexes, ionic liquids, etc. Most of these catalysts suffer low efficiency, high temperature, high pressure, low stability, water or moisture sensitivity or the need for co-solvent (Gong *et al.*, 2012; Wang *et al.*, 2011). Therefore, to improve the catalytic performance of this reaction, the catalysts need to simultaneously possess Lewis acid and base in order to activate epoxides and CO_2 respectively (Wilhelm *et al*., 2015,). Moreover, theoretical study also indicated that the formation of a hydrogen bond between catalyst and epoxide could accelerate the ring-opening reaction of the epoxide, thus enhancing the activity significantly (Taherimehr *et al.*, 2012). Catalyst contains "active sites", which are able to affect the kinetics of chemical reactions and make reactions go faster by reducing the activation energy.

Today, the development of greener technologies that eliminate the hazardous and environmentally undesirable phosgene is of paramount importance for the fixation of carbon dioxide. It is generally recognised that many homogeneous or heterogeneous catalysts catalyse this coupling reaction through an acid-base or electrophile-nucleophile bifunctional mechanism (Sarbu *et al.*, 2000). A wide range of homogeneous and heterogeneous catalysts have been developed to catalyse the CO_2 fixation process (Aluja *et al*., 2017). Homogeneous catalyst usually gives higher catalytic activity and selectivity in comparison to the heterogeneous catalyst (Luo *et al*., 2014) however, heterogeneous catalysts do not only offer advantages with regard to catalyst separation and reusability but also provides a reaction rate that can be increased through the proper use of the

supporting material. (Riduan, 2012). The following subsection explains different types of catalysts:

2.3.1 Bio-catalysis

Natural catalysts such as protein enzymes perform a chemical transformation on the organic compound through a process known as bio-catalytic processes. Bio-catalysis is an important aspect of catalysis and has been used widely to make small drugs in the pharmaceutical industry (Seibert and Tracy, 2014). Most of the living organisms' processes depend on the use of enzymes that consist of proteins and the amino acids, which are linked by bonds called peptide bonds and these bonds form the enzyme's structure. Enzymes use four types of interactions, these are electronic interactions, hydrogen bonding, hydrophobic interactions and Van der Waals interactions to bind its substrates. The bond between the active site and substrate is relatively weak and could not prevent enzymes' catalytic cycle if the bond is strong (Hagen *et al.*, 2006).

2.3.2 Homogenous catalysis

The separation of homogeneous catalysts from the reaction mixture is often associated with complicated procedures such as catalyst decomposition. These complications have limited its industrial application as it may require more energy and time (Liu *et al.*, 2015a). Moreover, homogenous catalytic reactions involving CO_2 are commonly carried out at high pressure, which may not be economically suitable and also pose safety concerns (Sarbu *et a*l. 2000; Styranec *et al.,* 2009; Beckman *et al*. 2015). The challenge is to develop efficient catalysts that are capable of activating CO_2 under low pressure and thus incorporating CO_2 into organic molecules catalytically (Mennicken *et al.*, 2016).

2.3.3 Heterogeneous catalyst

Heterogeneous catalysts are the workhorse of many industrial processes. Although they have many processing advantages over their soluble counterparts (Miao *et al.*, 2008), novel catalysts, which have high stability, superior efficiency and low cost, are urgently needed to facilitate the carbon dioxide conversion (Remya *et al.,* 2019). Therefore, heterogeneous catalysts are far more suitable for large scale industrial synthesis. However, it is important to design and synthesise more efficient heterogeneous catalysts due to the demand for environmentally friendly technologies. Heterogeneous catalysts are widely used in industries because of their advantages in the separation and recycling and their applicability for flow reaction systems. Unfortunately, conventional heterogeneous catalysts are sometimes less active and/or selective in comparison to some homogeneous catalysts such as metal complexes and organic bases including ionic liquids (Onyenkeadi *et al*, 2019).

In the past two decades, several attempts have been made to develop greener and sustainable catalytic systems for chemical fixation of CO_2. This includes conventional solid catalysts such as zeolites, metal oxides, quaternary onium salts, alkali metal halides, ionic liquids (ILs), transition metal complexes, etc. However, these attempts have failed to yield satisfactory results as most of these catalysts require high temperature and/or pressure (usually around 453 K and pressure higher than 8 atm), further separation and purification steps and low product yield (Kathalikkattil *et al.*, 2015). This is uneconomical from a commercial point of view and hence the research has been directed to employ a novel catalyst that provides solutions to all these shortfalls i.e. Metal-organic frameworks (MOFs). Although, traditional porous materials such as activated carbon, zeolites, aluminosilicates, etc have been known for their high ultra-specific surface area

and high porosity, however, their applications have been limited especially in the field of heterogeneous catalysis due to difficulty in pore modification.

2.4 Metal-Organic Frameworks (MOFs) catalysts

MOFs catalysts also known as multidimensional porous coordination polymers are a new class of microporous crystalline materials with exceptional properties such as ultrahigh specific surface area, enormous pore spaces and ordered crystalline structure (Karagiaridi *et al.*, 2012). MOFs have emerged as a suitable candidate for the cycloaddition of CO_2 and epoxide in the synthesis of organic carbonates due to their heterogeneity and reusability requirements (Beyzavi *et al.*, 2015a). It is noteworthy that solid MOF-based catalysts often display higher catalytic activity than their corresponding homogenous catalysts as evidenced in a broad range of reactions including ring-opening, addition reactions, oxidation reactions, hydrogenation, isomerisation (Rimoldi *et al.*, 2017). Zeolitic imidazolate frameworks, (ZIFs), is one of the subclasses of MOFs with a similar structure to zeolites. It has attractive structural properties and intrinsically lower density. Many experiments involving ZIF-8 have shown great applications in multidisciplinary fields such as catalysis, drug deliveries, purification, gas storage (Zhang *et al.*, 2016). MOF-Based catalytic systems for CO_2-epoxide coupling reaction

MOFs are intrinsically endowed with five different structural characteristics within its framework. These enhance its ability to activate epoxides for the coupling reaction of CO_2 and epoxide to produce desired cyclic organic carbonates (Liang *et al.*, 2019a). The earliest feature to be explored is the use of structural defects in MOFs frameworks. The second feature is the unsaturated coordination sphere around metals, which function as Lewis acid sites. These sites can be derived from the secondary building units (SBUs) and/or functional linker. Typically, these sites may require the use of a co-catalyst such as tetrabutylammonium bromide (TBAB), to get optimal results. The third is the Lewis base linkers, also refer to as

functional linkers. Sometimes, incorporating the Lewis acid, base or ionic sites into MOFs linkers has been found to enhances effective CO_2 fixation process. The fourth feature is the presence of Lewis acidic or basic sites on the surface or within the interior of defective MOF catalysts. The fifth and the last feature is the use of ionic linkers to catalyse the reaction of CO_2 and epoxide.

2.4.1 Defective MOFs for catalysis

MOFs with structural defects presents one of the earliest opportunities in the cycloaddition of CO_2 and epoxides. Sometimes, MOF based heterogeneous catalysts may contain linkers which are not catalytically active (no Lewis base site) and the metal centers are coordinatively saturated (no Lewis acid site) for cycloaddition reaction of CO_2 to epoxide. Thus, introducing defects to such MOF crystal structures can finely adjust their inherent structure-property relations, improve their catalytic performance, and can even confer the MOFs some unique properties that they did not previously possess (Ren *et al.*, 2017). Although, defects in MOFs may also occur naturally as a result of crystal imperfections such as vacant metal or linker sites, which could have served as an active site for the catalytic transformation of epoxide to carbonates (Fang *et al.*, 2015). Such MOFs with catalytic defects include ZIF-8, ZIF-68, MOF-5 (Song *et al.*, 2009), all of which are Zn^{2+}-containing materials.

The first trial using defective MOFs for the coupling reaction of CO_2 and epoxide was reported by Song et al. (2012) (Table 2.1, entry 1). The group synthesised classical MOF-5, constructed by Zn_4O SBUs and BDC linkers in the presence of a quaternary ammonium salt co-catalyst to catalyse the reaction of propylene oxide and CO_2. After several experiments, they found that the propylene carbonate yield increased with the alkyl chain length in the following order: Me_4N^+ < Et_4N^+ < n-Pr_4N^+ < n-Bu_4N^+ with a 97% yield achieved at a much higher CO_2

pressure of 60 bar. Impressed by this result, Jiang et al. (2015) prepared another defective Al-MOF, namely USTC-253-TFA to synthesise chloroprene carbonate. This MOF is built with alternating Al(III)-OH chain SBUs and 4,40-dibenzoic acid-2,20-sulfone linkers. Trifluoroacetic acid (TFA) was introduced during the catalyst synthesis to create the defect containing USTC-253-TFA with coordinatively unsaturated Lewis Al^{3+} sites and Brønsted acid (Al-OH) centers. After the synthesis, the catalytic performance of USTC-235-TFA was found to out-perform the defect-free catalyst USTC-253 (74.4%), USTC-253-TFA showed enhanced catalysis in the cycloaddition of CO_2 and ECH with the use of TBAB as a co-catalyst at room temperature under 1 bar CO_2 pressure giving a high yield of chloroprene carbonate (81%) (Table 2.1, entry 6).

Another successful trial using defective MOF for the coupling reaction of CO_2 and epoxide was reported in 2012 by Miralda et al. (2012b). The group used ZIF-8 to catalyse the reaction of CO_2 and epichlorohydrin without any solvent or co-catalyst to afford a 44% yield of chloropropene carbonate. The catalytic activity of ZIF-8 was attributed to its surface defects, derived from strong Lewis acidic Zn^{2+} sites as well as the basic nitrogen atoms from the imidazolate ligands. A post-synthetic modification (PSM) of the catalyst was carried out by introducing an amino group to its frameworks in order to improve its selectivity and yield. The crystalline structure of the catalyst was preserved throughout the synthetic operation. As a result of the PSM, the yield of chloropropene carbonate was found to increase from 44% to 73% under the same conditions as shown in (Table 2.1, entry 3) (Miralda *et al.*, 2012b). Regrettably, the catalyst was not stable at high pressures and lost its distinctive crystalline structure and superior catalytic performance during the recycled experiments. Further study revealed that the blocking/poisoning of the active sites by carbonate products and the presence of higher-pressure CO_2 might be responsible for the observed crystalline instability and catalytic deactivation of ZIF-8.

A year later, Zhu et al. (2013a) synthesised styrene carbonate from the reaction of CO_2 and SO using ZIF-8. As shown in (Table 2.1, entry 5), the cycloaddition reactions were performed at 7 bar, 323-373 K for 4 h. The catalyst exhibited high activity even at temperatures as low as 323 K. They also found that the catalytic reactions occurred at the defect sites of the catalyst surface. They have ascribed the reason for the fact that styrene oxide was too large to enter the pore of ZIF-8. The group concluded that both the acid sites and the N basic moieties in ZIF-8 favoured the activation and binding of the polar C-O bonds of CO_2 and also promoted its further conversion to styrene carbonate. Other research groups have also reported up to 93.3% yield of styrene carbonate at 393 K and 9.9 atm. in the absence of solvent and co-catalyst (North *et al.*, 2010). For example, the catalytic performance of ZIF-22 in the cycloaddition reaction of CO_2 to epoxide was also investigated by Hwang et al. (2016). The reaction was carried out in the absence of solvent and co-catalyst at 393 K and 11.8 atm. using epichlorohydrin as a substrate (Table 2.1, entry 2). The catalyst was reported to achieve TOF of 155 h^{-1}, which was significantly higher than other Zn-containing MOFs such as ZIF-8, ZIF-67 and ZIF-8-NH_2 with TOFs of 12, 22 and 17 respectively under same experimental conditions (Yang *et al.*, 2014; Miralda *et al.*, 2012; Kuruppathparambil *et al.*, 2016b). The higher efficiency of ZIF-22 compared with other ZIFs was attributed to the presence of the extra non-coordinated nitrogen atom in the 5-azabenzimidazolate linker, which was reported, to act as Lewis base cocatalyst, thus facilitated the cycloaddition reaction. ZIF-22 was also reported to be stable even after three repeated cycles as shown in (Table 2.1, entry 4, and 7)

Table 2. 1. MOFs with structural defects as heterogeneous catalysts for CO_2 conversion

Entry	MOF	Active site	Metal node	Lingards	substrate	Co-catalyst	T (K)	P_{CO2} (bar)	T (h)	Yield (%)	Ref
1	MOF-5	Defect	Zn^{2+}	H_2BDC	PO	TBAB	323	60	4	97	Song et al. (2009)
2	ZIF-22	Defect	Zn^{2+}	MeIM	ECH	-	393	11.8	2	99	North et al. (2010)
3	ZIF-8	Defect	Zn^{2+}	MeIM	ECH	-	343	7	4	44	Miralda et al (2012)
4	ZIF-67	Defect	Co^{2+}	MeIM	SO	-	393	10	6	87	Yang et al. (2012)
5	ZIF-8	Defect	Co^{2+}	MeIM	SO	-	373	7	4	27	Zhu et al. (2013)
6	USTC-253-TFA	Defect	Zn^{2+}	[AI-OH] Chain	ECH	TBAB	298	1	72	81	Jiang et al. (2015)
7	ZIF-67	Defect	Co^{2+}	MeIM	ECH	-	373	7	4	27	Hwang et al. (2016)

2.4.2 MOFs with acidic secondary building units (SBUs) (Active catalytic metal sites)

MOF catalysts with inherent coordinatively unsaturated sites (CUSs) around the metal ions or having a secondary building unit (SBUs) are sometimes used as Lewis or Brønsted centers after being immersed in protic solvents (North and Pasquale, 2009a; Xu *et al.*, 2018). Lewis acidic metal ions such as Cr^{3+}, In^{3+}, Fe^{3+}, $Zr^{4+,}$ and Hf^{4+} may function as a catalytic active site to initiate the cycloaddition of CO_2 and epoxide substrates (Liang *et al.*, 2019b; Beyzavi *et al.*, 2015a; Bhanage *et al*., 2017a). Typical examples of catalytically active centers include MIL-101(Cr or Fe) (Saptal and Bhanage, 2017b), M-MOF-74 (Beyzavi *et al.*, 2015a), Hf-NU-100 (Sabale *et al.*, 2016), PCN-700-Me (Guillerm *et al.*, 2014). The use of co-catalyst such as TBAB is usually employed to activate the opening of the epoxide ring where the MOF structures are without any Lewis base sites in order to achieve an optimal effect (Song *et al.*, 2009). Table 2.2 identified some examples of MOFs with catalytically active center nodes.

Cho et al. (2012a) reported the first successful approach to catalyse the reaction of styrene oxide and CO_2 using MOF-74 without any use of co-catalyst under 20 bar of CO_2 pressure at 373 K. The synthesised Co-MOF-74 catalyst displayed a promising catalytic performance with 99% conversion of styrene oxide (Table 2.2, entry 1). Furthermore, the group also found the catalyst to be efficient and reusable with no structural deterioration and no loss in catalytic activity after 3 experimental runs. A year after Cho's experiments, Yang et al. (2012) also reported the catalytic activity of mg-MOF-74 for the cycloaddition of CO_2 to styrene oxide at 373 K and 19.7 atm. They recorded an optimal 95% yield of styrene carbonate (SC) after 4 h of reaction time with only 30 mg of mg-MOF-74 in chlorobenzene solvent, surprisingly without any co-catalyst (Table 2.2, entry 2). The catalyst was stable after three repeated runs without any significant

loss in catalytic activity (Yang *et al.*, 2012). The group concluded from their experimental results, that the oxygen atoms present in the organic linkers may have acted as Lewis base site, while unsaturated mg atom acted as Lewis acid. Férey et al. (2013) discovered chromium terephthalate MOF catalyst named as MIL-101. According to the group, the presence of Lewis acidic Cr^{3+} centers on the metal cluster node and the interior large mesopores (29 Å and 34 Å) have enhanced substrate and product diffusion (Férey, G, C.Mellot-Draznieks, C.Serre, F.Millange, J.Dutour, S.Suble, 2013). Likewise, in 2013, Fedin and colleagues explored the catalytic features of MIL-101 to catalyse the reaction of styrene oxide and CO_2. An impressive 95% yield of SC was achieved with a temperature range of 298-393 K, 8 bar of CO_2 pressure and a reaction time 48 h. Although, the group admitted adding TBAB as a co-catalyst was greatly crucial to produce such a high yield of styrene carbonate. Post-reaction analysis of the spent catalyst revealed that all the ML-101 PXRD peaks disappeared just after the second reuse experiment. This indicated that the framework might have collapsed during the reaction. However, when doped with iron oxide, the obtained Fe-MIL-101 displayed a more higher catalytic performance than MIL-101 especially with PO as a substrate (Zalomaeva *et al.*, 2013) as shown in (table 2.2, entry 3 and 4).

Similar efforts were made in 2014 by Beyzavi and research group. They examined the catalytic performance of a mesoporous Hf-based MOF (Hf-NU-1000) as an efficient and multifunctional facile catalyst. In the presence of tetra-n-butylammonium bromide (TBAB) co-catalyst and acetonitrile used as a solvent, Hf-NU-1000 showed an outstanding catalytic performance in the quantitative cycloaddition of CO_2 to styrene oxide at room temperature and 1 atm pressure. 100% conversion of PO was recorded in 26 hr. Elsewhere, Beyzavi et al. had earlier reported a 46% conversion with Zr-

NU-1000 under in 4 hr (Table 2.2, entry 5). The two catalysts were believed to share similar coordination chemistry, however, catalyst characterisation results showed that Hf was more exophilic (stronger M-O bonds) than Zr-based. Thus Hf-based SBUs has a stronger Brønsted acid than Zr-based SBUs. The catalyst recovered good stability after three runs. A comparative catalytic efficiency test of Hf-Nu-1000 and other similar MOFs such as HKUSK-1, MOF-505, MMPF-9 and MMCF-2 conducted under the same reaction condition showed that Hf-Nu-1000 was found to be catalytically superior. Its performance was attributed to a high density of Hf Lewis acid site with relatively large pore size, ranging from 13 to 29 Å and a high Brunauer–Emmett Teller (BET) surface area of 1780 m^2/g (Beyzavi *et al.*, 2015b).

In a related study to Beyzavi's experiments, Zhou et al. (2019) reported on the catalytic performance of facile metal-organic frameworks named as Ni-TCPE1 for catalytic conversion of styrene oxide to styrene carbonate in the presence of tetrabutylammonium bromide (TBAB) as co-catalyst at 373 K and 9.9 atmospheric pressure. The catalyst was reported to retain its catalytic activity after 20 repeated runs (70 h), achieving a TON value of 35,000 with a 99% conversion of SO as shown in (Table 2.2, entry 6). Similarly, Duan and co-workers examined the catalytic effect of a single-walled metal-organic nanotube, called Ni-TCPE1 as a form of heterogeneous catalyst for CO_2 fixation (Zhou *et al.*, 2015). The catalyst was found to display outstanding catalytic performance with a turnover number (TON) of 35,000 per mole of the catalyst after repeating the reaction 20 times (70 h) as shown in (Table 2.2, entry 8). Liang et al. (2019b) recently investigated the catalytic efficiency a new rare earth nonnuclear carboxylate cluster-based gea-MOF (gea-MOF-1) in a solvent-free synthesis of styrene carbonate in the presence of a co-catalyst. This was found to be more

superior than Y_20_3/TBAB. The TGA and reusability analysis also confirmed that gea-MOF-1 has good thermal stability (up to 633 K under vacuum) and stable after three repeated use of the catalyst.

In a recent innovative design, Brozek and Dincă. (2014) used a cation exchange within the SBUs framework to develop new materials for gas exchange in heterogeneous catalysis. Two years later, in 2016, Zou et al. prepared a highly porous Zn-based MOF, called 1-Zn incorporated which two SBUs into its structures including dimeric paddlewheel units ($Zn_2(COO)_4$) and tetrahedron units ($Zn_4(O)$ $(CO_2)_6$) *via* the assembly of Zn^{II} ion and tricarboxylic ligands.1-Cu, 1-Zn and 1-Co were then introduced into the material in order to improve its catalytic performance. The resulting materials were then used to catalyse the cycloaddition of propylene oxide (PO). A 99% yield of propylene carbonate with 1-Zn followed by a 32% propylene carbonate yield with 1-Cu and 50% yield with 1-Co.

With the objective of designing a greener and highly efficient catalytic material for CO_2 fixation, recent research efforts have highlighted a group of newly developed MOF catalysts with acidic SBUs. Interestingly, these catalysts have demonstrated excellent catalytic activity without the need for solvent or co-catalyst even though they contain SBUs. These include BIT-103, BIT-102, BIT-101, CZ-ZIF and Ti-ZIF (Huang *et al.*, 2014). For example, Park and colleagues prepared and investigated the catalytic performance of a bimetallic ZIF: Co/Zn- ZIF (CZ-ZIF-8) to catalyse the coupling reaction of epichlorohydrin (ECH) and CO_2., (Kuruppathparambil *et al.*, 2016a). CZ-ZIF-8 possessed the same sodalite topology as that of the parent materials, ZIF-67 and ZIF-8, but a higher surface area of about 1400 m^2/g. The Co^{2+} and Zn^{2+} metal ions were shown to occupy equivalent sites in the porous framework at almost a ca. 1:1 ratio, as demonstrated by

energy-dispersive X-ray (EDX) analysis and inductively coupled plasma (ICP) atomic emission spectroscopy. It was expected that CZ-ZIF was designed to combine the high activity of ZIF-8(Zn) and high selectivity of ZIF-67(Co) for the desired product. This was confirmed by comparing the activities of ZIF-8, ZIF-67, CZ-ZIF and their components in the catalytic conversion of epichlorohydrin (ECH) into epichlorohydrin carbonate under relatively mild conditions (7 bar CO_2, 373 k, 4 h). The conversion of ECH by ZIF-8 was excellent (98%), while the selectivity was poor (33%). Conversely, ZIF-67 showed high selectivity (98%) and a moderate conversion (66%). Meanwhile, CZ-ZIF afforded both high conversion (94%) and selectivity (98%) for the epichlorohydrin carbonate (ECHC) (Table 2.2, entry 10) (Hwang *et al.*, 2016). On the other hand, the un-activated CZ-ZIF showed comparable activity (98%) and selectivity (96%) with activated CZ-ZIF as mentioned above. Moreover, CZ-ZIF was very stable and exhibited high reusability after four recycling tests. Additionally, ECHC could be obtained in a yield of 96% by exploiting CZ-ZIF as catalyst and TBAB as co-catalyst under ambient temperature over 36 h (7 bar CO_2, 313 K).

Table 2. 2. MOFs with acidic secondary building units (SBUs) for CO_2 conversion

Entry	MOF	Active site	Metal node	Lingards	substrate	Co-catalyst	T (K)	P_{CO2} (bar)	T (h)	Yield (%)	Ref
1	MOF-74	Co^{2+}	Co^{2+}	H_4DHBDC	SO	TBAB	373	20	4	99	Cho et al. (2012)
2	Mg-MOF-74	Mg^{2+}/Co^{2+}	Mg^{2+}/Co^{2+}	H_4DHBDC	SO/ECH	TBAB	373	20	4	99	Yang et al. (2012)
3	Cr-MIL-101	Cr^{3+}	$Cr_3O(CO_2)_6$	BDC	ECH	TBAB	298	8	24	82	Férey et al. (2013)
4	Fe-MIL-101	Fe^{2+}	$Fe_3O(CO_2)_6$	BDC	SO	TBAB	298	8	24	95	Zalomaeva et al. (2014)
5	Hf-NU-1000	Hf-OH/-OH_2	[Hf_6]	H_4TBAPy	ECH	TBAB	298	1	56	100	Beyzavi et al. (2014)
6	1-Zn	Zn^{2+}	$Zn_2(CO_2)_4$	H_3L	PO	TBAB	RM	10	60	99	Brozek et al (2014)
7	Ni-TCPE1	Ni^{2+}	Ni^{2+}	TCPE	SO	TBAB	373	12	10	86.2	Zhou et al. (2015)
8	Ni-TCPE2	Ni^{2+}	Ni^{2+}	TCPE	ECH	TBAB	373	12	10	99	Duan et al. (2015)
9	CZ-ZIF-8	Co^{2+},Zn^{2+}	Co^{2+},Zn^{2+}	MeIM	ECH	TBAB	373	7	4	92	Park et al. (2016)
10	gea-MOF-1	Y^{3+}	[Y_9(μ--OH)$_6$	BTB	SO	TBAB	393	20	6	85	Huang et al. (2016)

2.4.3 MOFs with acidic linkers-organic base systems (Dual catalytic metal centers)

Sometimes, the Lewis or Brønsted acid sites in the organic linkers of MOFs can be immobilised *via* a pre-designed approach or post-synthetic modification (PSM) method. The typical acidic linkers of MOFs include functional metallosalen, metalloporphyrin ligands, metallated azamacrocycle molecules and phosphorus-containing ligands (Ren *et al.*, 2013a; North *et al.*, 2010; Zheng *et al.*, 2015).

Recently, Ren et al. (2013b) prepared a highly porous Ni(salphen)-MOF by the assembly of a dicarbonyl functionalised Ni(salphen) ligand and Cd^{2+} ions. The catalyst was tested for cycloaddition of propylene oxide and CO_2. In the presence of TBAB as co-catalyst at 20 bar, 253 K for 4 h, 80% yield of PC was recorded as shown in (Table 2.3, entry 1). The same group prepared a 3D form of chiral Cd-MOF, Ni (saldpen)-MOF and compared its catalytic activity with Ni(salphen)-MOF for the cycloaddition of propylene oxide and CO_2, a disappointing 28% yield of PC was achieved with Ni (saldpen)-MOF. However, 86.1% yield of PC was recorded in the presence of a TBAB co-catalyst under 20 bar of CO_2 pressure, at 353 K as shown in (Table 2.3, entry 2).

Inspired by the catalytic activity of homogeneous metalloporphyrins catalysts in the presence of co-catalysts, Wang et al. (2016) investigated the catalytic performance of series of highly stable porous Zr-MOFs; PCN-224 (Ni, Co, Fe), incorporated with metalloporphyrin and six-connected Zr^6 clusters. They reported the catalytic efficiency of PCN-224 (Co) for the reaction of propylene oxide and CO_2 in the presence of TBAB. An encouraging 42% yield was obtained under 20 bar with CO_2 and at 373 K for 4 h as indicated in (Table 2.3, entry 3) (Kim *et al.*, 2013a).

Another notable efforts was made by Gao et al. (2017). The group prepared a nbo (niobium oxide like topology) MOFs, called MMCF-2 to catalyse the reaction of propylene oxide and CO_2 to produce propylene carbonate at a relatively mild reaction condition. A 95% yield of PC was achieved at room temperature and 1 atm CO_2 with the TBAB as a co-catalyst. In another separate experiment, the group carried out investigative experiments to study the relationship between active metal centers and the catalytic properties of MMCF-2 and other MOFs. The results concluded that MMCF-2 outperformed homogeneous Cu(TACTMB) (47.5% yield), as shown in (Table 2.3, entry 4 and 5) HKUST-1 (49.2% yield), and MOF-505 (48% yield) for the synthesis of propylene carbonate. The results indicated that the higher density of Cu^{2+} centers imparted by metal-macrocyclic linkers in each cage could significantly promote the catalytic activity by increasing the interactions between the catalytic sites and substrates.

Later in 2017, the same group, Gao et al. (2017) reported an ultrastable zirconium phosphonate framework, $Zr(H_4L)$, as a bifunctional catalyst for CO_2 transformation with a co-catalyst of TBAB for the coupling reaction of styrene oxide and CO_2. The experiment was carried out in the presence of 0.3 mmol of TBAB under CO_2 (1 MPa) at 646 K for 12 h as shown in (Table 2.3, entry 6). Although $Zr(H_4L)$ is a non-porous material, a high yield of 95% for styrene carbonate was achieved by $Zr(H_4L)$, with a remarkable turnover number (TON) of 2850 and turnover frequency (TOF) of 238 h^{-1}. When tested with smaller substrates, such as epibromohydrin and epichlorohydrin, a notable high carbonate yields were recorded within two hours under the same conditions, 97% and 91%, respectively (Li *et al.*, 2012). The Brønsted acid role of PAOH in protonated $[H4L]_{4-}$ anion in $Zr(H_4L)$ was further validated by experimental results, where the organophosphonate ligand HgL was used as the catalyst to achieve a yield of 63% and a lower TON of 1890 in the conversion of styrene oxide as

shown in (Table 2.3, entry 7). The active acidic site could be introduced into the linkers of MOFs by the PSM method. Demir et al. have synthesised a Zr-based MOF, MOF-53, with the same fcu topology of UiO- 67. The functional MOFs, MOF-53-VCl_3, and MOF0-53- VCl_4 were also prepared by post metalation of MOF-53 with vanadium ions for solvent-free cycloaddition reaction of epichlorohydrin with carbon dioxide (Demir *et al.*, 2017a).

In 2015, Liu and research group explored for the first time a novel zeolite-based MIL-101 supported Ag NPs named as Ag@MIL101 catalyst to catalyse cycloaddition reaction of CO_2 with terminal alkynes into propionic acids (Cai *et al.*, 2016). The prepared catalysts, labeled as 1a, 1b, 1c, and 1d, had different Ag loadings of 1.66, 2.58, 4.16, and 6.97 wt%, respectively. They found that all these composite samples had excellent catalytic performance, good reusability and high stability in the carboxylation of terminal alkynes with CO_2 at mild conditions (323 K and 1 atm of CO_2), and catalyst 1c with 0.027 mmol of Ag gave the highest 3-phenylpropiolic acid yield (96.5%). The catalytic activity decreased in the following order: 1c > 1d > 1b > 1a. The findings revealed a promising way of using NPs@MOF catalysts to synthesise carboxylic acids through C-H bond activation of terminal alkynes with CO_2 in synthetic and industrial chemistry.

Table 2. 3. MOFs with acidic linkers (Dual catalytic metal centers)

Entry	MOF	Active site	Metal node	Lingards	substrate	Co-catalyst	T (K)	P_{CO2} (bar)	T (h)	Yield (%)	Ref
1	Ni(Salphen)-MOF	Ni^{2+},Cd^{2+}	$[Cd_2]$	Ni(Salphen)	PO	TBAB	353	20	4	80	Ren et al. (2013a)
2	Ni(Salphen)-MOF	Ni^{2+},Cd^{2+}	$[Cd_4]$	Ni(Salphen)	PO	TBAB	353	20	4	86	Ren et al . (2013b)
3	PCN-224(Co)	Co^{2+}	$[Zr_6O_4(OH)_4(CO_2)_6]$	CoTCPP	PO	TBAC	373	20	4	42	Kim et al. (2013a)
4	MMCF-2	Cu^{2+}	$[Cu_2(CO_2)_4]$	Cu(tactmb)	PO	TBAB	RMT	1	48	95	Gao et al .(2014)
5	MMPF-9	Cu^{2+}	$[Cu_2(CO2)_4]$	(Cu)tdcbpp	ECH	TBAB	298	1	47.5	87	Ma et al. (2015)
6	$Zr(H_4L)$	Zr-OH, P-OH	[ZrAOAPAO] chain	H_gL	SO	TBAB	646	10	12	95	Gao et al. (2017a)
7	$Zr(H_4L)$	Zr-OH, P-OH	[ZrAOAPAO] chain	H_gL	ECH	TBAB	646	10	2	91	Gao et al. (2017b)

2.4.4 MOFs with functional (Lewis base) linkers

In a recent innovative research breakthrough, MOFs with functionalised organic linkers have made the synthesis of organic carbonates possible without the need for a co-catalyst by providing the Lewis basic site. Thus, MOF catalysts with functional groups such as NH_2 and OH, –S=O usually exhibit better catalytic activity compared to their parent MOFs that do not possess Lewis basic functionality. As such, the interaction between Lewis acid sites and Lewis basic sites within these MOFs results in the activation of both epoxide and CO_2, thereby facilitating the intramolecular reaction (North and Pasquale, 2009b). For example, Lescouet et al. (2012) developed amine-functionalised MIL-68(In)-NH_2 containing acid (indium metal nodes) and base (amine) pairs used to catalyse the reaction of styrene oxide to styrene carbonate. Without the use of a co-catalyst, the results show an improved catalytic performance compared with its pristine counterparts, MIL-68. The experimental results conducted by the group under the same reaction condition of 423 K, 8 atm. CO_2 pressure for 8 h (Table 2.4,entry 2), produced a styrene carbonate yields of 71% and 39% for MIL-68(In) NH_2 and MIL-68 respectively (Senthilkumar *et al.*, 2018).

Impressed by the report of Lescouet et al., Xiang and research group in 2017 prepared Amine functionalised UiO-66-NH_2 and compare its catalytic performance with its UiO-66 pristine counterpart. Under the same reaction condition of 373 K and 20 atm CO_2 pressure in chlorobenzene solvent, the group reported a yield of 70% and 48% for both UiO-66-NH_2 and UiO-66, respectively (Table 2.4, entry 6 and 8). In a recent, but separate report, Chao and co-workers used UiO-66-NH_2 (gel) for cycloaddition of styrene oxide in the presence of TBAB as co-catalyst. Although, the use of co-catalyst was not necessary to catalyse this reaction, however, adding TBAB has proven even more efficient conversion of styrene oxide into styrene

carbonate with a yield of 91% under 1 bar and 373 k over 8 h (Xiang *et al.*, 2017).

Sometimes, functional group such as -CONR(H)$_2$ (Xuan *et al.*, 2014), -F (Jia *et al.*, 2017), -NO$_2$, -NH$_2$ (Jia *et al.*, 2017), pyrazole groups and uncoordinated nitrogen atoms (Corey D. P. *et al.*, 2004) are incorporated into the ligands during the preparation of dual active sites (Jia *et al.*, 2017). These groups of MOFs tend to have a synergetic catalytic effect between acid and basic centers that catalyses the cycloaddition of CO_2 and epoxide. For instance, Beyzavi et al. (2015) proposed a tentative reaction mechanism for the CO_2 cycloaddition with epoxide by a catalyst with acid-base pairs. Typically, the epoxides are adsorbed and activated on the Lewis acidic metal nodes (A sites), while the basic organic linkers are used to activate the CO_2.

The presence of NH$_2$ groups in MOF can act as an electron donor (Lewis base) on the CO_2 which increases the CO_2 adsorption capacity (Phillips, 2012). In recent times, several research works have established the ‘‘amino effect” on CO_2 adsorption and activation on various MOFs. This includes such as MIXMOFs (Zalomaeva *et al.*, 2013), ZnW-PYI1, UMCM-1-NH$_2$ (Babu *et al.*, 2015), MIL-68(In)-NH$_2$, UiO- 66-NH$_2$, LCu (Kim *et al.*, 2013a), etc. They also established the MOFs with ANH$_2$ functional linkers usually exhibited better catalytic performance compared with MOFs without Lewis base groups (Vermoortele *et al.*, 2011). This confirms why MOFs with amine-functionalised links show high catalytic activities for cycloaddition of epoxide and CO_2.

Apart from the predesigned functionalised linkers, other catalytic active groups can also be incorporated into the MOF frameworks by post-synthetic

modification techniques or mixed or multivariate-ligand approaches (Zhou *et al.*, 2012). For example, Ma et al. (2015) introduced quaternary ammonium and quaternary phosphorous ionic liquids into MIL-101 by post-synthetic functionalisation to obtain MIL- 101-N-$(n\text{-}Bu)_3Br$ and MIL- 101-$P(n\text{-}Bu)_3Br$ (Table 2.4, entry 3 and 9) to catalyse the reaction of propylene oxide and CO_2 to produce propylene carbonate. At 353 K and 19.7 atm. after 8 h reaction duration in the absence of co-catalyst and a solvent. MIL-101-$P(n\text{-}Bu)_3Br$ and MIL-101-N- $(n\text{-}Bu)_3Br$ produced a PC yield of 98% and 96.1%, respectively (Senthilkumar *et al.*, 2018). Similarly, Li and co-workers also prepared two ILs functionalised bifunctional MOF catalysts, identified as MIL-101-N $(n\text{-}Bu)_3Br$ and MIL-101-$P(n\text{-}Bu)_3Br$, both of which contained two types of catalytic sites: CUS centers and functionalised ILs (Ma *et al.*, 2015). The two catalysts showed excellent catalytic performance for cycloaddition of propylene oxide (PO) and CO_2 to afford a 99% propylene carbonate (PC) yield and 98% PO conversion at a relatively mild reaction condition with a co-catalyst. Ding and Jiang also reported the use of immobilised imidazolium-based poly(ionic liquid)s. The resultant polyILs@MIL-101 composite contains both Lewis acid (in the MOF) and Lewis base active sites which both displayed excellent yield of organic carbonate in a cycloaddition reaction.

In another notable discovery, Liang and group synthesised a bifunctional decorated Zr-MOF, named (I^-)Meim-UiO-66 *via* isorecticular synthesis and a post-synthetic modification method (Liang *et al.*, 2017). The catalytic efficiency test of synthesised MOF was carried out over a wide range of substrates at 393 K under 1 atm. CO_2 pressure. ECH has the highest conversion with 100% ECHC yield. This was followed by 2-(allyloxymethyl) oxirane with a yield of 92%, while other substrates were reported to give moderate to low epoxide conversion (Arnold *et al.*, 2001). They further examined the catalytic performance of the nanoparticles (NPs) and

nanosphere (NS) of the MOF material for the cycloaddition of CO_2 with epichlorohydrin under similar experimental conditions. The nanoparticles (NPs) of the MOF material were found to exhibit higher efficient catalytic performance with a yield of 93% than nanosphere (NS) of MOF material with a yield of 59%, for the cycloaddition of epichlorohydrin with CO_2. The enhanced catalytic activity of the NPs form of the MOF was reported to indicate that the small nanoparticles with larger surface areas could provide many more active sites, thus enhanced the efficiency of cycloaddition reactions (Table 2.4, entry 1 and 7).

Cho et al. (2012) reported a rare example of porous bimetallic-based metal-organic frameworks called M-MOF-74 (Mg or Co). This was found to be a highly efficient heterogeneous catalyst for the coupling reaction of CO_2 to styrene oxide without the use of co-catalyst. M-MOF-74 (Mg or Co) was constructed by $[M_{2x}(OH_2)_{2x}(CO_2)x]$ chain SBUs and 2,5-dihydroxyterephthalate (DHBDC) linkers (Yang *et al.*, 2012). Although most MOF catalysts with strong acidic sites require a co-catalyst, MMOF- 74 was shown to exhibit high activity without basic additives. It was postulated that the five oxygen atoms from the organic linkers located around magnesium atoms acted as a base with low basicity, whereas the open metal atoms function as a Lewis acid site. Optimal yield of 95% for styrene carbonate was obtained when the reaction was conducted over 4 h at 373 K and 20 bar CO_2 pressure conditions over Mg-MOF-74 in chlorobenzene Yang *et al.*, (2012). M-MOF-74 showed no decrease in catalytic activity after three repeated runs and the structural integrity of M-MOF-74 remained. It was also observed that the reaction rates were not affected by pore diffusion under the given set of reaction conditions, perhaps due to the 1-D hexagonal channels of 1.1 nm diameter in the framework (Table 2.4, entry 4 and 5).

Table 2. 4. MOFs with functional (Lewis base) linkers

Entry	MOF	Active site	Metal node	Lingards	substrate	Co-catalyst	T (K)	P_{CO2} (bar)	T (h)	Yield (%)	Ref
1	UiO-67-IL	$ZrOH/OH_2I^-$	$[Zr6O4(OH)_4(CO_2)_{12}$	(I^-)Mein-BDC	ECH		363	1	8	95	Ding et al. (2007)
2	MIL-68(In)-NH_2	BDC-NH_2	$[In\text{-}OH\text{-}In]_n$chain	BDC-NH_2	SO	DMF	423	8	8	74	Lescouet et al. (2012)
3	MIL- 101-N-$(n\text{-}Bu)_3Br$	$Cr(II),Br^-$	$[Cr_3O(CO_2)_6]$	BDC-N-$(n\text{-}Bu)_3Br$	PO	-	353	20	8	99	Zhou et al. (2012)
4	Mg-MOF-74	Mg (II)	Mg(II)	H_4DHBDC	SO	-	373	20	4	95	Cho et al. (2012)
5	Co-MOF-74	Co(II)	Co(II)	H_4DHBDC	SO	-	373	20	4	96	Yang et al. (2012)
6	UiO-66-NH_2(gel)	NH2-BDCZr-OH/OH_2	$[Zr_6O_4(OH)_4(O_2)_{12}]$	NH_2-BDC	SO	TBAB	373	1	8	91	Xiang et al. (2017)
7	(I-)Mein-UiO-66	$ZrOH/OH_2I^-$	$[Zr6O4(OH)_4(CO_2)_{12\text{-}x}]$	(I^-)Mein-BDC	ECH	-	393	1	24	93	Liang et al. (2017b)
8	UiO-66-NH_2	NH2-BDCZr-OH/OH_2	$[Zr_6O_4(OH)_4(O_2)_{12}]$		SO	TBAB	373	1	8	91	Xiang et al. (2018a)
9	MIL- 101-P$(n\text{-}Bu)_3Br$	$Cr(II),Br^-$	$[Cr_3O(CO_2)_6]$	BDC-N-$(n\text{-}Bu)_3Br$	PO	-	353	20	8	98	Senthilkumar et al.. (2018)

2.4.5 MOFs with ionic linkers

In addition to the aforementioned categories of MOFs containing active sites, the use of ionic linkers such as tetraalkylammonium halides under mild reaction conditions have been recommended by many research groups according to Liang et al. (2019b). These have been found to make the catalytic systems optimally effective. Thus, the Lewis acid sites can work synergistically with a homogenous nucleophilic co-catalyst to assist the epoxide in changing into a haloalkoxide during the reaction. In the last five years, only a few MOFs with ionic groups (e.g. quaternary ammonium salts, imidazolium salts) have been used for the coupling reaction of CO_2 and epoxide. In general, the post-synthesis modification (PSM) method was proved to be helpful to obtain ionic MOFs, including F-IRMOF-3, IL-ZIF-90, MIL-101-N- $(n\text{-}Bu)_3Br$, MIL-101-P$(n\text{-}Bu)_3Br$ and (I^-)Meim-UiO-66.

Zhou et al. (2012) reported the catalytic performance of isorecticular functionalised metal-organic framework-3 (IRMOF-3) as an efficient heterogeneous catalyst for the synthesis of cyclic carbonates without co-catalyst and solvent. The catalyst was synthesised at room temperature by reacting methyl iodide with activated IRMOF-3 [$Zn_4O(NH_2\text{-}BDC)_3$] in the presence of N,N-dimethylformamide (DMF) solution. Although the catalyst has a low BET surface area, however, it was able to catalyse the reaction of PO and CO_2 into PC under 20 bar of CO_2 at 313 K over 1.5 h, achieving a yield of 98% (Table 2.5, entry 2). In addition, F-IRMOF-3-4d showed good reusability without any significant loss of activity, although atmospheric water should be separated from this system to retain the structure of F-IRMOF-3. The typical reaction mechanism was proposed as that C-O bond in epoxide is polarised by coordinating with Zn_4O or --NH_2 in FIRMOF-3, while I^- attacks the less sterically hindered carbon atom to open the epoxide ring. Then the halo-alkoxide conducts a nucleophilic reaction with CO_2

to form an alkylcarbonate anion, which is further converted to the targeted cyclic carbonates.

In one of the most recent discoveries, Liang et al. (2017) reported a bifunctional imidazolium functionalised Zr-MOF, called (I^-)Meim-UiO-66 by post-synthetic ionisation (PSI) of a new microporous imidazole functionalised MOF (Liang *et al.*, 2017). The presence of the Brønsted-acid (Zr-OH/OH_2) sites and nucleophilic iodide ions in this framework, (I^-)Meim-UiO-66 enhanced its catalytic efficiency and recyclability as a stable heterogeneous catalyst for the chemical CO_2 fixation into cyclic organic carbonates without the use any co-catalyst/solvent at ambient pressure. (I^-) Meim-UiO-66 exhibited highly efficient catalytic performance in the cycloaddition of epichlorohydrin and CO_2 into cyclic carbonate over 24 h at 393 K under 1 atm CO_2 pressure with a yield of 93%, which was superior to other MOFs, UiO-66 (trace), UiO-NH_2 (6.4%) and its counterpart with much larger particles (I^-)Meim-UiO-66 (NS) (59%) as shown in (Table 2.5, entry 5). It was rationalised that the small nanoparticles (20–30 nm) of (I^-) Meim-UiO-66 with the larger surface area could provide more active sites to improve the efficiency of heterogeneous catalysis. Additionally, (I^-)Meim-UiO-66 retained the good performance in several recycled experiments despite that the BET surface decreased from 328 m^2/g to 109 m^2/g (Liang *et al.*, 2019c).

Earlier in 2015, a zeolitic imidazolate framework (ZIF-90) was post-functionalised to form F-ZIF-90 using hydrazine followed by quaternisation (Jose *et al.*, 2015). Quaternised catalyst F-ZIF-90 showed a much higher yield than the unfunctionalised ZIF-90 for the synthesis of allyl glycidyl carbonate (96.6% vs 43.4%). A high yield of 94% in the formation of epichlorohydrin carbonate was also achieved over 6 h at 393 K and 11.7 bar of CO_2 pressure, without a co-catalyst and solvent as shown in (Table 2.5, entry 3). However, F-ZIF-90 partially lost its structural features and superior catalytic performance during the recycled

test. Similar trends were observed where ZIF-8 was used as a catalyst in the cycloaddition of CO_2 to epichlorohydrin as discussed earlier. Thus, temperature and CO_2 pressure should be carefully considered when ZIF type catalysts are used in the chemical CO_2 fixation process. Later, the same group reported another pyridinium based ionic liquid (IL) functionalised ZIF-90, IL-ZIF-90, utilising post-synthetic amine condensation (Tharun *et al.*, 2016). IL-ZIF-90 also showed enhanced catalytic activities than ZIF-90 in the formation of PC under the same conditions, with a yield of 95% and 49%, respectively as shown in (Table 2.5, entry 4). Despite that IL-ZIF-90 possessed a low BET surface area of 153 m^2/g, IL-ZIF-90 was found to be effective for a variety of terminal epoxides (Tharun *et al.*, 2016).

In 2017, Ding and research group reported another imidazolium-based ionic liquid decorated Zr-MOF, called UiO-67-IL, which was directly constructed from the imidazolium-based ligand and Zr(IV) ions. UiO-67-IL can be used as a highly heterogeneous catalyst for the conversion of epoxides into cyclic carbonates without the use of co-catalyst under 1 bar CO_2 pressure. In a typical reaction, epichlorohydrin was converted into chloropropene carbonate in a 95% yield by UiO-67-IL over 12 h at 363 K under 1 bar CO_2 without adding a co-catalyst (Kuruppathparambil *et al.*, 2016a). In contrast, the poor catalytic activity of pure UiO-67 was observed with only 8% yield after 14 h. When UiO-67-TBAB together was used as the catalytic system, a maximal yield of 98% was reached over 14 h, thus indicating the significant role of embedded imidazolium group in UiO-67-IL. Epoxides with larger groups, such as styrene oxide, and glycidyl phenyl ether, led to decrease yield with 51% and 52%, respectively when only UiO-67-IL has used the catalyst as shown in (Table 2.5, entry 6). However, the yield could be greatly improved by up to 99% by adding TBAB as a co-catalyst. The long-chain substituted epoxide 1,2-epoxydecane led to poor yield (6%), which was attributed to weak interactions between the framework and substrate (Liang *et al.*, 2019b).

Table 2. 5. MOFs with ionic linkers for the coupling reaction of CO_2 and epoxides

Entry	MOF	Active site	Metal node	Lingards	substrate	Co-catalyst	T (K)	P_{CO2} (bar)	T (h)	Yield (%)	Ref
1	F-IRMOF-3	Zn^{2+} and I^-	$[Zn_4O]$	BDC-$NH_4(Me)_{3-x}(i^-)$	PO	-	413	20	1.5	98	Zhou et al. (2012)
2	F-ZIF-90	Zn^{2+} and I^-	Zn^{2+}	ICA,F-ICA	ECH	-	393	1	8	95	Jose et al. (2015)
3	IL-ZIF-90	Zn^{2+} and I^-	Zn^{2+}	IL	PO	-	393	10	3	95	Tharum et al. (2016)
4	(I^-)Meim-UiO-66	$ZrOH/OH_2,I^-$	$[Zr_6O_4(OH)(CO_2)_{12-x}]$	In-BDC,(I^-) Meim-BDC	ECH	-	393	1	24	93	Liang et al ,. 2019
5	UiO-67-IL	$ZrOH/OH_2,Br^-$	$[Zr_6O_4(OH)(CO_2)_{12}]$	(Br^-)Allylin-2-bp	ECH	TBAB	363	1	14	98	Kuruppthaprambil et al. (2019b)

2.5 Recent progress in the catalytic activity of MOFs for CO_2 fixation to cyclic organic carbonate.

In recent years, significant advancements have been made to address the general reactivity and selectivity issues that are associated with metal-organic frameworks (MOFs) catalysts for the synthesis of cyclic organic carbonates. In this section, highlights will be made to the most important progress made and the opportunities that catalysis can bring about when the synthesis of these intermediates is optimised to a higher level of sophistication taking into account the challenging nature of the substrates that were involved. This section will discuss the scope and limitations of each strategy.

2.5.1 Catalytic activity of pristine MOFs

As discussed in the previous sub-sections, most MOF catalysts need modifications or the use of solvent or co-catalyst in order to activate epoxides for optimal effectiveness during cycloaddition reactions. However, a limited number of MOFs have been reported to be active on their own in converting CO_2 to epoxide. Although, this may require high temperature and pressure for the reaction to proceed. Thus, the activity of such catalysts and their cycloaddition selectivity and characteristics are discussed below.

MacIas et al. (2012) used a highly porous self–sustaining heterogeneous MOF $Cu_3(BTC)_2$ for the coupling reaction of CO_2-ECH to synthesise chloroprene carbonate. The reactions were performed in a high-pressure stainless-steel reactor under reaction conditions of 343 -373 K and 0.7 MPa CO_2 for 4 h without the use of any solvent or co-catalyst (Table 2.6, entry 7). They recorded a low conversion of epichlorohydrin, yield and selectivity of chloroprene carbonate of 63.8%, 51.8% and 33%, respectively. However, they have attributed the low results to significant formation of by-products such as diols of the epoxides and dimers of epichlorohydrin, especially at

low temperatures below 373 K due to the presence of a hydrophilic interior (with 12 water molecules per pore) in the catalyst. According to Zhao et al. (2015), the Cu^{2+} ions in the binuclear Cu^{2+} cluster of $Cu_3(BTC)_2$ are believed to be connected through a weak bond, and the residual axial coordination site is filled by a weakly bound water molecule. These weakly bound water molecules, which point towards the center of the pore, were suggested to be active centers in the hydration of the epoxide to the diol. Babu et al. (2015) explored a rare mixed-linker nanoporous polymer $Zn_2(HIP)_2(bipy)(H_2O)_2.2H_2O$ (ZnHipBipy) as an efficient catalyst to investigate the reaction of CO_2 to epoxide without the use of any solvent or co-catalyst. In a typical synthesis, allyl glycidyl ether (AGE) was converted to allyl glycidyl carbonate (AGC) under reaction conditions of 393 K and 1.2 MPa with a reaction time of 6 h (Table 2.6, entry 3). The single-crystal (ZinHipBipy-A) and bulk (ZnHipBipy-B) samples gave AGC yields of 34 and 41 %, respectively. However, their selectivities were approximately 68.4 and 64.1 %, respectively, and diol was produced as a side product.

2.5.2 Enhanced catalytic activity by solvents or co-catalysts

Ionic Liquids (ILs) are defined as those ionic salts which have a melting point below 373 K and are formed by positive and negative ions (Cota *et al*., 2017). In subsection 2.4.5 the catalytic effect of ionic liquids in ring-opening of epoxides for cycloaddition reactions has been discussed in substantial detail. However, ionic liquids are widely used as co-catalysts in MOF-catalysed cycloadditions because they allow MOFs to become fully functionalised while maintaining their high selectivity for cyclic carbonates and help to overcome the difficulty of separating diol/dimer side products from the final reaction mixture (Miralda *et al.*, 2012b).

For example Song et al. (2009) examined the catalytic performance of MOF-5 at a mild reaction condition using various epoxide substrates to synthesise several cyclic carbonates. In the absence of ionic co-catalyst such as quaternary ammonium salts (Me_4NCl, Me_4NBr, Et_4NBr, n-Pr_4NBr, and n-Bu_4NBr), the catalyst did not show much catalytic activity. However, a series of experiments were performed to examine the catalytic efficiency of 5/n-Bu_4NBr catalytic systems in the cycloaddition of CO_2 with propylene oxide to give propylene carbonate under various reaction conditions. The results obtained were promising with high PO conversion and a good yield of PC. When the catalyst was used with quaternary ammonium halide salt, an impressive 97.6 % yield was achieved at a low temperature of 323 K and CO_2 pressure with a range of 0.4–6.0 MPa. The PC yield was further increased when the length of the alkyl chains of the ammonium salts was increased. Using styrene oxide as a substrate, a longer reaction time of 7 h was needed for the reaction to reach 95 % under similar reaction conditions, which was attributed to the low reactivity of its b-carbon center. Cyclohexene oxide was the least active substrate, probably because of its high steric hindrance.

Among the various MOF-74 catalysts, Shi et al. (2003) reported that Co-MOF-74(M) showed a very high yield (96%) with chlorobenzene as the solvent and no ionic liquid co-catalyst. Furthermore, Co-MOF-74(M) showed selectivity near 100 % at 2.0 MPa and 373 K after 4h. Similar to Co-MOF-74, Mg-MOF-74(S) showed excellent catalytic performance in the cycloaddition of CO_2 to styrene oxide under mild reaction conditions of 2.0 MPa at 373 K without any co-catalyst and in the presence of chlorobenzene solvent, producing a 95 % yield of styrene carbonate (Kathalikkattil *et al.*, 2015).

The catalytic activity of MIL-125 and NH_2-MIL-125 for the cycloaddition of CO_2 to epichlorohydrin to give chloropropene carbonate using chlorobenzene as a solvent were investigated by Bhattacharjee et al. (2014). The NH_2-MIL-125 showed a higher chloropropene yield (95%) than MIL-125 (chloropropene yield: 64%) under reaction conditions of 373 K and 2.0 MPa with a reaction time of 6 h. NH_2-MIL-125 showed higher a concentration of basic sites as measured by the number of NH_2 groups than MIL-125. Acid-base analysis of the materials explained the higher cycloaddition activity of NH_2-MIL-125. The catalytic performances of MIL-68(In) and (MIL-68(In)-NH_2) catalysts were tested for the cycloaddition reaction of CO_2 to styrene oxide under conditions of 423 K and 0.8 MPa CO_2 with a reaction time of 8 h. MIL-68(In)-NH_2 showed better styrene oxide conversion (71(±3) %) than MIL-68(In) (39(±3) %) using DMF as a solvent (Büttner *et al.*, 2017).

Similarly, the catalytic activity of the UIO-66 MOFs was compared for the cycloaddition of CO_2 to styrene oxide using chlorobenzene as a solvent under reaction conditions of 373 K and 2 MPa with a reaction time of 4 h. The catalytic activities of these MOFs are in the following order: UiO-66-NH_2, UiO-66>Mg-MOF-74>MIL-101>CuBTC>IRMOF-3>ZIF-8 >MOF-5 (Senthilkumar *et al.*, 2018). UiO-66-NH_2 showed a high styrene oxide conversion (70%) under reaction conditions of 373 K and 2.0 MPa with a reaction time of 1h using chlorobenzene as a solvent. The presence of both Lewis acid and base sites inside the framework of UiO-66 could be the reason for its enhanced activity. The catalytic activity of the gea-mof-1 was also examined by Eddaoudi and co-workers (Kathalikkattil *et al.*, 2015) for various epoxides. This catalyst showed a propylene oxide conversion of 88 % under reaction conditions of 393 K and 2 MPa with a reaction time of 6 h.

2.5.3 Enhanced catalytic activity by nanocarbon-based catalysts

Carbon nanotubes possess high chemical and thermal stability, surface area, and tensile strength, and they are recently finding application in catalysis. Wang et al. (2014) employed oxidised multi-walled carbon nanotubes (MWCNTs) as support for immobilising a series of imidazolium-based ionic liquids with different anions and alkyl chains through the esterification of the carboxylic groups present on the nanotubes (Shi *et al.*, 2018).

Han et al. (2012) synthesised an MWCNTs coated with polyimidazolium bromide polymers. They have reacted 5,10,15,20-tetrakis(4-pyridyl)porphyrin zinc(II) 1,4-bis(bromomethyl)benzene(Bobadilla *et al.*, 2015a), and di(1H-imidazol-1-yl)methane (Srivastava *et al.*, 2005) in the presence of CNTs to form a catalyst with a nucleophile bromide anions. The bifunctional materials showed enhanced catalytic activity for coupling reaction of CO_2 and epoxide compared to its corresponding homogeneous counterpart, affording a TOF of up to 2602 h^{-1} with a substrate/catalyst ratio of 7100. The catalyst maintained its catalytic activity after seven recycles with no significant loss of activity and no sign of leaching was observed.

Graphene oxide (GO) represents an ideal support material for catalysts, for example, its 2D structure, which confers a high surface area. Moreover, once functionalised, GO may provide access to all the catalytic centers, avoiding mass transfer problems of the substrates. In addition, the presence in its structure of several oxygen-containing groups (–OH, –COOH, etc.) leads to a synergistic effect activating the CO_2 chemical fixation process by means of the instauration of hydrogen bonds with epoxide substrates. This fact was clearly demonstrated by Qu and co-workers, who used

commercially available GO as a carbocatalyst (in the presence of DMF) for cyclic carbonate synthesis. They found a direct correlation between the number of oxygenated groups and the catalytic activity of GO. For example, Calabrese et al. (2019) reported the preparation of a series of imidazolium-based IL grafted onto the surface of GO for the synthesis of PO. In the presence of hydroxy groups co-catalyst, the hybrid iodide counteranions catalyst gave a higher conversion of PO to the corresponding PC at 2 MPa pressure of CO_2 at 413 K for 4 h. Higher conversions of propylene oxide into the corresponding carbonate were obtained with 0.35 mol.% catalyst at 413 K in 4 h. The catalyst maintained high stability with up to seven times without loss of activity.

Table 2. 6. Comparison of the catalytic activity of pristine MOFs for coupling reaction of CO_2 and epoxides

Entry	MOF	Substrate	Cat. mol%	T (K)	P_{CO2} (MPa)	T(h)	TON	Yield (%)	Ref
1	ZIF-8	SO	0.7	373	0.7	5	79	55.0	Miralda et al. (2012)
2	ZIF-8	ECH	0.44	373	0.7	4	75	32.8	Carmen et al. (2012)
3	$Cu_3(BTC)_2$	ECH	2.75	373	0.7	4	12	33.0	Maclas et al. (2012)
4	ZIF-68	SO	4.81	393	1	12	21	99.1	Yang et al. (2014)
3	ZIF-90	AGE	0.43	393	1.17	6	101	43.4	Tharun et al. (2015)
4	CHB	AGE	1.6	393	1.2	6	55	87.4	Tharun et al. (2015)
5	ZnHipBipy-B	AGE	1.6	393	1.2	6	25	40.7	Babu et al.(2015)

2.6 Design of highly efficient and stable Zr/ZIF-8 catalyst for the greener synthesis of organic carbonates

Developing greener and stable catalytic systems for the effective transformation of CO_2 to organic carbonates has been a major highlight in many recent CO_2 management campaigns. In the foregoing section, the catalytic performance of Zr/ZIF-8 has been benchmarked against other reported ZIF based heterogeneous catalysts (due to similar sodalite topology) in order to achieve a fair and consistent benchmark assessment.

Recently, the stability of MOFs for large-scale industrial applications have been questioned in many literature (Bai *et al.*, 2016; Cavka *et al.*, 2008a; Jeong *et al.*, 2017; Marshall and Forgan, 2016; Yang *et al.*, 2018; Zhang *et al.*, 2016). This is due to their weak thermal, chemical and mechanical stability partly because of the structure of inorganic bricks and the nature of the chemical bonds it forms with the linker (Cavka *et al.*, 2008a). In order to improve this weak thermal functionality and to gain in-depth knowledge of their catalytic activity, Cavka et al. (2008) became the first group to synthesise Zr-based MOFs designated as zirconium 1,4-dicarboxybenzene, UiO-66 for photocatalysis (Jin and Yang, 2017). The test conducted by the group found that the increased stability of the Zr-based MOFs is owing to the Zr-O bonds formed between the cluster and carboxylate ligands (Cavka *et al.*, 2008b). Several other groups have thereafter explored this opportunity, which has seen increased in the application of Zr-based MOFs in many research activities. Demir et al. (2017b) utilised UiO (University of Oslo) type zirconium metal-organic frameworks in a solvent-free coupling reaction of ECH and CO_2 for the synthesis of epichlorohydrin carbonate (ECHC). The result of their experiments has seen an increase in the use of Zr-MOFs for the synthesis of organic carbonates.

From our experiments, the synthesis of Zr-doped MOF (Zr/ZIF-8) for the cycloaddition reaction of CO_2 and epoxide has demonstrated reasonable thermal stability under relatively mild reaction conditions without the use of solvent or co-catalyst. Although the synthesis of several Zr-based MOFs has been reported in recent times (albeit in early stages), only a few were employed for catalytic studies even more rarely for the synthesis of organic carbonates from CO_2 and epoxide. Zirconium-based MOFs (Zr-MOFs) have exhibited increased structural tolerability due to the presence of organic linkers (Karagiaridi *et al.*, 2012).

Zirconium based MOFs have demonstrated proof-of-concept applications in several areas such as toxic analyte, catalysis, gas storage, *vivo* drug delivery and therapeutic treatment, biosensing (Rimoldi *et al.*, 2017). In this research, a novel Zr/ZIF-8 has been successfully synthesised using the conventional solvothermal method. The prepared catalyst has been accessed as an innovative greener and sustainable heterogeneous catalyst for the direct synthesis of chloromethyl ethylene carbonate and from carbon dioxide and epichlorohydrin. The effect of various reaction parameters has been investigated and critically analysed. These include the effect of reaction temperature, CO_2 pressure, catalyst loading and reaction time. Catalyst reusability studies of Zr/ZIF-8 was also investigated to establish its stability and reusability for the synthesis of CMEC.

2.6.1 Zeolitic imidazolate framework-8 catalyst (ZIF-8)

Zeolitic imidazolate frameworks (ZIF) is a subclass of MOFs with emerging functional porous materials. ZIF-8 was first of the ZIF based catalysts to be used for CO_2-epoxide (Chen, 2016). In early 2013, Miralda and the research group reported the use of ZIF-8 catalysts for the cycloaddition of CO_2 and epichlorohydrin to form chloropropene carbonate in the absence of solvent

or co-catalyst. It was agreed that the co-existence of the Lewis acidic Zn center and the N basic moieties in the ZIF framework was responsible for its catalytic activities for the coupling reaction of CO_2 and epoxide (Hwang *et al.*, 2016). ZIF-8 has well-defined pore structures of diameter 11.6 Å, accessible through apertures of 3.4 Å suitable for hosting catalytically active guest species(Zhu *et al.*, 2013).

2.6.2 Zirconium (dopant)

Our idea of choosing zirconium (Zr^{4+}) as a suitable dopant for this catalytic system was in agreement with the experiments of Cavka et al. (2008b). Since Zr^{4+} has a comparable ionic size to zinc (Zn^{2+}) (i.e., 0.745 Å for Zr and 0.740 Å for Zn), Duan et al. (2011) and Gurav et al. (2013), believes this relationship will help minimise lattice distortion during the ion-exchange process. Zr^{4+} also has the ability to act as a dual donor (Ge, 2012), providing up to two extra free electrons per ion when substituted for Zn^{2+}(Jeong *et al.*, 2017)**.** According to Jin and Yang, (2017), zirconium is well known as an effective promoter of metal-based catalysts. It can also act as a phase stabiliser to increase the dispersion and stability of the active metal through strong metal-support interactions (Herodotou, 2015).

2.6.3 Benchmark evaluation of the catalytic performance of Zr/ZIF-8 with other ZIF based heterogeneous catalysts the for coupling reaction of CO_2 and epoxides

According to Liang et al. (2019b), benchmarking in heterogeneous catalysis is considered as cutting edge evaluation tool that sort to compare the performance of a new catalyst formulation against that of an accepted standard catalyst, under standard reaction conditions. Because evaluation by benchmarking is ideally transparent and replicable, it promotes research conduct that is collaborative, open, and ethical, thereby promoting

community-building (MacGillivray, 2010). Thus, it may be necessary to set a scope for benchmarking, even, if the primary objective is a mere comparison within a narrow class of catalytic materials (e.g. zeolitic imidazolate framework (ZIFs), or on different solid supports). This scope may include among others; selectivity, yield, conversion, TOF (turnover frequency), reusability, etc. Nonetheless, it becomes a great challenge when comparing huge disparity in different catalytic materials (e.g. MOFs catalysts vs metal oxides catalysts) due to vast differences in their operating conditions, or for optimising more than one performance metric. Therefore, the following benchmarking specifications have been set for this particular research work: Epichlorohydrin (ECH) has been chosen as the model substrate, only solvent-free/co-catalyst free carbonate synthesis has been considered at their optimum reaction conditions.

In chapter 4, we reported the catalytic performance of Zr/ZIF-8 from CO_2 and ECH. The catalyst displayed high epoxide conversion and high selectivity towards chloromethyl ethylene carbonate (CMEC) at 353 K. No co-catalysts or solvents were required for the reaction to proceed and activity of the reused catalyst showed consistent stability over seven subsequent use. The optimum reaction conditions for the experiments were found at 353 K, 8 bar of CO_2 pressure and 8 h using fresh 10% (w/w) of catalyst loading to achieve a conversion of ECH, selectivity and the yield of CMEC at 93%, 86% and 76%, respectively.

Recently, Liang et al. (2019) prepared a dual-ligand zeolitic imidazolate framework named as ZIF-8-90 to catalyse the reaction of ECH and CO_2 (Table 2.7, entry 9). A slightly higher temperature and pressure were recorded to achieve the result and the catalyst was only recycled three times before it lost its catalytic activity (Xiang *et al.*, 2019). While comparably, Zr/ZIF-8 was used up to seven consecutive runs without any significant loss of activity (Figures. 4.15 and 6.7: catalyst reusability studies). Although, the

group reported that no cocatalyst or solvent was used for the reaction to proceed. Similarly, in 2015, Jose and research group developed a functionalised F-ZIF-90 catalyst for coupling reaction of ECH and CO_2 as shown in (Table 2.7, entry 2), Zr/ZIF-8 exhibited higher TOF than most of the ZIF-based catalysts except F-ZIF-90, which was functionalised with quaternary ammonium groups (Jose *et al.*, 2015). The quaternary ammonium salts are commonly used as co-catalysts for cycloaddition of CO_2 to epoxides. However, in the present work, the use of co-catalyst and solvents were not required to activate the epoxide.

Very recently, Tharun and the research team explored the application of a rare one-component ionic liquid supported ZIF-90 (IL-ZIF-90) to synthesise chloropropene carbonate from CO_2 and ECH. Although, the catalyst afforded higher conversion and selectivity to chloropropene carbonate, but only after functionalisation with IL. In addition to that, the coupling reaction of CO_2 and ECH was performed at higher temperatures and pressure compared to Zr/ZIF-8 (Table 2.7, entry 3 and 7). The catalyst lost its stability only after four runs (Tharun *et al.*, 2016). It is noteworthy that functionalisation of ZIF-90 required additional steps to achieve the claimed results, this may have a knock-on effect on the overall production cost of the catalyst, whereas, Zr/ZIF-8 was synthesised *via* a simple traditional low-cost solvothermal method without functionalisation or any requirements for further purification steps. Kuruppathparambil et al. (2016) designed and synthesised a bimetallic heterogeneous catalyst composed of Co and Zn as active centers and 2-methylimidazole as a linker. CZ-ZIF possessed a sodalite topology, similar to the parent materials, ZIF-8 and ZIF-67 (table 2.7, entry 5). The catalyst was used to investigate the coupling reaction of ECH and CO_2. CZ-ZIF acts highly synergistically with the TBAB co-catalyst to change the pathway of the ECH–CO_2 reaction so that it may proceed at low temperatures.

Considering that economic feasibility and environmental benignity are crucial features of a catalytic system, the Zr/ZIF-8 possesses transparent advantages over other aforementioned ZIF catalysts discussed in this section. As previously mentioned, Zr/ZIF-8 is synthesisable with a low-cost simple traditional solvothermal method, most of the catalysts discussed in Table 2.7 require the use of either organic solvents, co-catalyst or the addition of extra bases, and higher temperatures or functionalisation. Thus, the ease, convenience, greener credentials, and energy efficiency of the Zr/ZIF-8 synthetic system impart have enhanced its sustainability. One major reason for using heterogeneous catalysts, despite their often lower activity profiles compared to their homogeneous counterparts, is their reusability. Hence, the reusability of the synthesised Zr/ZF-8 materials was also investigated with reference to the high thermal integrity of the doping material (zirconium). Zr/ZIF-8 exhibits very high reusability even after seven recycle tests, maintaining almost equal conversion rates to that of the fresh catalyst. The powder X-ray diffraction (XRD) pattern of the fresh Zr/ZIF-8 is similar to that of the reused catalyst under the reaction conditions employed (353 K, 8 bar, and 8 h) (Figure. 3.3). This is a promising result when considering that many of the ZIFs reported in the literature do not exhibit acceptable reusability profiles, even though they exhibit high catalytic activity when used fresh. Should the CO_2 transformation be applied on a large scale using ZIF based catalysts, this increased stability will be highly advantageous. Some other parameters, such as the amount of CO_2 adsorption on the surface of the catalyst, defects on the structure, and the size and volume of pores, may affect the reactivity and selectivity to desired carbonate products (Xiang *et al.*, 2019). Other ZIFs applied for the cycloaddition reaction of carbon dioxide are ZIF-67 (Table 2.7, entry 4) (Roshan *et al.*, 2016) and ZIF-95 (Table 2.7, entry 8) (Bhin *et al.*, 2017) all of which have been reported recently. Although, these ZIFs do not require

a co-solvent or a co-catalyst but require high temperature and pressure to achieve the required results.

Table 2. 7. Benchmark evaluation of the catalytic performance of Zr/ZIF-8 with other ZIF based heterogeneous for coupling reaction of CO_2 and epoxides

Entry	Catalyst	Reaction conditions T/P/t (K/bar/h)	Conversion (%)	Selectivity (%)	TOF (h^{-1})	Ref.
1	F-ZIF-8	373/7/4	100	49	18	Miralda et al. (2011)
2	F-ZIF-90	393/12/6	95	99	96	Jose et al. (2015)
3	IL-ZIF-90	393/10/3	94	88	31	Tharun et al. (2015)
4	ZIF-67	373/7/6	76	99	38	Jose et al. (2015)
5	CZ-ZIF	373/7/4	98	96	33	Kuruppathparambi et al. (2016)
6	ZIF-8	373/7/4	98	33	12	Kuruppathparambi et al (2016)
7	ZIF-90	393/12/8	89	91	16	Xiang et al. (2016)
8	ZIF-95	353/12/2	77	99	38	Tharun et al, (2017)
9	ZIF-8-90	373/20/4	96	99	80	Liang et al. (2019a)
10	Zr-ZIF-8	353/8/8	93	86	76	This work

2.7 Conclusions

The synthesis of cyclic carbonates for CO_2 and epoxides using various MOF catalysts have been elaborated extensively. Although, there is a need for more work to be done to obtain a better and more suitable Zr/Zn doping ratio in order to improve the catalytic activity of the novel catalyst. From the benchmark evaluation analysis, it can be concluded that the Zr/ZIF-8 catalyst has demonstrated to be a promising catalyst for effective CO_2 fixation. Table 2.7 has clearly shown that the catalyst lies within a competitive range among other reported ZIF based catalysts for cycloaddition of CO_2. The catalyst has shown a good substrate tolerance as demonstrated by its activity towards different epoxides including epichlorohydrin, styrene oxide and butylene oxide. More importantly, the reaction has been carried out under solvent-free and co-catalyst conditions. The heterogeneity nature of the catalyst has been proven by recovering and reusing the catalyst for up seven times without any significant loss in catalytic activity.

Chapter 3

Catalyst preparation and characterisation

Outline of the chapter

This chapter gives a detailed description of a greener synthesis of Zr/ZIF-8 catalyst *via* a simple low cost traditional solvothermal method. It also describes a detailed systematic characterisation of both pristine ZIF-8 and as-prepared Zr/ZIF-8 catalysts using multiple physicochemical characterisation techniques.

The chapter is organised as follows:

3.1. Introduction

3.2. Materials and methods

3.3. Synthesis of Zr/ZIF-8 catalyst

3.4. Catalyst characterisation

3.5. Conclusions

3 Catalyst preparation and characterisation

3.1 Introduction

This chapter discusses the greener synthesis and characterisation of a novel Zr/ZIF-8 catalyst *via* a simple low-cost solvothermal method. Zr/ZIF-8 catalyst has been successfully designed and assessed as a stable and highly efficient CO_2-reduction catalyst for the synthesis of organic carbonates. The characterisation of both pristine ZIF-8 and as-prepared Zr/ZIF-8 catalysts include multiple physicochemical techniques such as X-ray diffraction (XRD), transmission electron microscopy (TEM), scanning electron microscope (SEM), Brunauer–Emmett–Teller (BET), X-ray photoelectron spectroscopy (XPS), Thermal gravimetric Analysis (TGA), Fourier transform infrared (FTIR) and Raman spectroscopy (RM). Although ZIF-8 catalyst has been criticised by many researchers as thermally unstable for the cycloaddition reaction of epoxide and CO_2. However, several experiments carried out in this research work have indicated that incorporating zirconium into ZIF-8 could strengthen the weak functionality, thereby enhancing its tenability for large-scale industrial applications. It may also be worth mentioning that this research work has utilised a 10% dopant of zirconium for such a tremendous and improved catalytic activity of Zr/ZIF-8.

3.2 Chemicals and materials

Zinc nitrate hexahydrate ($Zn(NO_3)_2{\cdot}6H_2O$, purity: 99%), zirconium (IV) oxynitrate hydrate ($ZrO(NO_3)_2{\cdot}6H_2O$, purity: 99.99%), 2-Methylimidazole (2-MeIm) (purity: 99%) and ethanol (purity 99.8%) were purchased from Sigma-Aldrich Co. LLC, Dorset, UK. Methanol (MeOH, purity: 99%) and *n*-pentane (purity: 99.8%), dimethylformamide (DMF, purity: 99.8%) were both procured from Fisher Scientific UK Ltd, Loughborough, UK. Commercially available MOF catalyst ZIF-8 was purchased from Sigma-Aldrich Co. LLC under the trademark of Basolite Z1200. The liquid CO_2 cylinder and liquid nitrogen cylinder equipped with a dip tube were purchased from BOC Ltd., UK. All chemicals and catalysts were used without further purification or pre-treatment.

3.3 Synthesis of Zr/ZIF-8 catalyst

Zr/ZIF-8 catalyst has been synthesised by a simple traditional solvothermal method which has been previously described elsewhere by Schejn et al. (2015a), but with slight modifications. According to Bidokhti, (2017), MOF catalysts that are synthesised by solvothermal method have shown higher thermal stability. Thus, solvothermal method has been adopted as a preferred method of catalyst synthesis for this research work.

In a typical synthesis, a mixture containing 9 g of zinc nitrate hexahydrate and 1 g of zirconium (IV) oxynitrate hydrate in a molar ratio of Zn:Zr = 9:1 was dissolved in 54.7g of methanol labelled as A. In a separate flask, 6.1 g of 2–methyl imidazolate was dissolved in 54.7g of methanol labelled as B. Solutions A and B were then mixed vigorously by dropwise addition in a four-neck flask (labelled as C) under nitrogen flow at ambient temperature for 6 h as shown in figure 3.1. The Zr-doped ZIF-8 crystals were collected and separated by centrifugation at 400 rpm for 30 min. The solution was washed thoroughly with methanol three times and then dried at ambient temperature conditions. The crystals were left to dry overnight at 373 K. The greyish-white powders of Zr/ZIF-8 sample were further washed with DMF for 24 h in order to remove any excess of an unreacted organic linker. The solution was then heated at a temperature of 373 K in order to activate it. The sample was allowed to cool to room temperature naturally before been capped in a vial and refrigerated, ready for use in catalytic cycloaddition reactions. The obtained sample with a mass of 8.5 g was identified as Zr/ZIF-8 catalyst as shown in figure 3.2.

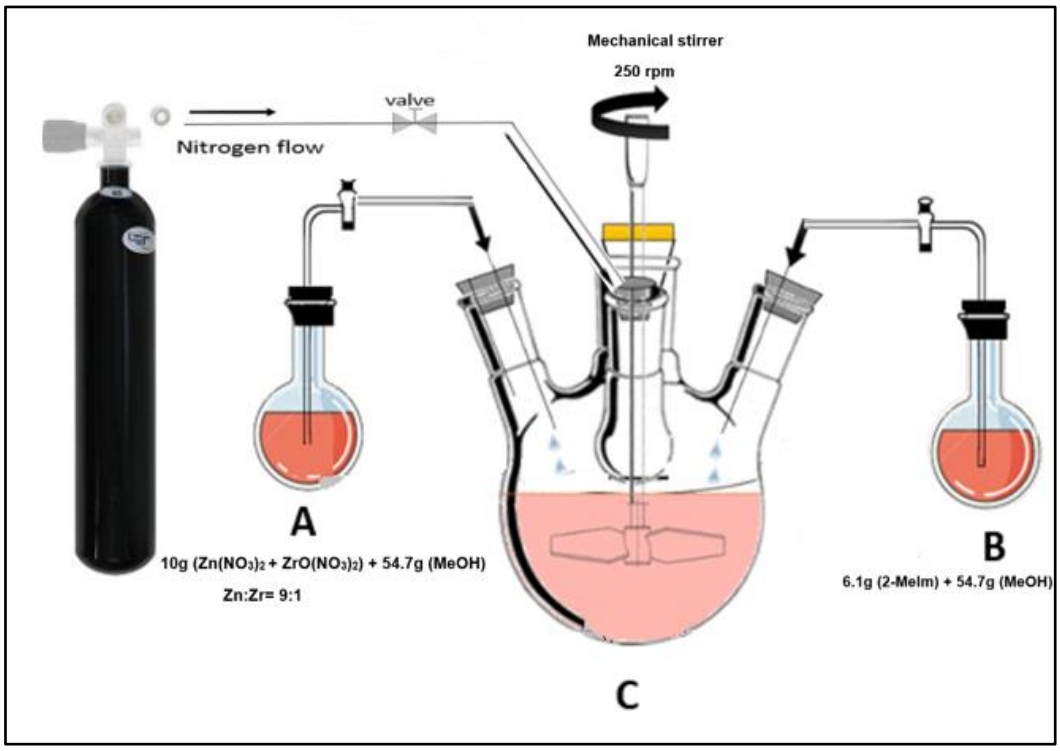

Figure 3. 1. Experimental set up for synthesis of Zr/ZIF-8 catalyst.

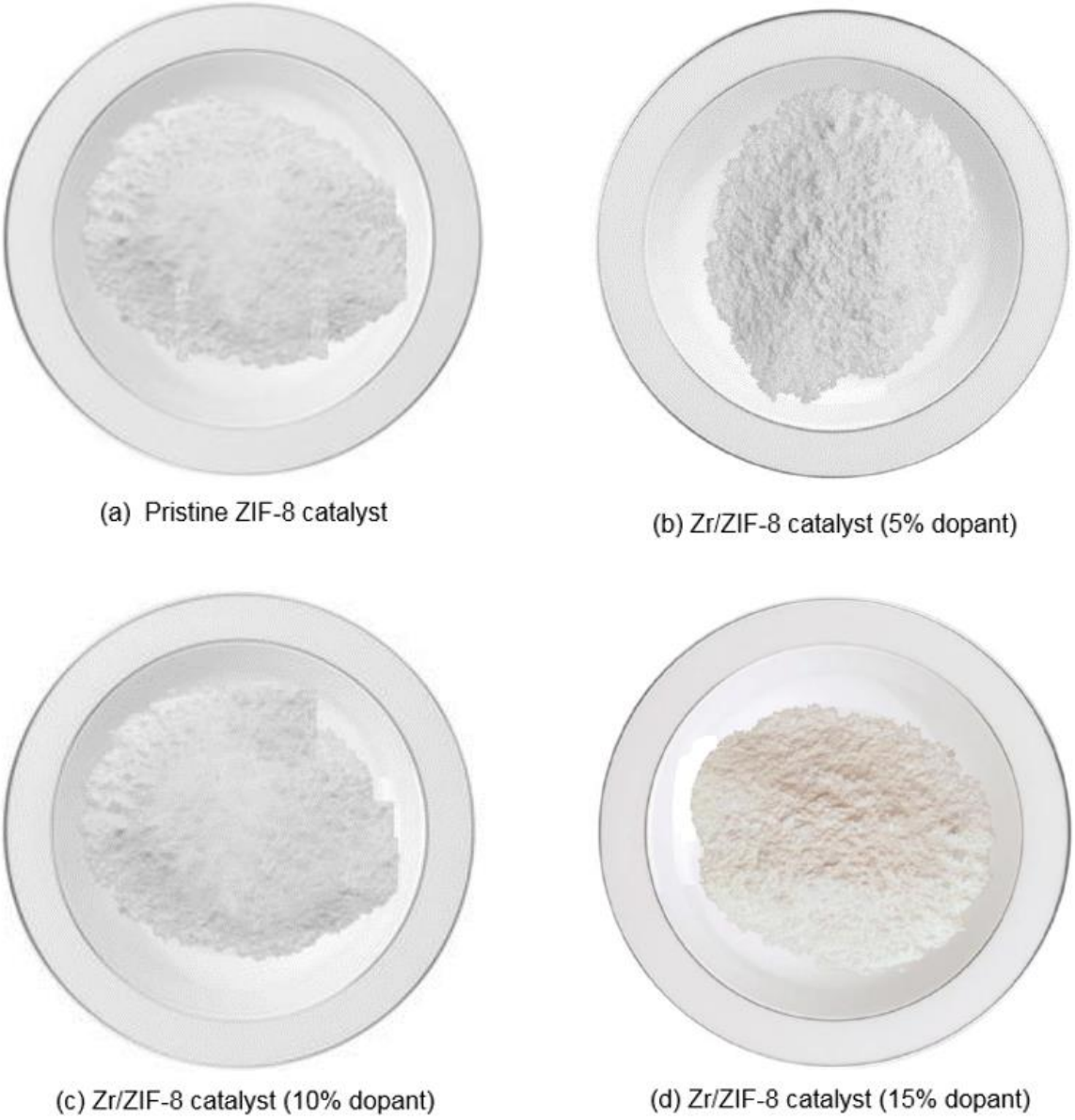

Figure 3. 2. Photographic images of (a) Pristine ZIF-8 catalyst and (b-d) Zr/ZIF-8 catalyst showing slight colour change upon increasing Zr/Zn percentage dopant.

3.4 Catalyst characterisation

3.4.1 Powder X-ray diffraction (XRD) analysis

3.4.1.1 Background

X-ray powder diffraction (XRD) is a rapid analytical technique primarily used for phase identification of a crystalline material and can provide information on unit cell dimensions. The analysed material is finely ground, homogenised, and average bulk composition is determined. The purpose to use XRD is one of the most efficient methods by which the quantitative determination of internuclear distances can be successfully made.

3.4.1.2 Procedure

The powder X-ray diffraction (XRD) patterns of the as-synthesised sample analysis were carried out at room temperature with a characteristics peaks range of $5 < 2\theta < 35$ at a scanning rate of $0.5°min^{-1}$. The catalyst was placed on a zero-background silicon sample holder using a Bruker D8 Advance x-ray diffractometer in transmission geometry with CuKα radiation (λ = 1.5406˚ A) at 40 kV and 40 mA. The samples were slightly grinded before measurements were taken so as to prevent the preferential orientation of individual crystals during sample analysis.

3.4.1.3 Observation and analysis

The X-ray diffraction patterns of ZIF-8, Zr/ZIF-8 and first recycled Zr/ZIF-8 are shown in Figure 3.3. The diffraction peaks appeared at small 2θ angles with eight diffraction peaks at 7.31, 10.31, 12.71, 14.71, 16.41, 18.01, 24.61, and 26.71 which are indexed to the (011), (002), (112), (022), (013), (222), (233), and (134) planes, respectively. The XRD patterns of both Zr/ZIF-8 and first recycled Zr/ZIF-8 catalysts are identical as shown in Figure 3.3, confirming that Zr/ZIF-8 has high crystal stability under the normal reaction conditions. These results are in agreement with simulated patterns reported in other literature (Gallardo-Fuentes *et al.*, 2016; Nabipour *et al.*, 2017; Fan

et al., 2018). The decrease in peak intensity of these diffractions was also observed at (2θ = 28–35°) indicating the effect of excess doping of Zr into the ZIF-8 framework. The XRD pattern of Zr/ZIF-8 also show a characteristic peak of ZIF-8 with no diffraction peak of zirconium nitrate, a similar observation was reported elsewhere by (Thi Thanh *et al.*, 2017).

Although, the peak intensity of Zr/ZIF-8 may be slightly lower when compared to ZIF-8 (commercial name: Basolite Z1200), purchased from Sigma Aldrich. Nevertheless, the experiments of (Nordin *et al.*, 2014) They establishes that guest molecules (such as zirconium) occupying MOF pore spaces may cause pattern destructive and subsequently, a retarded gas uptake capacity in the MOF. A further and in-depth examination of the XRD patterns of the specimen beyond this study could reveal some surprising details as doping of zirconium into ZIF-8 could enlarge its pore spaces, thereby inducing a crystallographic defect in the Zr/ZIF-8 catalyst.

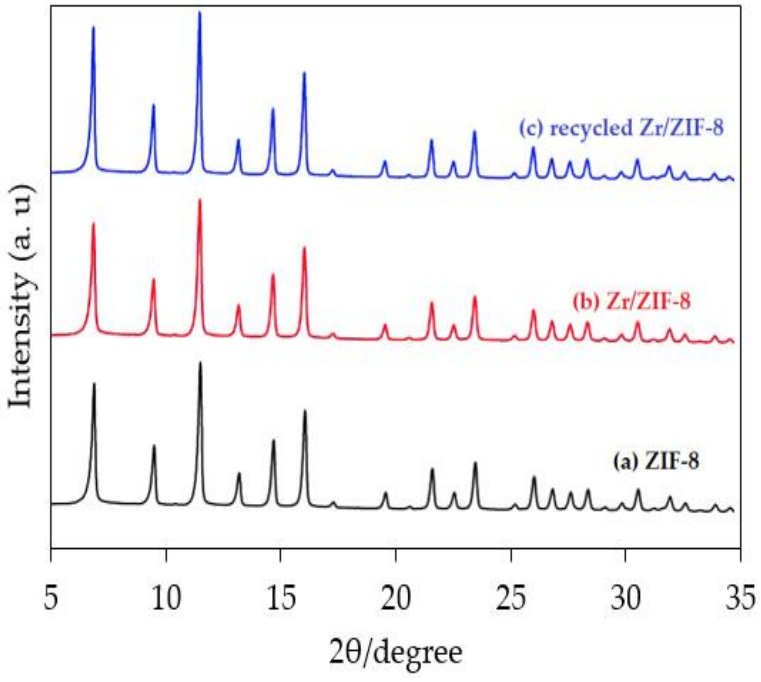

Figure 3. 3. Powered X-ray diffraction (PXRD) patterns of (a) ZIF-8, (b) Zr/ZIF-8 and (c) First recycled Zr/ZIF-8 catalyst.

3.4.2 Scanning electron microscopy (SEM)

3.4.2.1 Background

The scanning electron microscopy (SEM) involves the application of a microscope, which uses electrons instead of light to build a three-dimensional image of higher magnification to give structural information of the sample. This mainly works by scanning the surface of the sample in a raster pattern with a focused beam of electrons and detecting an image from the reflected electrons from and off the sample's surfaces.

3.4.2.2 Procedure

Particle size morphologies and microstructures of the as-synthesised Zr/ZIF-8 catalyst was examined using JEOL JSM-35C instrument operated at voltage 20 kV acceleration. Prior to imaging, the specimen was carbon-coated (5-10 nm) under a vacuum condition using Emitech K550X sputter coater, this was done to enhance material conductivity. The particle mean size of the specimen was calculated by taking a manual measurement of about 300 crystals in the SEM images using the field-emission scanning electron microscope (FE-SEM). FE-SEM spectra produced were used to examine the particle size and morphology.

3.4.2.3 Observation and analysis

Figure 3.4 shows the morphologies and microstructures of ZIF-8, fresh and first recycled Zr/ZIF-8 catalysts using the scanning electron microscope (SEM) with an average particle size diameter of 100 µm. Figure 3.4 (a) shows an evolution of ZIF-8 crystal from cubes with 6 faces [100] to intermediates shapes, and finally to a more stable equilibrium rhombic dodecahedral shape with edges exposing 12 faces [110] similar to the report of Zanon et al. (2017a). Figure 3.4 (b) (Zr/ZIF-8) revealed very slight morphological alterations to Figure 3.4 (a) (ZIF-8) framework. The slight alterations are a genuine indication of a stable Zr/ZIF-8 catalyst comparing to the report of Pang et al. (2016). Furthermore, the hexagonal shape of the recycled catalyst

in Figure 3.4 (c) showed a very small change after the cycloaddition reaction. A close examination of the SEM images of Figures 3.4 (a) and 3.4 (b) shows no significant effect of attrition on the overall particle aggregation between the two structures. The SEM image of recycled Zr/ZIF-8 in Figure 3.4 (c) showed rather small isolated monodispersed particles with a well-defined truncated rhombic dodecahedron structure caused by the presence of dopant in the host molecule. Essentially, the SEM images of the samples are consistent with the XRD results and the thermal stability of Zr/ZIF-8 as shown in the catalyst reusability studies. It is worth mentioning that, the increased average crystal size of the recycled Zr/ZIF-8 catalyst in the range of ~100–170 nm (Figure 3.4 (c)) may be attributed to Ostwald ripening and/or recrystallisation effect (Pang *et al.*, 2016), a phenomenon which explains a possible increase in the average crystal size of the reused catalyst during cycloaddition reaction, especially at a higher temperature (reaction temperature 353 K).

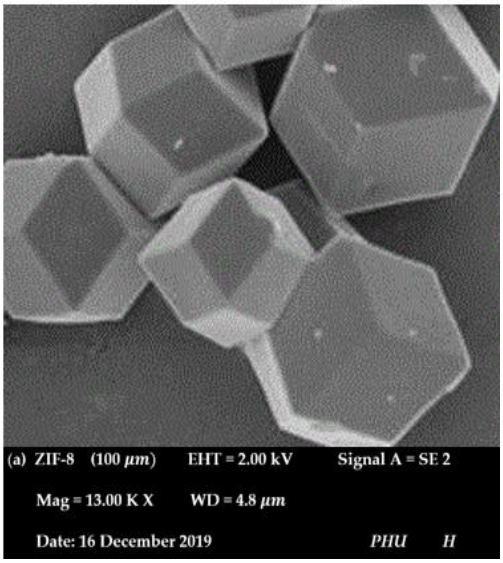

(a)

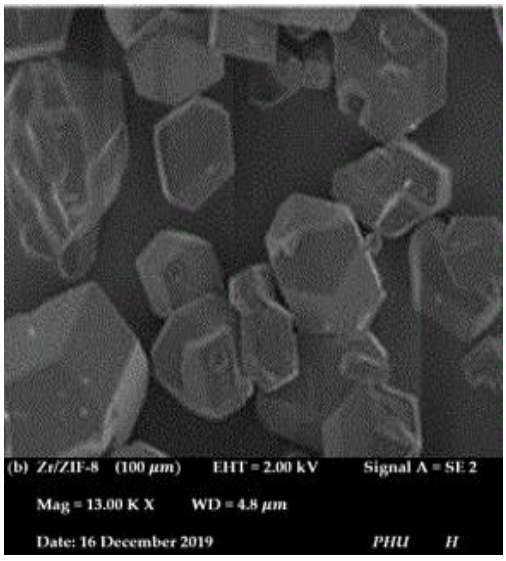

(b)

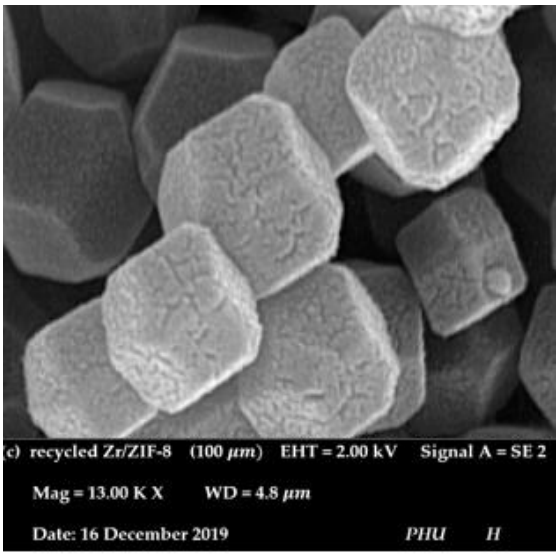

(c)

Figure 3. 4. Scanning Electron Microscopy (SEM) images of (a) Pristine ZIF-8 (b) Fresh Zr/ZIF-8 and (c) First recycled Zr/ZIF-8 with 10% dopant of Zr.

3.4.3 Transmission electron microscopy (TEM)

3.4.3.1 Background

The TEM uses a high voltage electron beam emitted by a cathode and produced from magnetic lenses. It uses electrons in place of light as a source to the targeted image. These electron beams are transmitted partially through the thin slice of the sample and carry information about the structure of the sample to the other side. The image is then magnified by a series of magnetic lenses until it is recorded by smashing on the fluorescent screen, photographic plate or light-sensitive sensor for example charge-coupled device (CCD) camera. The detected image by CCD is displayed in real-time on the computer. This is particularly good for learning as it has shown the component that the sample is made up to form the structure and a valuable tool for analysis in several professional fields, especially in material science due to its high resolution. The use of TEM for analysis is often time-consuming when preparing a sample of a thin layer that is electron transparent.

3.4.3.2 Procedure

Transmission electron microscopy (TEM) images of the catalyst were examined using a high-resolution TEM (HRTEM). A sample of the specimen was sonicated in ethanol for 15 min and was then placed by a dropwise onto a carbon film-supported copper grid. The as-prepared sample was allowed to dry at room temperature before inserting it into a sample holder.

3.4.3.3 Observation and Analysis

Low-magnification TEM images of the samples were carried out in order to examine the structural changes taking place on the surface of the samples. Figures 3.5 (a) and 3.5 (b) showed well-shaped high-quality homogenous crystals with a remarkable rhombic dodecahedral shape and average crystal size of about 100 μm which conforms to earlier literature (Pang *et al.*, 2016). It can be observed from the image in

Figure 3.5 (b) that there are no obvious aggregations or changes in particle size and morphology from Figure 3.5 (a). The TEM image of the first recycled catalyst (Figure 3.5 (c)) shows that the catalyst crystals were highly stable during the cycloaddition reaction of CO_2 and ECH.

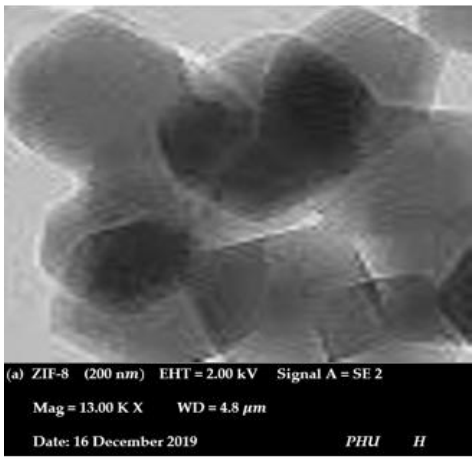

(a)

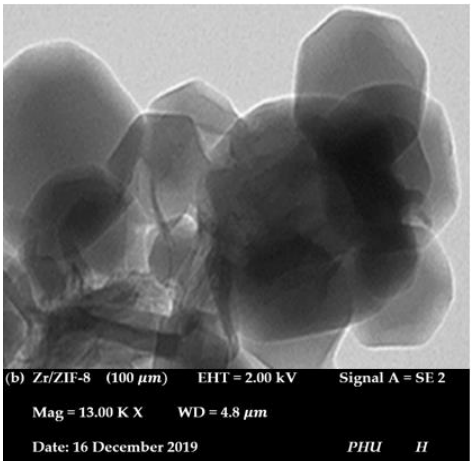

(b)

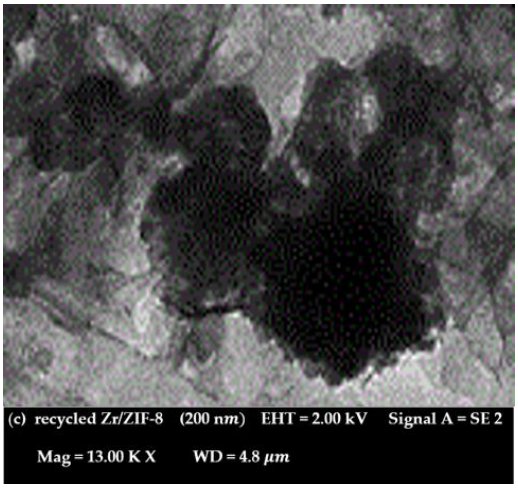

(c)

Figure 3. 5. High-Resolution Transmission Electron Microscopy (HRTEM) images of (a) pristine ZIF-8 crystals (b) Fresh Zr/ZIF-8 and (c) First recycled Zr/ZIF-8 with 10% dopant of Zr

3.4.4 Brunauer-Emmett (BET) surface area analysis

3.4.4.1 Background

The Brunauer-Emmett-Teller method (BET) is used to determine the physical adsorption of gas molecules in solid materials with complicated shapes, such as porous materials. In BET method, adsorption and desorption isotherms are used to identify the number of gas molecules adsorbed on the material. The BET equation describes adsorption where the adsorbate contains multilayer. Its main assumptions include:

- The adsorbed molecules are fixed;
- The enthalpy of adsorption for the layers is the same;
- The energy of adsorption for the layers is the same except the first one;
- A new layer can start before another is finished.

3.4.4.2 Procedure

The Brunauer–Emmett–Teller (BET) surface area of the as-prepared catalyst was analysed with a Micromeritics Gemini VII analyser at room temperature (291 K). Prior to BET analysis, the samples were degreased in a turbomolecular pump vacuum at 423 K for 8 h. The surface area and nitrogen adsorption/desorption isotherm measurements were taken at a liquid nitrogen temperature of 77 K (purge gas supplied by BOC, UK). In order to achieve a greater degree of accuracy in the accumulation of the adsorption data, the Micromeritics Gemini analyser was fitted with pressure transducers to cover the range of 133 Pa, 1.33 kPa, and 133 kPa.

3.4.4.3 Observation and analysis

The nitrogen adsorption-desorption isotherms of ZIF-8, Zr/ZIF-8, and the first recycled Zr/ZIF-8 catalysts are shown in Figure 3.6. The samples were measured at a liquid temperature of 77k at 373 K for 24 h. The three isotherms showed an attribute of a microporous framework with a sharp hysteresis loop of P/P0 between 0.8 and 1.0.

However, the pristine ZIF-8 catalyst demonstrates a typical type-I isotherm behaviour (Da Silva *et al.*, 2015) while Zr/ZIF-8 and the recycled Zr/ZIF-8 catalysts both shows typical type-IV isotherms with a type H_4 hysteresis loop in the range of P/P0 = 0.4–0.8 indicating the presence of mesopores (Fang *et al.*, 2010). Meanwhile, an increase in the volume adsorbed at low relative pressure is consistent with interparticle voids, which is indicative of dual macro-mesoporosity of the Zr/ZIF-8 lattice according to International Union of Pure and Applied Chemistry (IUPAC) classification (Liu *et al.*, 2016a; Panchariya *et al.*, 2018).

The specific BET surface area (S_{BET}) of the catalysts has been calculated using the BET equation. The pore size distribution was derived from the nonlinear density functional theory (DFT) model (calculated using computer software). The surface area and micropore volume of Zr/ZIF-8 were generally lower than ZIF-8 as shown in Table 3.1. The lower BET surface area and pore volume of Zr/ZIF-8 may be caused by the blockage of the pore cavities of the host molecule as a result of deposition of zirconium particles in the ZIF-8 shell, a phenomenon that has been previously reported by (Li-yan *et al.*, 2012). Surprisingly, the total pore volume and the BET specific surface area of recycled Zr/ZIF-8 catalyst both decreased after the reaction. This observation may be attributed to the agglomeration of coke deposits in the pore spaces, resulting in the blockage of some micropores and mesopores (Goyal *et al.*, 2018).

These results reflect a good pore size distribution of the samples microporous network (Cychosz *et al.*, 2017; Yin *et al.*, 2015). Although, variation may exist in particle BET surface area and pore volume from one literature to another, this may be attributed to post-synthesis work-up procedures such as further purification processes and activation of MOF samples. The BET surface area as shown in Figure 3.6 is in agreement with the previous literature (Bai *et al.*, 2015).

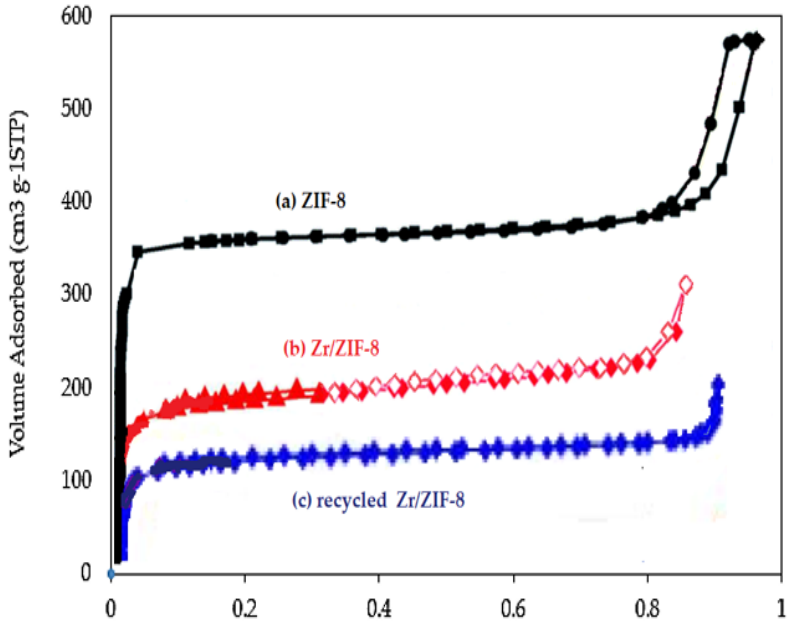

Figure 3. 6. N2 adsorption-desorption isotherms of (a) ZIF-8 (b) Zr/ZIF-8 and (c) first recycled Zr/ZIF-8 synthesised with 10% dopant of Zr.

Table 3. 1. Comparison of BET, pore-volume, and pore size for ZIF-8 and Zr/ZIF-8 crystals.

Entry	Material	$S_{(BET)}$ (m^2g^{-1})	Pore volume (Cm^3g^{-1})	Pore size (nm)
1	ZIF-8	1700	0.664	1.30
2	Zr/ZIF-8	1458	0.536	1.22
3	Zr/ZIF-8 (first recycled)	1378	0.498	1.21

3.4.5 The Fourier transform infrared (FTIR)

3.4.5.1 Background

Fourier transform infrared spectroscopy (FTIR) is a powerful technique which is used to confirm the surface functional groups and the molecular structure of a catalyst. It obtains an infrared spectrum by absorption or transmission through a solid, liquid or gas. It is a routine technique for the characterization of MOFs. Infrared spectroscopy can be used to confirm the coordination of the metal centers and the linker. It gives information about the available functional groups of MOFs. FT-IR spectra offer useful information about the presence of impurities or unreacted linkers. When IR (infra-red) radiation passes through a sample, some part of the electromagnetic radiation is absorbed and some is transmitted. The resulting spectrum shows the characteristics of the sample and also shows the unique molecular fingerprint of the sample. FTIR can measure all infrared frequencies and subsequently decodes them with the assistance of computer software, and the spectral information of the sample is then generated.

3.4.5.2 Procedure

The Fourier transform infrared (FTIR) spectra (4500-600 cm^{-1}) of the samples were obtained using Nicolet Magna-IR 830 spectrometer in KBr disks at room temperature with a resolution of 2 cm^{-1}. The specimen was mixed KBr in ratio 1:300, the mixture was ground in an agate mortar to a very fine powder. The product was oven dried for 12 h at 373 K, 250 mg of the dry samples were used to make a pallet; the pallet was analysed, and the spectra were recorded by 32 scans with 4 cm^{-1}.

3.4.5.3 Observation and analysis

Figure 3.7 shows the Fourier-transform infrared spectroscopy (FTIR) spectra of ZIF-8, Zr/ZIF-8, and first recycled Zr/ZIF-8 with an absorption region of 500–4000 cm^{-1}. The three samples show several bands with no substantial difference in the spectra.

For example, a typical adsorption band at 423 cm^{-1} is attributed to the Zn–N bond vibrations indicating that zinc molecules of the imidazole ring are well-knitted during the reaction to nitrogen atoms in 2-methylimidazolate (2-Hmim) linkers to form the ZIF frameworks (Bosch *et al.*, 2014a). The absorption spectra at 2926 cm^{-1} can be ascribed to the aromatic moieties, while the spectra at 3133 cm^{-1} can be attributed to the aliphatic imidazole ring due to C–H stretching (Xie *et al.*, 2013). The missing adsorption spectra in the region of 3400 to 2200 cm^{-1} is a strong indication of a fully deprotonated imidazole ring during the formation of the ZIF-8 frameworks (Xie *et al.*, 2013). The strong sharp peak at 1449 cm^{-1} can be assigned to the C–C bonding in the benzene ring. The peak at 1579 cm^{-1} can be attributed to C =N vibrations mode (Zhou *et al.*, 2019), while the spectra in the band range between 1100 and 400 cm^{-1} can be assigned to C–N stretching vibrations. The small peaks at 1245 and 1255 can be assigned to C–N and C≡N groups respectively indicating the presence of imidazole molecules in the sample frameworks. The Zr–N bonding vibration located between 550 and 620 cm^{-1} in Zr/ZIF-8 catalyst (Yao *et al.*, 2013). All characteristic peaks of ZIF-8 can be observed both in Zr/ZIF-8 and the recycled Zr/ZIF-8, indicating a successful combination and interaction between Zr and ZIF-8. This observation is a strong indication that the frameworks of ZIF-8 have not been affected after the incorporation of Zr. This results in agreement with the report of (Giraldo *et al.*, 2017) experiments.

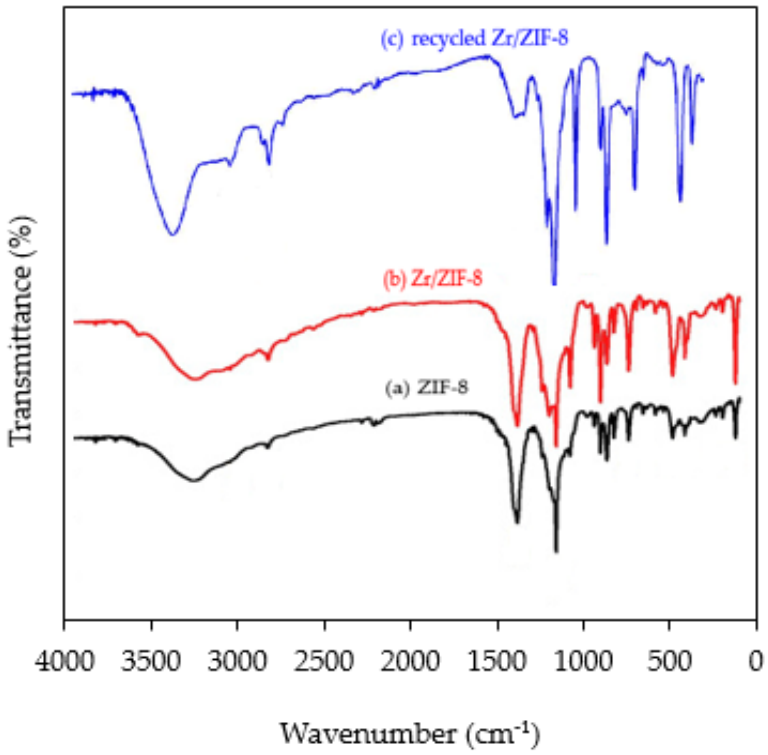

Figure 3. 7. Fourier-transform infrared spectroscopy (FTIR) spectra of (a) ZIF-8 (b) Zr/ZIF-8, and (c) first recycled Zr/ZIF-8 particles.

3.4.6 Raman spectroscopy

3.4.6.1 Background

Recently, the use of Raman spectroscopy technique to characterise zirconium doped MOF has gained significant attention partly because of its enhanced stability and resistance to fracture (Li *et al.*, 2001, 2016). Raman spectroscopy is a spectroscopic technique providing information about molecular vibrations that can be used for sample identification and quantification (Dallali Isfahani *et al.*, 2014). The technique involves shining a laser light source on a sample and detecting the scattered light. The majority of the scattered light is of the same frequency as the excitation source, which is known as elastic scattering. However, a very small amount of the scattered light is shifted in energy from the laser frequency due to interactions between the incident

electromagnetic waves and the vibrational energy levels of the molecules in the sample. Plotting the intensity of this "shifted" light versus frequency results in a Raman spectrum of the sample. In a Raman spectrum, the band positions correspond to the energy levels of different functional group vibrations.

Raman spectroscopy is a powerful technique to investigate carbonaceous materials. In the Raman spectra, the bond stretching of all pairs of sp^2 atoms in both rings and chains and the breathing modes of sp^2 atoms in rings. The G band at around 1590 cm^{-1} supports the presence of some nanocrystalline carbon and a high content of sp^2-hybridised carbon atoms caused by the carbonisation of the samples. The D band at around 1340 cm^{-1} is an indication of less disordered carbon. The parameters that affect the Raman bands include crystal size, structure and stresses of a catalyst (Kellici *et al.*, 2010).

3.4.6.2 Procedure

Raman spectroscopy measurements of the specimen were taken at room temperature with Horiba Jobin Yvon LabRAM spectrometer equipped with aHeNe laser operating at a wavelength of 633 nm (E_{ex}=1.96$_e$V) and Coherent Innova 70 ion laser at a wavelength of 458 nm, 488 nm and 514 nm.

3.4.6.3 Observation and analysis

Raman spectra of ZIF-8, Zr/ZIF-8 and first recycled Zr/ZIF-8 were observed using a Renishaw Ramascope 1000 (model: 52699). Figure 3.8 shows that Zr/ZIF-8 exhibited several Raman spectra at the following peaks 687, 892, 1149, 1186, 1462, 1568, 2931, 3114, and 3131 cm^{-1} similar to ZIF-8 spectra. The spectra at 1116 and 1484 cm^{-1} corresponding to bands D and G, respectively, found in the Raman spectrum of ZIF-8, have not been observed in the Zr/ZIF-8 and the recycled Zr/ZIF-8 spectra. This may be as a result of a split of the main bands at 1143 and 1508 cm^{-1} as previously reported by (Biswal *et al.*, 2013). The spectra found at 278 cm^{-1} may be

attributed to Zn–N stretching, while the spectra at 683, 1143, 1456, and 1508 cm^{-1} are attributed to imidazole ring puckering, C5–N vibrations, methyl bending, and C4=C5 stretching, respectively, which are similar to the observation of (Tanaka *et al.*, 2015). The remaining spectra can be assigned to stretching and bending on the imidazole ring (Pham *et al.*, 2018). With doping of Zr into the ZIF-8 frameworks, the peaks at 1116 and 1484 disappeared with no significant change in main peaks on spectra (Pham *et al.*, 2018). The spectra of the three samples show similar vibration modes, which confirms structural equality in the frameworks.

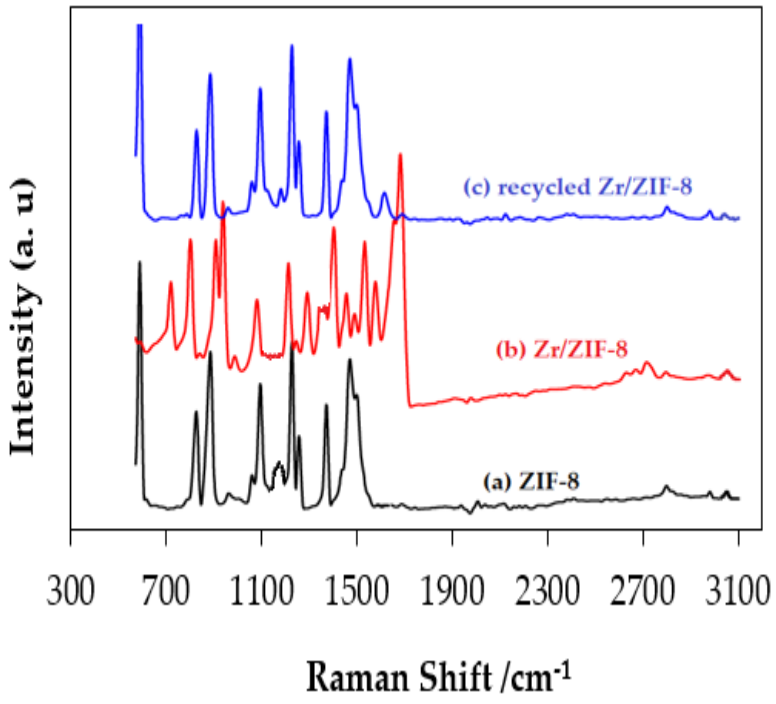

Figure 3. 8. Raman spectra of the crystal-size (a) ZIF-8 (b) Zr/ZIF-8 and (c) first recycled Zr/ZIF-8 samples

3.4.7 Thermogravimetric analysis

3.4.7.1 Background

Thermogravimetric analysis (TGA) of ZIF-8 and Zr/ZIF-8 was investigated under nitrogen in the temperature range of 0 to 800 K. The influence of Zr doping on the thermal stability of ZIF-8 has also been monitored.

3.4.7.2 Procedure

All samples were run on a Q-500 series thermal gravimetric analyzer (TA Instruments, New Castle, DE) with samples held in platinum pans in a continuous-flow nitrogen atmosphere. Samples were heated at a constant rate of 278 K/min during all TGA experiments.

3.4.7.3 Observation and analysis

There are three distinct phases of weight loss experienced by both samples as indicated in Figure 3.9. It can be observed from the thermogram that, both catalysts experienced a very small initial weight loss of about 3% in the region from 298 to 373 K in the first phase. This can be attributed to the loss of water and some guest molecules (e.g., methanol) and possibly some unreacted species trapped in the pore cavities of the framework (Yin *et al.*, 2015). As the temperature was further increased through the second phase, Zr/ZIF-8 experienced a gradual and steady weight loss up to 723 K and then remained stable thereafter until 973 K. Conversely, ZIF-8 experienced a rapid and significant weight loss of around 54% up to 823 K, attributing the decomposition of some absorbed organic ligand and the final weight loss phase experienced the collapse of the ZIF-8 structure at high temperature (Pham *et al.*, 2018). It is worth noting that materials stability of the ZIF-8 framework can be attributed to the incorporation of zirconium in ZIF-8. A similar observation was reported by (Wang *et al.*, 2018) in the doping of lanthanum into ZIF-8. After the decomposition, approximately 39% of the starting weight remained. From this observation, it can be

concluded that the Zr/ZIF-8 catalyst frameworks have remained structurally stable and this is consistent with XRD and SEM.

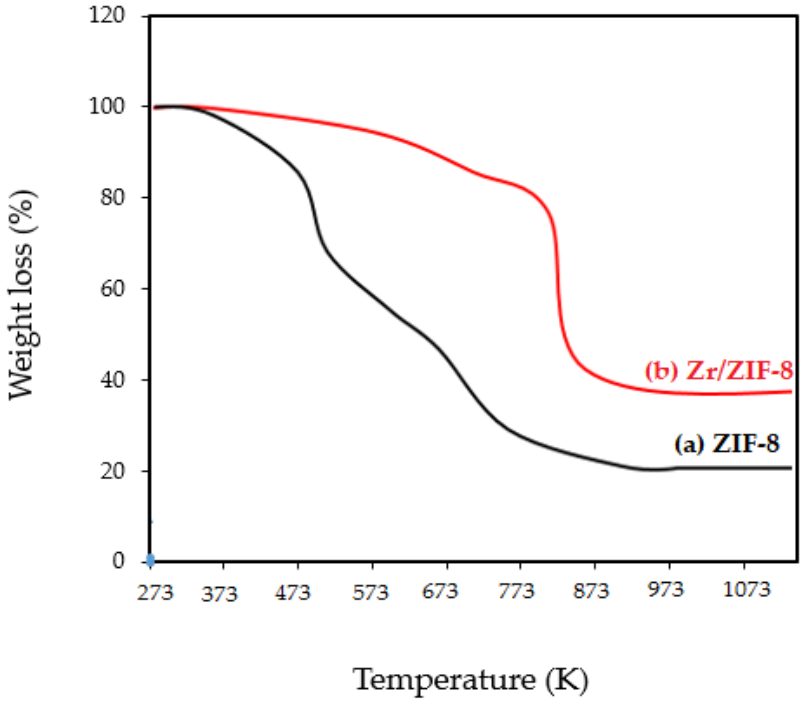

Figure 3. 9. Thermal stability curve of (a) ZIF-8 and (b) Zr/ZIF-8

3.4.8 X-ray photoelectron spectroscopy

3.4.8.1 Background

XPS analysis provides qualitative, quantitative and chemical state information for surface elements of solid materials. XPS analysis was employed to investigate the changes in the concentration of Zirconium and Zinc within the crystal lattice, their oxidation and chemical states.

3.4.8.2 Procedure

X-ray photoelectron spectroscopy (XPS) of the samples was recorded on krato axis ultra DLD photoelectron spectrometer, a surface science instrument SSx-100 using a monochromatic Al KR X-ray source operating at 144 W. The chemical states and surface composition of the as-synthesised catalyst was characterised using NIST X-ray photoelectron spectroscopy (XPS). The samples were carefully placed in a conductive tape and allowed to dry before analysis. The samples were kept in vacuum overnight before XPS measurements were carried out.

3.4.8.3 Observation and analysis

The X-ray photoelectron spectroscopy (XPS) spectra in Figure 3.10 clearly shows the chemical state of the element present in pristine ZIF-8 frameworks (Zn, C, N) and O, while those elements present in Zr/ZIF-8 sample include Zn, C, N, O, and Zr species. Figure 3.10a exhibits high-resolution XPS spectra showing two strong peaks with the binding energy of 1044.3 and 1021.1 eV which can be assigned to Zn $2p^{½}$ and Zn $2p^{3/2}$ components, respectively, confirming the presence of Zn (II) ions attached with nitrogen in the imidazole ring [48]. This result is consistent with the XRD results. With the incorporation of Zr into ZIF-8, the binding energy of Zn $2p^{1/2}$ and $2p^{3/2}$ have slightly increased, this could be as a result of the chemical environment of zinc and the interaction between zinc and zirconium. All spectra have been normalized to the magnitude of the Zn $2p^{3/2}$ and Zn $2p^{1/2}$ peaks so that changes in intensity are relative to the amount of Zn in the surface region. Similarly, Figure 3.10b shows the high-resolution N1s spectra of all samples. The N1s spectra can be deconvoluted into three characteristic peaks found at 399.0 and 399.8 and 398 eV which can be assigned to the pyridinic, pyrrolic, and graphitic, respectively. These can be related to the N species of the 2-methyl imidazole ring (Song *et al.*, 2012). C1s spectra show four different characteristic peaks corresponding to C–C at 284.1 eV, C–N at 285.8 eV, C–O at 286.4 eV, all assigned to the 2-methyl imidazole ring (Yuan *et al.*, 2012). The low peak found at 283.4 eV could be as a result of Zr doping into ZIF-8 frameworks (Ye *et*

al., 2015). Figure 3.10d shows high-resolution O1 spectra that have been deconvoluted into two characteristic peaks with binding energy 532.3 and 531.8 eV corresponding to O^{2-} found in Zn–O bonding and carboxylate species, respectively (Luanwuthi *et al.*, 2015). The relatively low peak intensity of Zr–O in O1s, C1s, and N1s is a strong indication that the ZIF-8 frameworks are not affected by the presence of dopant, which perfectly agreed with the result of (Mao *et al.*, 2017).

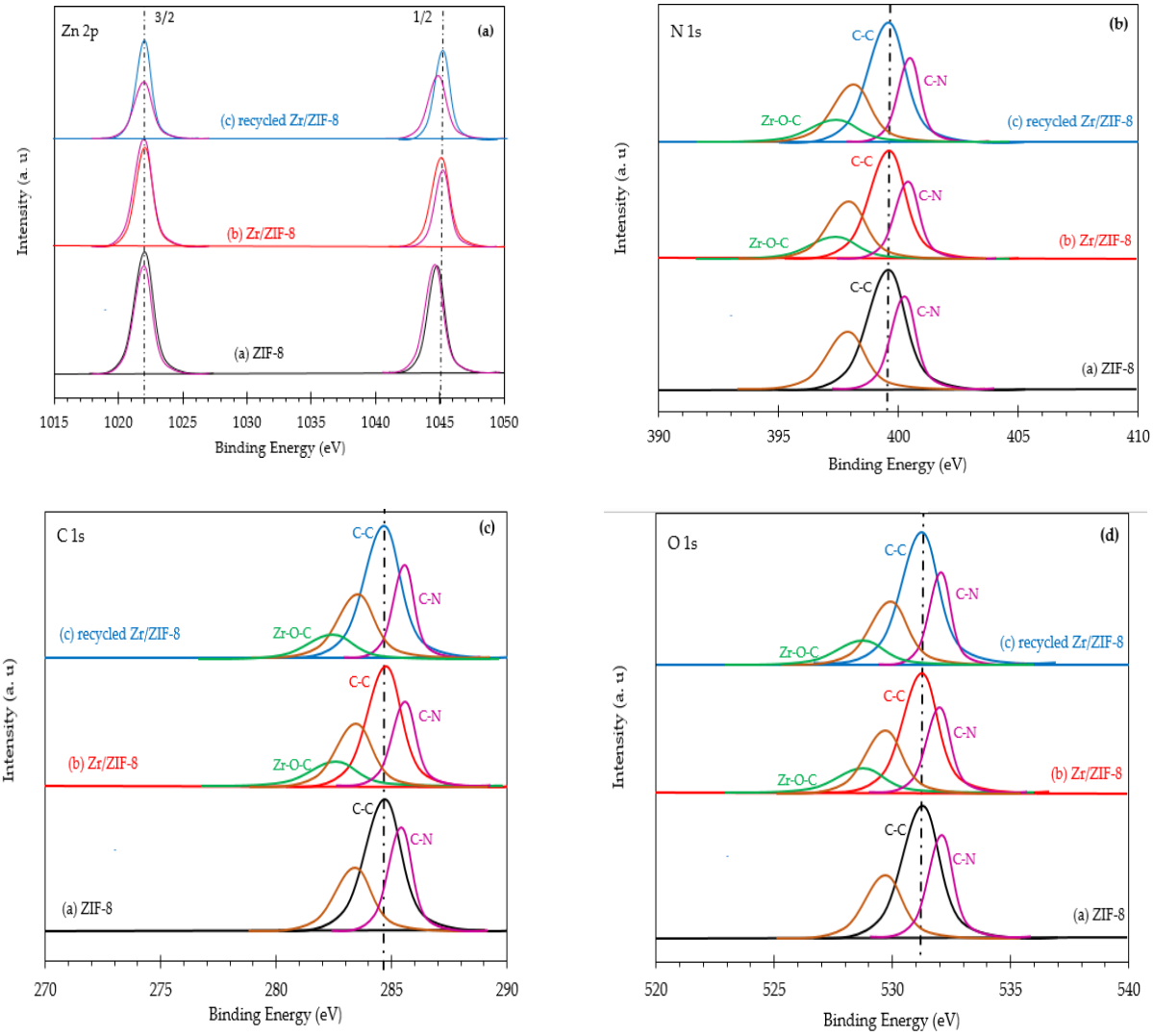

Figure 3. 10. X-ray photoelectron spectroscopy (XPS) spectra showing deconvoluted regions of ZIF-8, Zr/ZIF-8 catalyst, and first recycled Zr/ZIF-8 catalysts. (a) Zn 2p, (b) N 1s, (c) C 1s, (d) O 1s.

3.5 A plausible mechanism for cycloaddition of CO_2 and Zr/ZIF-8

In order to develop an efficient MOF-based catalytic systems, it is important to explore the interactive relationship between the CO_2 and epoxide *via* a reaction mechanism. Thus, we proposed a possible reaction mechanism for catalytic cycloaddition of CO_2 and epichlorohydrin (ECH) with Zr/ZIF-8 as shown in Figure 3.11. The proposed reaction mechanism was catalysed by incorporating CO_2 into ECH in the presence of Lewis acid catalyst in the following four key stages:

(i) Activation of epoxide by Lewis acid catalyst.
(ii) Nucleophilic attack that provokes the opening of the epoxide ring leading to an alkoxide.
(iii) Incorporation of CO_2
(iv) Subsequent cyclisation to afford the desired cyclic carbonate

In stage (i) of the reaction system, the Zr/ZIF-8 cation accelerates the coordination of epoxide *via* non-covalent interactions. Then the ring-opening of epichlorohydrin through a nucleophilic attack of chlorine at the least-hindered carbon atom, producing an oxy anion species in stage (ii). Incorporation of CO_2 into anionic intermediate species to form an acyclic ester at the ring stage (iii) and subsequent cyclisation *via* an intermolecular nucleophilic attack in the final stage (iv). The activation of CO_2 can occur both through a nucleophilic attack with the oxygen atom as a nucleophile or an electrophilic attack with the carbon atom as an electrophile (Gallardo-Fuentes *et al.*, 2016). After series of experiments, Liang et al. postulated a tentative mechanism that supports the use of tetra-*n*-butylammonium bromide (MOFs-TBAB) as a co-catalyst in order to optimise the synthesis of cyclic organic carbonates (COCs). This idea of using a co-catalyst was also supported by North and Pasquale. (2009a) through a series of controlled kinetic experiments. A plausible reaction mechanism for the Zr/ZIF-8-catalysed cycloaddition of CO_2 with ECH is proposed in Figure 3.11.

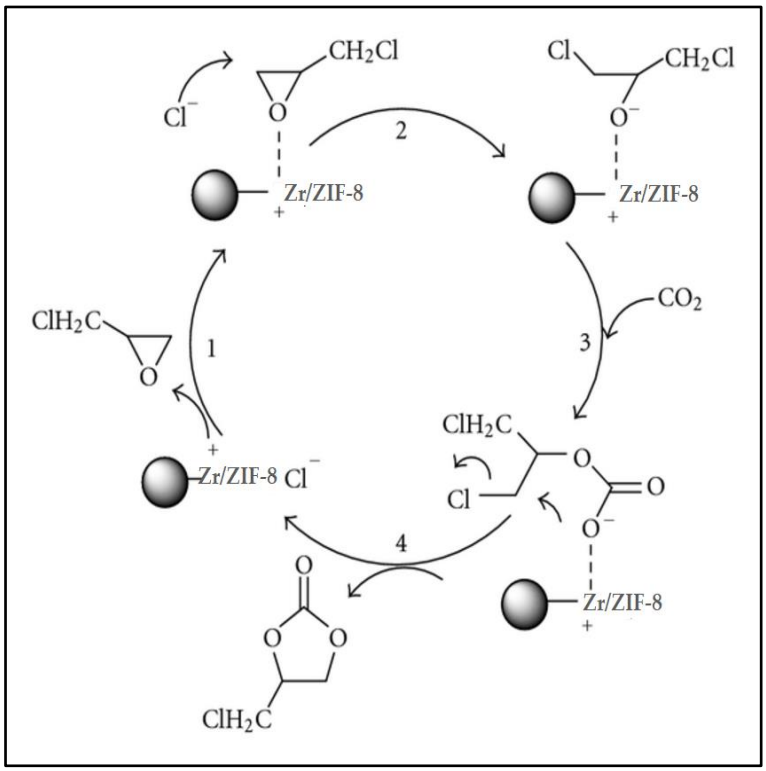

Figure 3. 11. Proposed mechanism for Zr/ZIF-8 catalysed cycloaddition of CO_2 with ECH

3.5.1 Reaction pathways

Zr/ZIF-8 is a bi-functional catalyst, which contains both the acidic and basic sites that are associated with the Lewis acid Zn^{2+} ions and the basic imidazole groups, respectively. The side products associated with the coupling reaction of CO_2 and ECH as identified by the gas chromatography (GC) analysis are 3-chloropropane 1,2-diol and 2,5-bis (chloromethyl)-1,4-dioxane (see Figure. 3.12).

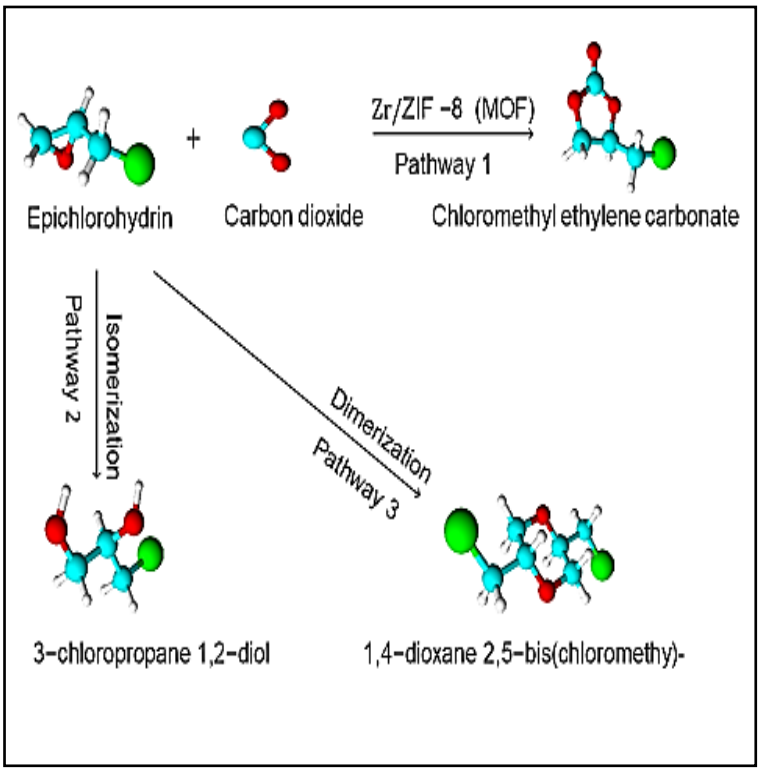

Figure 3. 12. Reaction pathways for cycloaddition reaction of ECH and CO_2

3.6 Conclusions

The characterisation of commercially available ZIF-8 and as-prepared Zr/ZIF-8 catalysts have been examined critically using multiple physiochemical techniques such as X-ray diffraction (XRD), transmission electron microscopy (TEM), scanning electron microscope (SEM), Brunauer–Emmett–Teller (BET), X-ray photoelectron spectroscopy (XPS), Thermal gravimetric Analysis (TGA), Fourier transform infrared (FTIR) and Roman spectroscopy (RM). Although ZIF-8 is criticised by many researchers as thermally unstable for the cycloaddition reaction of epoxide and CO_2. However, incorporating zirconium into ZIF-8 has proven to be effective in strengthening this weak functionality. Zr/ZIF-8 has shown similar physiochemical properties

Chapter 4

Comparison of catalytic activity of ZIF-8 and Zr/ZIF-8 for the greener synthesis of chloromethyl ethylene carbonate by carbon dioxide utilisation

Outline of the chapter

This chapter compares the catalytic activity of both pristine ZIF-8 and as-prepared Zr/ZIF-8 catalysts. It also examines the effects of different reaction conditions (temperature, CO_2 pressure, reaction time and catalyst loading) on the conversion of epichlorohydrin (ECH), selectivity and yield of chloromethyl ethylene carbonate (CMEC). Finally, it examines the reusability studies of both catalysts in order to assess their suitability (stability) for subsequent reuse.

The chapter is organised as follows:

4.1. Introduction

4.2. Experimental methods

4.3. Effects of different heterogeneous catalysts

4.4. Results and discussion

4.5 Reusability studies

4.6. Conclusions

4 Comparison of catalytic activity of ZIF-8 and Zr/ZIF-8 for synthesis of CMEC

4.1 Introduction

The catalytic activity of both ZIF-8 and Zr/ZIF-8 has been investigated for the synthesis of chloromethyl ethylene carbonate (CMEC) using carbon dioxide (CO_2) and epichlorohydrin (ECH) under solvent-free conditions. Many literatures have highlighted the weak thermal, chemical, and mechanical stability of ZIF-8 catalyst which has limited its large-scale industrial applications. The synthesis of a novel Zr/ZIF-8 catalyst for cycloaddition reaction of ECH and CO_2 to produce CMEC has provided a remarkable reinforcement to this weak functionality, which is a significant contribution to knowledge in the field of green and sustainable engineering. The enhancement in the catalytic activity of Zr/ZIF-8 has been explained based on acidity/basicity studies. The comparison of the catalytic activity of the two catalysts has been drawn based on the effect of various reaction conditions such as reaction temperature, CO_2 pressure, catalyst loading, reaction time, stirring speed and reusability studies. Zr/ZIF-8 has been assessed as a suitable heterogeneous catalyst outperforming the catalytic activity of ZIF-8 catalyst with respect to the conversion of epichlorohydrin, selectivity and yield of chloromethyl ethylene carbonate. Experimental results at optimum reaction conditions for direct synthesis of chloromethyl ethylene carbonate agree well with similar literature on Zr/MOF catalytic performance, where the conversion of ECH, selectivity and the yield of CMEC is 93%, 86% and 76%, respectively.

4.2 Experimental methods

4.2.1 Chemicals and materials

Acetone (purity: 99%), epichlorohydrin (purity: 99%), chloromethyl ethylene carbonate (purity: 99 %), Methanol (purity 99%) and *n*-pentane (purity 99.8%) were both procured

from Fisher Scientific UK Ltd, Loughborough, UK. ZIF-8 catalyst was purchased from Sigma-Aldrich Co. LLC, Dorset, UK and as-prepared Zr/ZIF-8 catalyst. The liquid CO_2 cylinder equipped with a dip tube was purchased from BOC Ltd., UK. Supercritical fluid (SCF) pump (model: SFT-10) was procured from Analytix Ltd., UK. A Parr high-pressure stainless-steel autoclave reactor (model: 5500) of 100 mL capacity equipped with a reactor controller (model: 4848) was purchased from SCIMED (Scientific and Medical Products Ltd.), UK. All chemicals and catalysts were used without further purification or pre-treatment.

4.3 Experimental procedure for synthesis of chloromethyl ethylene carbonate (CMEC) using Zr/ZIF-8 catalyst

In a typical cycloaddition reaction, a 25 mL stainless steel high-pressure reactor was initially charged with a specific amount of Zr/ZIF-8 catalyst and the limiting reactant, epichlorohydrin. A desired temperature was set on the reactor's panel controller; the reactor was then sealed and stirred continuously at a known stirring speed. As shown in figure 4.1, at the desired temperature, a specific amount of liquid CO_2 was charged through a supercritical fluid (SCF) pump into the reactor. The reaction was left for the desired reaction time. After the reaction was completed, the reactor was cooled down to room temperature and the mixture was collected and filtered. The catalyst was separated, washed with acetone, and dried in a vacuum oven. A known amount of methanol (used as internal standard) was added to the product and analysed using a gas chromatograph (GC). The effect of different reaction parameters was investigated. These include catalyst loading, stirring speed, CO_2 pressure, temperature, and reaction time. Reusability studies of both catalysts were also carried out in order to investigate the stability of the catalysts for the synthesis of chloromethyl ethylene carbonate.

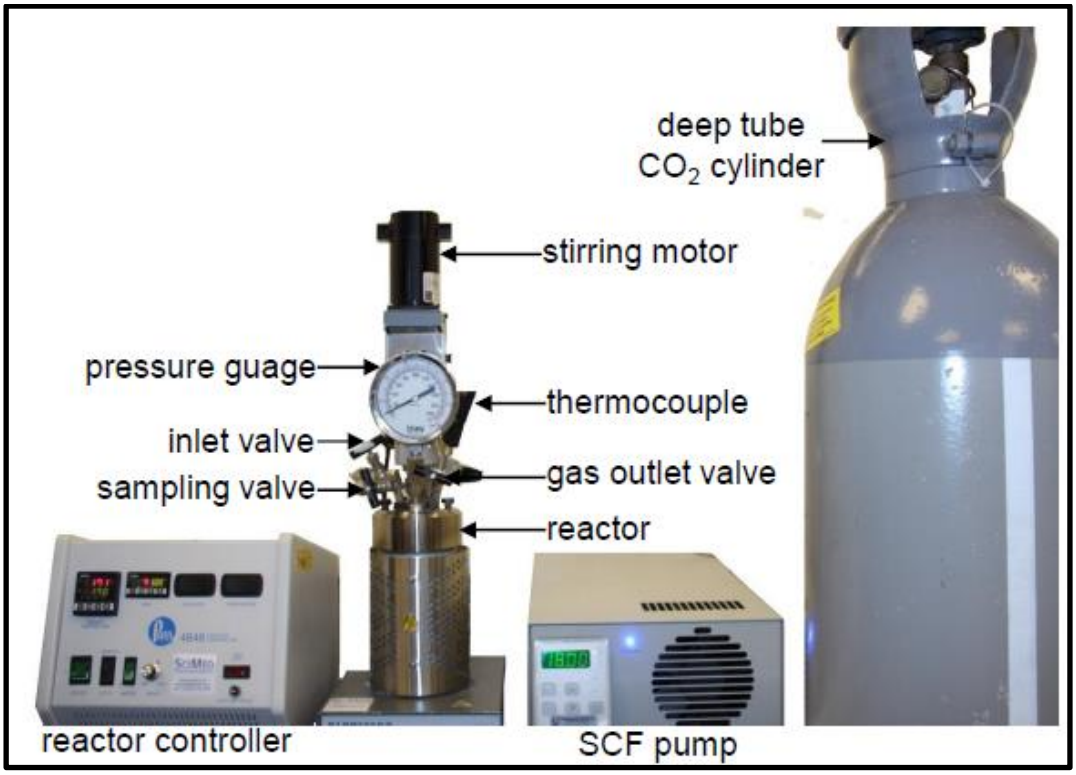

Figure 4. 1. Batch experimental set-up for the synthesis of organic carbonates

4.3.1 Method of sample analysis

A specific quantity of methanol (used as internal standard) was added to a known amount of sample of the product to be analysed by Shimadzu GC-2014 gas chromatography (GC). The set-up in figure 4.2 shows the stationary phase was a capillary column with a length of 30 m, an inner diameter of 320 µm and a film thickness of 0.25 µm. Oxygen (purity: 99.9%) and hydrogen (purity: 99.9%) were used as ignition gases. The carrier gas used was high purity helium (purity: 99.9%) with a gas flow rate maintained at 1 mL min^{-1}, helium being used as the carrier gas for the mobile phase.

A temperature program was developed for the system where both the injector and detector temperatures were maintained isothermally at 523 K. A spilt ratio of 50:1 and

an injection volume of 0.5 µL were chosen as part of the GC method. The sample was injected by an auto sampler for analysis. The column temperature was held at 323 K for 5 min after the sample had been injected. Afterward, a temperature ramp was applied that increased the temperature linearly at a rate of 50 K min^{-1} to a temperature of 523 K. The total run time for each sample was 12 min. The injection needle was washed twice after the sample injection using *n*-pentane. After each sample run, the column temperature was cooled down to 313 K so that the following sample could be analysed. The component mass fractions were directly calculated from the chromatograms *via* internal standard method using methanol as an internal standard. A typical chromatogram of the sample mixture analysed using GC revealed that methanol peak emerged at a retention time of ~4.10 min followed by ECH peak at ~7.10 min and CMEC at ~11.9 min as shown in figure 4.3.

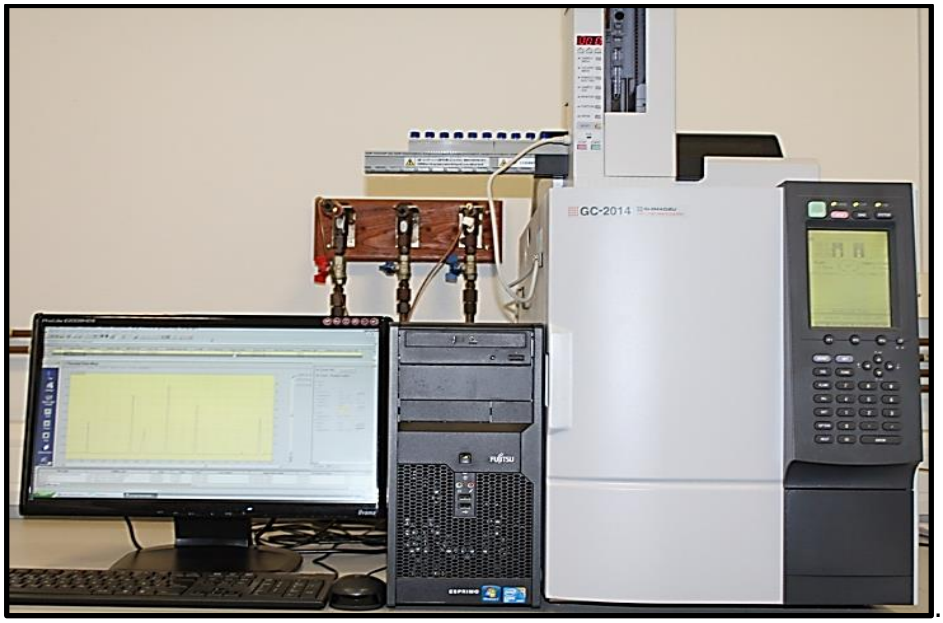

Figure 4. 2. Shimadzu gas chromatography (GC-2014) used for sample analysis.

4.3.2 Chromatogram

A known volume of the mixtures of internal standard (IS) and reaction mixture samples were injected into Shimadzu GC-2014 gas chromatograph. A typical chromatogram of the internal standard and the chemical components present in the reaction mixture obtained from the cycloaddition reaction of CO_2 and epichlorohydrin (ECH) to produce chloromethyl ethylene carbonate (CMEC) are presented in Figure. 4.3

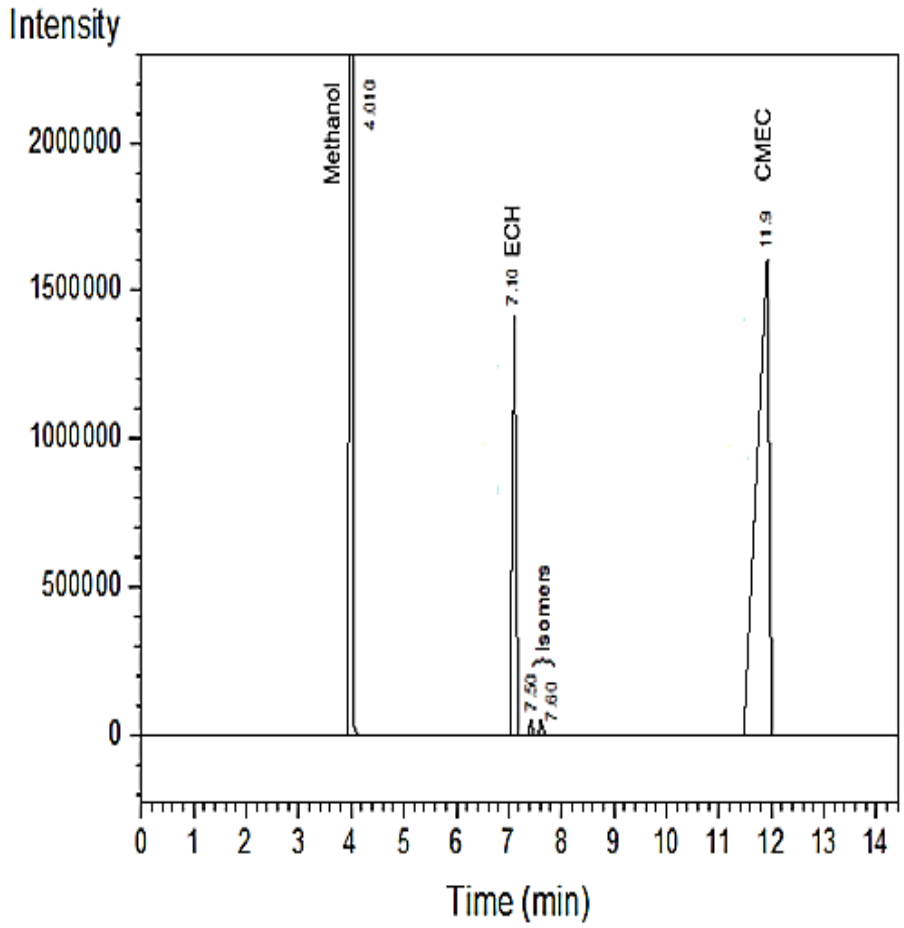

.

Figure 4. 3. A typical chromatogram of a reaction mixture and internal standard analysed by a Shimadzu GC-2014 gas chromatograph.

Methanol peak emerged first at the response time of ~4 min followed by ECH at the response time of ~7min and CMEC at the response time of ~12 min. The total run for each sample for this study was 14 min

4.3.3 Calibration method

In analytical chemistry, a calibration curve is a general method of determining the concentration of an unknown substance by comparing it with the concentration of known samples. This process is called a calibration method. There are three known methods to develop calibration curves, which are the standard addition, internal standards and externals standards. This research has focused on the use of **internal standards (IS)** method of calibration curve.

4.3.4 Preparation of calibration curves

Calibration curves were developed to determine the composition of all the components present in the samples collected from the batch reactor. An internal standards (IS) method was used to develop the calibration curves. To achieve this, several standard samples with known concentrations were prepared and a specific amount of internal standard (IS) was added to each sample. A constant volume of the samples was then injected into a gas chromatograph (GC) for sample analysis. A chromatogram was then obtained for each injected sample and the result was analysed using a GC.

4.3.5 Internal standardisation

An internal standards (IS) method is used in the quantitative analysis of a reaction mixture. This analytical technique compares the responses of an unknown compound in the sample to the response of known standards. In concept, an Internal standard itself is a chemical substance that is added in a constant amount to every sample to

be analysed. It behaves similarly to the analyte provides a signal that can be distinguished from that of the analyte.

The peak area's ratio for each component (A_i) to the internal standard (A_{is}) can be calculated using *equation 4.1*. The concentration ratio of each component (C_i) to the internal standard (C_{is}) can also be calculated using e*quation 4.2*. This formed the calibration curve of area ratio against the concentration ratio of all the components present in the samples. The slope of the curve is known to be the response factor**.** The response factor is useful for the calculation of quantitative percentage conversion and yield of organic carbonates.

$$\textbf{Area ratio (AR)} = \frac{\text{Area of the ith component } (A_i)}{\text{Area of internal standard } (A_{is})} \qquad \textbf{equation 4. 1}$$

$$\textbf{Concentration ratio (CR)} = \frac{\text{Concentration of the ith component } (C_i)}{\text{concentration of internal standard } (C_{is})} \qquad \textbf{equation 4. 2}$$

$$\textbf{Response factor of the ith component } (RF_i) = \frac{\text{Area ratio } (AR_i)}{\text{Concentration ratio } (CR_i)} \qquad \textbf{equation 4. 3}$$

By linearising equation 4.3 to form equation of a straight-line graph.

We obtain:

$$AR_i = RF_i x \; CR_i \qquad \textbf{equation 4. 4}$$

This form equation of a straight line is *y=mx+c* **equation 4. 5**

Where:

y = concentration ratio (CR_i)

m= response factor of the i^{th} component (RF_i)

x =area ratio (AR_i).

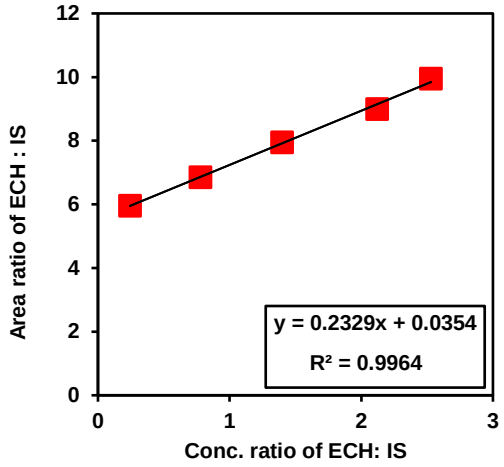

Figure 4. 4. Calibration curve for response factor determination of ECH using methanol as an internal standard

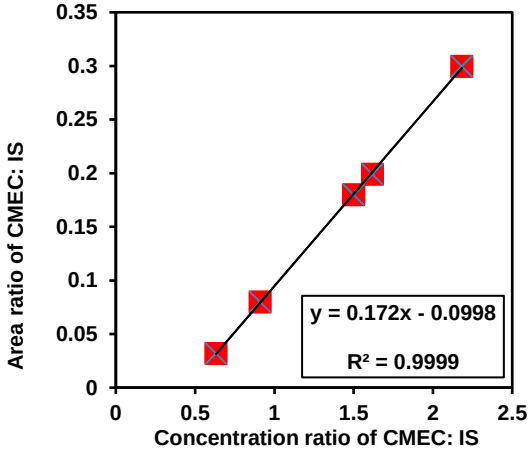

Figure 4. 5. Calibration curve for response factor of CMEC using methanol as an internal standard.

Figures. *4.4* and 4.5 show the calibration curves for ECH and CMEC as prepared respectively, prepared based on known concentration samples. These samples were injected into the GC and a chromatogram was obtained for each of the samples. The peaks area ratios of the three samples were used to calculate the area ratio and response factors for ECH and CMEC. The response factors for ECH and CMEC were 0.9964 and 0.999 respectively.

4.3.5.1 Selection of internal standards

The followings are the guidelines toward the selection of an internal standard:

- The internal standard can be similar in analytical behaviour to the compound of interest but have different signals.
- The internal standard must be miscible with samples that need to be analysed.
- The elute of the used internal standard must be near to the desired product or before the last sample in order to limit processing time. (Saving energy).
- The internal standard must be stable and under the set conditions.

4.3.5.2 Advantages of internal standardisation

- It accounts for routine variation in the response system of the chromatographic.
- It accounts for the variations in the exact volume of sample extract introduced into the system of the chromatographic.
- The retention times of the target compound and the internal standard can be used to obtain the relative retention time (RRT) of the target compound and can as well be used to compensate the shifts for small retention time.

4.3.5.3 Determination of ECH conversion, CMEC yield, and selectivity

The conversion of ECH, CMEC yield and selectivity were determined using equations 4.6, 4.7 and 4.8, respectively.

$$\textbf{ECH Conversion (\%)} = \frac{\text{Initial moles of ECH - Moles of ECH remaining}}{\text{Initial moles of ECH}} \times 100 \qquad \textbf{equation 4. 6}$$

$$\textbf{CMEC Yield (\%)} = \frac{\text{Moles of products formed}}{\text{Initial moles of ECH}} \times 100 \qquad \textbf{equation 4. 7}$$

$$\textbf{Selectivity (\%)} = \frac{\text{CMEC Yield (\%)}}{\text{ECH Conversion (\%)}} \times 100 \qquad \textbf{equation 4. 8}$$

Equation 4.6 was used to calculate the ECH conversion (%) from the difference of the initial moles of ECH and moles of ECH remaining to the initial moles. The result was multiplied by 100% to get the ECH conversion in percentage.

Equation 4.7 was used to calculate the CMEC yield (%) from the ratio of moles of the products formed to the initial moles of ECH. The result was multiplied by 100% to have the CMEC yield in percentage.

Equation 4.8 was used to calculate the selectivity (%) from the ratio of CMEC yield (%) to the ECH conversion (%). The result was multiplied by 100% to get the selectivity in percentage

4.3.6 Preliminary batch experimental studies for the synthesis of cyclic organic carbonate

In chapter 3, we carried out the synthesis of Zr/ZIF-8 catalyst in different ZnZr molar ratios. The as-prepared catalysts were identified as Zr_5/ZIF-8, Zr/ZIF-8 and Zr_{15}/ZIF-8, representing Zn/Zr= 5, 10 and 15 molar ratios, respectively. This sub-section explains the initial batch experimental studies to determine the most suitable Zn/Zr molar ratio of Zr/ZIF-8 catalyst for optimal effectiveness for cycloaddition of epoxide and CO_2.

Table 4. 1. First preliminary batch experiments

Entry	catalyst	Zr/Zn mol ratio	Conversion (%)	Selectivity (%)	Yield (%)
1	$Zr_{0.5}$/ZIF-8	0.5	61	40	21
2	Zr/ZIF-8	1.0	68	59	48
3	$Zr_{1.5}$/ZIF-8	1.5	36	30	10

Model substrate: ECH, reaction conditions: T(313 K) /P(1 bar)/ t(2 h)

Table 4. 2. Second preliminary batch experiments

Entry	catalyst	Zr/Zn Mol ratio	Conversion (%)	Selectivity (%)	Yield (%)
1	$Zr_{0.5}$/ZIF-8	0.5	64	40	23
2	Zr/ZIF-8	1.0	72	63	56
3	$Zr_{1.5}$/ZIF-8	1.5	39	31	12

Model substrate: ECH, reaction conditions: T(318 K)/ P(1.5 bar)/ t(2 h)

Table 4. 3. Third preliminary batch experiments

Entry	catalyst	Zn/Zr Mol ratio	Conversion (%)	Selectivity (%)	Yield (%)
1	$Zr_{0.5}$/ZIF-8	0.5	69	46	21
2	Zr/ZIF-8	1.0	80	67	58
3	$Zr_{1.5}$/ZIF-8	1.5	41	34	16

Model substrate: ECH, reaction condition: T(323 K)/ P(2 bar)/T(2 h)

4.3.7 Carbonate synthesis using ZIF-8 catalyst

The experimental procedure stated in subsection 4.3 has been repeated using ZIF-8 catalyst under the same experimental reaction conditions. This is to enable a more realistic and effective comparison between the catalytic activity of pristine ZIF-8 and as-prepared Zr/ZIF-8 catalysts for the greener synthesis of organic carbonates. Similarly, all the product samples collected from the reactor have been analysed using the same gas chromatography (GC) program as prescribed in subsection 4.3.1.

4.4 Catalytic activity

Theoretical studies from the literature have indicated that the combination of synergetic effects of both acidic and basic sites (Lewis and Brönsted site) existing in the MOF catalysts could contribute to the catalytic performance of the two frameworks. Hence, the catalytic activity of the novel material (Zr/ZIF-8) was compared with pristine ZIF-8 for the cycloaddition reaction of CO_2 and ECH to synthesise CMEC under solvent-free conditions. The reactions have been carried out under the same conditions of 353 K reaction temperature, 8 bar CO_2 pressure, 10% (w/w) catalyst loading, 8 h reaction time and 350 rpm of stirring speed.

Table 4. 4. Summary of catalytic performance of ZIF-8 and Zr/ZIF-8 for coupling reaction of CO_2 and ECH to produce CMEC

Entry	Catalyst	T (K)	EHC Conversion (%)	CMEC Selectivity (%)	CMEC Yield (%)
1	ZIF-8	323	65	57	37
2	ZIF-8	333	69	64	44
3	ZIF-8	343	73	69	49
4	ZIF-8	353	77	74	52
5	ZIF-8	363	81	71	51
6	ZIF-8	373	85	69	49
7	Zr/ZIF-8	323	80	67	58
8	Zr/ZIF-8	333	86	74	64
9	Zr/ZIF-8	343	90	80	70
10	Zr/ZIF-8	353	93	86	76
11	Zr/ZIF-8	363	95	85	75
12	Zr/ZIF-8	373	97	82	72

From Table 4.4, it follows that at optimum CO_2 pressure of 8 bar, the reaction time of 8 h, catalyst loading of 10 % w/w and variable temperature, Zr/ZIF-8 exhibits higher catalytic activity than ZIF-8 (Zr/ZIF-8: 93%, 86%, 76%; and ZIF-8: 77%, 70%, 52%) for conversion, selectivity and yield respectively at the same reaction conditions. The presence of acidic and/or basic sites in heterogeneous catalysts has significantly catalysed the reaction of CO_2 and ECH to produce CMEC (Zhou *et al.*, 2017).

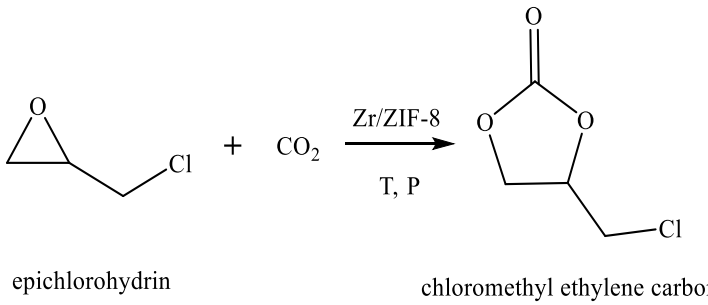

Figure 4. 6. Schematic representation of ECH-CO_2 cycloaddition reaction

4.5 Effect of different heterogeneous catalysts

Catalysts are very important parts of any chemical reaction; they contain active sites, which are able to speed up the kinetics of chemical reaction by reducing the activation energy. Different types of homogenous and heterogeneous catalysts have been synthesised to catalyse the reaction of CO_2 and epoxide to produce corresponding organic carbonates. In order to assess the stability and effectiveness of the samples, the catalytic activity of both ZIF-8 and Zr/ZIF-8 was investigated in the synthesis of chloromethyl ethylene carbonate from CO_2 and epichlorohydrin. Table 4.4 shows the effects of the two catalysts for the conversion of epichlorohydrin, selectivity and yield of chloromethyl ethylene carbonate. The catalyst was synthesised using a solvothermal method as per standard procedures. The sample was heat-treated at about 373 K in order to enhance an improved catalytic activity and were labelled as ZIF-8 and Zr/ZIF-8 for pristine and as-prepared catalysts, respectively. The reaction of CO_2 and ECH to produce CMEC was carried out in a 25 mL high-pressure reactor at 353 K reaction temperature, 8 bar CO_2 pressure, 10% catalyst loading, and 8 h reaction time. It can be seen from Table 4.4 that when ZIF-8 was used to catalyse the reaction of CO_2 and ECH, the conversion of ECH, selectivity, and the yield of CMEC were 77%, 74%, and 52% respectively. However, figure 4.7 shows that incorporating zirconium into ZIF-8 has significantly increased catalytic performance of Zr/ZIF-8 with the conversion of ECH, selectivity and the yield of CMEC being 93%, 86%, and 76% respectively, although, the presence of side products were reported in both reactions

by GC analysis. These side products include 3-chloropropane 1,2-diol and 2,5-bis (chloromethyl)-1,4-dioxane.

With similar pore spaces and same embedded Lewis acid metal sites in both ZIF-8 and Zr/ZIF-8 catalysts, the increase in the catalytic activity of Zr/ZIF-8 may be ascribed to high CO_2 affinity *via* the introduction of zirconium into ZIF-8 frameworks, which has significantly increased its pore spaces (Li *et al.*, 2016). A fine balance of proximity between pristine and Zr -doped MOF was critically examined by Demir et al. (2017b). Their experimental results in the solvent-free coupling reaction of ECH and CO_2 to produce epichlorohydrin carbonate (ECHC) concluded that 79.6% yield of ECHC and 97.3% selectivity were achieved after 2 h using Zr-MOF catalyst (Zr/MOF-53). It is however interesting to note that GC analysis of the product of Zr/ZIF-8 identified 3-chloropropane-1,2-diol (diols of epichlorohydrin- 14.2%) as the main reaction by-products.

To affirm the superior catalytic performance of Zr/ZIF-8 over ZIF-8, nitrogen adsorption and desorption isotherms of the two frameworks were collected and presented in Table 3.1. Zr/ZIF-8 showed higher CO_2 adsorption capacity which explains in part the improved catalytic performance.

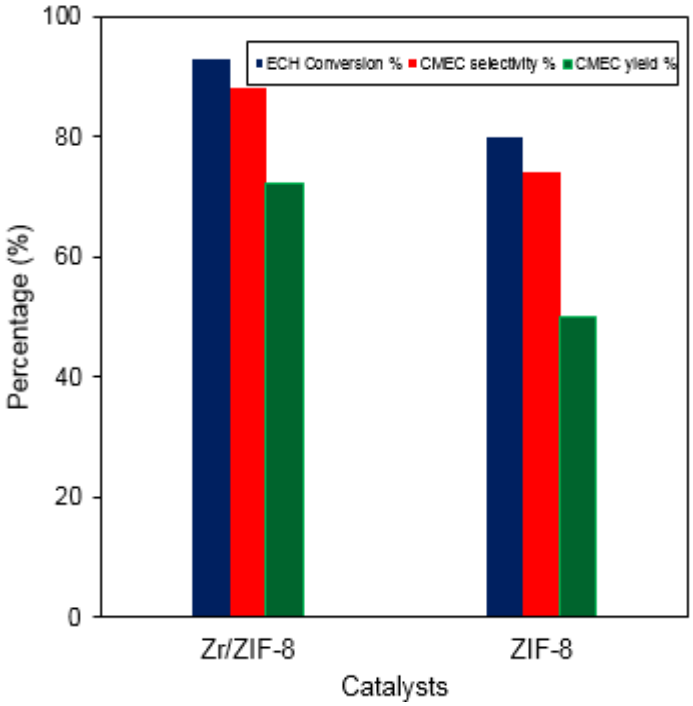

Figure 4. 7. Effect of different catalysts on the cycloaddition reaction of epichlorohydrin (ECH) and carbon dioxide (CO_2) to produce chloromethyl ethylene carbonate (CMEC) with reaction conditions of 353 K reaction temperature, 8 bar CO_2 pressure, 10% catalyst loading, 8 h reaction time, and 350 rpm of stirring speed.

4.6 Results and discussion

4.6.1 Effect of temperature

The cycloaddition reaction of CO_2 and epoxide can be referred to as exothermic in nature. The influence of temperature on the cycloaddition of CO_2 to ECH to produce CMEC was investigated between temperature ranges of 323 to 373 K. All experiments were conducted with optimised reaction conditions, which were determined during our previous studies with a 10% catalyst loading and 8 bar CO_2 pressure for 8 h and a stirring speed of 350 rpm. Table 4.4 shows the catalytic performance of Zr/ZIF-8 and ZIF-8 as a function of temperature, CO_2 pressure, reaction time, and catalyst loading.

It can be depicted from Figures 4.8 and 4.9 that the conversion of epichlorohydrin, selectivity and yield of CMEC were temperature-dependent. Generally speaking, variation in temperature has similar trends in the catalytic activity of both frameworks; the conversion of epichlorohydrin, the selectivity and yield of CMEC increases as temperature increases from 323 to 353 K. However, incorporating zirconium into ZIF-8 has significantly improved the performance of Zr/ZIF-8 with the conversion of ECH, selectivity and yield of CMEC as 93%, 86%, and 76% respectively, while ZIF-8 gave a conversion of ECH, selectivity and yield of CMEC as 77%, 74%, and 52%, respectively, under the same optimum reaction temperature.

Further increase in reaction temperature beyond 353 K was unfavourable to selectivity and yield of CMEC in both systems. A slight decrease of the CMEC yield (from 76% to 75%; Zr/ZIF-8 and 52% to 51%; ZIF-8) was observed upon an increase in temperature. This may be due to the formation of diols and dimers of epichlorohydrin (Abhang *et al.*, 2015) and a small amount of by-products such as polymerised CMEC could also affect the yield. Adeleye, (2015) reported that the increase in the reaction temperature caused a decrease in carbonate yield, due to the decomposition of the catalyst at a higher temperature. Kim et al. (2017) also concluded that the reaction temperature for optimal performance is dependent on the nature of the catalyst employed. Therefore, for this set of experiments, the optimised reaction temperature for both frameworks in the synthesis of chloromethyl ethylene carbonate was 353 K. All the subsequent experiments for the chloromethyl ethylene carbonate were conducted at 353 K.

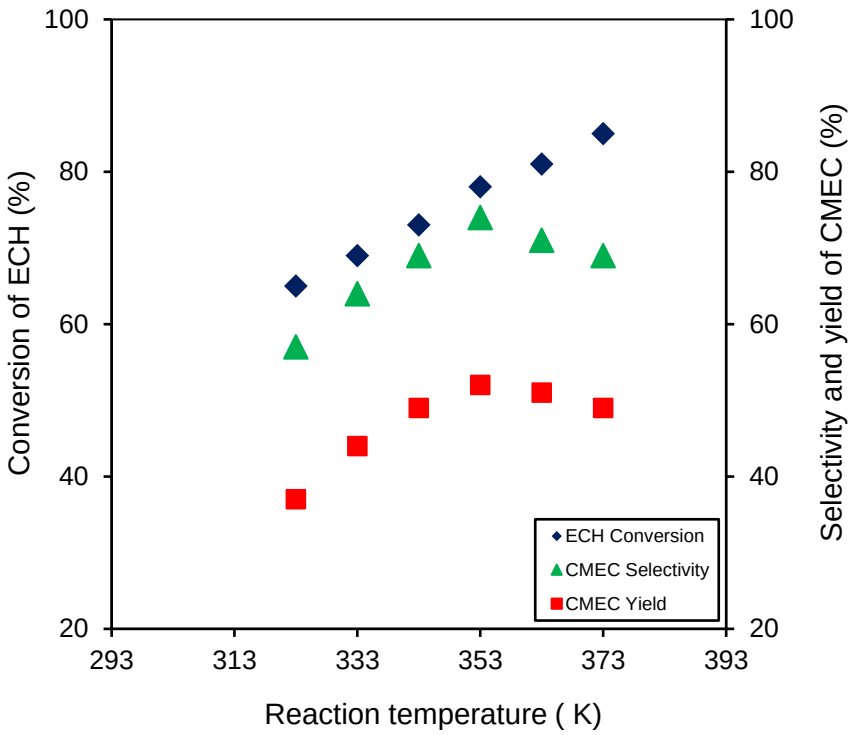

Figure 4. 8. Temperature dependence on the conversion of epichlorohydrin (ECH) versus selectivity and yield of chloromethyl ethylene carbonate (CMEC). Experimental conditions: catalyst used ZIF-8; catalyst loading 10% (w/w); reaction time 8 h; CO_2 pressure 8 bar; stirring speed 350 rpm.

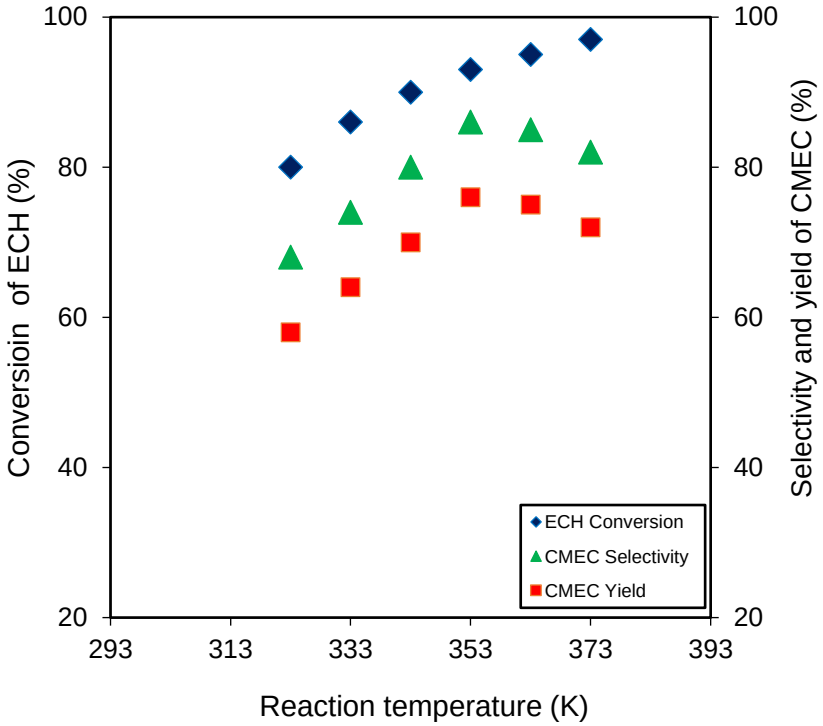

Figure 4. 9. Temperature dependence on the conversion of epichlorohydrin (ECH) *versus* selectivity and yield of chloromethyl ethylene carbonate (CMEC). Experimental conditions: catalyst used Zr/ZIF-8; catalyst loading 10% (w/w); reaction time 8 h; CO_2 pressure 8 bar; stirring speed 350 rpm.

4.6.2 Effect of CO_2 pressure

CO_2 pressure is another important factor influencing the cycloaddition of CO_2 to epoxides. The pressure of carbon dioxide has been established as one of the most crucial factors affecting the conversion, yield, and selectivity of cyclic carbonate (Kim *et al.*, 2013b). The reaction of epichlorohydrin and CO_2 to produce chloromethyl ethylene carbonate was examined by varying the CO_2 pressures. For this study, the experiments were carried out at 353 K, 10% catalyst loading, and 350 rpm for 8 h.

The selectivity and yield of CMEC were found to increase steadily from 67% and 58% to 86% and 76%, respectively, as the CO_2 pressure increases from 2 to 8 bar. These results indicate that the catalytic performance of the Zr/ZIF-8 depends on the concentration of available CO_2 at the reactive sites. Similar variation was observed in the catalytic activity of the two frameworks with changing CO_2 pressure where the selectivity and yield of CMEC increased from 57% and 37% to 77% and 52%, respectively, at the same pressure of 8 bar of CO_2 as in the case of Zr/ZIF-8.

Figures 4.10 and 4.11 demonstrates the dependence of CO_2 pressure on the yield of CMEC. It can be observed from the graph that the CMEC yield increased with increasing pressure, the maximum of the CMEC yield was reached at 8 bar. By increasing the CO_2 pressure more than 8 bar, a negative effect was observed on both reaction systems, where both yield and conversion experience a slight drop. Li et al. (2016) observed that the introduction of too much CO_2 dissolves in epoxide may result in the formation of CO_2-epoxide complex, and retards the interaction resulting in a lower conversion. Similar results were also reported by Xiang et al. (2019), where the introduction of higher pressure of CO_2 dissolved in the epoxide and becomes an unfavourable factor due to the difficulty of separating CO_2 and ECH. This condition inhibits the reaction between ECH and catalyst, thus resulting in lower carbonate yield (Jang *et al.*, 2015). Liang et al. (2017) also reported that many diols and dimers of epichlorohydrin were produced as side products at high pressure. Based on the experimental results and theoretical study, it can be concluded that 8 bar CO_2 pressure was optimum and all subsequent experiments for the CMEC synthesis were carried out at a CO_2 pressure of 8 bar.

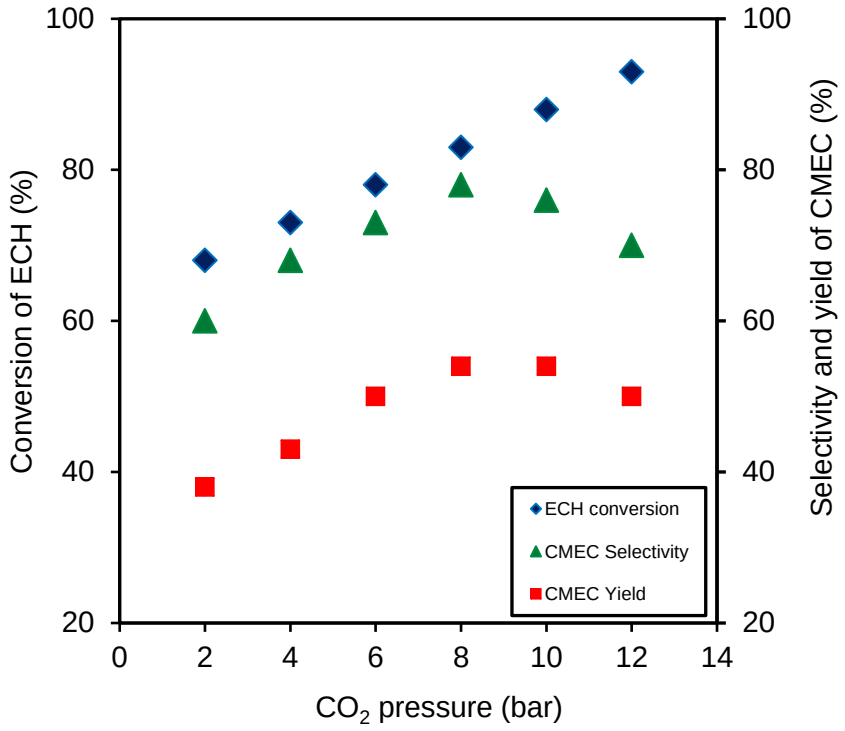

Figure 4. 10. Pressure dependence on the conversion of epichlorohydrin (ECH) *versus* selectivity and yield of chloromethyl ethylene carbonate (CMEC). Experimental conditions: catalyst used ZIF-8; catalyst loading 10% (w/w); reaction time 8 h; reaction temperature 353 K; stirring speed 350 rpm.

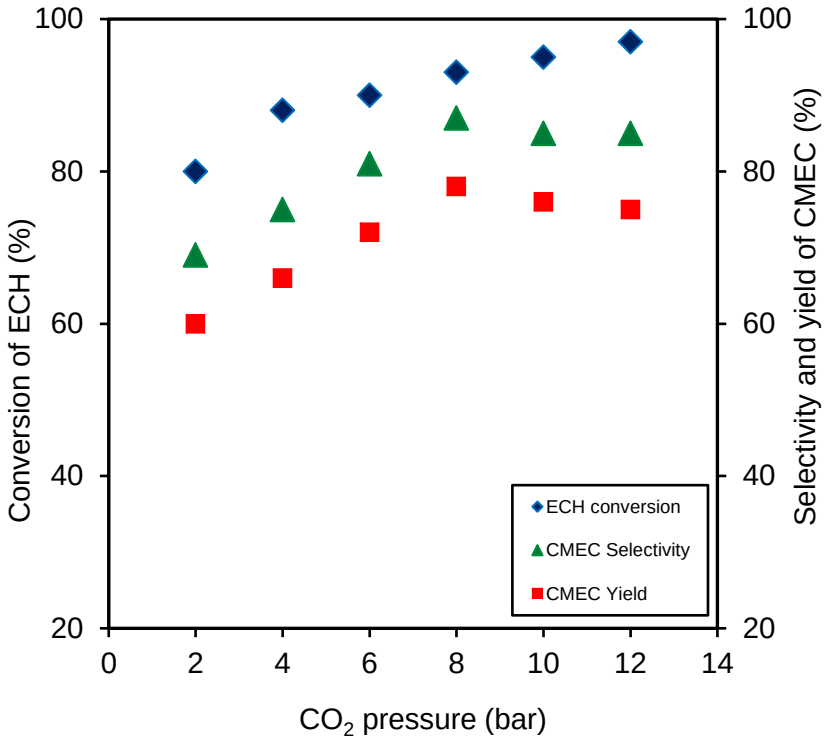

Figure 4. 11. Pressure dependence on the conversion of epichlorohydrin (ECH) versus selectivity and yield of chloromethyl ethylene carbonate (CMEC). Experimental conditions: catalyst used Zr/ZIF-8; catalyst loading 10% (w/w); reaction time 8 h; reaction temperature 353 K; stirring speed 350 rpm.

4.6.3 Influence of reaction time

The effect of varying the reaction time on the yield of CMEC was investigated by carrying out a set of coupling reaction of CO_2 and epichlorohydrin using both ZIF-8 and Zr/ZIF-8 catalysts. For this study, all experiments were conducted at 353 K and 8 bar CO_2 pressure with 10% (*w/w*) catalyst loading of ZIF-8 and Zr/ZIF-8. Figure 4.12 demonstrates the influence of reaction time on CMEC yield and selectivity. The results shown on the graph illustrates that the yield increased continuously at the beginning and reached 76% and 52% within 8 h for Zr/ZIF-8 and ZIF-8, then decreased to 75% and 51% respectively, indicating that a slight change in the reaction condition can

influence the product formation in a reaction. Similarly, the conversion of ECH was observed to increase from 353 to 366 K when the reaction time was increased from 2 to 8 h. However, when the reaction time was increased further to 10 h and above, a progressive decrease in conversion of ECH was recorded. A similar observation was previously reported in the conversion of ECH to chloropropene carbonate with Zn-ZIF-67 by Wang et al. (2011a). According to them, conversion of epoxides reaches an equilibrium plateau at optimum reaction time. This phenomenon is referred to as induction period. The induction period is attained when the CO_2 and epoxides sufficiently diffuse into the catalytic frameworks of the ZIF-material to reach the active sites of the catalyst and then be converted to the organic carbonate. Beyond the induction period, low conversion of epoxides, as well as organic carbonates, may be observed. From Figure 4.12, it can be concluded that prolonged reaction time produces lesser ECH conversion and consequently lesser CMEC yield and selectivity. Based on the experimental results and theoretical study, the reaction time of 8 h was considered the optimum for ZIF-8 and Zr/ZIF-8.

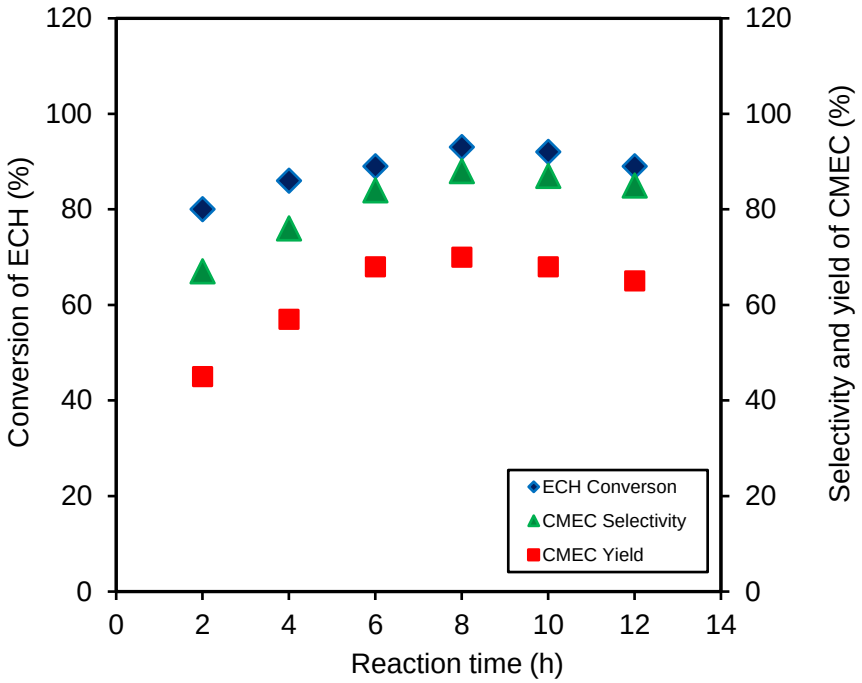

Figure 4. 12. Time dependence on conversion of epichlorohydrin (ECH) versus selectivity and yield of chloromethyl ethylene carbonate (CMEC). Experimental conditions: catalyst Zr/ZIF-8; catalyst loading 10% (w/w); reaction temperature 353 K; CO_2 pressure 8 bar; stirring speed 350 rpm.

4.6.4 Effect of external mass transfer in heterogeneous catalytic processes

Mass transfer limitations play significant roles in chemical reactions by controlling the rate of reaction towards the desired product. In homogenous catalytic reaction, the effect of mass transfer between the phases is mostly negligible. However, in a heterogeneous catalytic reaction, the reaction rate significantly relies on the mass or diffusion between these phases. Mass transfer is typically higher in porous solid or fine particles of nanoscale than large nonporous catalyst (Sathe *et al.*, 2017a) transfer of material from the exterior to the interior of a particle happens through pores that open to the external surface, which provides access to the interior of the crystalline material (Li and Niu, 2011).

In the heterogeneous catalytic conversion of CO_2 and epoxide, the internal and external gradient of transport materials between system phases lowers the activity and selectivity of the catalyst towards the desired product (Dibenedetto *et al.*, 2011). It is important to know that when designing a new catalyst and directing such a catalyst to be selective towards a particular desired product mass transfer resistance and kinetics are key functions. In cycloaddition reaction of CO_2 with ECH (Jang *et al.*, 2015), the physicochemical properties of the catalyst and the operating conditions all have a direct effect on the activity of the catalyst as well as the quality of CMEC formed. When a chemical reaction occurs on an active surface, intraparticle diffusion takes place through the pores and the film surrounding the solid catalyst (Mousavi *et al.*, 2017).

The coupling reaction of ECH with CO_2 to produce chloromethyl ethylene carbonate is an exothermic reaction. In order to reduce or eliminate the effects of mass transfer resistance, it is recommended to employ a highly porous heterogeneous catalyst (Al-Qaisi *et al.*, 2016). The influence of mass transfer on the reaction of ECH and CO_2 to synthesize CMEC at 353 K reaction temperature for 8 h with a range of stirring speed between 320 and 550 rpm in an autoclave reactor. It was observed that there was no significant change in the conversion of ECH (~93), selectivity (~86), and the yield of CMEC (~76) when the stirrer speed was maintained above 330 rpm. Therefore, it was concluded that there was no effect of external mass transfer resistance on the experimental conditions.

4.6.5 Effect of catalyst loading

To investigate the influence of catalyst loading on the CMEC synthesis, several numbers of experiments were performed by varying the molar ratio of both ZIF-8 and Zr/ZIF-8 catalyst to ECH. For this study, all experiments were conducted at 353 K and 8 bar CO_2 pressure for 8 h. The results of varying catalyst loading are presented in Figure 4.13. It can be observed from the graph that by increasing the catalyst loading,

there was a corresponding increase in ECH conversion, yield, and selectivity of CMEC. For example, for the experiments conducted with catalyst loadings from 2.5%–7.5%, there was a significant increase in ECH conversion, yield, and selectivity of CMEC. Also, for the experiment conducted at 10% (*w/w*) of catalyst loading, there was a sharp increase of ECH conversion, yield, and selectivity of CMEC from 90%–96%, 45%–56%, and 73%–79%, respectively. According to Maeda et al. (2014), the decrease in epoxide conversion may be ascribed to a decrease in the substrate concentration around the pore cavities of the catalyst at higher catalyst loading. This effect neutralizes the Brönsted acid centers of the catalyst, thereby preventing the interaction between the acidic sites of the catalyst and the oxygen atom of epoxide from the ring-opening. This consequently reduces the epoxide conversion to organic carbonates. Considering the percentage error of ±2%, it can be concluded that the number of active sites for ECH and CO_2 to react and produce CMEC was large enough at 10% (*w/w*) catalyst loading. From the results obtained with respect to catalyst loading, 10% (*w/w*) was the optimum. From the experimental results for both ZIF-8 and Zr/ZIF-8 catalysts, it is satisfactory to conclude that 10% (*w/w*) catalyst loading was considered the optimum and further experiments were carried out at 10% (*w/w*) catalyst loading.

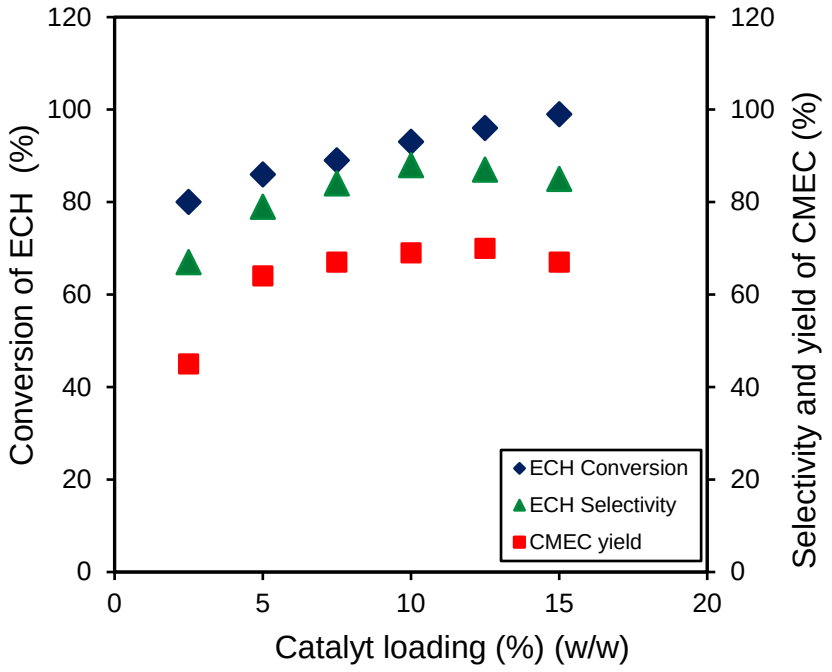

Figure 4. 13. Catalyst loading dependence on conversion of epichlorohydrin (ECH) *versus* selectivity and yield of chloromethyl ethylene carbonate (CMEC). Experimental conditions: catalyst Zr/ZIF-8; reaction temperature 353 K, (w/w); reaction time 8 h; CO_2 pressure 8 bar; stirring speed 350 rpm**.**

4.6.6 Effect of reaction conditions on catalyst selectivity to chloromethyl ethylene carbonate

The effect of varying reaction temperature on catalysts' selectivity towards CMEC was demonstrated in Figures 4.8 and 4,9. For example, it was observed that when the temperature was increased from 323 to 353 K, both catalysts show a corresponding increase in selectivity from 68% and 50% to 86% and 74%, respectively. However, when the temperature was increased beyond the 353 K, a marginal decrease in

selectivity was observed in both frameworks, demonstrating that the 353 K was the optimum temperature for the reaction. Meanwhile, the gas chromatography-mass spectroscopy (GC-MS) analysis of the samples shows that 17.3% of 2,5-bis (chloromethyl)-1,4-dioxane (by-product) formed at 353 K, this may explain in part why a drop in catalysts' selectivity was recorded for both samples. Similar results and by-products have been previously reported with ZIF-8 by Carreon, (2012). He also agreed that almost 100% selectivity of ZIF-8 to chloropropene carbonate was achieved at a temperature of 393 K, but decreased to 78.6% when the temperature was increased to 403 K.

In addition to the effect of temperature on catalysts' selectivity, the influence of varying CO_2 pressure on catalysts' selectivity was also investigated. According to Figures 4.10 and 4.11, the selectivity of the catalysts towards CMEC was found to increase steadily from 67% and 58% to 86% and 76%, respectively, as the CO_2 pressure was increased from 2 to 8 bar. These results indicate that the activity and selectivity of both catalysts were influenced by the concentration of available CO_2 at the reactive sites. Although, a similar effect was observed in the responses of both catalysts to variation in CO_2 pressure, however, the results show that Zr/ZIF-8 has higher selectivity than the ZIF-8 catalyst, where the selectivity of both catalysts increased from 69% and 60% to 87% and 77%, respectively, for Zr/ZIF-8 and ZIF-8catalysts. Conversely, both samples experienced a decline in selectivity from 87% and 77% to 85% and 70% for ZIF-8 and Zr/ZIF-8, respectively, when the CO_2 pressure was increased beyond the optimum level of 8 Bar.

Miralda et al. (2012a), further argued that ZIF-8 is a dual-functional catalyst with both acidic and basic sites that have been associated with the Lewis acid Zn^{2+} ions and the basic imidazole groups, respectively. This bifunctional characteristic enhances the catalyst selectivity for cycloaddition reaction. In a separate report, (Stewart, (2015),

also ascertained that it is likely that Lewis acid sites associated with Zn^{2+} ions in the ZIF-8 framework play a vital role in catalysing the reaction of epichlorohydrin and CO_2 to chloropropene carbonate. They further explained that the presence of basic nitrogen atoms of the imidazole ligand, probably, favours the adsorption and binding of CO_2 as well as activation of the carbon-oxygen bonds in CO_2**.** In agreement with other similar doped ZIF-8, the open metal centers in the Zr/ZIF-8 has the potential to easily activate the epoxides and the basic sites present in the frameworks. This could be the reason for the higher selectivity that was observed in the solvent-free ECH–CO_2 cycloaddition reactions under mild conditions. Comparatively, the higher selectivity of Zr/ZIF-8 than ZIF-8 towards CMEC may be attributed to the presence of zirconium (Zr). According to a 2019 publication by de Caro et al. (2019), the effect of Zr doping on Mg-Al hydrotalcite, the catalyst has significantly increased its selectivity from 90% to >99% towards glycerol carbonate (GC).

4.7 Reusability of ZIF-8 catalysts

Reusability is an important and essential feature of any heterogeneous catalyst in order to be considered useful in industrial applications (MacIas *et al.*, 2012b). The influence of catalyst reusability on the catalytic properties of ZIF-8 and Zr/ZIF-8 in the cycloaddition reaction was investigated. The experiments were carried out in a high-pressure reactor at optimum reaction conditions, i.e., at 353 K, 8 bar with fresh 10% (*w/w*) ZIF-8 catalyst loading, for 8 h, and at a stirring speed of 350 rpm. The catalysts after Run 1 in the cycloaddition reaction were washed with ethanol and acetone, centrifuged, and oven-dried at 343 K for 12 h before reuse. The recovered catalysts were reused for up to 7 subsequent experiments following the same experimental procedure. ZIF-8 showed a progressive loss in catalytic activity after each run as shown in Figure 4.14, while Zr/ZIF-8 (Figure 4.15) exhibited no loss of activity indicating the catalyst stability for cycloaddition reaction of CO_2 epichlorohydrin. Yuan et al. (2016) stated that the presence of dopant in ZIF-8 show that zirconium is more stable and resilient during the reaction. There was no significant change in the

conversion of ECH, selectivity, and yield of CMEC using Zr/ZIF-8. Although, a very slight decrease in the yield of CMEC from 70% (fresh) to 69% (first recycled) was observed. The low catalytic activity of the recycled Zr/ZIF-8 catalyst may be ascribed to the formation of carbonaceous materials during the cycloaddition reaction as previously reported by Liang et al. (2019b). Furthermore, the XRD and FT-IR analyses results confirmed that Zr/ZIF-8 maintained its crystallinity throughout the reaction process.

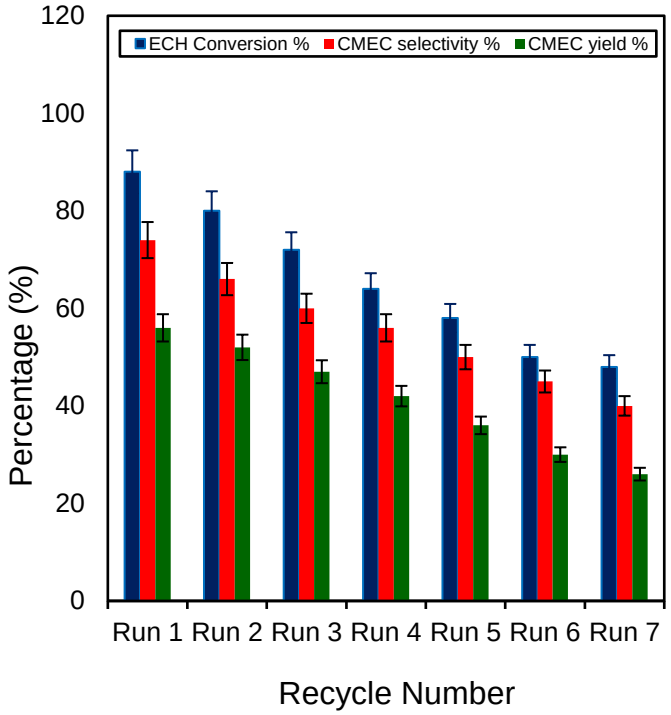

Figure 4. 14. Catalyst reusability studies on conversion of epichlorohydrin (ECH), selectivity and yield of chloromethyl ethylene carbonate (CMEC). Experimental conditions: catalyst: used: catalyst used ZIF-8; catalyst loading 10% (w/w); reaction temperature 353 K; CO_2 pressure 8 bar; reaction time 8 h; stirring speed 350 rpm.

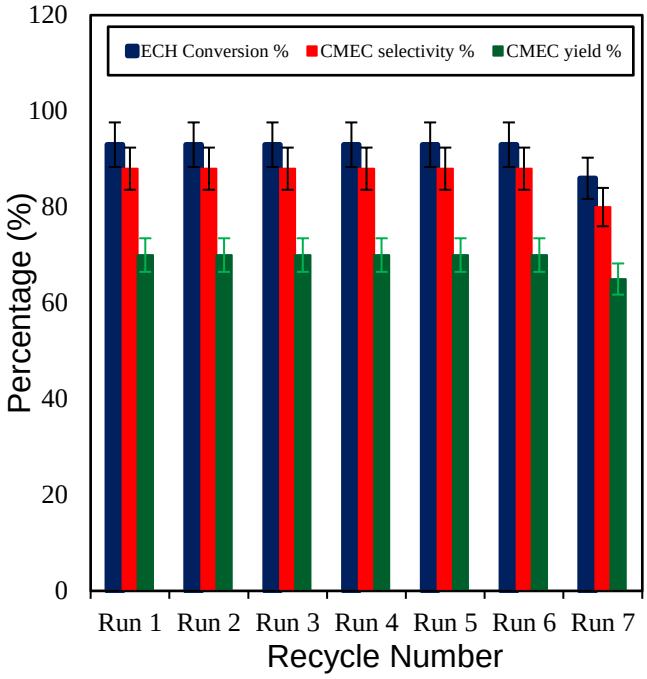

Figure 4. 15. Catalyst reusability studies on conversion of epichlorohydrin (ECH), selectivity and yield of chloromethyl ethylene carbonate (CMEC). Experimental conditions: catalyst used: Zr/ZIF-8; catalyst loading 10% (w/w); reaction temperature 353 K; CO_2 pressure 8 bar; reaction time 8 h; stirring speed 350 rpm.

4.8 Conclusions

Zr/ZIF-8 has been successfully designed and assessed as a greener and highly efficient CO_2-reduction catalyst for the synthesis of CMEC. Although ZIF-8 is criticised by many researchers as thermally unstable for the synthesis of organic carbonates from CO_2 and epoxide, however, our experiments have confirmed that the introduction of zirconium into ZIF-8 could strengthen the weak functionality, making it tenable for large-scale industrial applications. Several authors have utilised zirconium to reinforce different kinds of MOF experiments in order to achieve optimum results. However, their attempts have been unsatisfactory, partly because a firm balance between the required percentage of zirconium dopant and their host molecules was not established

for those particular experiments. It may also be worth mentioning that this work has utilised a 10% dopant of zirconium for such a tremendous catalytic activity of Zr/ZIF-8. The stability tests carried out on both samples show that Zr/ZIF-8 demonstrates higher stability compared with single metal ZIF-8.

It has been concluded from the experimental results that there is a direct relationship between variation in the reaction conditions and ECH conversion, CMEC yield, and selectivity. From the experimental results, it can be observed that Zr/ZIF-8 catalyst displayed high epoxide conversions and high selectivity to chloromethyl ethylene carbonate at 353 K, without using any solvent or co-catalyst. Lewis acid copper (II) sites in the ZIF-8 frameworks promote adsorption of CO_2 on the solid surface and its further conversion to CMEC. The activity of the reused Zr/ZIF-8 catalyst showed consistent stability over seven subsequent runs. The optimum reaction condition for the experiments was found at 353 K, 8 bar CO_2 pressure, and 8 h using fresh 10% (*w/w*) Zr/ZIF-8 catalyst loading for this reaction. Therefore, the development of a novel Zr/ZIF-8 catalyst for the synthesis of CMEC from CO_2 and ECH provided an efficient and promising greener route for CO_2 utilisation

Chapter 5

Multiobjective optimisation for the greener synthesis of CMEC by CO_2 and ECH *via* response surface methodology

Outline of the chapter

Following the experimental synthesis of CMEC in the preceding chapter, this chapter gives a concise account of process optimisation *via* response surface methodology.

The chapter is organised as follows:

5.1. Introduction

5.2. One-factor-at-a-time analysis (OFAT)

5.3. Multiobjective experimental design

5.4. Results and discussions

5.5. Effects of one-factor-at-a-time experiments on responses

5.6. Interactive effects of process variables on responses

5.7. Multiobjective process optimisation

5.8. Conclusions

5 Multiobjective optimisation for the greener synthesis of CMEC by CO_2 and ECH via response surface methodology

5.1 Introduction

In chapter 4, the experimental synthesis of chloromethyl ethylene carbonate was discussed in detail. This included the effect of individual reaction variables on ECH conversion as well as CMEC yield and selectivity. In this chapter, a statistical analysis with response surface methodology (RSM) has been used to investigate and optimise process variables for the greener synthesis of chloromethyl ethylene carbonate (CMEC) by carbon dioxide (CO_2) and epichlorohydrin (ECH).

Within the context of chemical engineering, low product yields have been attributed to a number of factors including the use of unsuitable choice of catalyst (JK *et al.*, 2017), problems achieving the right optimum reaction conditions (Olaniyan *et al.,* 2020), and inappropriate application of other input parameters (Manohar *et al.*, 2013). In recent years, optimising system variables to improve product yields has been the focus of many different fields of research. Response surface methodology (RSM) is a collection of statistical and mathematical techniques based on the multivariate non-linear model for optimising processes (Jeirani *et al.*, 2012). RSM has received considerable interest in many industrial processes in an attempt to construct empirical models able to correlate the statistical relationships (if any) between a set of variables making up an industrial system (Khuri and Mukhopadhyay, 2010). Saada et al. (2018) have successfully modelled and optimised the synthesis of organic carbonates with five independent variables at three-level (3^5) factorial design. Their results have been validated using regression analysis.

Several authors including Aboelazayem et al. (2018a) and Onyenkeadi et al. (2019a), have criticised the traditional “trial-and-error” optimisation methods and “one-factor-at-a-time” (OFAT) as time-consuming and considered quite expensive due to a large number of samples and experimental trials involved. Another drawback identified with traditional optimisation methods is low overall efficiency (Kumar *et al.*, 2017). Sadeghi et al. (2018), describes OFAT as a method that excludes the interactive effects among the variables and does not express the complete effects of the parameters on the process. In order to overcome these drawbacks, Yu and He, (2017) suggested multivariate statistical techniques, which are full three-level factorial designs: Box-Behnken designs, central composite designs, and Doehlert designs.

A multivariate optimisation technique is a statistical tool for analysing complex non-linear processes. This is especially useful when interactions are not known or optimal process parameters are to be determined in order to make a process more robust (Yuan *et al.*, 2015). It is cost-effective as fewer experimental trials are required, high computational efficiency (Nwabueze, 2010), and it requires very little or no human experience to obtain accurate and satisfactory results (Mostafaei *et al.*, 2015). Therefore, the systematic application of RSM optimisation for the catalytic conversion of epichlorohydrin (ECH) and carbon dioxide (CO_2) to chloromethyl ethylene carbonate (CMEC) can be regarded as an innovative way of CO_2 utilisation.

In the present research work, using the design expert software, a quadratic model was developed to study the effect of the interaction between four selected independent variables and two reaction responses. The adequacy of the model was validated by the correlation between the experimental and predicted values of the responses using an Analysis of Variance (ANOVA) method. The proposed Box-Behnken Design (BBD) method suggested 29 runs for data acquisition and modelling the response surface.

The optimum reaction conditions of 353 K, 8 bar CO_2 pressure and 8 h using fresh 10% (w/w) Zr/ZIF-8 catalyst loading produced 93% conversion of ECH and 76% yield of CMEC. It was concluded that the predicted and experimental values are in excellent agreement with ±1.55% and ±1.54% relative errors from experimental results for both the conversion of ECH and CMEC yield, respectively. Therefore, statistical modelling using RSM can be used as a reliable prediction tool for system optimisation for greener synthesis of chloromethyl ethylene carbonate via CO_2 utilisation.

5.2 One-factor-at-a-time (OFAT) analysis

OFAT analysis was developed to determine the preliminary effective range of the selected parameters for statistical analysis. The effect of four-single factors (temperature, pressure, reaction time, and catalyst loading) was evaluated for the synthesis of chloromethyl ethylene carbonate. The OFAT analysis investigated all the four parameters in the following range: Reaction temperature K (313, 323, 333, 343, 353, 363, 373); pressure (bar) (4, 6, 8, 10, 12, 14, 16); catalyst loading (%) (*w*/*w*) (5, 7.5, 10, 12.5, 15); reaction time (h) (4, 6, 8, 10, 12, 14, 16).

5.3 Experimental design

Based on the OFAT results, a three-level, four-factor (3^4) factorial design with 29 runs of experiments were suggested for this study in order to determine the responses (conversion and yield). In this design, all four factors were varied simultaneously over a set of experimental runs. To avoid bias, the suggested set of experiments was carried out randomly and the four factors, temperature, pressure, catalyst loading, and reaction time have been labelled as x_1, x_2, x_3, *and* x_4, respectively as shown in Table 5.1. The variables and their coded and uncoded values are presented with each level and range as given below in Table 5.1 (i.e., −1, 0, 1).

Table 5. 1. Experimental design variables and their coded levels

Variables	Code	Range and Levels		
		−1	0	+1
Temperature (K)	x_1	313	353	373
Pressure (bar)	x_2	4	8	16
Catalyst loading (*w*/*w*)	x_3	5	7	15
Time (h)	x_4	4	8	16

The total number of experiments (N) is given by eq. 5.1

$$N = k^2 + K + C_p \quad \text{eq. 5.1}$$

Where k is the number of independent variables, Cp is the replicate number of the center point.

5.3.1 Statistical analysis

The empirical mathematical model showing the effect of the independent variables x_1, x_2, x_3, and x_4 on the predicted response Y was investigated using the second-order polynomial regression equation with backward elimination.

A quadratic equation derived using RSM for the model is shown using eq. 5.2:

$$Y = b_o + \sum_{i=1}^{n} b_i x_i + \sum_{i=1}^{n} b_{ii} x_i^2 + \sum_{i=1}^{n-1} \sum_{j>1}^{n} b_{ij}\, x_i x_j + \mathcal{E} \quad \text{eq. 5.2}$$

where Y is the predicted response, x_i and x_j are the independent variables in coded levels ($I \neq j$), b_i, b_{ii}, and b_{ij} are the coefficients for linear, quadratic, and interaction effects, respectively, b_0 is the model coefficient constant, n is the number of factors, and $\mathcal{E}$ is the model random error (Saada *et al.*, 2018).

The adequacy of the predicted models was validated by a number of statistical tools such as correlation coefficient (R^2), adjusted coefficient of determination (R^2_{adj}), and the predicted coefficient of determination (R^2_{pred}). The statistical significance of the predicted model was analysed by (ANOVA) using a regression coefficient by conducting Fisher's F-test at a 95% confidence level (Gallardo-Fuentes *et al.*, 2016). Design Expert 11 software (Stat-Ease Inc., Minneapolis, MN, USA) was used for the design of experiment, regression, and graphical analysis. Statistical significance of the results has been presented by $p < 0.05$ and mean ± SE. The fit quality of the polynomial equation has been proved by R^2.

Table 5. 2. Experimental design matrix with the actual and predicted responses

Run	T x_1 (K)	P x_2 (bar)	t x_3 (h)	Catalyst Loading x_4 (*w*/*w*)	Actual ECH Conv. (%)	Predicted ECH Conv. (%)	Actual CMEC Yield (%)	Predicted CMEC Yield (%)
1	313	4	8	7	42	46.33	16	14.63
2	353	8	16	5	67	68.17	33	32.29
3	353	8	8	7	84	84.00	64	64.00
4	313	16	16	7	58	59.88	29	31.67
5	353	8	8	7	84	84.00	64	64.00
6	353	8	4	5	52	55.67	26	26.46
7	353	4	16	7	75	72.96	40	41.04
8	313	8	8	5	54	55.79	23	24.88
9	353	16	16	7	93	93.29	65	66.04
10	313	8	8	15	58	56.46	31	30.38
11	353	16	8	5	86	81.21	36	35.00
12	373	16	8	7	86	81.67	45	46.13
13	373	4	8	15	75	82.33	54	57.63
14	353	16	8	15	88	91.38	68	68.00
15	373	8	4	7	68	62.38	38	33.33
16	353	8	8	7	84	84.00	64	64.00
17	373	8	16	15	90	85.38	64	60.67
18	373	16	8	5	54	59.29	26	28.88
19	313	16	8	7	90	82.67	55	51.13
20	373	8	8	15	86	87.96	64	64.38
21	353	4	4	7	68	64.46	35	36.21
22	353	8	8	15	84	84.00	64	64.00
23	353	8	8	7	84	84.00	64	64.00
24	353	16	4	15	70	75.79	35	36.21
25	313	8	4	15	52	52.88	23	24.33
26	353	8	16	15	89	85.33	65	64.29
27	353	4	8	5	66	58.88	37	33.50
28	353	4	8	15	77	78.04	44	43.00
29	373	8	4	15	69	67.83	35	35.46

Table 5. 3. Analysis of variance of the developed model for ECH

Source	Sum of square	Diff.	Mean Square	F Value	p-value	Significance
Model	5014.09	14	362.01	11.21	< 0.0001	HS
x_1-temperature	827.75	1	827.75	26.02	0.0001	HS
x_2-pressure	854.08	1	854.08	27.10	< 0.0001	HS
x_3-catalyst loading	871.33	1	871.33	18.68	0.0006	HS
x_4-reaction time	619.00	1	619.00	21.58	0.0005	HS
x_1x_2	308.25	1	308.25	9.44	0.0060	HS
x_1x_3	177.00	1	177.00	4.98	0.0283	S
x_1x_4	58.00	1	58.00	1.95	0.1842	NS
x_2x_3	18.25	1	18.25	0.62	0.4451	NS
x_2x_4	38.25	1	38.25	1.29	0.2754	NS
x_3x_4	5.15	1	5.15	0.19	0.6691	NS
x_1^2	789.39	1	789.39	25.73	0.0001	HS
x_2^2	4.16	1	4.16	0.15	0.7030	NS
x_3^2	353.82	1	353.82	11.13	0.0049	S
x_4^2	336.95	1	336.95	9.40	0.0061	S
Residual	448.08	14	34.86			
Lack of Fit	448.08	10	44.81	0.44	0.56	NS
Pure Error	0.000	4	0.000			
Cor Total	5553.17	28				

S: significant.

NS: not significant.

HS: highly significant

Table 5. 4. Analysis of variance of the developed model for CMEC yield.

	Sum of square	Diff.	Mean Square	F Value	p-value	Significance
Model	7335.55	14	431.90	68.68	< 0.0001	HS
x_1-temperature	1023.00	1	1023.00	139.85	< 0.0001	HS
x_2-pressure	468.75	1	468.75	60.53	< 0.0001	HS
x_3-catalyst loading	1260.75	1	1260.75	162.80	< 0.0001	HS
x_4-time	901.33	1	901.33	116.39	< 0.0001	HS
x_1x_2	576.00	1	576.00	74.38	< 0.0001	HS
x_1x_3	225.00	1	225.00	29.05	< 0.0001	HS
x_1x_4	100.00	1	100.00	12.91	0.0029	HS
x_2x_3	119.00	1	119.00	15.62	0.0014	HS
x_2x_4	146.25	1	146.25	20.18	0.0005	HS
x_3x_4	128.25	1	128.25	17.08	0.0010	HS
x_1^2	1258.78	1	1258.78	176.11	< 0.0001	HS
x_2^2	347.29	1	347.29	42.52	< 0.0001	HS
x_3^2	897.34	1	897.34	128.27	< 0.0001	HS
x_4^2	897.05	1	897.05	120.62	< 0.0001	HS
Residual	104.24	14	7.87			
Lack of Fit	104.24	10	10.43	1.35	0.325	NS
Pure Error	0.000	4	0.000			
Cor Total	7444.79	28				

S: significant.

NS: not significant.

HS: highly significant

5.4 Results and discussion

5.4.1 Analysis of Variance (ANOVA)

An analysis of variance (ANOVA) was performed using the Design-Expert software in order to investigate the fitness and significance of the model for each regression coefficient. The empirical analysis of RSM model used to correlate the interactive relationship between the controlling factors (x_1, x_2, x_3, *and* x_4) and the predicted response *Y* (conversion of ECH and yield of CMEC) are shown in Table 5.2 above. The results of the experimental trials at various process conditions show the range of the responses from 42% to 93% of ECH conversion and 16% to 68% of CMEC yield. This trend is consistent with the results published by Onyenkeadi and colleagues. The predicted values sufficiently correlate with the observed values and fit the RSM model design for this study. The best-fitting model was established by a regression analysis using Design-Expert software. Fitting of the data to various models (linear, two factors interactions (2FI), quadratic, and cubic polynomials) and their following analysis of variance (ANOVA).

5.4.2 Development of regression model

In this study, the purpose of using the RSM was to generate a statistical model that demonstrated mutual interaction between the responses and the effective variables. Through the experimental matrix generated in a randomised run of experiments, the obtained responses are given using a second-order polynomial regression equation with backward elimination as shown below. The equations show the empirical relationship between the conversion of ECH and the yield of CMEC and the experimental factors in coded forms.

$$Y_1 = 84.15 + 8.75\,x_1 + 8.86\,x_2 + 7.22\,x_3 + 7.500x_4 - 9.005\,x_1x_2 + 7.25\,x_1x_3 + 4.15\,x_1x_4 - 2.150\,x_2x_3 + 2.10\,x_2x_4 + 1.10\,x_3x_4 - 11.45\,x_1^2 + 0.80x_2^2 - 7.10\,x_3^2 - 7.30\,x_4^2 \quad (1)$$

$$Y_2 = 64.15 + 9.10\,x_1 + 6.30\,x_2 + 10.30\,x_3 + 8.70\,x_4 - 12.15\,x_1x_2 + 7.25\,x_1x_3 + 5.25\,x_1x_4 + 5.40\,x_2x_3 + 6.30\,x_2x_4 + 5.60\,x_3x_4 - 14.40\,x_1^2 - 7.55\,x_2^2 - 12.75\,x_3^2 - 12.15x_4^2 \quad (2)$$

Y_1 and Y_2 are the response variables: ECH conversion and CMEC yield. The independent variables are x_1, x_2, x_3, and x_4 which are reaction temperature, pressure, catalyst loading, and reaction time, respectively. The results of interaction effects between the independent variables were deduced as follows: Temperature-pressure; x_1x_2, temperature-catalyst loading; x_1x_3, temperature-reaction time; x_1x_4, pressure-catalyst loading; x_2x_3, pressure–time; x_2x_4 and catalyst loading–reaction time; x_3x_4. Finally, the excess of each independent variable was represented as follows: Temperature-temperature; x_1^2, pressure-pressure; x_2^2, catalyst loading-catalyst loading; x_3^2 and reaction time-reaction time; x_4^2.

5.4.3 Statistical analysis of regression model

The response model calculated for this study has demonstrated a high degree of accuracy with an R^2 of 0.9973 and an R^2_{adj} of 0.9954 at a confidence level of 95%. This agrees well with the result of Onyenkeadi et al. (2018), where the determination coefficient values, R^2 and R^2_{adj}, for the reliability of the model fitting, were calculated to be 0.9932 and 0.9658, respectively. Mäkelä, (2017) also suggested that a good model fit should yield an R^2 of at least 0.8. Furthermore, the values of R^2 and R^2_{adj} are close to 1.0. This demonstrates that a mutual correlation exists between the experimental and the predicted values. Therefore, the statistical significance of the

second-order polynomial equation for this design shows that the regression model is statistically significant ($p < 0.0001$) and the lack of fit test is non-significant ($p > 0.05$) relative to the pure error.

The following assumptions have been used to conclude the statistical adequacy checking of the model based on the ANOVA results. The first assumption is the similarity between the predicted and actual data of the two models as shown in Figures 5.1 and 5.2. This demonstrated that the variations between the experimental and predicted values of the ECH conversion and CMEC yield are statistically non-significant (NS), hence the predicted model can be said to show a high level of accuracy and adequacy. Another assumption is the normality of the residuals. The plot of residuals has been investigated using a normal plot where most of the points approximately form a straight line as shown in both Figures 5.3 and 5.4. This shows that residuals for both ECH conversion and CMEC yield are in a normal distribution. This assumption is consistent with the report of Muthusamy et al. (2019). Thirdly, the randomisation of the residuals has also been assessed using a plot between the residuals versus predicted responses. The random distribution shows a lack of clear structure with a normal distribution at zero mean and variance (Zhu *et al.*, 2018). It can be observed in Figures 5.5 and 5.6 that points above and below the diagonal line show areas of over or under prediction with no definite structure.

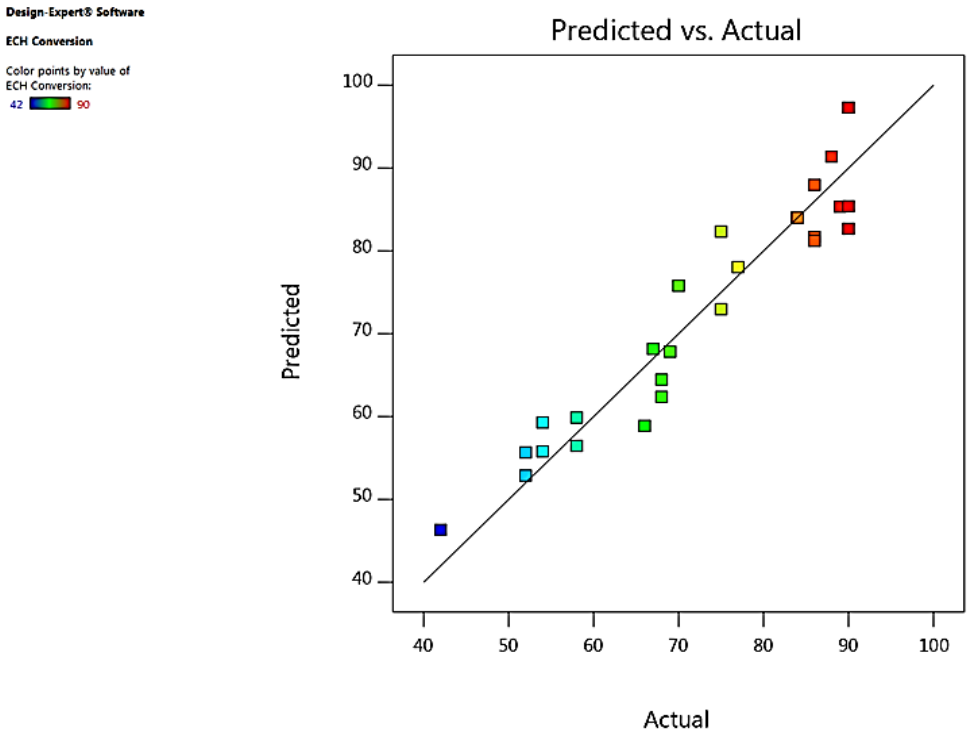

Figure 5. 1. Predicted *versus* actual values models for ECH conversion

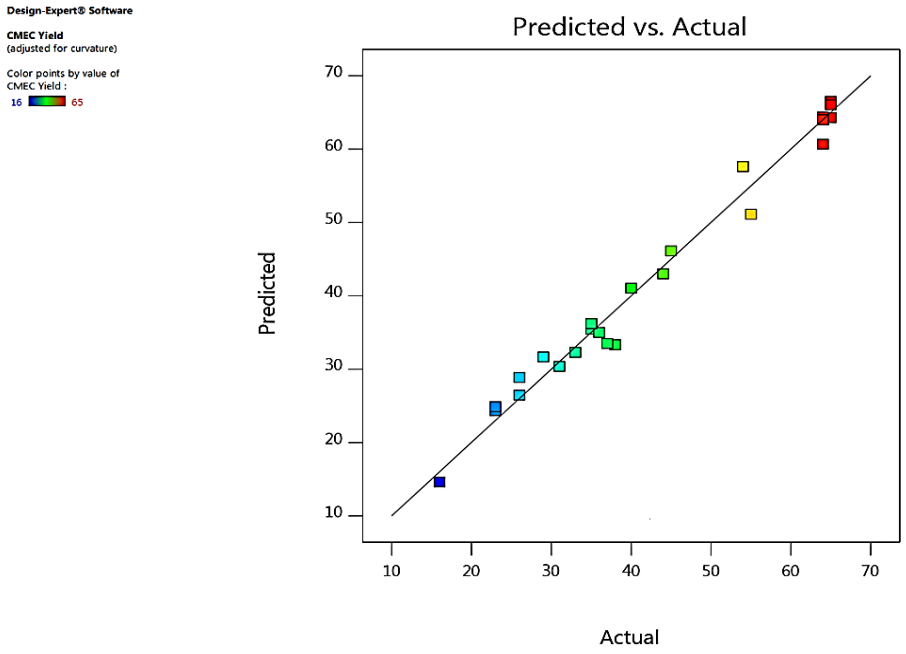

Figure 5. 2. Predicted *versus* actual values models for CMEC yield

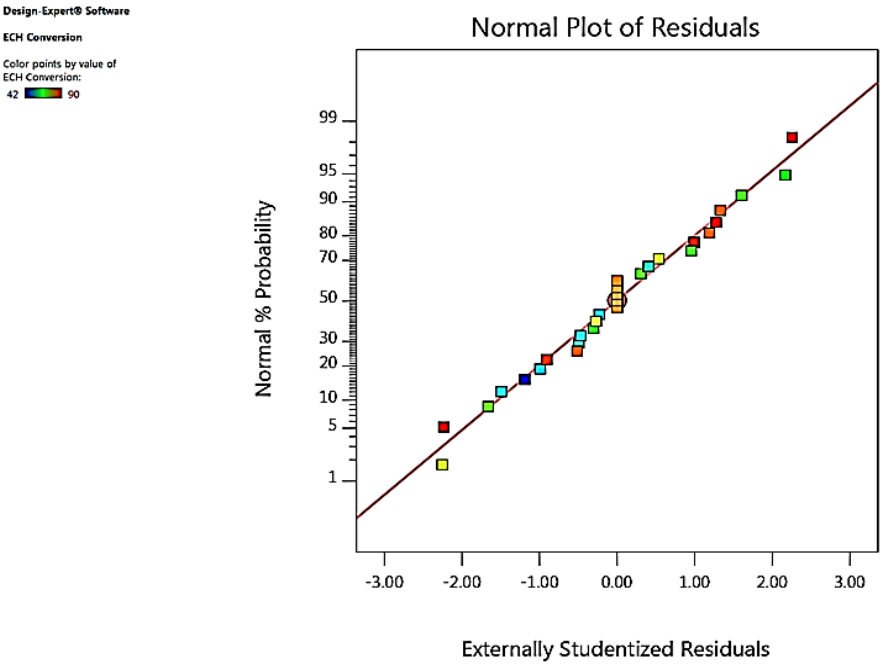

Figure 5. 3. Normal plot of residuals for ECH conversion

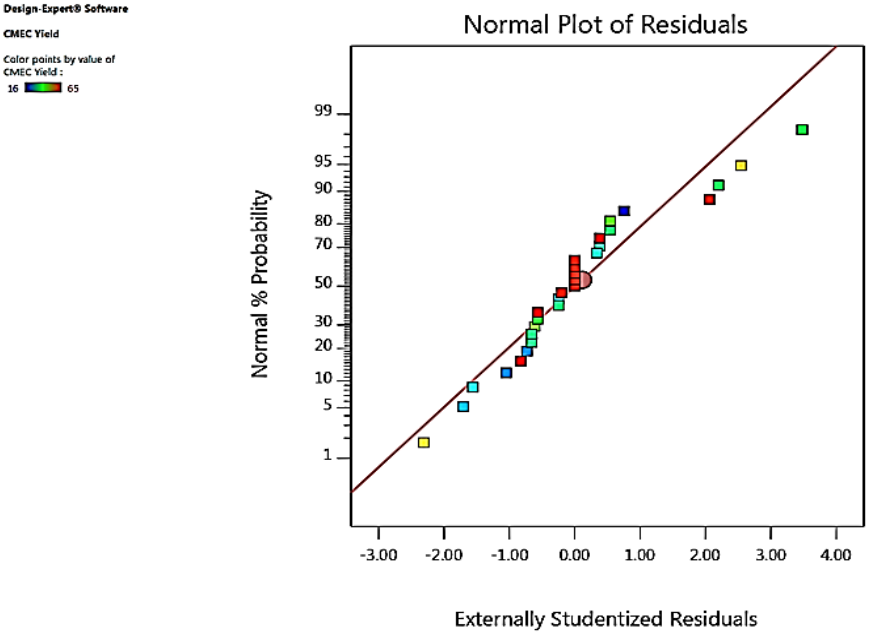

Figure 5. 4. Normal plot of residuals for CMEC yield

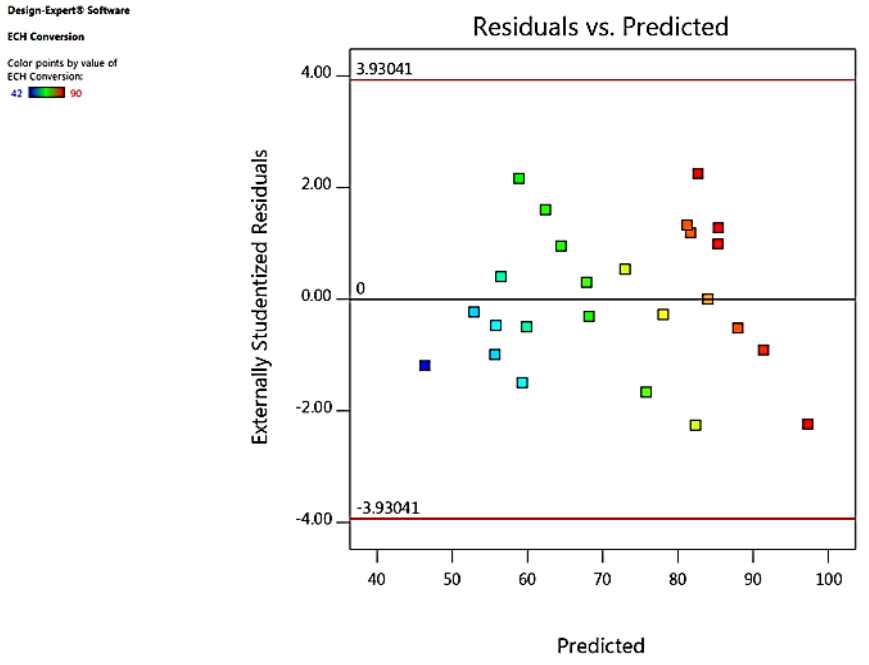

Figure 5. 5. The plot of residuals *versus* predicted response for ECH conversion

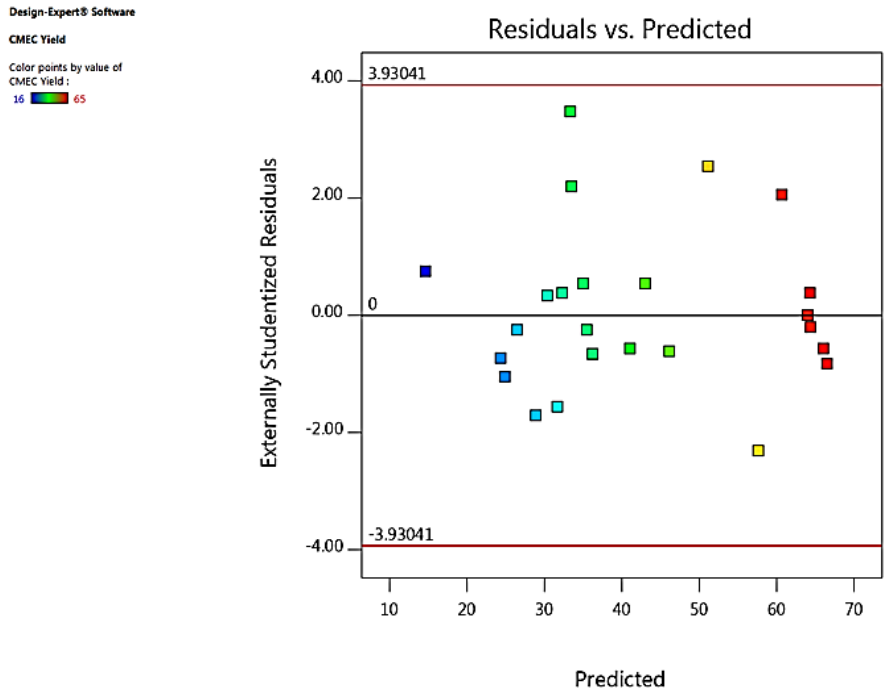

Figure 5. 6. The plot of residuals *versus* predicted response for CMEC yield.

In order to verify the model for fitting and adequacy test at a 95% confidence level, it was necessary to apply Analysis of variance (ANOVA). As shown in Tables 5.3 and 5.4, the ANOVA results indicated a good model fit with the model. F-value is 0.44 (Table 5.3) and the probability > F of less than 0.0001 implied that this model was significant. The lack of fit test (non-significant: $p > 0.05$) was also considered a good statistical indicator for the model adequacy checking as it relates the residual error to the pure error from the replica design point (Lee *et al.*, 2014). As indicated in ANOVA Tables 5.3 and 5.4, the conversion of ECH and CMEC yield was significantly ($p < 0.05$) influenced by the interactive and quadratic effects of all the independent variables.

5.4.4 Model fitting and adequacy checking

In order to verify the model for fitting and adequacy test at a 95% confidence level, it was necessary to apply Analysis of variance (ANOVA). As shown in Tables 5.3 and 5.4, the ANOVA results indicated a good model fit with the model. F-value is 0.44 (Table 5.3) and the probability > F of less than 0.0001 implied that this model was significant. The lack of fit test (non-significant: $p > 0.05$) was also considered a good statistical indicator for the model adequacy checking as it relates the residual error to the pure error from the replica design point (Lee *et al.*, 2014). As indicated in ANOVA Tables 5.3 and 5.4, the conversion of ECH and CMEC yield was significantly ($p < 0.05$) influenced by the interactive and quadratic effects of all the independent variables.

5.4.5 Response surface plots analysis

After the regression models had been built and model adequacy checking was tested, 3D response surface plots and their corresponding 2D contour plots were drawn for a model equation. Different shapes of the contour plots indicate different levels of interaction between two variables. For example, an oval plot represents significant interactions between the two selected variables while a circular plot means otherwise (Khuri and Mukhopadhyay, 2010). According to Rabiee and Mahanpoor, (2018), 3D response surface promotes understanding of system behaviour. It is also significant in recognising the characters of the response surface (Long *et al.*, 2019).

5.5 Effect of one factor at a time experiment on responses (OFAT)

The effects of individual reaction variables (temperature, pressure, time, and catalyst loading) and their interactions on reaction responses (conversion and yield) have been investigated using the 3D-surface and 2D-contour plots generated from the predicted quadratic model as evidenced in Figures 5.7–5.10. The experiments have been

carried out by varying one reaction parameter at a time while keeping other parameters constant at the following reaction conditions: Reaction temperature 353 K, CO_2 pressure 11 bar, reaction time 12 h, catalyst loading 12% (*w*/*w*).

Although, both ECH conversion and CMEC yield have been used by RSM for system optimisation. However, for the reasons of consistency and to enable quantitative evaluation in the overall system optimisation, only CMEC yield has been focused in this section for variable determination process.

5.5.1 Effect of reaction temperature

To a significant extent, it is largely agreed that a directly proportional relationship exists between temperature and CMEC yield as shown in the results of ANOVA in Table 5.4. The influence of reaction temperature on CMEC yield has been investigated by varying temperature over the range of 323 K to 373 K. As evidenced in Figure 5.7, CMEC yield increased steadily from 40% to 68% as temperature increased from 323 K to 353 K. However, a gradual decrease in CMEC yield was observed at higher temperature values beyond 353 K. This may be due to the formation of diols and dimers of epichlorohydrin above optimum temperature (Mohammadifard and Amiri, 2018). Chen et al. (2014) explained that higher reaction temperatures caused a shift in the equilibrium to the reactant side and resulted in a reduced DMC yield. The same temperature effect was also reported by Kilic et al. (2018); they have observed that as they increased the reaction temperature from 348 K to 373 K (while keeping other variables constant), there was a corresponding increase in ECHC yield from 65.8% to 97.0%. However, a further increase in temperature beyond 373 K, caused a slight decrease both in the ECHC yield and catalyst selectivity.

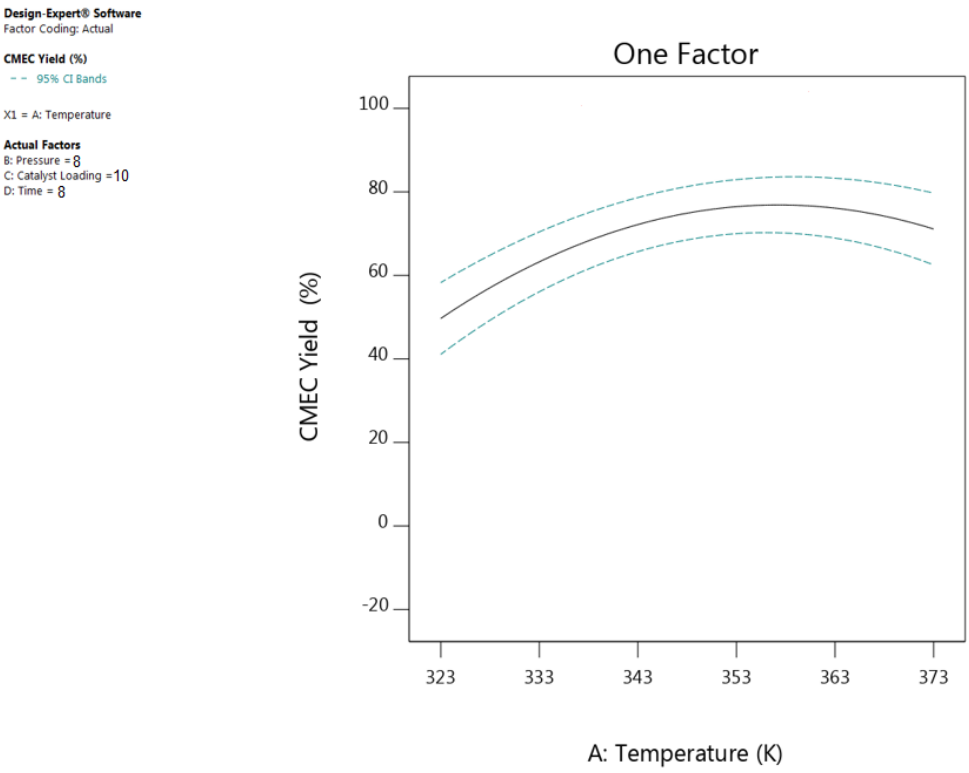

Figure 5. 7. The plot showing the effect reaction of temperature on CMEC yield.

5.5.2 Effect of CO_2 pressure

ANOVA Table 5.4 demonstrates the dependence of CO_2 pressure on CMEC yield, since CO_2 acts both as reactant and reaction medium simultaneously (Abhang *et al.*, 2015). As indicated in Figure 5.8, when CO_2 pressure was increased from 8 to 11 bar, the CMEC yield also increased from 50% to 68%. Conversely, with the CO_2 pressure of 11.5 bar, a 59% CMEC yield was recorded indicating a declining effect. Zhong et al. (2014) demonstrated the effect of variation in CO_2 pressure on organic carbonates. They have enhanced more propylene carbonate (PC) yield when CO_2 pressure was increased from 1 MPa to 3 MPa. However, when CO_2 pressure was further increased to 4 MPa, they observed that the concentration of propylene oxide (PO) in the gas

phase had decreased as a result of dilution by CO_2 and consequently resulted in a reduced PC yield. It is therefore concluded that the optimum CO_2 pressure based on OFAT analysis for this set of experiments was 11 bar of CO_2 pressure.

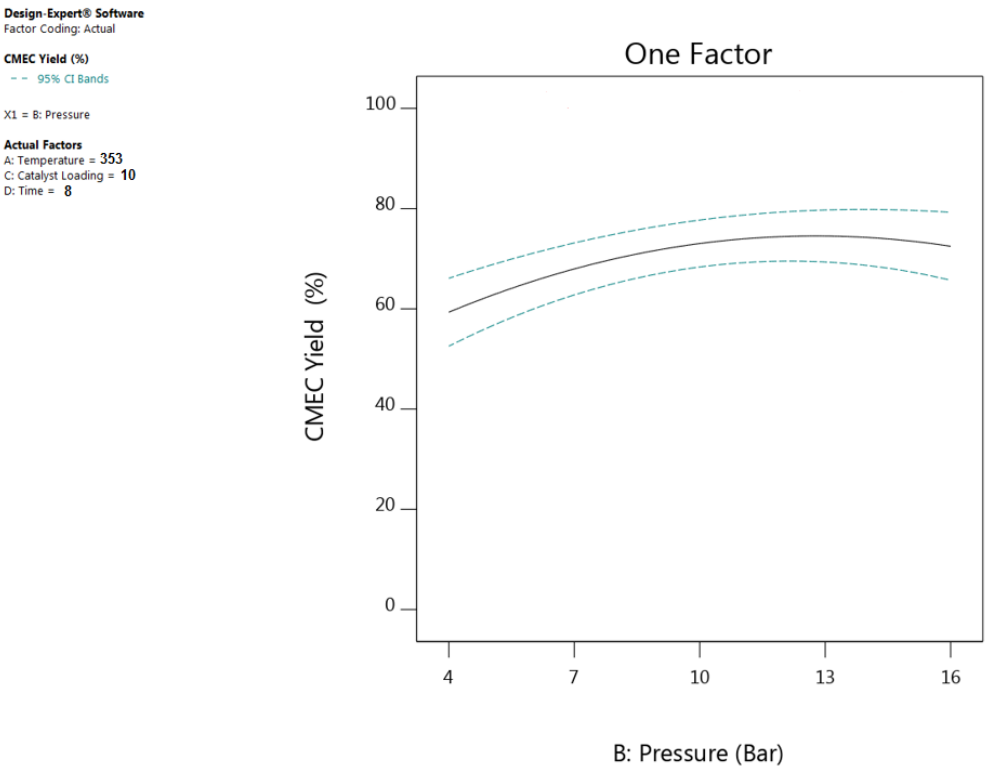

Figure 5. 8. The plot showing the effect of CO_2 pressure on CMEC yield.

5.5.3 Effect of reaction time

Reaction time is one of the crucial factors in a catalytic reaction. Figure 5.9 shows a direct proportionality effect between reaction time and the CMEC yield; the yield increased gradually as the reaction time increased until it reached 68% in 12 h. Further increase in reaction time beyond 12 h resulted in a continuous decline in CMEC yield as shown in Figure 5.9. This could be as a result of the formation of polymerised CMEC

caused by prolonged reaction time (Shi *et al.*, 2013). A similar phenomenon was also reported by Onyenkeadi et al. (2018), where an increase in reaction time from 8 to 16 h was directly proportional to butylene carbonate (BC) yield. However, prolonged reaction time beyond this time resulted in a decrease in BC yield.

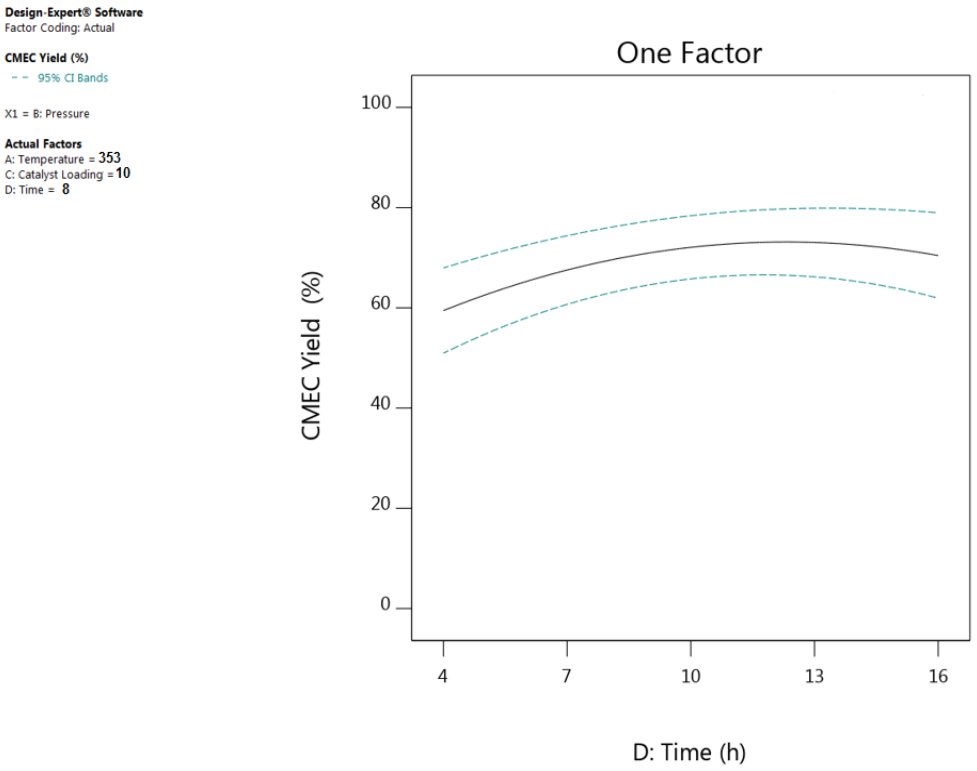

Figure 5. 9. The plot showing the effect of reaction time on CMEC yield

5.5.4 Effect of catalyst loading

The effect of catalyst loading on CMEC yield was investigated by varying Zr/ZIF-8 loading from 5% to 15% (*w*/*w*). As shown in Figure 5.10, it can be observed that as catalyst loading was increased, CMEC yield also increased proportionally from 42% reaching a maximum of 68% at 12% (*w*/*w*) catalyst loading. It was then decreased progressively when the amount of catalyst was further increased to 13% (*w*/*w*),

indicating that optimum catalyst loading had been exceeded. It would be expected that the number of active sites available for the reaction of ECH and CO_2 would increase as catalyst loading increased (Xuan *et al.*, 2018). However, Han et al. (2019) argued that an excessive increase in catalyst loading tends to provoke the formation of undesirable side-products (in their experiment, a by-product of diglyceride (GDL) or triglyceride (GTL) was formed), thereby causing a drop in glycerol monolaurate (GML) selectivity as they increased the amount of catalyst beyond 2% (*w*/*w*). Similarly, in the present work, an increase in the amount of catalyst loading beyond the optimum level was unfavourable to the reactive system resulting in a reduced CMEC yield. Therefore, the optimum catalyst loading for this reactive system is 12% at a reaction temperature of 353 K for 12 h at 11 bar of CO_2 pressure.

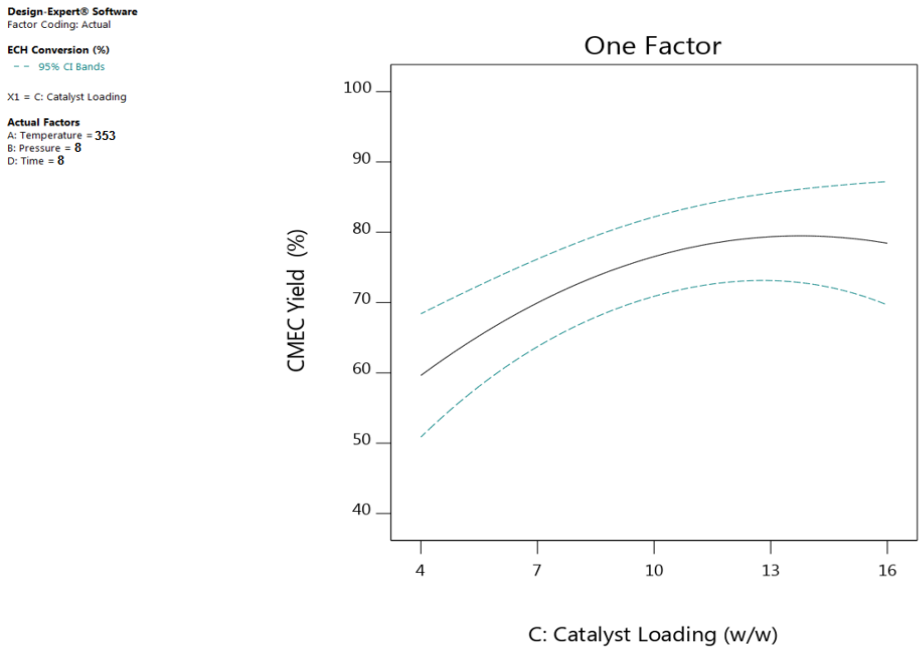

Figure 5. 10. The plot showing the effect of catalyst loading on (a) ECH conversion and (b) CMEC yield.

5.6 Interactive effect of process variables on responses

The interaction effect of each pair of reaction variables has been investigated using ANOVA results, 3D surface, and 2D contour plots. The interaction effect of some process variables on ECH conversion and CMEC yield produce different effects at different levels of other variables. Therefore, 3D plots have played a crucial role in making accurate predictions about process optimisation (Bahrami *et al.*, 2019). From ANOVA Tables 5.3 and 5.4, it can be observed that all the four reaction parameters are deemed significant and can affect the process response tremendously at different levels of interaction. Hence, the interactive effect of process variables has a direct influence on system optimisation. The interaction effect between a pair of variables would be negligible if the contour plot of the response surface is circular. Conversely, the effect of the interaction would be significant if the contour plot is elliptical (Nandiwale and Bokade, 2014). Therefore, instead of studying single variable (as in conventional method) the interactions were investigated which is significant for a comprehensive optimisation study.

5.6.1 Interactive effect of temperature and pressure

As depicted in Figure 5.11 and the ANOVA Tables 5.3 and 5.4, the interaction effect of reaction temperature and CO_2 pressure has played significant roles in both ECH conversion and CMEC yield (while keeping reaction time and catalyst loading at their optimum: 12 h and 12% (*w*/*w*), respectively). At lower reaction temperature (e.g., at 323 K), an increase in the CO_2 pressure from 4 to 16 bar increases the CMEC yield from 47% to 68%. However, higher reaction temperature beyond 353 K showed a negative effect on CMEC yield (Figure 5.11); this could be as a result of the formation of by-products at elevated temperature as indicated in the reaction mechanism (Figure 3.11). However, at a different level of interaction between temperature and pressure (e.g., from 358 K to 373 K and 13–16 bar), a notable effect was also recorded where

there was a gradual decline in the CMEC yield indicating optimum condition had been exceeded. This shows that variation in reaction temperature had a negative effect on both responses at higher values. Therefore, the temperature-pressure relationship has a significant effect on process responses. Similarly, the elliptical shape of the 2D contour plot in Figure 5.12 exemplifies a mutual interactive effect of the reaction variables on responses.

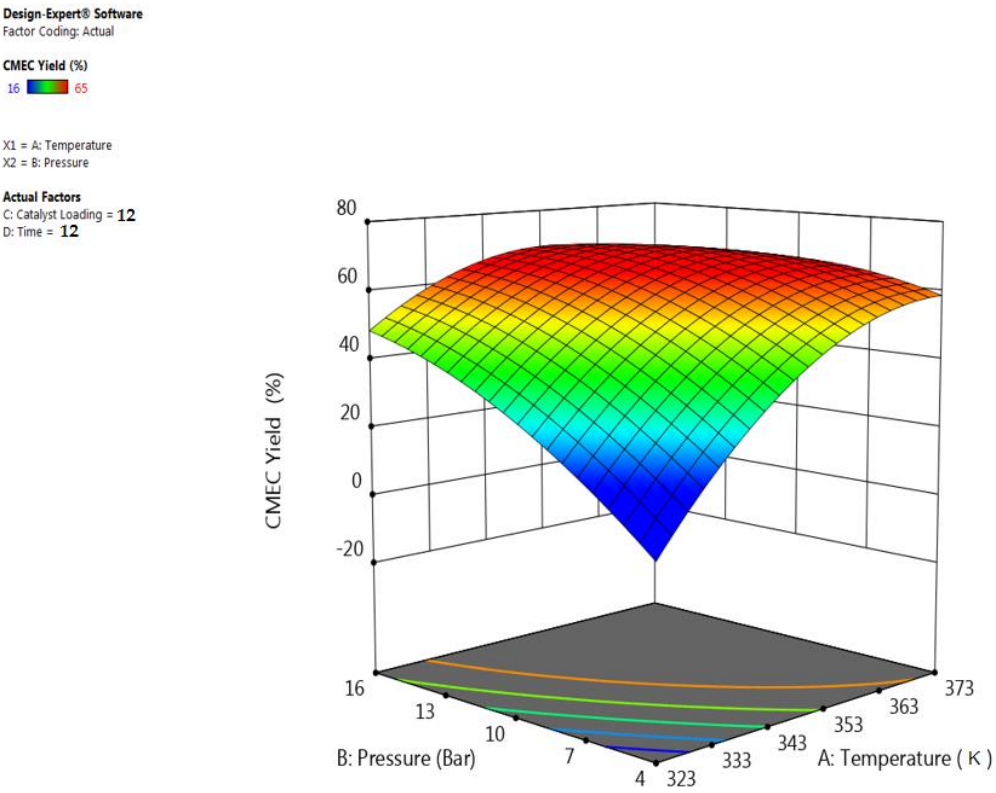

Figure 5. 11. 3D response surface plot showing the effect of temperature and pressure on CMEC yield

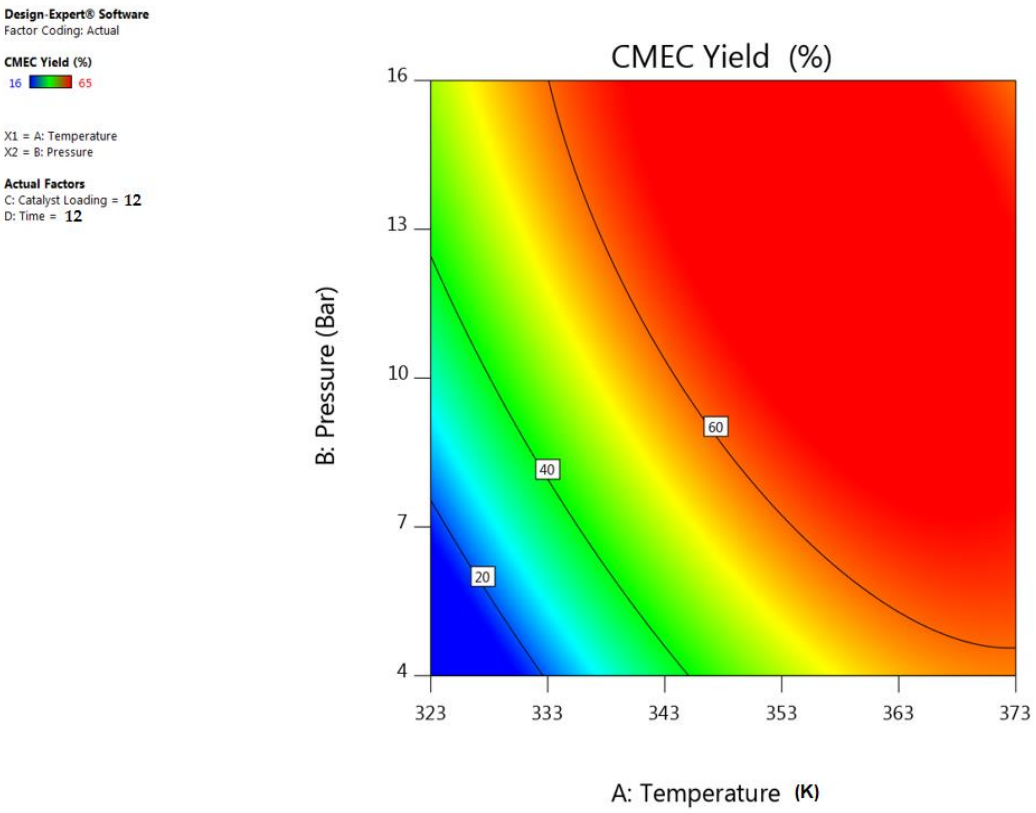

Figure 5. 12. Contour plot showing the effect of temperature and pressure on CMEC yield

5.6.2 Interactive effect of temperature and time

Figure 5.13 illustrates the interaction effect of reaction time and temperature on CMEC yield (while keeping the other two variables at their optimum: Catalyst loading: 12% (*w*/*w*), CO_2 pressure: 11 bar). The surface plot suggested that the CMEC yield was highest (68%) at a reaction time of 12 h and a temperature of 353 K, indicating that an increase in the reaction temperature from 313 K to 353 K favours ECH conversion and consequently enhances CMEC yield as shown in Figure 5.13. However, an increase in reaction temperature beyond 353 K at 12 h of reaction time was unfavourable to the reactive system causing a marginal drop in CMEC yield from 68% to 65%. Onyenkeadi

et al. (2017) reported that the formation of oligomers and isomers are possible at extended reaction time at a higher temperature. Product quality and stability may also be affected due to chemical degradation or losses by thermal decomposition at higher reaction temperatures (Peng *et al.*, 2018). Response surface and contour plots in Figures 5.13 and 5.14, respectively clearly show that CMEC yield had a linear effect with increasing reaction temperature until the optimum condition was achieved. This phenomenon agrees with the Arrhenius law (Redissi and Bouallou, 2013); higher temperature results in a higher conversion rate and consequently leading to higher CMEC yield. It can be concluded from the ANOVA Table 5.4 that the reaction temperature was found to be a highly influencing parameter on both the conversion of ECH and CMEC yield as evident from low *p*-value (<0.0001).

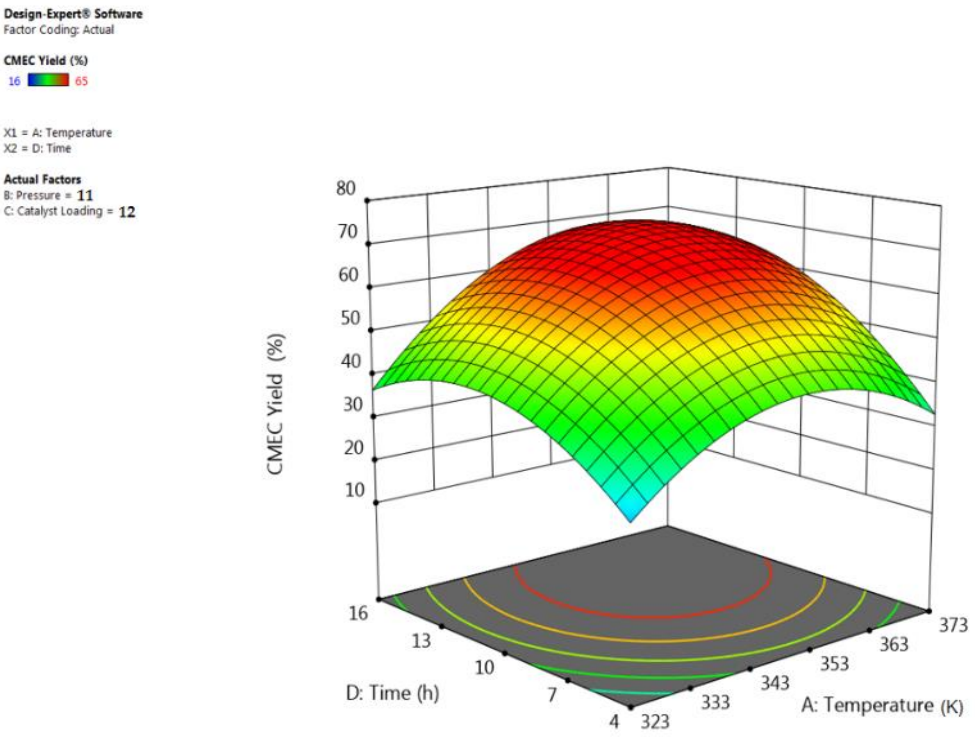

Figure 5. 13. 3D response surface of the effect of reaction time and temperature on CMEC yield

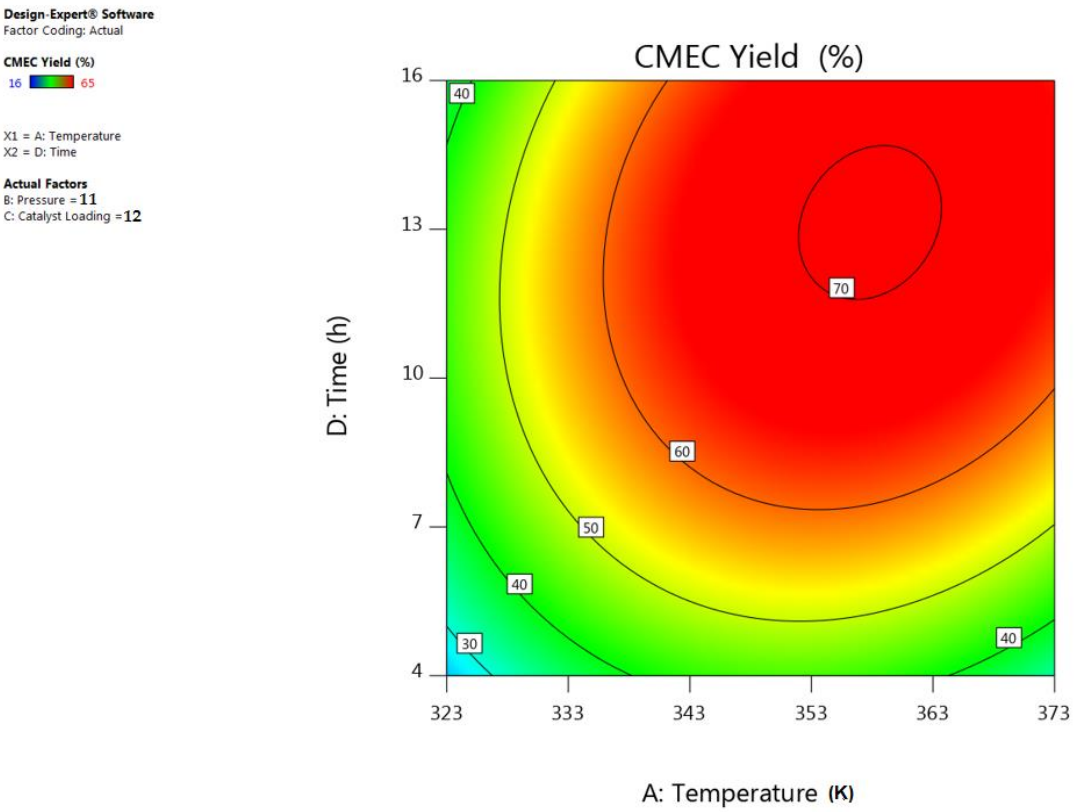

Figure 5. 14. Contour plot of the effect of reaction time and temperature on CMEC yield

5.6.3 Interactive effect of temperature and catalyst loading

The overall CMEC yield has been significantly influenced by the interaction between the catalyst loading and reaction temperature while CO_2 pressure and time have been kept at optimum values of 11 bar and 12 h, respectively. For example, Figure 5.15 shows that at lower catalyst loading of 5% (*w*/*w*), only 34% of CMEC yield was recorded as a result of low ECH conversion at low catalyst loading. The CMEC yield increased steadily up to 68% as reaction temperature increased at moderate levels of catalyst loading from 333 K to 353 K. This phenomenon could be attributed to the increase in the catalyst surface area, which provides more contact area between the

limiting reactant ECH and the active sites of the catalyst. Higher catalyst loading gives higher ECH conversion resulting in higher CMEC yield—an effect which is more pronounced at higher temperatures. However, at a higher temperature above 353 K, a marginal decrease in CMEC yield was observed, which may be due to catalyst deactivation at very high temperatures (Baş and Boyacı, 2007). The contour plot in Figure 5.16 with elliptical shape demonstrated the significant and combined effect of the catalyst loading and reaction temperature. The result has also supported lower *p*-value (0.0005) of the interaction x_1x_3 term. As shown in Figure 5.15, at any designated value of reaction temperature from 333 K to 353 K, the CMEC increased proportionally with catalyst loading. This observation was also supported by low *p*-value (<0.0001).

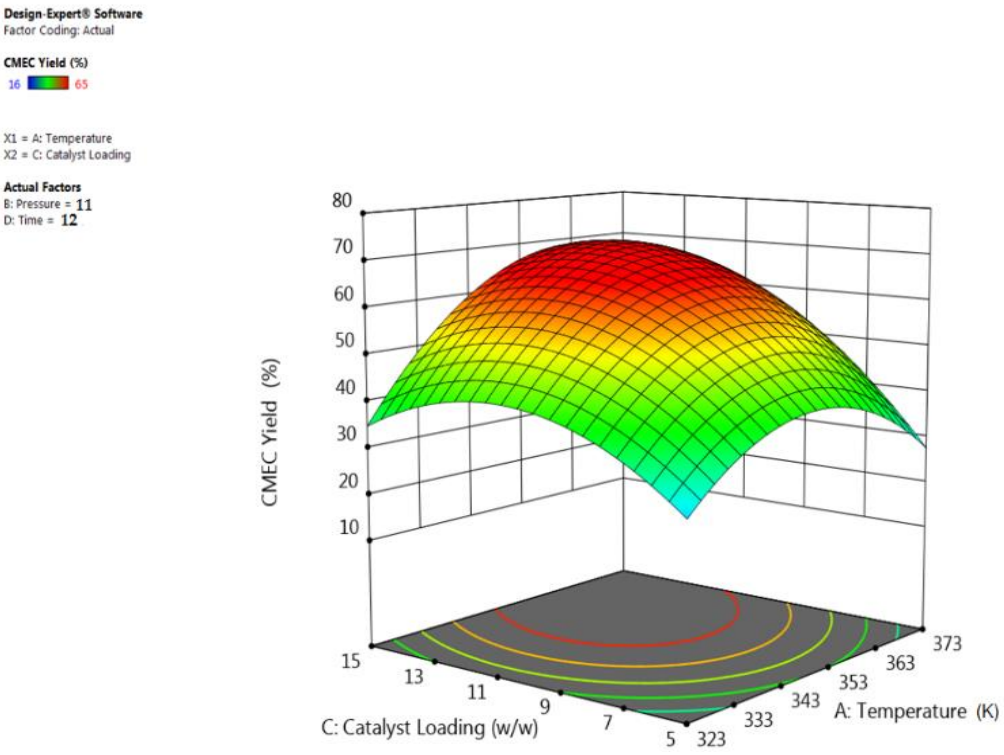

Figure 5. 15. 3D response surface of the effect of temperature and catalyst loading on CMEC yield

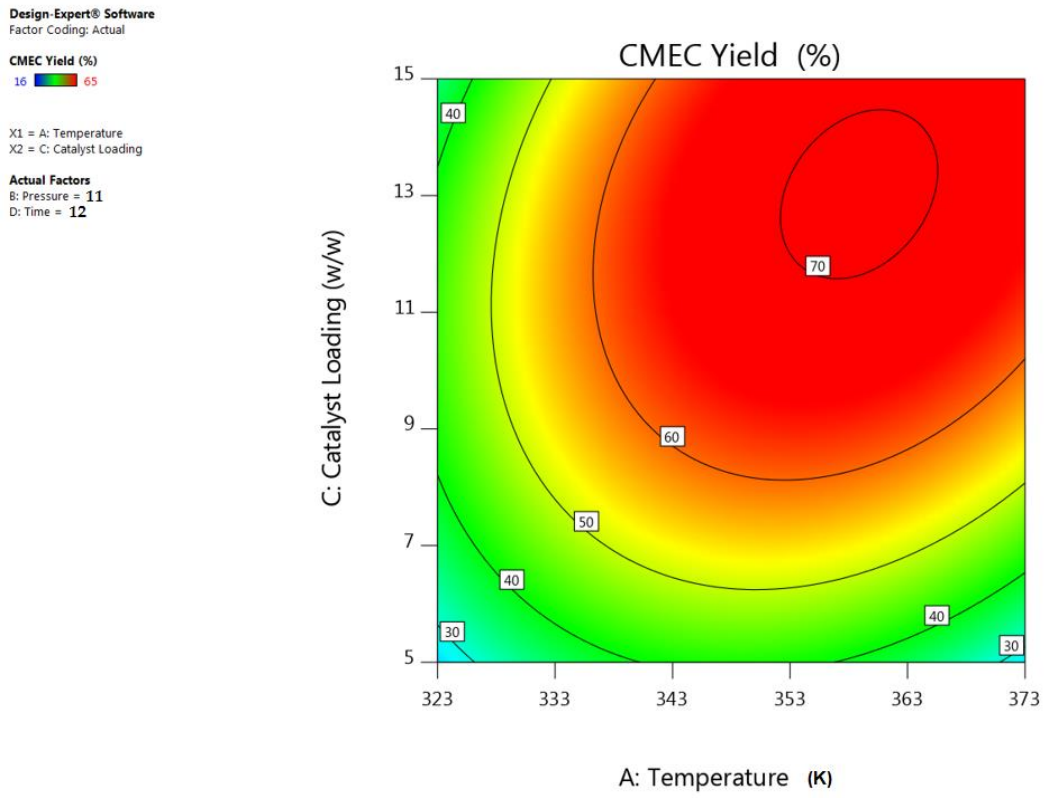

Figure 5. 16. Contour plot of the effect of temperature and catalyst loading on CMEC yield

5.6.4 Interactive effect of time and pressure

Similar to the previous observation of the interaction effect of temperature and pressure, Figure 5.17 demonstrates the interaction effect of CO_2 pressure and time on CMEC yield while maintaining reaction temperature and catalyst loading at 353 K and 12% (*w*/*w*), respectively. For example, at a shorter reaction time of 4 h, there was a negligible effect of CO_2 pressure in the CMEC yield. Figure 5.17 shows that optimum reaction time of 8.1 h was observed at a CO_2 pressure of about 8 bar with a 68% of CMEC yield. It has been observed that the CMEC yield reached a maximum at a reaction time of 8.1 h, thereafter, it was stable. A further increase in reaction time beyond this

value caused a sharp drop in CMEC yield as indicated in the surface plot of Figure 5.18.

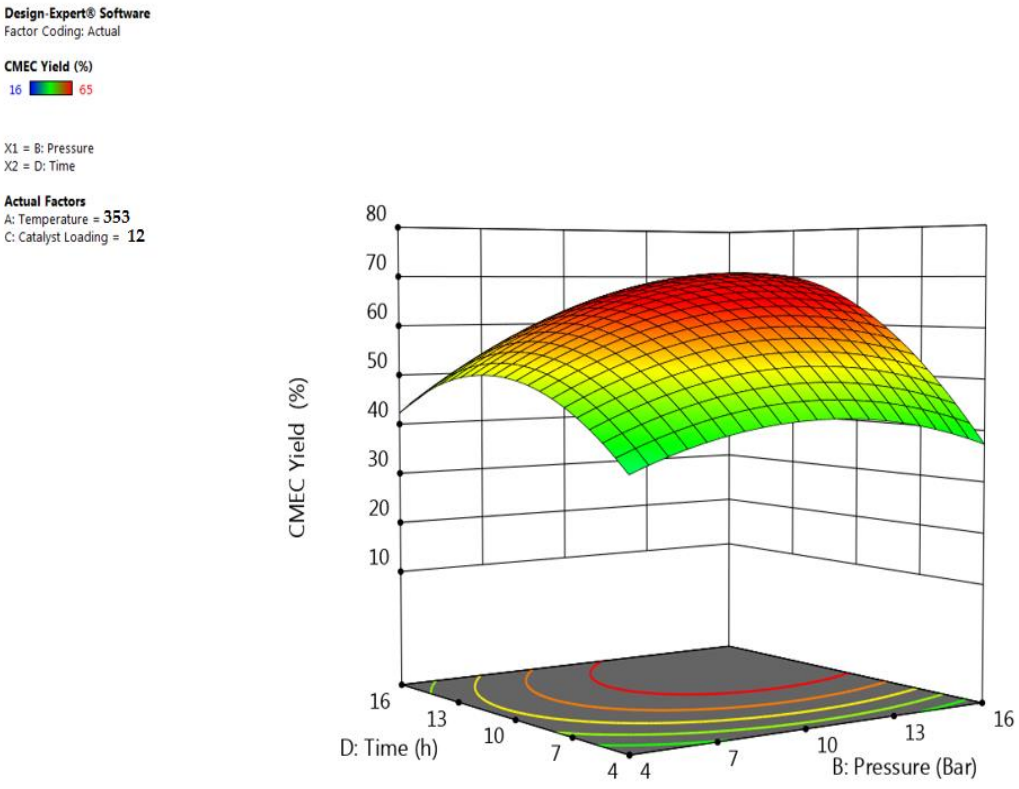

Figure 5. 17. 3D response surface of the effect of reaction time and pressure on CMEC yield.

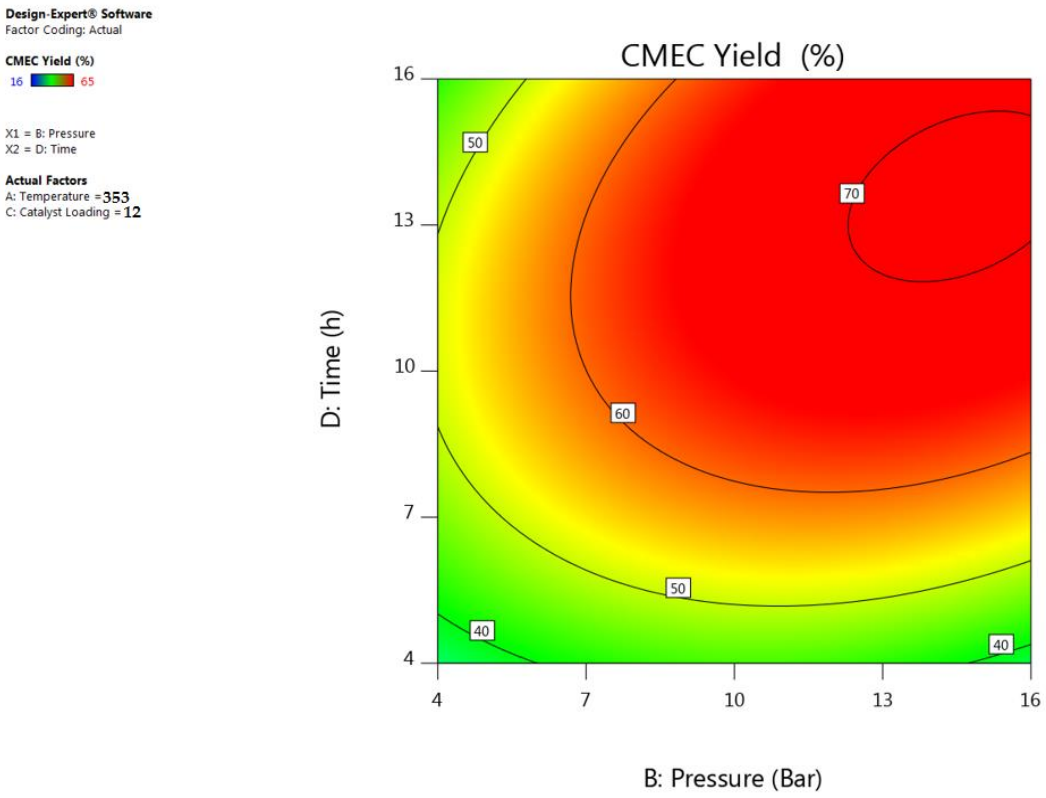

Figure 5. 18. Contour plot of the effect of reaction time and pressure on CMEC yield

5.6.5 Interactive effect of time and catalyst loading

The contour and 3D surface plots in Figures 5.19 and 5.20 show the interaction effect between the reaction time and the catalyst loading at a constant temperature of 353 K and CO_2 pressure of 12 bar. The contour plots show less curvature up to 7 h of reaction time, which implied less influence of catalyst loading on CMEC yield between the reaction time of 2 to 6 h. However, a maximum CMEC yield of 68% was achieved at higher catalyst loading and reaction time of 12% (*w*/*w*) and 12 h, respectively. A declining effect was observed in Figure 5.19 as the catalyst loading goes above 12% (*w*/*w*). This reflects that the optimum catalyst loading had been exceeded. A similar trend was reported by Onyenkeadi and research team on the declining effect of

catalyst loading beyond the optimum reaction time. An increase in the amount of catalyst loading can increase the number of active sites on the catalyst surface, and consequently, increases the number of radicals. However, an excessive increase in catalyst concentration beyond the optimum reaction time can result in catalyst deactivation. This phenomenon is totally in agreement with the recent reports of Feilizadeh et al. (2017).

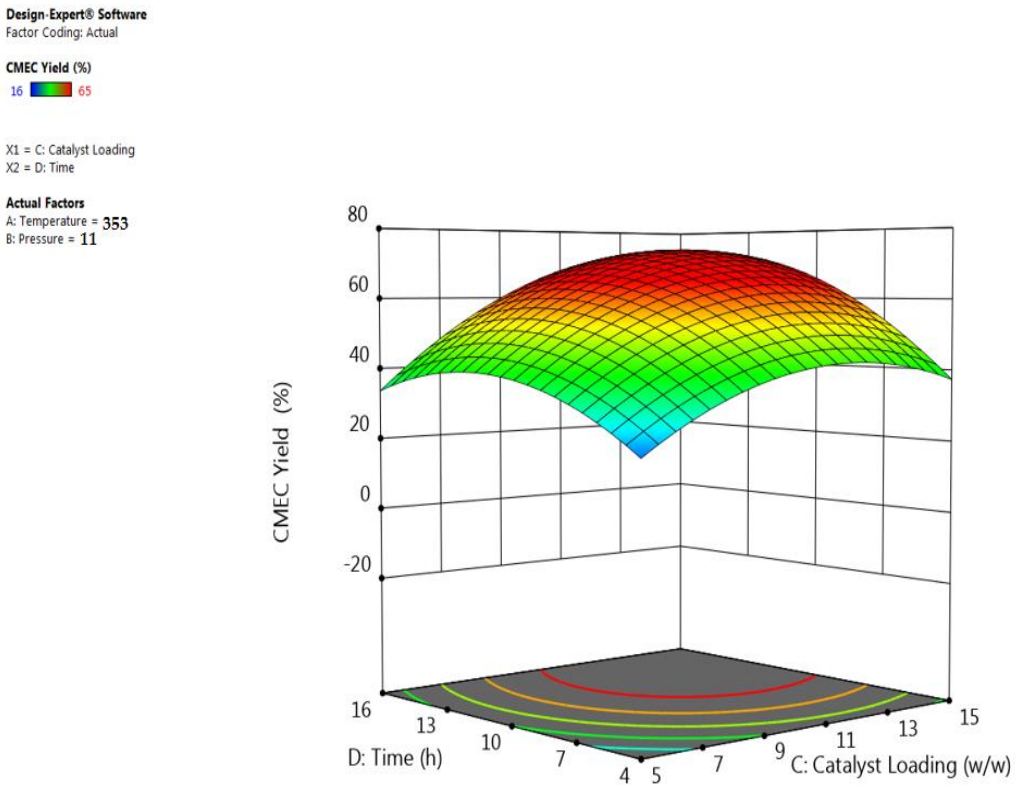

Figure 5. 19. 3D response surface of the effect of reaction time and catalyst loading on CMEC yield

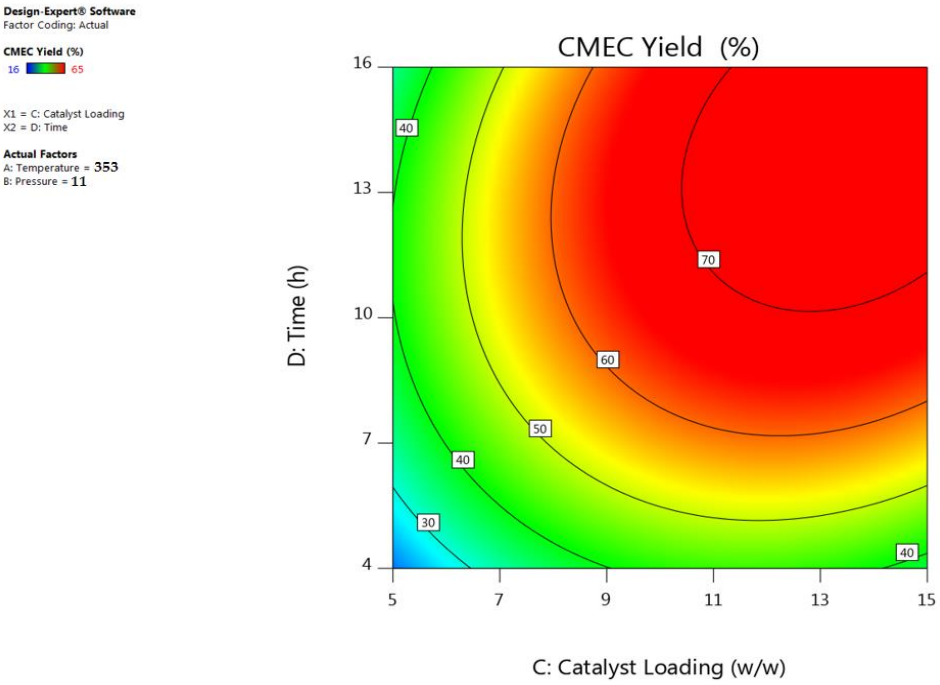

Figure 5. 20. Contour plot of the effect of reaction time and catalyst loading on CMEC yield

5.6.6 Interactive effect of catalyst loading and pressure

The exponential interaction effect between catalyst loading and pressure at a constant reaction time of 12 h and a temperature of 353 K is presented in Figure 5.21. However, the interaction produced a different effect on CMEC yield at different levels of interaction (i.e., different levels of interaction produce different effects on the ECH conversion). For example, Figure 5.21 shows that at the start of the reaction, 5% (*w*/*w*) of catalyst loading at 7 bar of CO_2 pressure produced an increasing effect on the CMEC yield. As the catalyst loading was further increased from 5% to 10% (*w*/*w*), the CMEC yield was observed to increase steadily from 40% to 68% corresponding to an increase in CO_2 pressure from 7 to 11 bar. The CMEC yield was highest (68%) at a maximum catalyst loading of 12 % (*w*/*w*) when the CO_2 pressure was maintained at

11 bar as shown in Figure 5.21. However, a negative effect of excessive increase in CO_2 pressure was observed on CMEC yield (a drop to 64%) at this level of interaction between catalyst loading and pressure. This phenomenon can be attributed to catalyst deactivation at increased CO_2 pressure beyond the optimum. A similar experience was reported earlier by Zhang et al. (2012). The group has recorded a higher propylene carbonate (PC) yield with a fixed amount of immobilised ionic liquid/$ZnCl_2$ at a CO_2 pressure of 1.5 MPa, however, a lower PC yield was observed at a higher CO_2 pressure of 2 MPa. Furthermore, they claimed that this phenomenon occurs when acidic CO_2 dissolves in basic epoxide to form a liquefied CO_2−epoxide complex, thereby inducing catalyst deactivation.

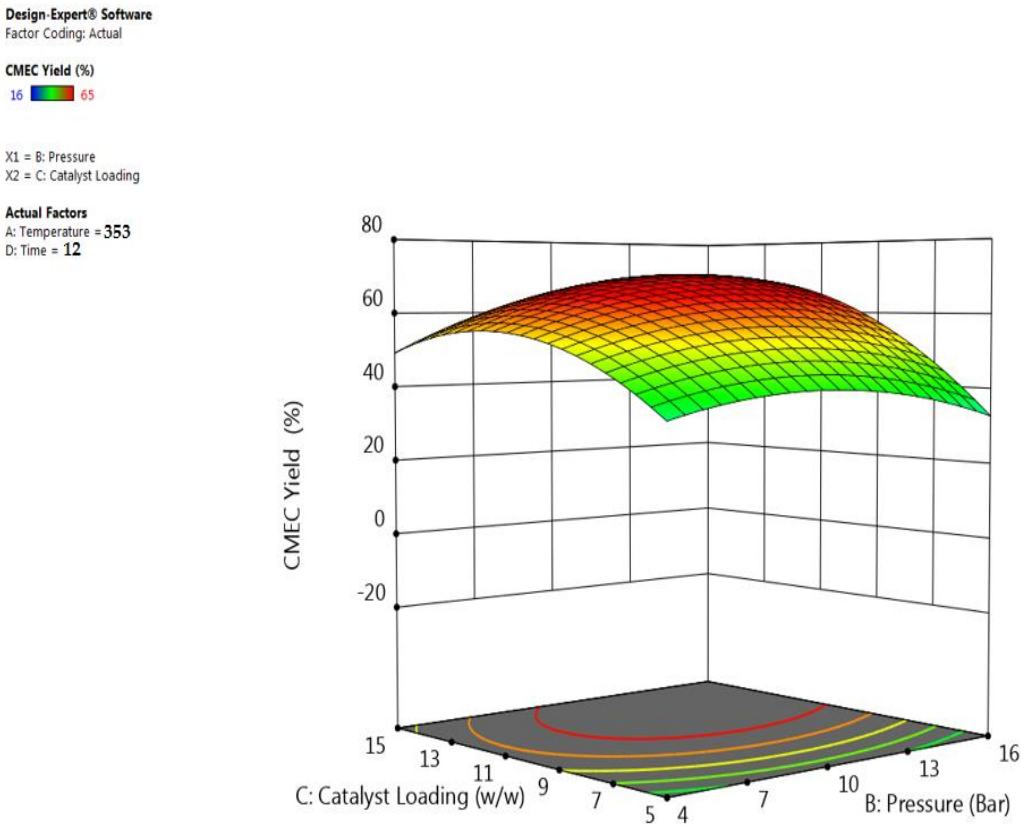

Figure 5. 21. 3D response surface of the effect of catalyst loading and pressure on CMEC yield

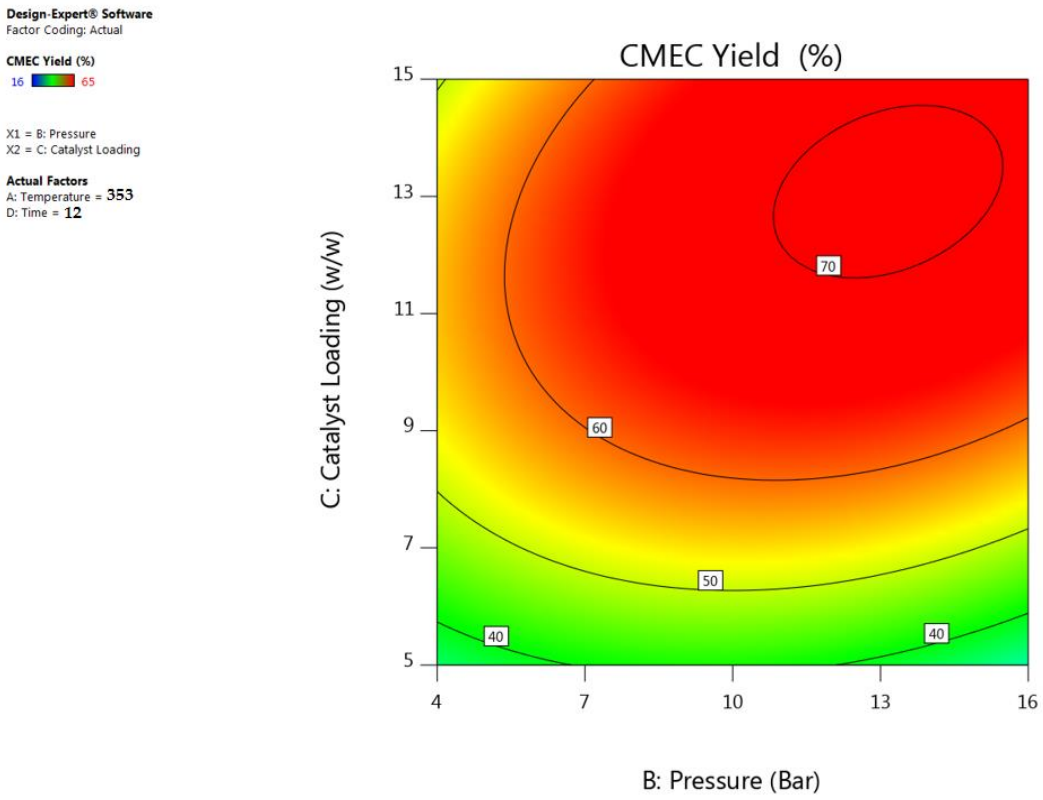

Figure 5. 22.Contour plot of the effect of catalyst loading and pressure on CMEC yield.

5.7 Multiobjective process optimisation

The growing quest for greener substitute for fossil fuel has led to increased production, process optimisation, and application of organic carbonate. As a result, the use of RSM has received more attention over conventional optimisation methods in order to investigate process optimum conditions and the interactive relationships between effective working variables. Although, finding the optimal reaction parameters for a single response using RSM is relatively simple; however, the optimisation of several responses at the same time is not an easy matter. Table 5.5 shows the optimisation targets for this study, the values have been set to maximise the process productivity. Targets for both ECH conversion and CMEC yield have been set to reach the maximum values while both the reaction temperature and time have been targeted to

minimum values with a viewpoint of reducing production cost at a maximum economic gain. Because of the catalyst efficiency and stability at optimum conditions, as a result, no specific target has been set for catalyst loading.

Based on the models generated and the accuracy between the actual experimental and predicted results, it can be construed that the model shows high consistencies between the two results where the relative errors of the predicted results from the experimental data are 1.55% and 1.54% for ECH conversion and CMEC yield, respectively. The similarity between the predicted and experimental results at the optimum conditions has validated the predicted optimum conditions. The experimental results concluded that an increase in reaction parameters increases ECH conversion and CMEC yield being 93% and 68%, respectively.

Table 5. 5. Optimisation constraints used to predict optimum conditions for chloromethyl ethylene carbonate synthesis

Factor	Code	Goal	Limits	
			Lower	Upper
Temperature (K)	x_1	Minimise	313	373
Pressure (bar)	x_2	In range	2	16
Catalyst loading (%)	x_3	In range	5	15
Time (h)	x_4	Minimise	2	16
ECH conversion	Y_1	Maximise	60	93
CMEC yield	Y_2	Maximise	30	68

5.8 Catalyst reusability studies

In view of large scale industrial applications and to minimise production cost, the reusability studies of Zr/ZIF-8 catalyst have been investigated. The catalyst reusability process has also followed strict eco-regulation after all the predicted optimum parameters have been derived from BBD of RSM. The experiments were carried out in a high-pressure reactor at optimum reaction conditions, at 353 K, 8 bar with fresh 10% (*w*/*w*) ZIF-8 catalyst loading, for 8 h, and at a stirring speed of 350 rpm. The catalyst after Run 1 in the cycloaddition reaction was washed with ethanol and acetone, centrifuged, and oven-dried at 343 K for 12 h before reuse. The recovered catalysts were reused for up to seven subsequent experiments as shown in Figure 5.23, following the same experimental procedure. The catalyst exhibited no loss of activity indicating the catalyst stability for the cycloaddition reaction of CO_2 epichlorohydrin. Incorporating zirconium into ZIF-8 has significantly increased the catalytic performance of Zr/ZIF-8 with the conversion of ECH and the yield of CMEC being 93% and 68%, respectively. The activity of reused Zr/ZIF-8 catalyst showed consistent stability over seven subsequent runs as indicated in Figure 5.23. Although, a very slight decrease in the yield of CMEC from 68% (fresh) to 67% (first recycled) was observed in the seventh run. Carbonaceous material formed during the reaction may explain in part the lower activity of the recycled catalysts (Bezerra *et al.*, 2008).

Although the difference in the error bars status between the ECH conversion and CMEC yield may be statistically significant, this may be attributed to the formation of some side products associated with the coupling reaction of CO_2 and ECH. The following side products have been identified by the GC analysis; 3-chloropropane 1,2-diol and 2,5-bis (chloromethyl)-1,4-dioxane.

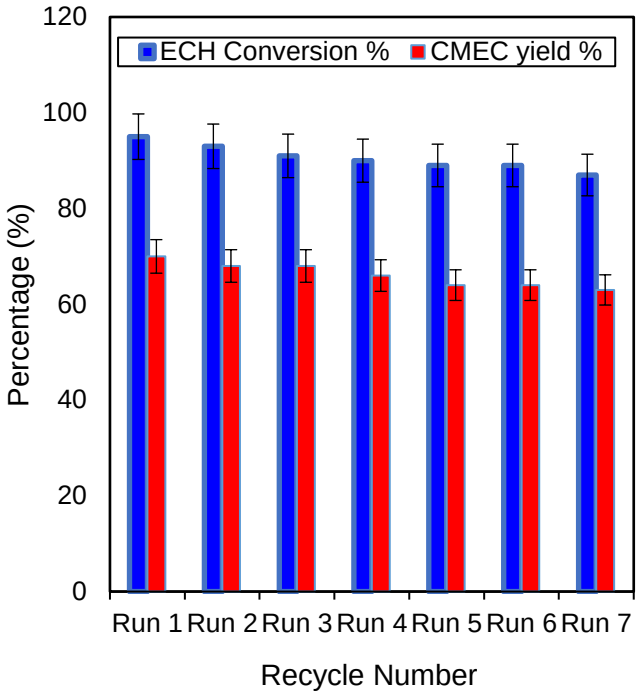

Figure 5. 23. Catalyst reusability studies of Zr/ZIF-8 on conversion of ECH, and CMEC yield using predicted response surface methodology's optimum condition of catalyst loading 12% (*w*/*w*); reaction temperature 353 K; CO_2 pressure 11 bar, reaction time 12 h, stirring speed 350 rpm

5.9 Conclusions

In this study, Zr/ZIF-8 catalyst has been successfully used for process optimisation in the synthesis of CMEC using RSM. In total, 29 runs of experiments were conducted for optimum design and modelling. The developed model was validated to assess the agreement between its predictions and a set of experimental data. The development of a novel Zr/ZIF-8 catalyst via a simple low-cost solvothermal method has demonstrated that the catalyst is viable for large-scale industrial applications. The catalyst has shown a good substrate tolerance as demonstrated by its activity towards epichlorohydrin. More importantly, the reaction has been carried out under solvent-

free and co-catalyst free conditions. The heterogeneity of the catalyst has been proven by recovering and reusing the catalyst for up to seven times without any significant loss in catalytic activity. Furthermore, PXRD, FT-IR, and TGA analysis of the recycled catalyst shows that the catalyst framework is quite stable after recycled experiments. The high selectivity towards epichlorohydrin carbonate, simple separation of the catalyst by centrifugation, and excellent recyclability demonstrated that the catalyst is viable for industrial applications. We believe that this work could provide a new direction for designing more sustainable heterogeneous catalysts for the greener synthesis of organic carbonates via CO_2 utilisation.

Chapter 6

A greener approach and system optimisation of styrene carbonate (SC) synthesis *via* CO_2 utilisation

Outline of the chapter

This chapter is divided into two parts. The first part focuses on the experimental catalytic synthesis of styrene carbonate. The second part evaluates and compares the results of both the experimental synthesis and the predicted values for the synthesis of styrene carbonate. It has used a modelling *via* response surface methodology (RMS) with a 3-level, 4-factor (3^4) factorial Box–Behnken design to predict an optimal outcome for the design.

The chapter is organised as follows:

6.1. Introduction

6.2. Materials and methods

6.3. CO_2-styrene oxide cycloaddition

6.4. Results and discussion (OFAT- one-factor-at-a- time)

6.5. RSM modelling and optimisation

6.6. Results and discussion (process optimisation)

6.7. Effects of process variables (interactive effects)

6.8. Multiple responses optimisation

6.9. Conclusions

6 A greener approach and system optimisation for styrene carbonate synthesis *via* CO_2 utilisation

6.1 Introduction

This chapter has highlighted the importance of using response surface methodology (RSM) to optimise system variables for the greener synthesis of styrene carbonate (SC) from carbon dioxide (CO_2) and styrene oxide (SO) using a highly efficient Zr/ZIF-8 catalyst. Box-Behnken Design (BBD) with four independent variables has been used to evaluate and predict the influence and the interaction effect of four independent reaction variables, *i.e.* temperature, pressure, reaction time and catalyst loading on two selected responses, *i.e.* conversion of SO and SC yield. The adequacy of the predicted models has been validated using numerous statistical techniques including analysis of variance (ANOVA) at a 95% confidence level. The experimental and model-predicted values have shown an excellent agreement for Zr/ZIF-8 as efficient CO_2- reduction heterogeneous catalyst for the synthesis of SC from SO and CO_2. Approximative relative errors of ±1.25% for SO conversion and ± 0.75% for SC yield, respectively were calculated. The use of RSM to optimise process variables for the synthesis of SC has offered a new direction in maximising the production of value-added chemicals and effectively utilise CO_2 gas emissions.

6.2 Materials and methods

6.2.1 Chemicals and materials

Acetone (purity: 99%), styrene oxide (purity: 99.5%), styrene carbonate (purity: 98%), butylene oxide (purity: 99%) and butylene carbonate (purity: 99.8%) were purchased from Sigma-Aldrich Co. LLC, Dorset, UK. Methanol (purity: 99%), 4-vinyl-1-cyclohexene epoxide (purity: 98%) and *n*-Pentane (purity 99.8%) were purchased from Fisher Scientific UK Ltd, Loughborough, UK. As-prepared Zr/ZIF-8 catalyst. The purity of all the chemicals was verified by gas chromatography (GC) analysis. All chemicals

were used without further purification. Helium gas and liquid CO_2 (purity: 99.9%) cylinder equipped with a dip tube was purchased from SOC Ltd., UK. Supercritical fluid (SCF) pump (model: SFT-10) was procured from Analytix Ltd., UK. A Parr high-pressure stainless-steel autoclave reactor (model: 5500) of 100 mL and (model 4590) of 25 mL capacity equipped with a reactor controller (model: 4848) was purchased from SCIMED (Scientific and Medical Products Ltd.), UK. Risk assessment (RA) for batch reactor experiments were carried out before conducting the experiments.

6.2.2 Experimental procedure for the synthesis of styrene carbonate (SC)

In a typical cycloaddition reaction, a 25 mL stainless steel high-pressure reactor was initially charged with a specific amount of Zr/ZIF-8 catalyst and the limiting reactant, styrene oxide. A desired temperature was set on the reactor's panel controller; the reactor was then sealed and stirred continuously at a known stirring speed. At the desired temperature, a specific amount of liquid CO_2 was charged through a supercritical fluid (SCF) pump into the reactor. The reaction was left for the desired reaction time. After the reaction was completed, the reactor was cooled down to room temperature and the mixture was collected and filtered. The catalyst was separated, washed with acetone, and dried in a vacuum oven. A known amount of methanol (used as internal standard) was added to the product and analysed using a gas chromatograph (GC). The effect of different reaction parameters was investigated. These include catalyst loading, stirring speed, CO_2 pressure, temperature, and reaction time. Reusability studies of both catalysts were also carried out in order to investigate the stability of the catalysts for the synthesis of styrene carbonate.

6.2.3 Sample analysis

A specific quantity of internal standard, methanol added to a known sample of the product was analysed using gas chromatography (GC) (Model: Shimadzu GC-2014).

The stationary phase was a capillary column with dimensions (30 m length, 320 µm inner diameter, and 0.25 µm film thickness). Oxygen (99.9%) and hydrogen (99.9%) were used as ignition gases. The carrier gas used for the mobile phase was high purity helium (99.9%) with a flow rate maintained at 1 mL min^{-1}. A temperature program was developed for the system where both the injector port and detector temperatures were kept isothermally at 523 K. The other selected program includes a split ratio of 50:1 and an injection volume of 0.5 µL. The column temperature was initially maintained at 323 K for 5 min, then followed by a temperature ramp at a flow rate of 50 K min^{-1} to a temperature of 523 K with a 12 min run for each subsequent sample. The chromatogram shows that SO peak at ~3.5 min, methanol at ~3.8 min, SC at ~11 min. This observation is parallel to the work published by (Adeleye *et al.*, 2014).

6.2.4 The catalytic activity of Zr/ZIF-8 in the cycloaddition of SO and CO_2

Herein we report the catalytic performance of Zr/ZIF-8 for the coupling reaction of CO_2 and SO. Our experience using Zr/ZIF-8 to synthesise chloromethyl ethylene carbonate (CMEC) from epichlorohydrin (ECH) and carbon dioxide (CO_2) (Olaniyan and Saha, 2020) has proved that the catalyst has a high CO_2 adsorption capacity for cycloaddition reaction. According to Beyzavi et al. (2015a), ZIF-8 is a bi-functional catalyst containing both acidic and basic sites associated with the Lewis acid Zn^{2+} ions and the basic imidazole groups, respectively. The dual functionality of the catalyst enhances its affinity for cycloaddition reaction. In a separate report, Zhu et al. (2013b) have ascertained that it is likely that Lewis acid sites associated with Zn^{2+} ions in the ZIF-8 framework play a vital role in catalysing the reaction of SO and CO_2 to SC. Meanwhile, Zanon et al. (2017b) had earlier reported that the presence of basic nitrogen atoms of the imidazole ligand, probably, favours the adsorption and binding of CO_2 as well as activation of the carbon-oxygen bonds in CO_2**.** In agreement with other similar doped ZIF-8, the open metal centers in the Zr/ZIF-8 has the potential to easily activate the epoxides and the basic sites present in the frameworks. This could be the reason for the higher catalytic performance observed in the solvent-free CO_2-SO cycloaddition

reactions under mild conditions (Kim *et al.*, 2018). Figure 6.1 shows the cycloaddition reaction of CO_2 and SO to synthesise SC.

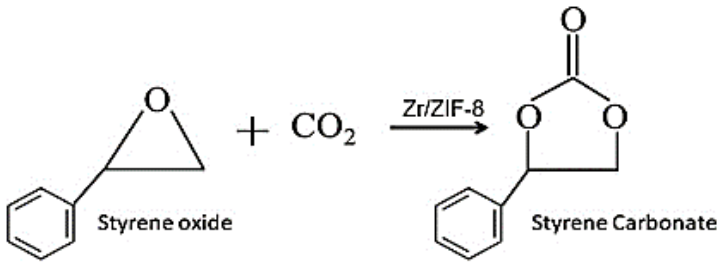

Figure 6. 1. Reaction of CO_2 and epoxide

Our idea of choosing zirconium (Zr^{4+}) as a suitable dopant for this catalytic system was in perfect agreement with the experiments of Cavka et al. (2008b). Since Zr^{4+} has comparable ionic size to Zinc (Zn^{2+}) (i.e., 0.745 Å for $Zr^{4+}$and 0.740 Å for Zn^{2+}), Duan et al. (2011) and Gurav et al. (2013), believes this relationship will help to minimise lattice distortion during the ion-exchange process. Zr^{4+} also has the ability to act as a dual donor (Ge, 2012), providing up to two extra free electrons per ion when substituted for Zn^{2+} (Jeong *et al.*, 2017)**.** According to Jin and Yang, (2017), Zr^{4+} is well known as an effective promoter of metal-based catalysts. It can also act as a phase stabiliser to increase the dispersion and stability of the active metal through strong metal-support interactions (Herodotou *et al.*, 2015). Furthermore, by comparing with other reported ZIF based heterogeneous catalysts, Zr/ZIF-8 presents a higher conversion of epoxide and carbonate yield under relatively mild reaction conditions. This may be associated with the synergetic effects of the multi-functional active sites on the catalyst rather than just mere interaction between SO and catalyst (Liu *et al.*, 2018).

In the current research work, the catalytic efficiency of Zr/ZIF-8 has been further extended to a few other commercially available representative epoxides, such as

epichlorohydrin (ECH), butylene oxide (BO), and cyclohexene oxide (CHO). By using our optimum reaction conditions of 353 K of reaction temperature, 6 bar of CO_2 pressure, 6 % (w/w) of catalyst loading for 8 h, to run the experiments, these representative epoxides produced their corresponding cyclic carbonates with reasonable yields as shown in Table 6.1. However, cyclohexene oxide produced a lesser yield of cyclic carbonate than other epoxides. Cui et al. (2015) have reported similar observations in their series of experiments. However, they have attributed the low carbonate yield of cyclohexene oxide to its high steric hindrance. This condition is also known to cause difficulty in interactions between the internal epoxide and the active sites of the porous catalyst (Paquin *et al.*, 2015). Lai et al. (2016) also concluded after several experiments that high steric hindrance of cyclohexene oxide has the possibility to deter nucleophilic attack of anion on to the epoxide (which may have been the case in their experiments). In another separate account, Taherimehr et al. (2012) also reported that SO is more difficult to convert to styrene carbonate due to its less reactive-carbon atom. To the best of our knowledge, this claim has not yet been refuted by any research group at the time of this report.

Xiang et al. (2019) investigated the catalytic activity of other ZIF-based catalysts for the cycloaddition reaction of CO_2 and epoxide. They reported a highly selective conversion of styrene oxide to styrene carbonate (100% selectivity) by ZIF-68 catalyst at 393 K. ZIF-22 afforded a significantly higher activity than ZIF-90 with TOF of 237 h and 17 h respectively for the synthesis of propylene carbonate (PC) from propylene oxide (PO) and carbon dioxide (CO_2) (Hwang *et al.*, 2016).

Table 6. 1. Comparison of catalytic activity of different representative epoxides for coupling reaction of CO_2 and epoxides with Zr/ZIF-8

Entry	Substrate	Conversion (%)	Selectivity (%)	Yield (%)	Ref.
1	SO	98	72	68	Current work
2	BO	89	70	53	Onyenkeadi et al. (2018)
3	*ECH	93	83	76	Olaniyan et al. (2020)
4	CHO	62	55	17	Adeleye PhD thesis

Reaction conditions: T (K) =353, P (Bar) =6, t (h) =8, Catalyst loading % (w/w) =6

*T (K) =353, P (Bar) =8, t (h) =8, Catalyst loading % (w/w) =10

6.2.5 Reaction mechanism

On the basis of our experimental results and theoretical study, we proposed a plausible reaction mechanism for the coupling reaction of SO and CO_2. In Figure 6.2, the reaction was initiated by the coordination of styrene oxide with Lewis acid site Zn^{2+} to form the adduct of zinc-epoxide complex, then nucleophilic interaction on the electrophilic carbon of CO_2. At the same time, the acidic sites (unsaturated coordinative Zn or structural defects) of Zr/ZIF-8 interact with the oxygen atom of an epoxide. The activated CO_2 attacks the less sterically hindered carbon atom of epoxide, which results in the epoxide ring-opening. Finally, the ring-closure step takes place between the O−anion and carbon atom in the intermediates to produce the desired five-membered cyclic carbonate (Zhu, 2013).

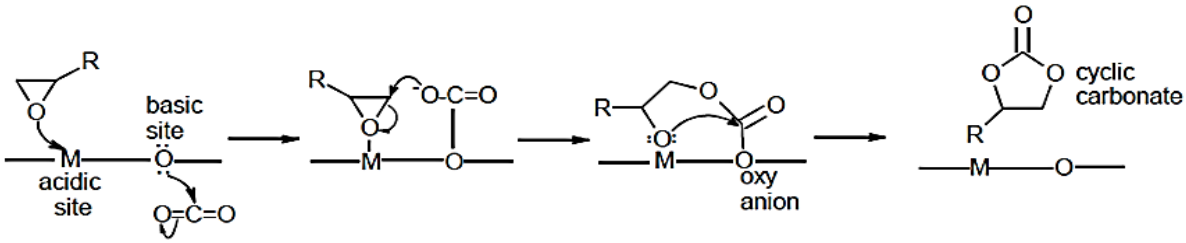

R is an alkyl group, M is a metal atom (acidic site) and O is oxygen atom (basic site).

Figure 6. 2. Proposed reaction mechanism for the cycloaddition reaction of CO_2 to SO over an acid-base pair.

6.3 Results and discussion

6.3.1 Effect of reaction temperature

The heterogeneous catalytic synthesis of styrene carbonate (SC) *via* cycloaddition of styrene oxide (SO) and carbon dioxide (CO_2) was carried out within temperature range of 313-373 K in order to determine the effect of reaction temperature on the conversion of SO, selectivity and yield of SC and also to establish the optimum temperature for the system. A 98% conversion of SO was recorded at 373 K, indicating that most of the reactant molecules attained the activation energy for the ring-opening cycloaddition reaction (Luo *et al.*, 2016).

Figure 6.3 shows the graph of SO conversion, selectivity and SC yield at different reaction temperatures. It can be observed that as the reaction temperature increases gradually, the conversion of SO, selectivity and SC yield also increases until the optimum temperature was reached. For example, when the reaction temperature was increased from 313 to 333 K, the conversion of SO also increased steadily from 81 to 96%, selectivity and SC yield also increased linearly from 55 to 71% and 45 to 68%, respectively demonstrating that 333 K was high enough for the catalytic system. Conversely, selectivity and SC yield experienced a marginal decrease from 71% to 69% and 68% to 67%, respectively as the temperature was further increased beyond

353 K. Meanwhile, a corresponding increase in SO conversion from 96 to 98% was recorded at the same temperature. This indicated that temperature had a significant effect on the conversion of SO, yield and selectivity of SC.

Based on our experimental analysis, the decline in selectivity and SC yield was expected because our gas chromatography-mass spectroscopy (GC-MS) analysis of the samples shows that 17.3% of benzaldehyde and 14.1% of benzoic acid (by-products) have been formed at 353 K, which was similar to the by-products and results published by Sun et al. (2005). This may explain in part why a drop in selectivity and yield of SC was recorded. Another similar experience was reported by Onyenkeadi et al. (2018a). They have investigated the effect of varying temperatures on the cycloaddition reaction of butylene oxide–carbon dioxide (BO-CO_2). In their experiments, Low butylene carbonate yield was recorded when the reaction temperature was increased above the optimum (408 K). Further sample analysis *via* the (GC-MS) shows that more by-products (such as isomers and oligomers) have been formed when the reaction temperature was increased above the optimum. They concluded that the formation of these by-products was responsible for the low BC yield. The account of Jasiak et al. (2016) is another typical example of demonstrating the effect of excessive increase temperature on selectivity and SC yield. They have attributed the negative results in selectivity and yield of SC to polymerisation of SC at a temperature above the optimum.

Similarly, Sun et al. (2004) and Qiao et al. (2009) have also reported that at extreme temperature, decomposition of SC to SO could be observed. This phenomenon has been widely published in many literatures. Another possible explanation many researchers have attributed to a marginal decrease in SC yield could be as a result of less SO conversion due to low solubility of CO_2 at a higher temperature. For example, Xiang et al. (2009) achieved a 95.8% conversion of SO at 353 K. However, a slight

increase in temperature to 358 K resulted in a drop of SO conversion to 90%. Therefore, on the basis of our experimental results and theoretical study for this heterogeneous catalytic synthesis of styrene carbonate, 353 K is believed to be the optimum temperature for the reaction between SO and CO_2 with Zr/ZIF-8 catalyst.

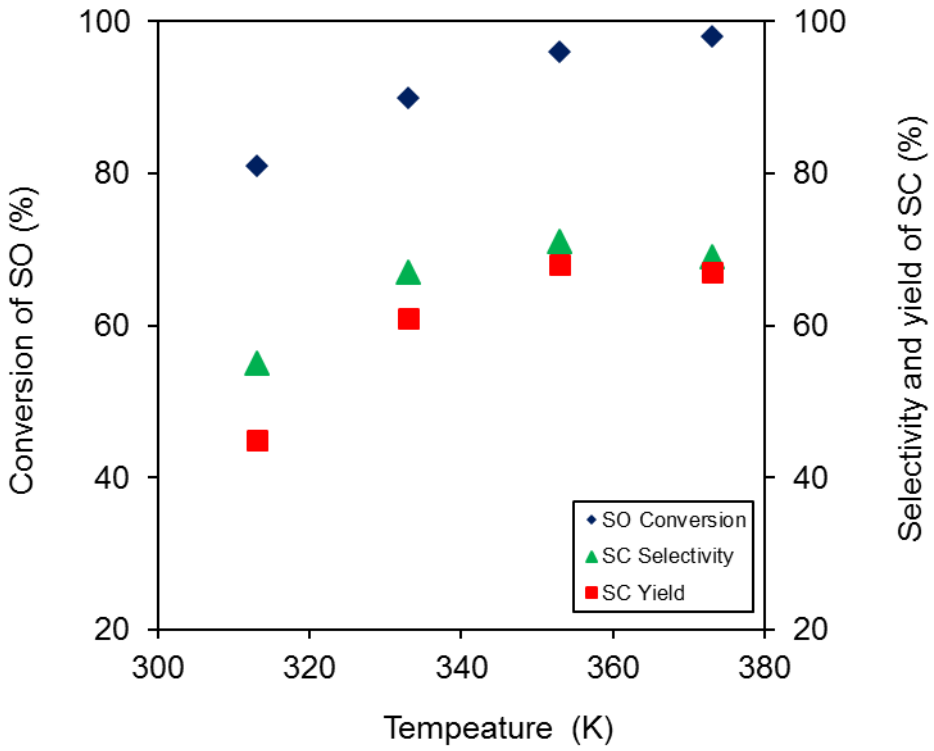

Figure 6. 3. Effect of reaction temperature on the cycloaddition reaction of CO_2 and styrene oxide.

6.3.2 Effect of CO_2 pressure

CO_2 pressure plays a pivotal role in the cycloaddition reaction of styrene oxide and CO_2. Cheng et al. (2013) reported CO_2 pressure is a vital factor that affects conversion, yield and selectivity of organic carbonates. The current experiment was carried out in a high-pressure reactor at 353 K, 10% catalyst loading at various CO_2 pressure ranging from 4 bar to 12 bar.

Figure 6.4 shows the effect of CO_2 pressure on the conversion of SO, selectivity and yield of SC. This was a study to determine the optimum CO_2 pressure for the reaction of SO and CO_2. It can be observed from the graph that at a fixed reaction time and reaction temperature, an increase in CO_2 pressure from 2 to 6 bar, leads to a corresponding increase in SO conversion from 74 to 97% and consequently increases the selectivity and yield of SC from 55 to 72% and 46 to 68%, respectively. According to Montoya et al. (2015), when more acidic CO_2 dissolves in the liquid phase, the reaction system facilitates the formation of CO_2-epoxide complex and more organic carbonates are formed. Similarly, in the present work, when the CO_2 pressure was increased beyond 6 bar, a progressive decrease in selectivity and SC yield was observed from 72 to 71% and 68 to 67%, respectively while SO conversion increases continually. Several factors have been investigated for these results. Wu et al. (2018) reported that the decomposition of SC to form oligomers is one of the major factors. Another significant factor which has been reported in many CO_2-epoxide reactions is CO_2 phase change. For example, in the experiments of Sun et al. (2009), they have attached transparent sapphire windows to the reactor in order to study the phase behaviour of a multi-phase cycloaddition reaction. According to their visual observations report, a three-phase reaction mixture was noticed. This was assumed to be a gas-liquid-solid phase system, whilst the reaction primarily occurs in the SO-rich liquid phase. It was observed that as CO_2 pressure was increased from 1 to 8 Mpa, more CO_2 concentration was enhanced in the liquid phase thereby promoting the interaction between the gas-liquid phases (CO_2-rich gas, SO-rich liquid), and subsequently increases SC yield. They also noted that further increase in CO_2 pressure to 15 MPa, induced more acidic CO_2 to dissolve in liquid phase causing a SO-epoxide complex, hence a marginal drop in SC yield was observed. A similar experience was later reported by Appaturi and Adam, (2013). In the current research work, the GC analysis of the product has identified many isomers and oligomers in samples that have been synthesised above 6 bar of CO_2 pressure. Therefore, based on our experimental analysis, it can be concluded that the optimum CO_2 pressure for

the reaction of SO and CO_2 using Zr/ZIF-8 is 6 bar with yield and selectivity of 68% and 72%, respectively.

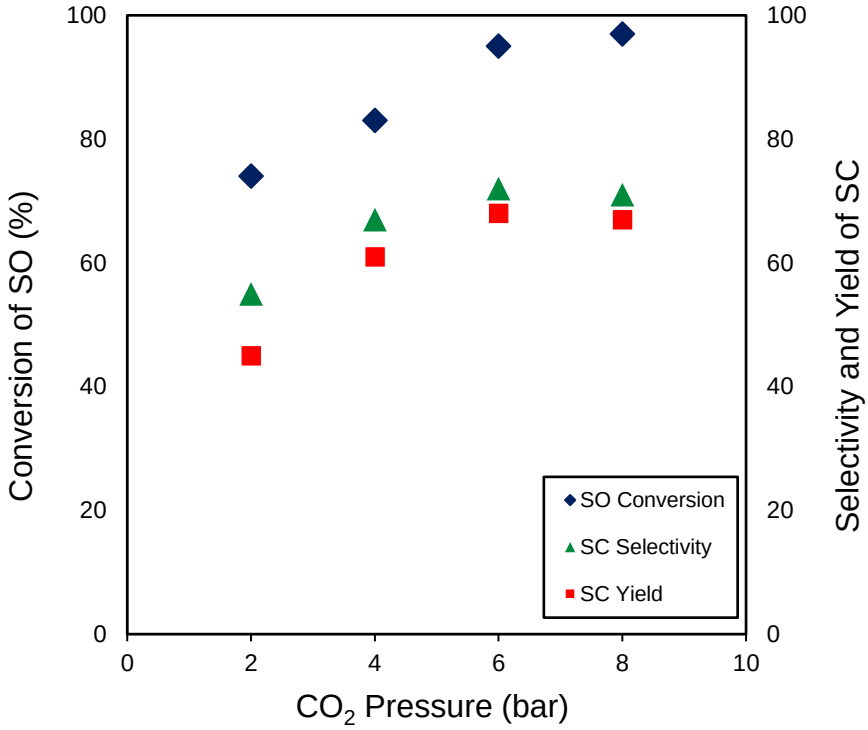

Figure 6. 4. Effect of reaction pressure on the cycloaddition reaction of CO_2 and styrene oxide.

6.3.3 Effect of reaction time

The effect of reaction time on SC yield was studied by carrying out a set of cycloaddition of CO_2 and SO using Zr/ZIF-8 catalyst. For this study, different experiments were carried out by varying the reaction time from 4 to 10 h at 353 K, 6 bar CO_2 pressure with 10% catalyst loading of Zr/ZIF-8.

Figure 6.5. shows the influence of reaction time on SC yield, selectivity and conversion. The graph shows an increase in SO conversion as reaction time increases

from 4 to 8 h, after which no significant change in SO conversion at 98% even with prolonged reaction time beyond 8 h. From the graph, no significant effect was also reported on the SC yield after 8 h (stays at 68%). Meanwhile, about a 5% drop (72% to 70%) in the SC selectivity was observed at a longer reaction time which was similar to the observation of Ravi et al. (2015). Therefore, it can be concluded that prolonged reaction time has very little or no effect on both the SO conversion and SC yield beyond 8 h of reaction time. Whereas a further increase in reaction time beyond 8 h was unfavourable to SC selectivity with a 5% drop. Carreon, (2012) already reported that prolonged reaction time could lead to the decomposition of organic carbonates. Polymerised SC may also cause a decrease in overall percentage yield of SC as previously experienced by Onyenkeadi et al., (2019). Therefore, the optimum reaction time for this study is 8 h.

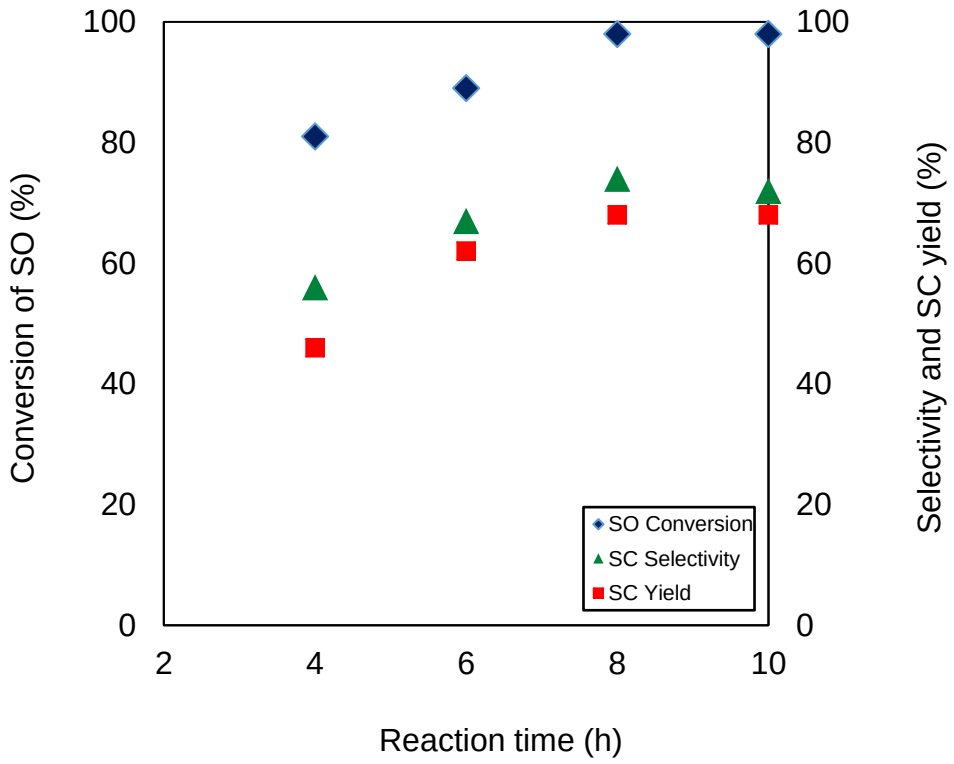

Figure 6. 5. Effect of reaction time on the cycloaddition of CO_2 and styrene oxide.

6.3.4 Effect of catalyst loading

In this experiment, the effect of catalyst loading was carried out by cycloaddition reaction of SO to CO_2 using different amounts of Zr/ZIF-8 catalyst ranging from 2.5%-10%(w/w) at 353 K, 6 bar CO_2 pressure for 8 h.

Figure 6.6 shows the varying impact of catalyst loading on SO conversion, selectivity and SC yield. It can be seen from the graph that as catalyst loading was gradually increased from 2.5% (w/w) to 10% (w/w), there was a corresponding increase in SO conversion, SC yield and selectivity. For example, a 44.6% yield of SC was achieved at a conversion of 73% of SO with a 2.5% (w/w) of catalyst loading. Positive significant changes were observed in SO conversion and SC yield when more catalyst was added to the reactive system, which signifies more active sites at higher catalyst loading (Bhanage *et al.*, 2001). At 6 % (w/w) catalyst loading, 86.2% of SO conversion and 68% of SC yield was achieved. When the catalyst loading was increased beyond 6% (w/w), both selectivity and SC yield experienced a decline from 73% to 70% and 68% to 66%, respectively. According to Zalomaeva et al. (2013), an increase in catalyst loading increases active sites of the catalyst and subsequently increases the SO conversion, selectivity and yield of respectively. In the present work, a reduced SC yield was recorded in all experiments above 6% (w/w). One of the major explanations for reduced carbonates yield at higher catalyst loading could be the synergistic effect of high CO_2 pressure and high temperature along with poisoning/blocking of the active sites by carbonaceous products (Bosch *et al.*, 2014b; Kuznetsova *et al.*, 2019). This synergetic and poisoning effect was first observed and reported by Zhou et al. (2008). Similarly, Khan et al. (2019) reported that coke deposited on the surface of the catalysts may block access to active sites in the micropores leading to rapid catalyst deactivation. This condition can ultimately lead to a complete catalyst deactivation and crystalline instability of ZIF-8 frameworks as earlier reported by Yuan et al. (2016). Therefore, based on our experimental results and analysis, it can be concluded that

6% (w/w) catalyst loading is the optimum catalyst loading for this experiment at 353 K, 6 bar CO_2 pressure in 8 h.

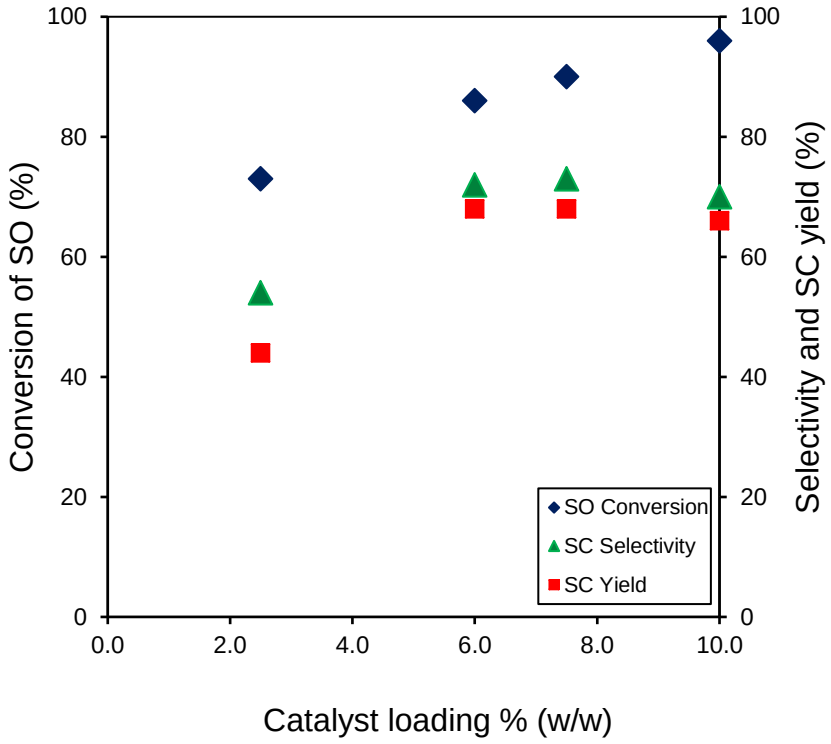

Figure 6. 6. Effect of catalyst loading on the cycloaddition reaction of CO_2 and styrene-oxide.

6.3.5 Catalyst reusability studies

Catalyst reusability is an important and essential feature of any catalyst to be considered in industrial applications. According to Figure 6.7, Zr/ZIF-8 has demonstrated notable and excellent reusability in terms of SO conversion, selectivity and SC yield with no significant loss in catalytic for seven subsequent experiments following the same experimental procedure. Although, a very slight decrease in the yield of SC from 57.4% (fresh) to 56.3% (first recycled) was observed. Jutz et al. (2008) claimed that poisoning/blocking of the active sites by carbonaceous products could be the reason for the slight catalyst deactivation and crystalline instability of the catalyst.

The experiments were carried out in a high-pressure reactor at optimum reaction conditions, at 353 K, 6 bar with fresh 6% (w/w) Zr/ ZIF-8 catalyst loading, for 8 h and at a stirring speed of 350 rpm. The catalyst after Run 1 in the cycloaddition reaction was washed with ethanol and acetone, centrifuged, and oven-dried at 343 K for 12 h before reuse. Srivastava et al. (2005) stated that the presence of dopant in ZIF-8 show that zirconium is more stable and resilient during the reaction.

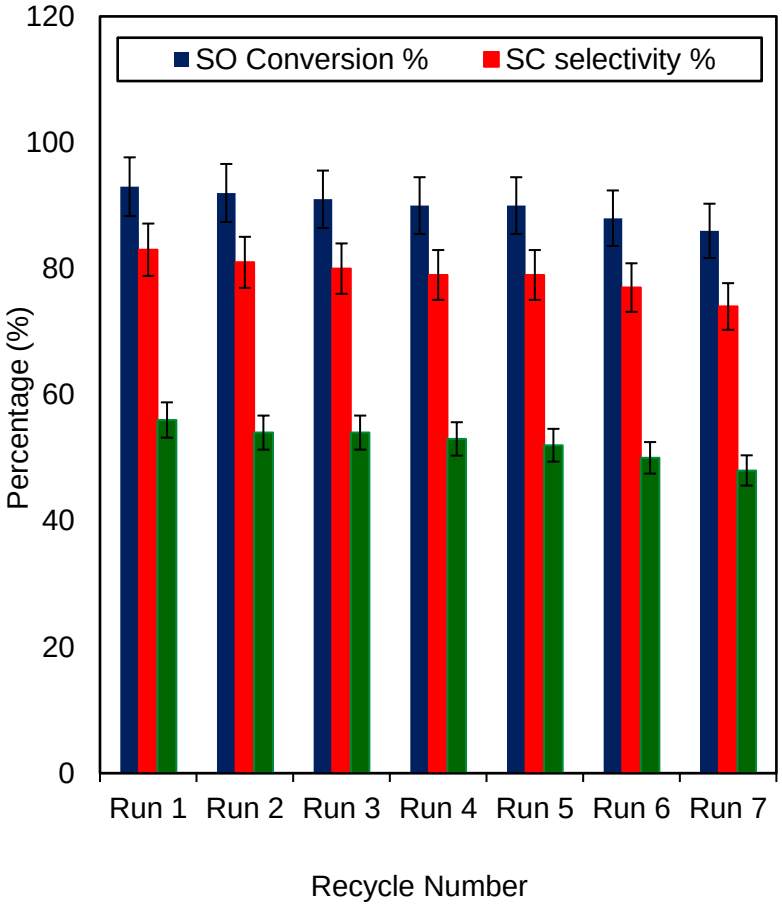

Figure 6. 7. Catalyst reusability studies on the conversion of styrene oxide (SO), selectivity and yield of styrene carbonate (SC).

6.4 RSM modelling and optimisation

On the basis of the reaction results obtained from the experimental synthesis of styrene carbonate using (one-factor-at-a-time) OFAT analysis, it was deemed necessary to optimise the reaction variables to further examine the efficiency of the new catalyst using response surface methodology (RSM). RSM is a multivariate optimal design technique used as a prediction tool for development, improvement and optimising process variables (Chi *et al.*, 2012). Apart from its cost-effectiveness compared to other traditional optimisation techniques, RSM can also be used to study the interaction effect of the process variables on the response through regression fitting (Aboelazayem *et al.*, 2018b).

6.4.1 Experimental design

The number of experiments (n) required for Box–Behnken design (BBD) design matrix is given as $n= 2^n + 2n + m.$ Where n is the number of independent variables, m is the number of replicated center points. Thus, a 3-level, 4-factor (3^4) factorial BBD with 29 runs of experiments were proposed for this study in order to effectively optimise the interaction effects of the reaction variables on system responses. Conversion of styrene oxide (SO) (%) and yield of styrene carbonate (SC) (%) have been selected as focused responses denoted as Y1 and Y2, respectively. While the four independent reaction variables analysed include the reaction temperature (K), CO_2 pressure (bar), catalyst loading (%) (w/w) and reaction time (t). All the four independent variables have been varied in a randomised manner over a set of experiments in order to minimise the effect of unexplained inconsistency in the responses. The variables and their coded values are presented with each level and range as given below in Table 6.2 (i.e. −1, 0, 1).

Table 6. 2. Experimental design variables and their coded levels

Variables	Code	Range and Levels		
		-1	0	+1
Temperature (K)	A	313	353	373
Pressure (bar)	B	2	8	10
Catalyst loading (w/w)	C	2	5	10
Time (h)	D	4	8	12

6.4.2 Statistical analysis

The experimental data were fitted to the general quadratic equation as shown in eq. 7.1 to illustrate each response variable (Y1 and Y2) as a function of the independent variables. Y was investigated using the second-order polynomial regression equation with backward elimination

A quadratic equation derived using RSM for the model is shown using eq. 7.1

$$Y = b_o + \sum_{i=1}^{n} b_i x_i + \sum_{i=1}^{n} b_{ii} x_i^2 + \sum_{i=1}^{n-1} \sum_{j>1}^{n} b_{ij} x_i x_j + \mathcal{E}$$

where Y is the predicted response, x_i and x_j are the independent variables in coded levels ($i \neq j$), b_i, b_{ii}, and b_{ij} are the coefficients for linear, quadratic and interaction effects, respectively, b_0 is the model coefficient constant, n is the number of factors, and Ɛ is the model random error (Liu *et al.*, 2016b).

The adequacy of the predicted models was validated by a number of statistical tools such as correlation coefficient (R^2), adjusted coefficient of determination (R^2_{adj}) and the predicted coefficient of determination (R^2_{pred}). The statistical significance of the

predicted model was analysed by (ANOVA) using the regression coefficient by conducting Fisher's F-test at 95% confidence level (Saada *et al.*, 2018). Design Expert 11 software (Stat- Ease Inc., Minneapolis, MN, USA) was used for the design of experiment, regression and graphical analysis. Statistical significance of the results has been presented by $p < 0.05$ and mean ± SE. The fit quality of the polynomial equation has been proved by R^2.

6.4.3 Model development and adequacy checking

The fitting accuracy of the predicted model has been examined for adequacy in terms of the experimental results obtained for the SO conversion (39 to 96%) and SC yield (15 to 67%) as indicated in Table 6.3. Different statistical and experimental validation techniques have been employed, these include ANOVA test at 95% confidence level for model statistical significance, R^2 and R^2_{adj} have also been used for the model empirical test. According to Table 6.3, the variations in the results have indicated that there has been a huge interaction between the reaction variables and the responses. Multiple regression analysis of the experimental data in Table 6.3 has been performed using Design-Expert software. It has generated two polynomial regression equations for each response variable representing an empirical relationship between reaction variables and each response variable as shown in eq. 6.2 and 6.3.

$$Y1 = 81.00 + 7.21\,A + 6.98\,B + 10.45\,C + 8.24\,D - 8.00\,AB + 8.79\,AC + 6.10\,AD - 3.50\,BC + 4.45\,BD + 1.45\,CD - 14.78\,A^2 - 0.39B^2 - 9.78\,C^2 - 8.67\,D^2 \quad \text{eq. 6.2}$$

$$Y2 = 53.00 + 5.54\,A + 6.67\,B + 4.84\,C + 7.29\,D - 12.90\,AB + 6.65\,AC + 4.98\,AD + 3.39\,BC + 5.72\,BD + 5.40\,CD - 13.54\,A^2 - 3.81^2 - 8.74\,C^2 - 811\,D^2 \quad \text{eq. 6.3}$$

Where, Y1, Y2 represents response variables including SO conversion and SC yield, respectively. A, B. C. and D represent independent variables including temperature, pressure, catalyst loading and time, respectively. Further, AB, AC, AD, BC, BD and CD represent the interaction between independent variables. Finally, A^2, B^2, C^2 and

D^2 represent the excess of each independent variables. The developed models have demonstrated the effect of each independent variables, variable interactions and excess of each variable on the response. The positive sign of each variable coefficient represents the synergetic effect of the variable on the response; however, the negative sign represents the antagonistic effect on the response.

The predicted RSM models have been examined for adequacy to report the possible problems associated with the normality assumptions. The RSM models have been validated by ANOVA at 95% confidence level. Fisher's F-test and p-value have been used to determine the significance of the corresponding variable.

Table 6. 3. Design matrix with the actual and predicted yield

Run	T *A* (K)	P *B* (bar)	t *C* (h)	Catalyst loading *D* (w/w)	Actual SO Conv. (%)	Predicted SO Conv. (%)	Actual SC Yield (%)	Predicted SC yield (%)
1	313	8	4	10	43	45.47	19	14.63
2	353	4	8	10	68	67.87	36	32.29
3	353	4	8	5	83	85.60	57	54.00
4	353	8	10	10	59	58.82	26	31.67
5	313	8	4	10	83	86.00	55	54.00
6	353	10	4	10	53	56.77	28	26.46
7	353	8	8	7	76	76.96	46	43.05
8	353	8	4	10	52	55.79	26	26.75
9	353	4	8	7	98	96.29	68	68.01
10	373	8	8	10	59	57.46	33	32.38
11	313	10	8	7	84	85.21	37	37.20
12	373	10	8	5	85	84.67	47	47.43
13	373	8	10	10	76	83.33	56	55.61
14	353	8	8	7	87	90.38	47	47.52
15	373	8	4	7	69	62.38	39	35.35
16	353	10	8	10	83	84.00	60	60.10
17	373	4	8	10	92	85.38	44	42.37
18	373	10	8	7	53	59.29	28	29.88
19	353	16	8	5	91	82.67	54	53.13
20	313	8	8	10	84	87.96	46	46.38
21	353	10	10	7	67	64.46	36	35.24
22	313	8	8	5	85	84.00	54	56.00
23	353	4	10	7	85	84.00	45	47.00
24	353	8	4	5	71	75.79	37	36.21
25	353	8	8	7	54	52.88	24	24.33
26	313	10	10	7	87	85.33	56	56.29
27	353	8	8	7	68	58.88	39	33.50
28	353	8	10	5	79	78.04	46	45.00
29	313	4	8	7	67	67.83	37	37.66

Table 6. 4. Analysis of variance of the developed model for SO conversion

Source	Sum of Squares	Diff	Mean Square	F-value	p-value	Significance
Model	5194.09	14	371.01	26.31	< 0.0001	HS
A-Temperature	918.75	1	918.75	28.02	0.0812	HS
B-Pressure	954.08	1	954.08	29.10	< 0.0001	HS
C-Catalyst Loading	645.33	1	645.33	19.68	0.0006	HS
D-Time	675.00	1	675.00	20.58	0.6360	HS
AB	342.25	1	342.25	10.44	0.0060	S
AC	196.00	1	196.00	5.98	0.0283	S
AD	64.00	1	64.00	1.95	0.1842	S
BC	20.25	1	20.25	0.6175	0.4451	S
BD	42.25	1	42.25	1.29	0.2754	S
CD	6.25	1	6.25	0.1906	0.6691	NS
A^2	876.59	1	876.59	26.73	0.0001	S
B^2	4.97	1	4.97	0.1514	0.7030	S
C^2	364.86	1	364.86	11.13	0.0049	S
D^2	340.95	1	340.95	10.40	0.0061	S
Residual	459.08	14	32.79			
Lack of Fit	459.08	10	45.91		0.123	NS
Pure Error	0.0000	4	0.0000			
Cor Total	5653.17	28				

S: significant, NS: not significant, HS: highly significant

Table 6. 5. Analysis of variance of the developed model for SC yield

Source	Sum of Squares	Difference	Mean Square	F-value	p-value	Significance
Model	7446.55	14	531.90	68.68	< 0.0001	HS
A-Temperature	1083.00	1	1083.00	139.85	< 0.0001	HS
B-Pressure	468.75	1	468.75	60.53	< 0.0001	HS
C-Catalyst Loading	1260.75	1	1260.75	162.80	< 0.0001	HS
D-Time	901.33	1	901.33	116.39	< 0.0001	HS
AB	576.00	1	576.00	74.38	< 0.0001	S
AC	225.00	1	225.00	29.05	< 0.0001	S
AD	100.00	1	100.00	12.91	0.0029	S
BC	121.00	1	121.00	15.62	0.0014	S
BD	156.25	1	156.25	20.18	0.0005	S
CD	132.25	1	132.25	17.08	0.0010	NS
A^2	1363.78	1	1363.78	176.11	< 0.0001	S
B^2	329.29	1	329.29	42.52	< 0.0001	S
C^2	993.34	1	993.34	128.27	< 0.0001	S
D^2	934.05	1	934.05	120.62	< 0.0001	S
Residual	108.42	14	7.74			
Lack of Fit	108.42	10	10.84	2.81489	0.22476	NS
Pure Error	0.0000	4	0.0000			
Cor Total	7554.97	28				

S: significant, NS: not significant, HS: highly significant

6.4.4 Statistical analysis of regression model

Equations 7.2 and 7.3 have concluded a good visualisation of the effect of significant variables and their interaction on each response. High values of determination coefficients (R^2 = 0.947 and 0.975 for SO conversion and SC yield, respectively) show a good correlation between actual and predicted results. These results indicated that only 0.053 and 0.025 of the total variation have not been well clarified for SO conversion and SC yield, respectively, which indicates a very high fitting of the predicted models with the experimental data. The ANOVA for the developed models has been applied to examine the significance of the model for fitting the experimental data. Table 6.4 and 6.5 summarises the ANOVA results for both SO conversion and SC yield models. The significance of the model is determined at high Fisher's F-value and low probability p-value. Based on the ANOVA results for SO conversion (Y1), F-value and p-value have been reported as 26.31 and <0.0001, respectively. While for SC yield (Y2), F-value and p-value have been evaluated as 68.68 and <0.0001, respectively. These results indicate that the model is statistically significant with a 95% confidence level. Moreover, the validity of the models has been confirmed by p-values of lack of fit i.e. 0.123 and 0.225 (more than 0.05) for SO conversion and SC yield, respectively, which indicates that the models have represented most of the experimental data successfully.

The appropriateness of the model has been investigated using various diagnostic residuals plot including normal plots of residuals, residuals *vs* predicted and predicted vs actual in order to study the behaviour of the model. Figure 6.8 depicts a normal distribution of residuals where most of the points follow an ideal straight line of regression, indicating the accuracy and significance of the model for the SO conversion (Abu *et al.*, 2017). Therefore, it can be construed that the normal plot residuals for SO conversion agree well with experimental data. In addition to the normality of the residuals plot, the equal variance of residuals above and below of the

X-axis at each level of the parameters validates the assumptions of the empirical model. For example, Figure 6.9 shows that there were no definite patterns in the plots while the majority of the plots fall within a horizontal band centered at zero. Deviation from these systemic patterns may suggest a violation of the constant variance assumption (Jeffries, 2003). Finally, the third hypothesis of ANOVA to test the validity of the predicted model is the randomisation of errors. The actual *vs* predicted response values shown in Figure 6.10 demonstrates the real response data plotted against the predicted responses. It can be observed that points above or below the horizontal line show areas of over or under prediction.

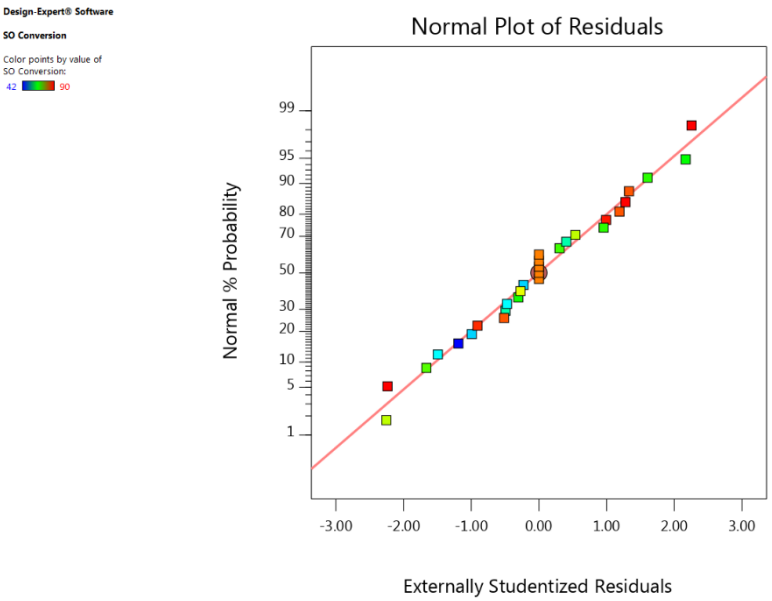

Figure 6. 8. Normal plot of residuals for SO conversion

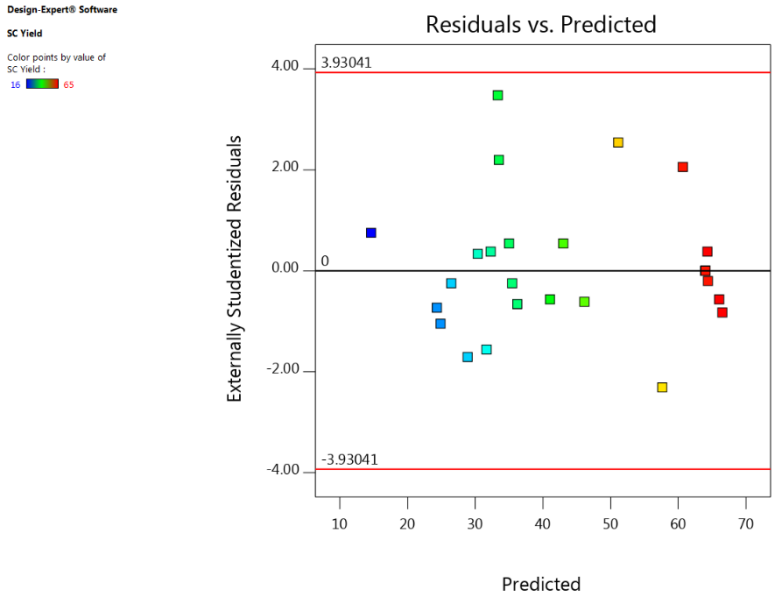

Figure 6. 9. Normal plot of residuals for SC yield

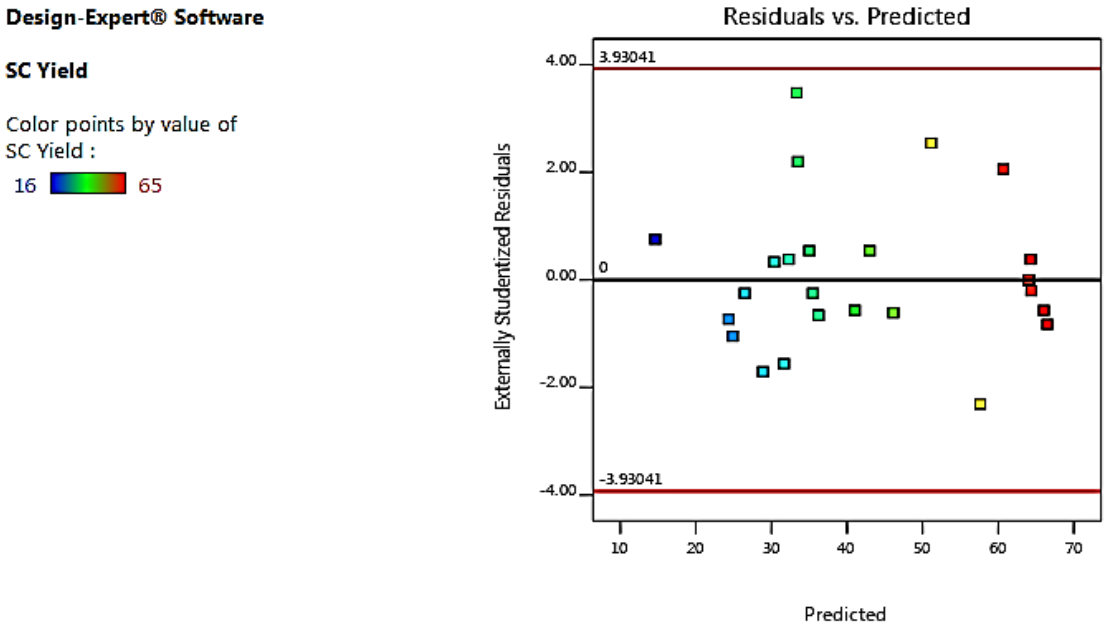

Figure 6. 10. Plot of residuals versus predicted values for the styrene carbonate yield model

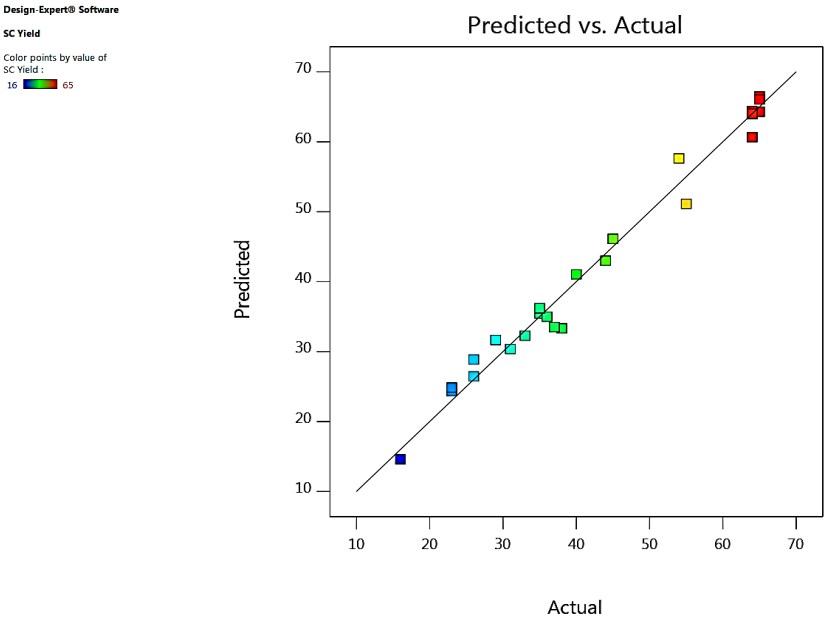

Figure 6. 11. Plot of predicted versus Actual values for the styrene carbonate yield model

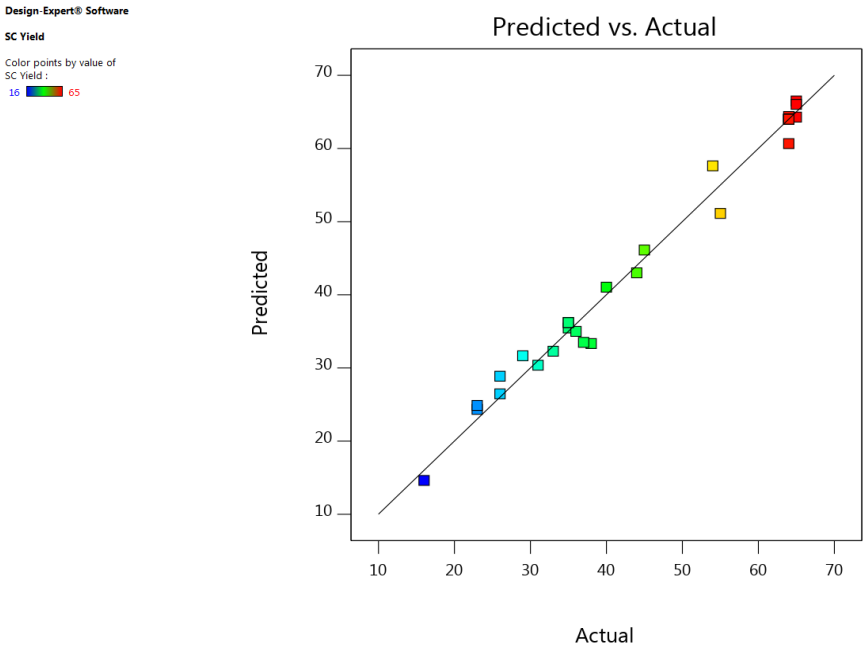

Figure 6. 12. Plot of residuals versus predicted values for the styrene carbonate yield model

6.5 Effect of process variables (One factor –at- a -time- OFAT)

The effects of individual reaction variables (temperature, pressure, time and catalyst loading) and their interactions on reaction responses (SO conversion and SC yield) have been investigated using the 3D-surface and contour plots generated from the predicted quadratic model as evidenced in Figures 6.13 to 6.15. The experiments have been carried out by varying one reaction parameter at a time while keeping other parameters constant at the following reaction conditions: reaction temperature 353 K, CO_2 pressure 6 bar, reaction time 8 h, catalyst loading 6 % (w/w).

6.5.1 Effect of reaction temperature

ANOVA results reported in Tables 6.4 and 6.5 shows that temperature has a highly significant effect on the process response. Figure 6.13 demonstrates that the direct proportionality relationship exists between temperature and SO conversion within the temperature of 323 K and 353 K. However, further increase in temperature beyond 353 K resulted in a slight drop in SO conversion. These negative results may be attributed to catalyst decomposition above the optimum as reported by Kawanami et al., (2003). They have observed that increasing the reaction temperature beyond the optimum of 408 K resulted in a marginal drop of propylene carbonate yield. Another possible factor reported by North, (2012) is a low solubility of CO_2 at a higher temperature. They have observed that less CO_2 was soluble at high temperatures resulting in low SC yield.

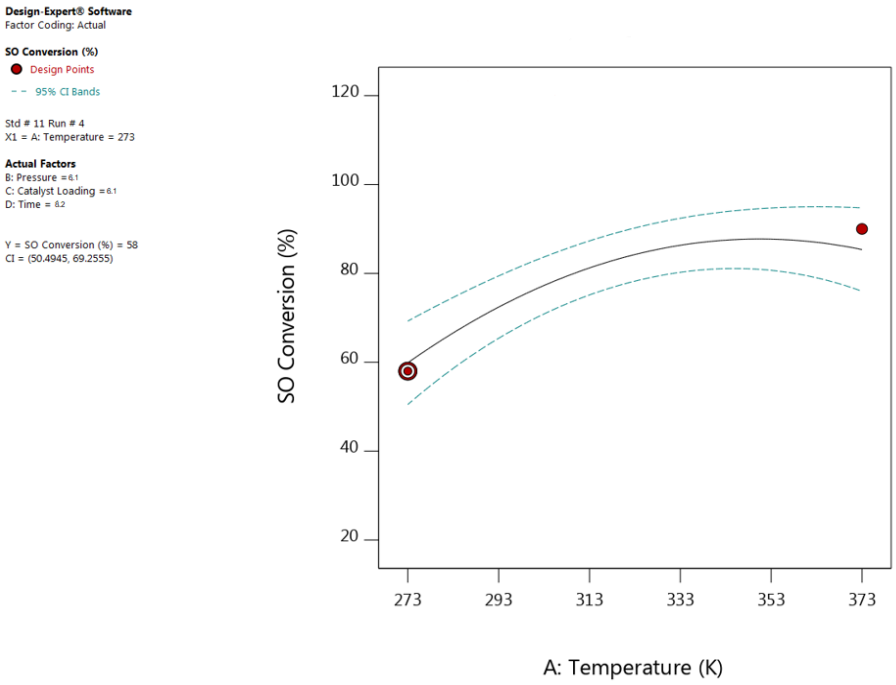

Figure 6. 13. The plot showing the effect reaction temperature on SO conversion

6.5.2 Effect of CO_2 pressure

From the ANOVA results in Table 6.4 and 6.5, it can be observed that variation in CO_2 pressure shows a significant effect on both the SO conversion and SC yield. According to Da Silva et al. (2012), the influence of CO_2 pressure on the two responses may have resulted from several factors including the volume of the phases present, the concentration of the reacting species, the activity of catalytically active species and the reaction kinetics in these phases. For example, Figure 6.14 shows that when CO_2 pressure was increased from 2 to 6 bar, the SC conversion also increased steadily from 69% to 85%. Conversely, when the CO_2 pressure was increased beyond 6.1 bar, the SO conversion drop to 83%. This demonstrated the effect of variation in CO_2 pressure on SO conversion was significant. It is therefore concluded that the optimum CO_2 pressure based on OFAT analysis for this set of experiments was 6.1 bar of CO_2 pressure.

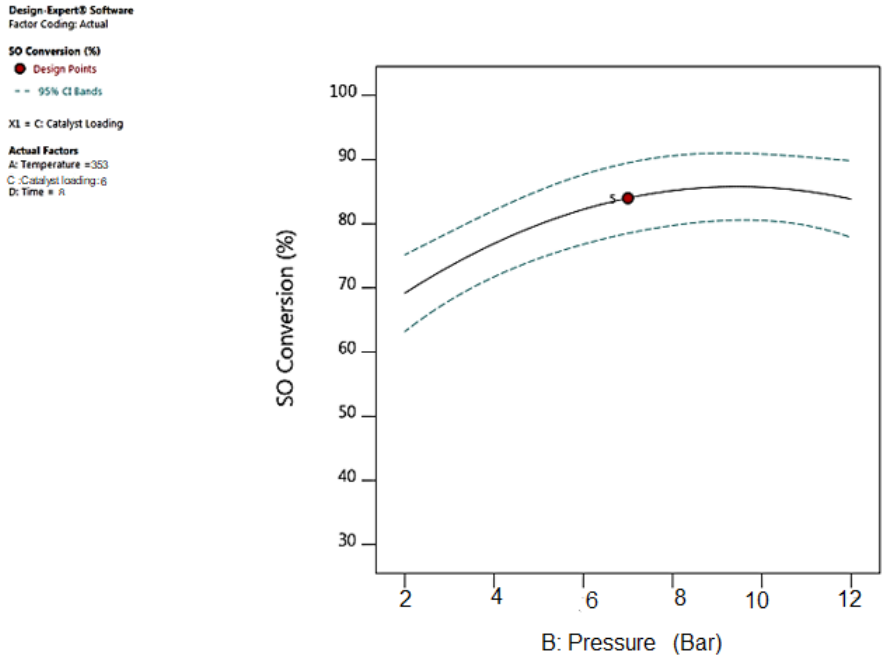

Figure 6. 14. The plot showing the effect CO_2 pressure on SO conversion

6.5.3 Effect of catalyst loading

The effect of varying the amount of catalyst used for SO conversion was also examined as shown in Figure 6.15. It was observed that a gradual increase in catalyst loading has a positive impact on the SO conversion as this increases the number of active sites taking part in the reaction. However, a sharp decrease in SO conversion was observed when the catalyst loading was increased beyond 6 % (w/w), indicating that the optimum level of catalyst loading has been exceeded. This phenomenon has been reported earlier by Unnikrishnan and Darbha, (2016).

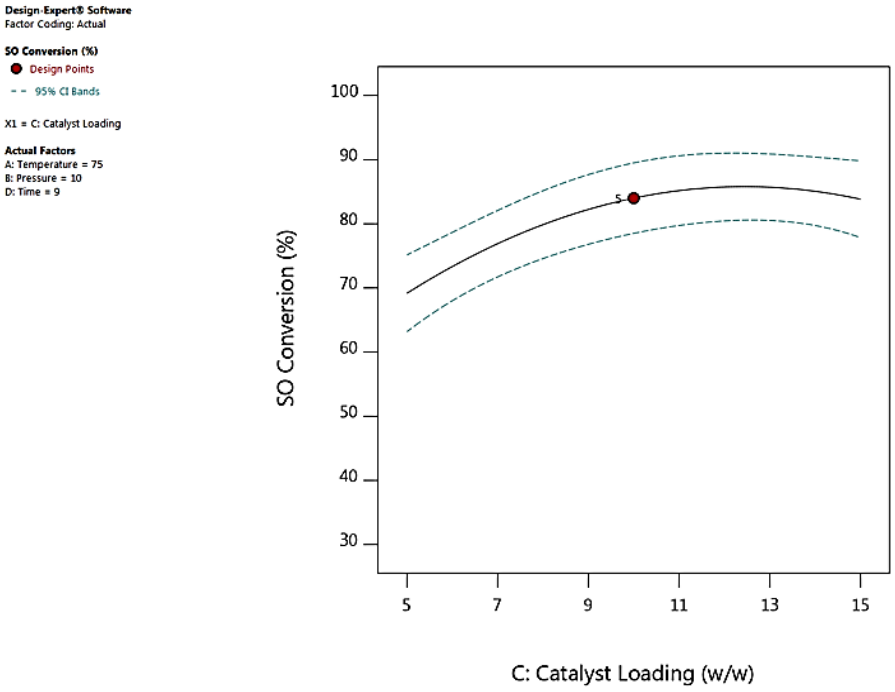

Figure 6. 15. The plot showing the effect catalyst loading on SO conversion.

6.6 Interaction effects of process variables

The interaction effect of each pair of reaction variables was investigated from both interaction plots and ANOVA results. Moreover, 3D-surface and contour plots for SO conversion and SC yields *versus* interaction of two independent variables have been used to illustrate the effect of interaction. In each plot, the two remaining independent variables have been kept constant at their center points.

6.6.1 Interactive effect of temperature and pressure

According to the ANOVA results in Tables 6.4 and 6.5, the interaction effect between reaction temperature and CO_2 pressure has significant effects on both SO conversion and SC yield (while keeping reaction time and catalyst loading at their optimum: 8 h and 6% w/w, respectively). As shown in Figure 6.16, the effect of reaction temperature at 4 bar of CO_2 pressure has an increasing effect on SC yield from 51% to 65% as the

temperature was increased from 313 K to 353 K. Further increase in temperature at the same level of CO_2 pressure shows no noticeable effect on the SC yield. Meanwhile, when the CO_2 pressure was further increased to 6 bar while maintaining the temperature at 353 K, a completely different effect was observed where a further 2% SC yield was recorded (67%). Conversely, when both temperature and CO_2 pressure were varied simultaneously to higher levels, a marginal decrease in SC yield was observed, similar to the report of Gallardo-Fuentes et al. (2016). This result implies that both temperature and CO_2 pressure has a negative effect on SC yield at higher values. The elliptical shape of the contour plot in Figure 6.17 exemplifies the interactive effect of the reaction variables on responses.

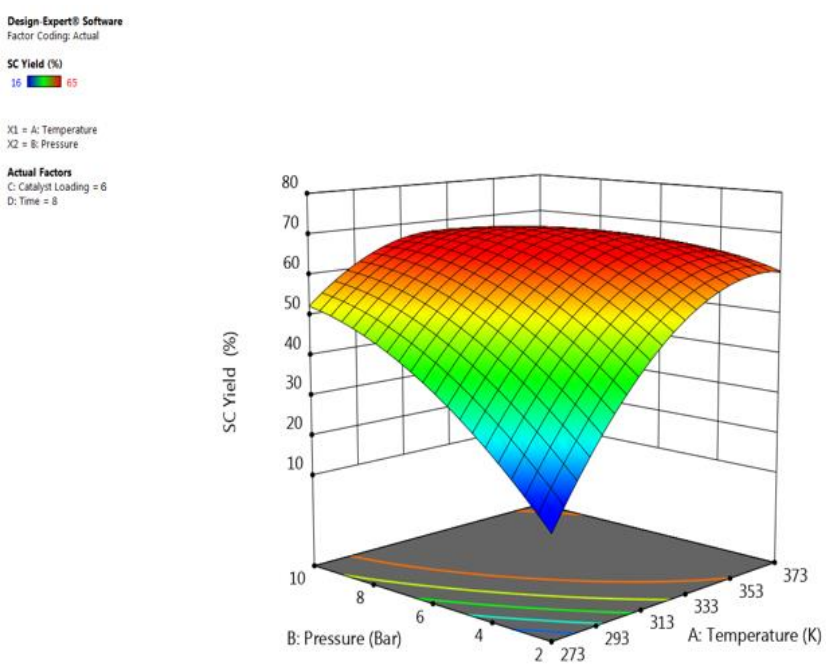

Figure 6. 16. 3D response surface plot of reaction temperature and pressure versus SC yield

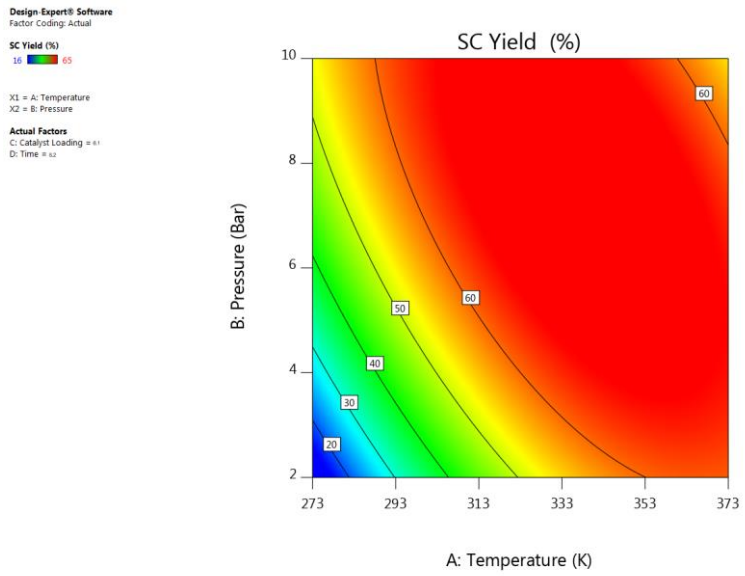

Figure 6. 17. Contour plot of reaction temperature and pressure *versus* SC yield

6.6.2 Interactive effect of time and catalyst loading

The contour and 3D surface plots in Figures 6.18 and 6.19 show the interaction effect between the reaction time and the catalyst loading at a constant temperature of 353 K and CO_2 pressure of 6 bar. The contour plots show less curvature up to 4 h of reaction time, which implies less influence of catalyst loading on SO conversion between the reaction time of 2-4 h. However, a maximum SO conversion of 96% was achieved at higher catalyst loading and reaction time of 6% (w/w) and 8 h, respectively. A declining effect was observed in Figure 6.18 as the catalyst loading goes above 6% (w/w) even when the reaction time was maintained at 8 h. This reflects the optimum catalyst loading and reaction time had been achieved. A similar trend was reported by (Shaikh and Sivaram, (1996) on the declining effect of catalyst loading beyond the optimum reaction time. An increase in the amount of catalyst loading can increase the number of active sites on the catalyst surface, and consequently, increase the number of radicals. However, an excessive increase in catalyst concentration beyond the optimum reaction time can result in a catalyst deactivation (Adeleye *et al.*, 2015). This

phenomenon is totally in agreement with the reports of Feilizadeh et al., (2017). Figure 6.19 shows an elliptical shape of the contour plot which indicates the interactive effect of the reaction variables on responses.

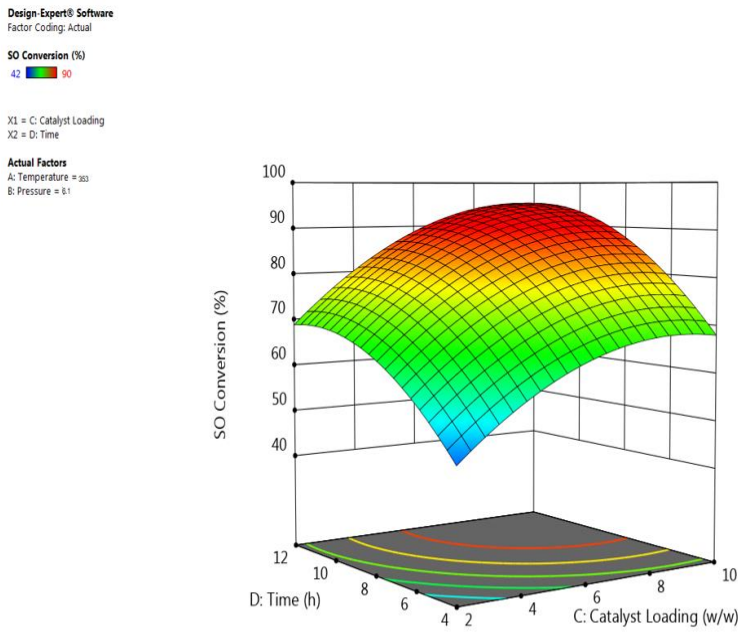

Figure 6. 18. 3D response surface plot of catalyst loading and time versus SO conversion

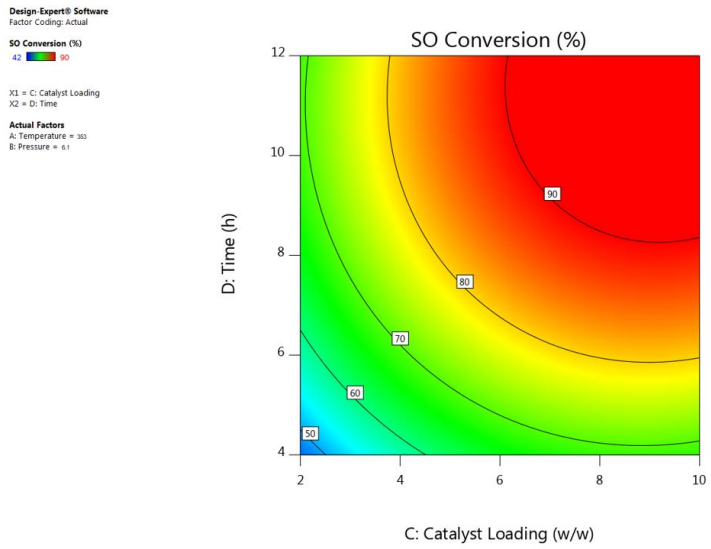

Figure 6. 19. Contour plot of catalyst loading and time *versus* SO conversion

6.6.3 Interactive effect of catalyst loading and pressure

The exponential interaction effect of catalyst loading and pressure on SO conversion at constant temperature and reaction time is shown in Figure 6.20 reaction time. Initially, a gradual increase in catalyst loading leads to a corresponding increase in the SO conversion, however, SO conversion became steady as the CO_2 pressure increases from 3-6 bar. The SO conversion was highest at the maximum catalyst loading of 6.1% (w/w) as shown in Figure 6.20. More catalyst loading indicates more active sites which participate in the reaction to catalyse the SC yield Olaniyan et al. (2020). It can be observed from Figure 6.21 that an increase in CO_2 pressure had a significant effect on SO conversion at different amounts of catalyst loading. More dilution of reactants and the catalyst enhances the mass transfer rate between limiting reactant SO and active sites of the catalyst which in turn increases the SO conversion.

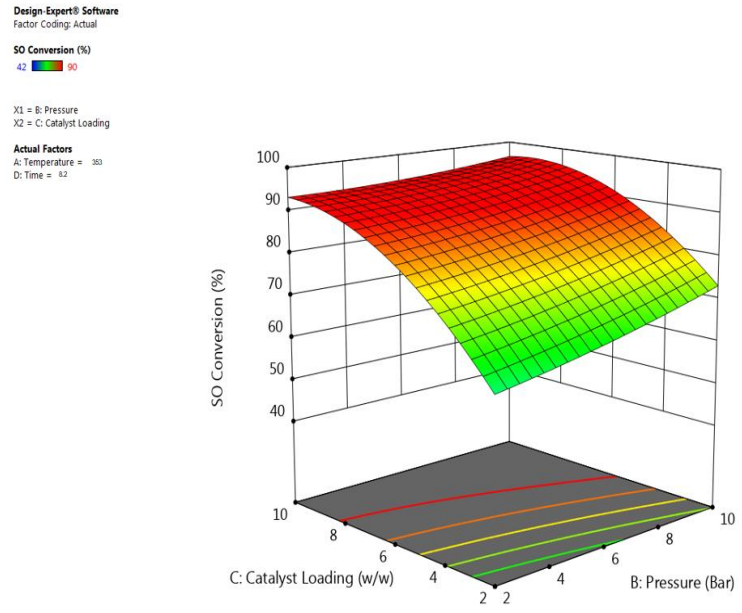

Figure 6. 20. 3D response surface plot of catalyst loading and pressure *versus* SO conversion

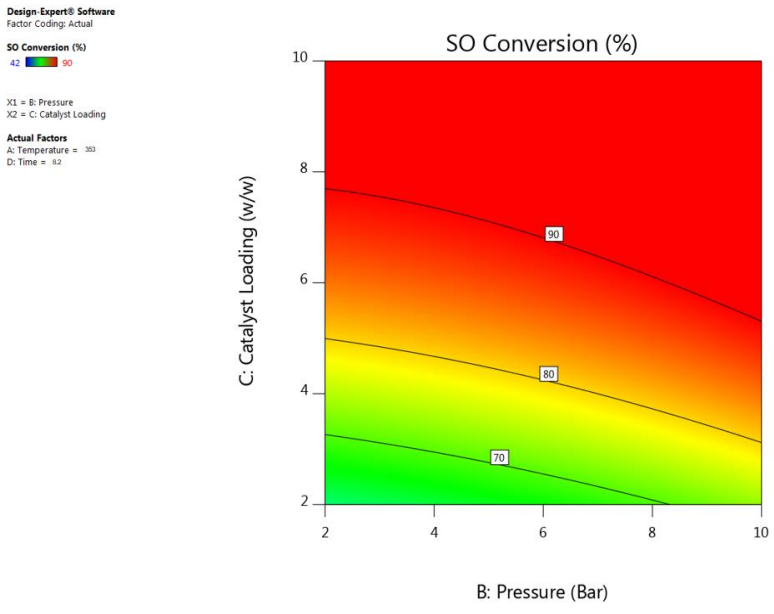

Figure 6. 21. Contour plot of catalyst loading and pressure *versus* SO conversion

6.6.4 Interactive effect of temperature and catalyst loading

The overall SC yield has been significantly influenced by the interaction between the catalyst loading and reaction temperature. Figure 6.22 shows that at lower catalyst loading of 3% (w/w), the SC yield was low. The SC yield increased as reaction temperature increased at moderate levels of catalyst loading. However, at a higher temperature above 353 K, a marginal decrease in SC yield was observed, which may be due to catalyst deactivation according to. A considerable increase in SC yield with an increased catalyst loading between 333-353 K was observed in Figure 6.22. This phenomenon could be attributed to the increase in the catalyst surface area, which provides more contact area between the limiting reactant SO and the active sites of the catalyst (Chen *et al.*, 2015). Higher catalyst loading gives higher SO conversion, an effect which is more pronounced at higher temperatures. The result is also supported lower p-value (0.0005) of the interaction AC term. The elliptical shape of the contour plot in Figure. 6.23 exemplifies the interactive effect of the reaction variables on responses.

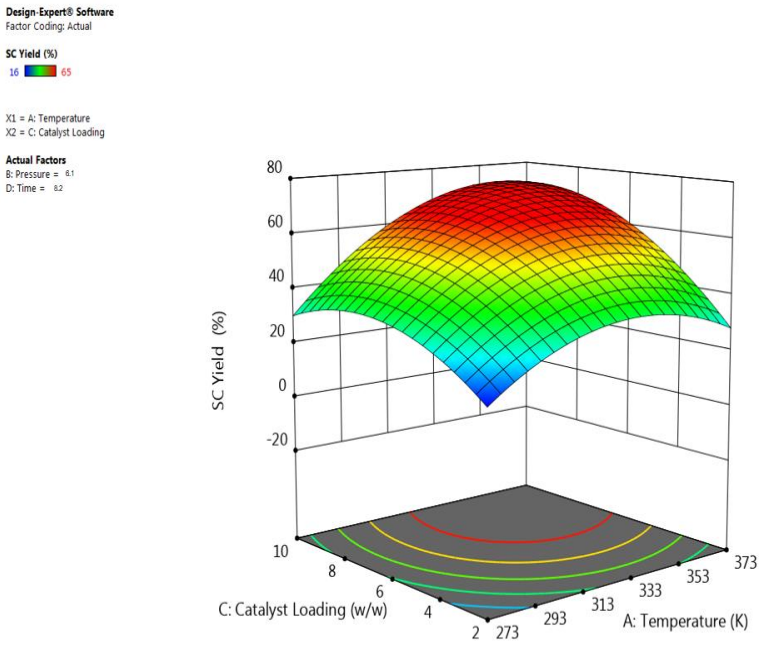

Figure 6. 22. 3D response surface plot of catalyst loading and reaction temperature *versus* SC yield

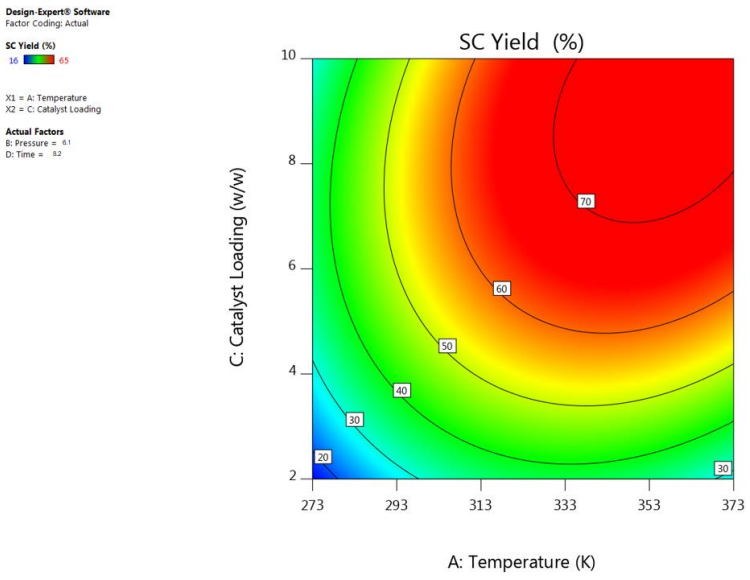

Figure 6. 23. Contour plot of catalyst loading and reaction temperature *versus* SC yield

6.7 Multiple responses optimisation

The optimisation process for the greener synthesis of styrene carbonate *via* cycloaddition reaction of styrene oxide and CO_2 has been carried out to define the optimum values for the effective reaction variables affecting the selected response variables. Design-Expert software has been used to develop the numerical optimisation step by combining the desirability of each independent variable into a single value and then search for optimum values for the specified response. Lastly, in order to conclude the optimum conditions of the independent variables, a set of targets must be defined on the software to guide the optimisation process (Thi Thanh *et al.*, 2017).

The targets of the independent variables have been set bearing in mind the economic and environmental implications of these variables. As a result, the high cost and energy-consuming variables i.e. reaction temperature (A), CO_2 pressure (B) and reaction time (D) have all been set to minimum, while catalyst loading (C) has been targeted to be between the range of minimum and maximum levels without restrictions since the used catalyst can be recovered and reused for subsequent reactions. Finally, the focused responses: SO and SC have both been set to be maximised in order to achieve optimal conversion and yield respectively within the independent variables targets restrictions. The numerical optimisation concluded that 98% and 67.7% of SO conversion and SC yield, respectively, could be achieved at optimal reaction conditions of 353 K, 6 bar, 6.1% catalyst loading in 8.2 h.

Table 6. 6. Optimisation constraints used to predict optimum conditions for the synthesis of styrene carbonate**.**

Factor	Code	Goal	Limits	
			Lower	Upper
Temperature (K)	*A*	Minimise	313	373
Pressure (bar)	*B*	Minimise	2	10
Catalyst loading (%)	*C*	In range	2	10
Time (h)	*D*	Minimise	4	12
SO conversion	Y_1	Maximise	70	100
SC yield	Y_2	Maximise	40	80

6.8 Validation of predicted optimum conditions

The optimal response values of the predicted quadratic equation have been validated experimentally at optimum effective reaction condition at 353 K reaction temperature, 6.1 bar of CO_2 pressure, 6.1 w/w catalyst loading and 8.2 hr of reaction time. The experimental results showed similar response value to the predicted optimal responses of 98% and 67% for SO conversion and SC yield respectively. These results ensured the validity of the optimisation steps with a relative error from the experimental results of 0.335% and 0.731% for SO conversion and SC yield, respectively. The similarity between the experimental response results and the predicted optimal response confirms and verifies the accuracy and adequacy of the optimisation technique conducted by the predicted quadratic model. The desired target was to maximise the yield of SC and SO conversion while minimising reaction parameters used in the regression model.

6.9 Conclusions

Styrene carbonate has been experimentally synthesised in a solvent-free cycloaddition reaction of SO and CO_2 and the effect of all the reaction variables on the conversion of SO and yield of SC have been successfully analysed using a traditional optimisation technique (OFAT). It has been established that the optimum reaction conditions using the OFAT method at 353 K, 6 bar, 6% (w/w) catalyst loading in 8 h reaction time gave a conversion of SO and SC yield of 98% and 68%, respectively. However, the use of RSM numerical optimisation technique at the optimum reaction conditions of 353 K, 6.1 bar, 6.1% (w/w) catalyst loading in 8.2 h reaction time and gave SO conversion of 96.5% and SC yield of 67%. The predicted optimum conditions have been validated experimentally with 0.335% and 0.731% relative error for both SO conversion and SC yield, respectively. The reaction temperature, pressure, time and catalyst loading have been determined as the significant variables affecting reaction responses using the OFAT method. Therefore, the experimental results and systematic optimisation of process variables in this study have clearly demonstrated an efficient and greener route for the synthesis of styrene carbonate from styrene oxide and CO_2 *via* CO_2 utilisation. The catalyst has shown a good substrate tolerance towards SO in solvent-free conditions with high selectivity towards SC. Its heterogeneity has been proven by recovering and reusing up seven times without any significant loss in catalytic activity. This property has shown that the catalyst is viable for large-scale industrial application

Chapter 7

Conclusions and recommendations for future work

Outline of the chapter

This chapter provides the overall conclusions of the thesis where the achievement of each research objective has been discussed. Furthermore, research recommendations for future work have been addressed.

The chapter is organised as follows:

7.1. Conclusions

7.2. Challenges and recommendations

7 Conclusions and recommendations for future work

7.1 Conclusions

This research has opened a new direction in heterogeneous catalytic conversion of CO_2 to organic carbonates. The development of a novel Zr/ZIF-8 catalyst *via* a simple low-cost solvothermal method has demonstrated that the catalyst is viable for large-scale industrial applications. The catalyst has shown good substrates tolerance as demonstrated by its activity towards different epoxides including epichlorohydrin (ECH), styrene oxide (SO), butylene oxide (BO) and cyclohexene oxide (CHO). More importantly, the reaction has been carried out under solvent-free and co-catalyst conditions. The heterogeneity nature of the catalyst has been proven by recovering and reusing the catalyst for up to seven times without any significant loss in catalytic activity. Furthermore, powder X-ray diffraction (PXRD), Fourier transform infrared (FTIR) spectra, and thermal gravimetric analysis (TGA) of first recycled catalyst described in Chapter 3 shows that the catalyst frameworks are quite stable after reusability performance. The high selectivity towards chloromethyl ethylene carbonate and styrene carbonate, simple separation of the catalyst by centrifugation, and excellent reusability studies have demonstrated that the catalyst is viable for large scale industrial applications. The physicochemical properties of the new catalyst have been satisfactorily consistent with pristine ZIF-8 catalyst using multiple characterisation techniques. We believe that this work could open up a new direction for designing a more sustainable, non-toxic catalyst for the transformation of CO_2 to organic carbonates and other valuable chemicals.

Finally, Zr/ZIF-8 has been assessed as a suitable heterogeneous catalyst outperforming the catalytic activity of ZIF-8 catalyst with respect to the conversion of epoxides selectivity and yield of organic carbonates. The catalyst has provided a remarkable reinforcement to the weak thermal functionality of ZIF-8. This has formed

one of the significant contributions to knowledge in the field of green and sustainable engineering. The enhancement in the catalytic activity of Zr/ZIF-8 has been explained based on acidity/basicity studies. The comparison of the catalytic activity of two catalysts has been drawn based on the effect of various reaction conditions such as reaction temperature, CO_2 pressure, catalyst loading, reaction time, stirring speed and reusability studies.

7.1.1 Review the existing technologies for the production of cyclic organic carbonates

Several production methodologies for the synthesis of organic carbonates have been critically examined in Chapter 2. Each methodology has been defined by highlighting the advantages and disadvantages of implementation. In addition, previously reported results have been reviewed by highlighting the operational conditions. A summary of the reviewed operational conditions of each process has also been highlighted.

7.1.2 Highlight one of the cyclic carbonate production technologies that could be implemented for a sustainable methodologies

After reviewing all the recent methodologies for carbonates synthesis, more emphases have been drawn to the cycloaddition reaction of CO_2 and epoxide as it provides a 100% atom economy and hence satisfying the green chemistry requirements. More importantly, section 2.3 of Chapter 2 has carried out an extensive critical review of the catalytic synthesis of both chloromethyl ethylene carbonate (CMEC) and styrene carbonate (SC) under various reaction conditions using different MOF catalysts.

7.1.3 Greener synthesis and characterisation of Zr/ZIF-8

Essentially, Zr/ZIF-8 has been successfully designed and tested as a greener, highly stable and efficient CO_2-reduction catalyst for the synthesis of various organic

carbonates. The catalyst has been designed by varying Zn/Zr ratio until Zn:Zr = 9:1 stoichiometric ratio was established as the most appropriate ratio for the catalytic system. Also in Chapter 3, the catalyst has been characterised using multiple physicochemical characterisation techniques. These properties have been found to be consistent with the properties displayed by pristine ZIF-8 catalyst. Experimental results show that the incorporation of zirconium into ZIF-8 has significantly increased ZIF-8 stability as well as the catalytic performance of Zr/ZIF-8. The catalyst displayed high epoxide conversions and high carbonate selectivity. The optimum experimental conditions and results for the synthesis of chloromethyl ethylene carbonate were found to be 353 K, 8 bar of CO_2 pressure and 8 h using fresh 10% (w/w) Zr/ZIF-8 catalyst loading for a 93% ECH conversion, 86% and 76% of CMEC selectivity and yield, respectively. While the optimum experimental conditions and results for the synthesis of styrene carbonate were found to be 353 K, 6 bar of CO_2 pressure and 8 h using fresh 6% (w/w) Zr/ZIF-8 catalyst loading for a 98% SO conversion, 72% and 68% of SC selectivity and yield, respectively. Similarly, the optimised reaction conditions and results using RSM techniques for the synthesis of chloromethyl ethylene carbonate were found at 353 K, 11 Bar of CO_2 pressure 12 h using 12% (w/w) fresh catalyst loading for a 96% ECH conversion and 68% CMEC yield while 353 K, 6.1 Bar of CO_2 pressure and 8.2 h using fresh 6% (w/w) Zr/ZIF-8 catalyst loading for 98% SO conversion and 68% SC yield for the synthesis of styrene carbonate.

7.1.4 Apply response surface methodology (RSM) technique to model and optimise the reaction process

In the current work, response surface methodology (RSM) has been employed to investigate and optimise process variables for the greener synthesis of chloromethyl ethylene carbonate and styrene carbonate. Using the design expert software, a quadratic model was developed to study the interactions between four independent variables (temperature, CO_2 pressure, catalyst loading and time) and two reaction

responses (conversion of epichlorohydrin (ECH) and yield of chloromethyl ethylene carbonate (CMEC) as well as the conversion of styrene oxide (SO) and yield of styrene carbonate (SC)). The adequacy of the model has been validated by the correlation between the experimental and predicted values of the responses using an Analysis of variance (ANOVA) Table. With a coefficient of the determination being R^2 of 0.9973 and an R^2_{adj} of 0.9954 and a *p*-value ($P<0.0001$) for CMEC while R^2 of 0.9470 and an R^2_{adj} of 0.9841 and a *p*-value ($P<0.0001$) for SC. The model was highly significant and could be recommended for process optimisation in the synthesis of both CMEC and SC. The experimental results concluded that an increase in reaction parameters increases the conversion of epoxide and carbonate yield.

7.2 Challenges and recommendations

Synthesis of organic carbonates *via* cycloaddition of CO_2 and epoxide has numerous environmental benefits and potentials for sustainable development in comparison with other conventional synthesis methodologies in terms of higher carbonate yield, easy product separation and lower reaction temperature and/or CO_2 pressure. However, many limitations and challenges need to be resolved before implementing the method on a commercial scale. This section covers some recommendations for improving the process and enhancing its applicability and profitability.

7.2.1 Improving the activity of Zr/ZIF-8

This research has demonstrated that Zr/ZIF-8 catalyst is a promising candidate for chemical fixation of CO_2 to organic carbonates. Its catalytic activity and stability show that it performed beyond average when compared with most of the existing ZIF based MOF catalysts. It requires less energy input, no solvent/co-catalyst to catalyse the reaction and easy product separation. More importantly, Zr/ZIF-8 follows a simple and easy and low cost traditional solvothermal synthesis method. However, further

investigations are recommended in order to improve its catalytic performance. This include:

- Varying Zr/Zn ratio in order to establish a more suitable stoichiometric ratio for the catalytic design.
- Establishing an ideal catalyst/reactant ratio in the cycloaddition reaction of CO_2 and epoxide for optimal results.
- Determining the best temperature range for catalyst activation.
- Possibilities to improve the reusability of the catalyst may also be areas of great interest. Comparatively, the solvothermal approach of synthesising MOFs may be slightly more expensive than producing zeolite. Therefore, future work can be focused on reducing the production cost of ZIF-8 to make Zr/ZIF-8 catalyst a more economically efficient by exploring the effects of impure solvent, different gel composition and cheaper zinc sources. Furthermore, the Zr/ZIF-8 is decently active in the conversion of CO_2 to carbonates in the laboratory using pure carbon dioxide, its performance with CO_2 gas mixture is not clear. It is important to study the catalytic ability of Zr/ZIF-8 when using CO_2 mixed with other gases because CO_2 does not come in pure form but rather as in flue gas (a mixture of gases).

7.2.2 Catalyst characterisation

The activity of the catalyst relies in part on the synergistic effect between the polarisation of Lewis acidic zinc species and nucleophilic attack of halides on epoxide, which promotes the epoxy ring-opening for effective carbonate synthesis. Therefore, investigating of redox properties of the catalyst is highly recommended in order to identify appropriate information needed for improving the novelty of the catalyst.

7.2.3 Synthesis of other valuable organic carbonates

Our studies illustrated that Zr/ZIF-8 is a promising material for a catalyst. It performed more active, stable and reusable than most of the reported ZIF-based catalysts. It catalyses the reaction at lesser energy usage and was easier to be separated from the products. However, future work could be focused on further extensive synthesis to achieve a lesser reaction optimum condition. Its catalytic activity also could be tested on other popular epoxides such as propylene oxide, ethylene oxide, dimethyl carbonate.

7.2.4 Use of CO_2 gas mixture (flue gases) for organic carbonate synthesis

CO_2 does not come in pure form but rather as a mixture of gases, the catalytic performance of Zr/ZIF-8 could be studied when using CO_2 mixed with other gases. Although Zr/ZIF-8 is active in the conversion of CO_2 to organic carbonates in the lab using pure carbon dioxide. It would be desirable and very useful to develop a technological way to directly utilise CO_2 from CO_2 mixture of gases (flue gas) for organic carbonate synthesis. The development of this process would avoid the cost associated with carbon capture and storage (CCS).

7.2.5 Techno-economic analysis

This research work has provided a step forward towards the greener synthesis of several organic carbonates and more importantly, CO_2 utilisation. Zr/ZIF-8 served as a standalone catalyst (in the absence of any organic solvent or co-catalyst). However, a comprehensive economic assessment and environmental benefits of the process would be helpful for comparison to the conventional way of cyclic carbonate synthesis using homogeneous catalysts in the presence of organic solvents. This analysis would suggest the potential advantage of the current method. Life cycle assessment (LCA)

could be an important tool to evaluate the environmental impact and economic feasibility study of this process.

Chapter 8

References

8 References

Abhang, R. M., Wani, K. S. and Patil, V. S. (2015) Synthesis and Characterization of ZIF-8 Filler for Preparation of Mixed Matrix Membrane, *International Journal of Science & Engineering Research*, 6 (8), pp. 1276–1280. DOI:10.1002/slct.201600162.

Aboelazayem, O., El-Gendy, N. S., Abdel-Rehim, A. A., Ashour, F. and Sadek, M. A. (2018a) Biodiesel production from castor oil in Egypt: Process optimisation, kinetic study, diesel engine performance and exhaust emissions analysis, *Energy*, 157, pp. 843–852. DOI:10.1016/j.energy.2018.05.202.

Aboelazayem, O., Gadalla, M. and Saha, B. (2018b) Valorisation of high acid value waste cooking oil into biodiesel using supercritical methanolysis: Experimental assessment and statistical optimisation on typical Egyptian feedstock, *Energy*, 162, pp. 408–420. DOI:10.1016/j.energy.2018.07.194.

Abu, M. L., Nooh, H. M., Oslan, S. N. and Salleh, A. B. (2017) Optimization of physical conditions for the production of thermostable T1 lipase in Pichia guilliermondii strain SO using response surface methodology, *BMC Biotechnology*, 17 (1), pp. 1–10. DOI:10.1186/s12896-017-0397-7.

Adeleye A.I. (Supervisor-Saha. B) Catalytic Conversion of Carbon Dioxide (CO_2) into Value Added Chemicals. Ph.D. Thesis, *London South Bank University*, London, UK, 2015.

Adeleye, A. I., Kellici, S., Heil, T., Morgan, D., Vickers, M. and Saha, B. (2015) Greener synthesis of propylene carbonate using graphene-inorganic nanocomposite catalysts, *Catalysis Today*, 256 (2), pp. 347–357. DOI:10.1016/j.cattod.2014.12.032.

Adeleye, A. I., Patel, D., Niyogi, D. and Saha, B. (2014) Efficient and greener synthesis of propylene carbonate from carbon dioxide and propylene oxide, *Industrial and Engineering Chemistry Research*, 53 (49), pp. 18647–18657. DOI:10.1021/ie500345z.

Agarwal, A. S., Rode, E., Sridhar, N. and Hill, D. (2016) Conversion of CO_2 to Value-Added Chemicals: Opportunities and Challenges, *Handbook of Climate Change Mitigation and Adaptation*. 17 (4), pp. 1-4. DOI:10.1007/978-1-4614-6431-0.

Al-Qaisi, F. M., Nieger, M., Kemell, M. L. and Repo, T. J. (2016) Catalysis of Cycloaddition of Carbon Dioxide and Epoxides Using a Bifunctional Schiff Base Iron(III) Catalyst, *ChemistrySelect*, 1 (3), pp. 545–548. DOI:10.1002/slct.201600162.

Aluja, C. and Laia (2017) Towards green synthesis of organic carbonates : Utilization of CO_2 as a chemical feedstock, Ph.D. Thesis, *Universitat Rovira i Virgili, 2015.*

An, S., Lee, J. S., Joshi, B. N., Jo, H. S., Titov, K., Chang, J. S., (2016) Freestanding fiber mats of zeolitic imidazolate framework 7 via one-step, scalable electrospinning, *Journal of Applied Polymer Science*, 133 (32), pp. 1–8. DOI:10.1002/app.43788.

Andraos, J. (2011) A green metrics assessment of phosgene and phosgene-free syntheses of industrially important commodity chemicals, *Pure and Applied Chemistry*, 84 (3), pp. 827–860. DOI:10.1351/pac-con-11-06-12.

Appaturi, J. N. and Adam, F. (2013) A facile and efficient synthesis of styrene carbonate via cycloaddition of CO_2 to styrene oxide over ordered mesoporous MCM-41-Imi/Br catalyst, *Applied Catalysis B: Environmental*, 136 (137), pp. 150–159. DOI:10.1016/j.apcatb.2013.01.049.

Arends, I., Sheldon, R., Hanefeld, U., Arends, I. and Hanefeld, U. (2007) *Introduction: Green Chemistry and Catalysis*, *Green Chemistry and Catalysis*. *Catalysis today*, 122-245, pp, 1122-126 DOI:10.1002/9783527611003.ch.

Arnold, P. L., Scarisbrick, A. C., Blake, A. J. and Wilson, C. (2001) Chelating alkoxy-N-heterocyclic carbene complexes of silver and copperElectronic supplementary information (ESI), *Chemical Communications*, 10 (22), pp. 2340–2341. DOI:10.1039/b107855k.

Babu, R., Kathalikkattil, A. C., Roshan, R., Tharun, J., Kim, D. W. and Park, D. W. (2015) Dual-porous metal organic framework for room temperature CO2fixation via cyclic carbonate synthesis, *Green Chemistry*, 18 (1), pp. 232–242. DOI:10.1039/c5gc01763g.

Bahrami, M., Amiri, M. J. and Bagheri, F. (2019) Optimization of the lead removal from aqueous solution using two starch based adsorbents: Design of experiments using response surface methodology (RSM), *Journal of Environmental Chemical Engineering*, 7 (1), pp. 102-793. DOI:10.1016/j.jece.2018.11.038.

Bai, D., Zhang, Z., Wang, G. and Ma, F. (2015) Cycloaddition of epoxide and CO_2 to cyclic carbonate catalyzed by VO(IV) porphyrin, *Applied Organometallic Chemistry*, 29 (4), pp. 240–243. DOI:10.1002/aoc.3278.

Bai, Y., Dou, Y., Xie, L.-H., Rutledge, W., Li, J.-R. and Zhou, H.-C. (2016) Zr-based metal–organic frameworks: design, synthesis, structure, and applications, *Chem. Soc. Rev.*, 45 (8), pp. 2327–2367. DOI:10.1039/C5CS00837A.

Baj, S., Krawczyk, T., Jasiak, K. and Siewniak, A. (2014) General Catalytic coupling of epoxides and CO_2 to cyclic carbonates by carbon nanotube-supported quaternary ammonium salts, *Applied Catalysis A* , 488 (3), pp. 96–102. DOI:10.1021/ja508626n

Baş, D. and Boyacı, İ. H. (2007) Modeling and optimization I: Usability of response surface methodology, *Journal of Food Engineering*, 78 (3), pp. 836–845. DOI:10.1016/j.jfoodeng.2005.11.024.

Bazzanella, A. M. (2014) Carbon Dioxide, *Energy system,* 4 (2), pp. 21-30. DOI:10.1002/14356007.a05.

Beckman, E. J. (2004) Supercritical and near-critical CO_2 in green chemical synthesis and processing, *Journal of Supercritical Fluids*, 28 (2–3), pp. 121–191. DOI:10.1016/S0896-8446(03)00029-9.

Beyzavi, M. H., Klet, R. C., Tussupbayev, S., Borycz, J., Vermeulen, N. A., Cramer, C. J., Stoddart, J. F., Hupp, J. T. and Farha, O. K. (2014) A hafnium-based metal-organic framework as an efficient and multifunctional catalyst for facile CO_2 fixation and regioselective and enantioretentive epoxide activation, *Journal of the American Chemical Society*, 136 (45), pp. 15861–15864. DOI:10.1021/ja508626n.

Beyzavi, M. H., Stephenson, C. J., Liu, Y., Karagiaridi, O., Hupp, J. T. and Farha, O. K. (2015) Metal Organic Framework-Based Catalysts: Chemical Fixation of CO_2 with Epoxides Leading to Cyclic Organic Carbonates, *Frontiers in Energy Research*, 2 (January), pp. 1–10. DOI:10.3389/fenrg.2014.00063.

Bezerra, M. A., Santelli, R. E., Oliveira, E. P., Villar, L. S. and Escaleira, L. A. (2008) Response surface methodology (RSM) as a tool for optimization in analytical chemistry, *Talanta*, 76 (5), pp. 965-977. DOI:10.1016/j.talanta.2008.05.019.

Bhanage, B. M. and Arai, M. (2014) *Transformation and Utilization of Carbon Dioxide*. *Journal of the American Chemical Society*, 178 (40), pp. 39-53, DOI:10.1007/978-3-642-44988-8.

Bhanage, B. M., Fujita, S. I., Ikushima, Y. and Arai, M. (2001) Synthesis of dimethyl carbonate and glycols from carbon dioxide, epoxides, and methanol using heterogeneous basic metal oxide catalysts with high activity and selectivity, *Applied Catalysis A: General*, 219 (1–2), pp. 259–266. DOI:10.1016/S0926-860X(01)00698-6.

Bhattacharjee, S., Jang, M. S., Kwon, H. J. and Ahn, W. S. (2014) Zeolitic Imidazolate Frameworks: Synthesis, Functionalization, and Catalytic/Adsorption Applications, *Catalysis Surveys from Asia*, 18 (4), pp. 101–127. DOI:10.1007/s10563-014-9169-8.

Bhin, K. M., Tharun, J., Roshan, K. R., Kim, D. W., Chung, Y. and Park, D. W. (2017) Catalytic performance of zeolitic imidazolate framework ZIF-95 for the solventless synthesis of cyclic carbonates from CO_2 and epoxides, *Journal of CO_2 Utilization*, 17, pp. 112–118. DOI:10.1016/j.jcou.2016.12.001.

Bidokhti, N. S. (2017) Synthesis , Characterisation and Application of Carbonised Metal Organic Frameworks, *Journal of the American Chemical Society*, 19 (28), pp. 15861–15864. DOI:10.1021/ja508626n.

Biotecnologia, M. (2016) Małgorzata Ewa Zakrzewska Towards carbon dioxide utilisation : dense phase carbon dioxide and its mixtures with ionic liquids. *Applied Organometallic Chemistry*, 29 (4), pp. 240–243. DOI:10.1002/aoc.3278.

Biswal, B. P., Shinde, D. B., Pillai, V. K. and Banerjee, R. (2013) Stabilization of graphene quantum dots (GQDs) by encapsulation inside zeolitic imidazolate framework nanocrystals for photoluminescence tuning, *Nanoscale*, 5 (21), pp. 10556–10561. DOI:10.1039/c3nr03511e.

Bobadilla, L. F., Lima, S. and Urakawa, A. (2015) *Cycloaddition of CO_2 and Epoxides over Reusable Solid Catalysts*, *Advanced Catalytic Materials*. 28 (2–3), pp. 121–191 DOI:10.1002/9781118998939.ch8.

Bosch, M., Zhang, M. and Zhou, H.-C. (2014) Increasing the Stability of Metal-Organic Frameworks, *Advances in Chemistry*, 2 (9), pp. 1–8. DOI:10.1155/2014/182327.

Brozek, C. K. and Dincă, M. (2014) Cation exchange at the secondary building units of metal-organic frameworks, *Chemical Society Reviews*, 43 (16), pp. 5456–5467. DOI:10.1039/c4cs00002a.

Butterworth, B. (2006) Reversing Global Warming?, The potential of using wastes, 7 (5), pp. 54–55. DOI:10.1016/S1471-0846(06)70701-6.

Büttner, H., Longwitz, L., Steinbauer, J., Wulf, C. and Werner, T. (2017) Recent Developments in the Synthesis of Cyclic Carbonates from Epoxides and CO_2, *Topics in Current Chemistry*, 375 (3), pp. 4-8. DOI:10.1007/s41061-017-0136-5.

Cai, S., Zhu, D., Zou, Y. and Zhao, J. (2016) Porous polymers bearing functional quaternary ammonium salts as efficient solid catalysts for the fixation of CO_2 into cyclic carbonates, *Nanoscale Research Letters*, 11 (1), pp. 0–8. DOI:10.1186/s11671-016-1529-z.

Calabrese, C., Giacalone, F. and Aprile, C. (2019) Hybrid Catalysts for CO_2 Conversion into Cyclic Carbonates, *Catalysts*, 9 (4), pp. 325 (1-10). DOI:10.3390/catal9040325.

Carreon, M. A. (2012) Metal organic frameworks as catalysts in the conversion of CO_2 to cyclic carbonates, *Indian Journal of Chemistry - Section A Inorganic, Physical, Theoretical and Analytical Chemistry*, 51 (9–10), pp. 1306–1314. DOI: 10.1021/cs200638h

Cavka, J. H., Jakobsen, S., Olsbye, U., Guillou, N., Lamberti, C., Bordiga, S. and Lillerud, K. P. (2008) A New Zirconium Inorganic Building Brick Forming Metal Organic Frameworks with Exceptional Stability, *JACS communications*, 130 (42), pp. 13850–13851. DOI:10.1021/ja8057953.

Chen, B. (2016) Zeolitic imidazolate frameworks (ZIFs) and their derivatives : synthesis and energy related applications. Ph.D. Thesis, University of Exeter, UK.

Chen, D., Zhang, X. and Lee, A. F. (2015) Synthetic strategies to nanostructured photocatalysts for CO_2 reduction to solar fuels and chemicals, *Journal of Material Chemistry. A*, 3 (28), pp. 14487–14516. DOI:10.1039/C5TA01592H.

Chen, L., Wang, S., Zhou, J., Shen, Y., Zhao, Y. and Ma, X. (2014) Dimethyl carbonate synthesis from carbon dioxide and methanol over CeO_2 versus over ZrO_2 : comparison of mechanisms, *Royal Society of Chemistry Advance.*, 4 (59), pp. 30968–30975. DOI:10.1039/C4RA03081H.

Cheng, W., Su, Q., Wang, J., Sun, J. and Ng, F. (2013) Ionic Liquids: The Synergistic Catalytic Effect in the Synthesis of Cyclic Carbonates, *Catalysts*, 3 (4), pp. 878–901. DOI:10.3390/catal3040878.

Cheng, W., Xu, F., Sun, J., Dong, K., Ma, C. and Zhang, S. (2016) Superbase/saccharide: An ecologically benign catalyst for efficient fixation of CO_2 into cyclic carbonates, *Synthetic Communications*, 46 (6), pp. 497–508. DOI:10.1080/00397911.2016.1151050.

Chi, G., Hu, S., Yang, Y. and Chen, T. (2012) Response surface methodology with prediction uncertainty: A multi-objective optimisation approach, *Chemical Engineering Research and Design*, 90 (9), pp. 1235–1244. DOI:10.1016/j.cherd.2011.12.012.

Cho, H. Y., Yang, D. A., Kim, J., Jeong, S. Y. and Ahn, W. S. (2012) CO_2 adsorption and catalytic application of Co-MOF-74 synthesized by microwave heating, *Catalysis Today*, 185 (1), pp. 35–40. DOI:10.1016/j.cattod.2011.08.019.

Choe, H., Joo, J. C., Cho, D. H., Kim, M. H., Lee, S. H., Jung, K. D. and Kim, Y. H. (2014) Efficient CO_2-reducing activity of NAD-dependent formate dehydrogenase from Thiobacillus sp. KNK65MA for formate production from CO_2 gas, *PLoS ONE*, 9 (7), pp. 14–16. DOI:10.1371/journal.pone.0103111.

Clark, J. and Macquarrie, D. (2002) *Handbook of Green Chemistry and Technology*., Catalysis, 5 (9), pp. 2-6. DOI:10.1002/9780470988305.

Corey D. P., Garcia-Anoveros J., Holt J. R., Kwan K. Y., Lin S., Vollrath M. A. (2004) TRPA1 is a candidate for the mechanosensitive transduction channel of vertebrate hair cells, *Nature*, 432 (8), pp. 723–730. DOI: /10.1038030665c.

Cota, I. and Fernandez Martinez, F. (2017) Recent advances in the synthesis and applications of metal organic frameworks doped with ionic liquids for CO_2 adsorption, *Coordination Chemistry Reviews*, 351 (10), pp. 189–204. DOI:10.1016/j.ccr.2017.04.008.

Cucciniello, R. and Cespi, D. (2018) Recycling within the Chemical Industry: The Circular Economy Era, *Recycling*, 3 (2), pp. 22. DOI:10.3390/recycling3020022.

Cui, K., Liang, Z., Zhang, J. and Zhang, Y. (2015) Synthesis of Cyclohexene Carbonate Catalyzed by Polymer-Supported Catalysts, *Synthetic Communications*, 45 (6), pp. 712–723. DOI:10.1080/00397911.2014.979297.

Cychosz, K. A., Guillet-Nicolas, R., García-Martínez, J. and Thommes, M. (2017) Recent advances in the textural characterization of hierarchically structured nanoporous materials, *Chem. Soc. Rev.*, 46 (2), pp. 389–414. DOI:10.1039/C6CS00391E.

Da Silva, E., Dayoub, W., Mignani, G., Raoul, Y. and Lemaire, M. (2012) Propylene carbonate synthesis from propylene glycol, carbon dioxide and benzonitrile by alkali carbonate catalysts, *Catalysis Communications*, 29, (7) pp. 58–62. DOI:10.1016/j.catcom.2012.08.030.

Da Silva, J. D. S. F., Malo, D. L., Bataglion, G. A., Eberlin, M. N., Ronconi, C. M., Alves, S. and De Sá, G. F. (2015) Adsorption in a fixed-bed column and stability of the antibiotic oxytetracycline supported on Zn(II)-[2-methylimidazolate] frameworks in aqueous media, *PLoS ONE*, 10 (6). DOI:10.1371/journal.pone.0128436.

Dai, W. L., Luo, S. L., Yin, S. F. and Au, C. T. (2009) The direct transformation of carbon dioxide to organic carbonates over heterogeneous catalysts, *Applied Catalysis A: General*, 366 (1), pp. 2–12. DOI:10.1016/j.apcata.2009.06.045.

Dallali Isfahani, T., Javadpour, J., Khavandi, A., Goodarzi, M. and Rezaie, H. R. (2014) Nanocrystalline growth activation energy of zirconia polymorphs synthesized by mechanochemical technique, *Journal of Materials Science and Technology*, 30 (4), pp. 387–393. DOI:10.1016/j.jmst.2013.10.012.

Darensbourg, D. J. (2010) Chemistry of carbon dioxide relevant to its utilization: A personal perspective, *Inorganic Chemistry*, 49 (3), pp. 10765–10780. DOI:10.1021/ic101800d.

de Caro, P., Bandres, M., Urrutigoïty, M., Cecutti, C. and Thiebaud-Roux, S. (2019) Recent progress in synthesis of glycerol carbonate and evaluation of its plasticizing properties, *Frontiers in Chemistry*, 7 (5), pp. 1–13. DOI:10.3389/fchem.2019.00308.

de Falco, M., Iaquaniello, G. and Centi, G. (2013) CO_2: A valuable source of carbon, *Green Energy and Technology*, 137, (6) pp. 27–44. DOI:10.1007/978-1-4471-5119-7.

Demir, S., Usta, S., Tamar, H. and Ulusoy, M. (2017a) Solvent free utilization and selective coupling of epichlorohydrin with carbon dioxide over zirconium metal-organic frameworks, *Microporous and Mesoporous Materials*, 244, (4) pp. 251–257. DOI:10.1016/j.micromeso.2016.10.043.

Demir, S., Usta, S., Tamar, H. and Ulusoy, M. (2017b) Solvent free utilization and selective coupling of epichlorohydrin with carbon dioxide over zirconium metal-organic frameworks, *Microporous and Mesoporous Materials*, 244, (3) pp. 251–257. DOI:10.1016/j.micromeso.2016.10.043.

Dibenedetto, A., Angelini, A., Aresta, M., Ethiraj, J., Fragale, C. and Nocito, F. (2011) Converting wastes into added value products: From glycerol to glycerol carbonate, glycidol and epichlorohydrin using environmentally friendly synthetic routes, *Tetrahedron*, 67 (6), pp. 1308–1313. DOI:10.1016/j.tet.2010.11.070.

Duan, X. M., Stampfl, C., Bilek, M. M. M., McKenzie, D. R. and Wei, S. H. (2011) Design of shallow acceptors in ZnO through early transition metals codoped with N acceptors, *Physical Review B - Condensed Matter and Materials Physics*, 83 (8). DOI:10.1103/PhysRevB.83.085202.

EIA (2017) Today in Energy - U.S. Energy Information Administration (EIA), *US Energy Information Administration*. *Topics in Current Chemistry*, 375 (3). pp. 5-6. DOI:10.1007/s41061-017-0136-5.

Extavour, M. and Bunje, P. (2016) CCUS: Utilizing CO_2 to reduce emissions, *Chemical Engineering Progress*, 112 (6), pp. 52–59. DOI:10.1016/j.jmst.2013.10.012.

Fan, G., Zheng, X., Luo, J., Peng, H., Lin, H., Bao, M., Hong, L. and Zhou, J. (2018) Rapid synthesis of Ag/AgCl@ZIF-8 as a highly efficient photocatalyst for degradation of acetaminophen under visible light, *Chemical Engineering Journal*, 351 (2), pp. 782–790. DOI:10.1016/j.cej.2018.06.119.

Fang, Q.-R., Makal, T. A., Young, M. D. and Zhou, H.-C. (2010) Recent Advances in the Study of Mesoporous Metal-Organic Frameworks, *Comments on Inorganic Chemistry*, 31 (5–6), pp. 165–195. DOI:10.1080/02603594.2010.520254.

Fang, Z., Bueken, B., De Vos, D. E. and Fischer, R. A. (2015) Defect-Engineered Metal-Organic Frameworks, *Angewandte Chemie - International Edition*, 54 (25), pp. 7234–7254. DOI:10.1002/anie.201411540.

Feilizadeh, M., Rahimi, M., Zakeri, S. M. E., Mahinpey, N., Vossoughi, M. and Qanbarzadeh, M. (2017) Individual and interaction effects of operating parameters on the photocatalytic degradation under visible light illumination: Response surface methodological approach, *Canadian Journal of Chemical Engineering*, 95 (7), pp. 1228–1235. DOI:10.1002/cjce.22808.

Férey, G, C.Mellot-Draznieks, C.Serre, F.Millange, J.Dutour, S.Suble, I. M. (2013) A Chromium Terephthalate – Based Solid with Unusually Large Pore Volumes and Surface Area, 2040 (2005). DOI:10.1126/science.1116275.

Gaikwad, V. V. and Bhanage, B. M. (2018) Palladium-Catalyzed Aerobic Oxidative Carbonylation of C–H Bonds in Phenols for the Synthesis of p-Hydroxybenzoates, *European Journal of Organic Chemistry*, 2018 (22), pp. 2877–2881. DOI:10.1002/ejoc.201800538.

Gallardo-Fuentes, S., Contreras, R., Isaacs, M., Honores, J., Quezada, D., Landaeta, E. and Ormazábal-Toledo, R. (2016) On the mechanism of CO_2 electro-cycloaddition to propylene oxides, *Journal of CO_2 Utilization*, 16, pp. 114–120. DOI:10.1016/j.jcou.2016.06.007.

Gao, C. Y., Ai, J., Tian, H. R., Wu, D. and Sun, Z. M. (2017) An ultrastable zirconium-phosphonate framework as bifunctional catalyst for highly active CO_2 chemical transformation, *Chemical Communications*, 53 (7), pp. 1293–1296. DOI:10.1039/c6cc08773f.

Gaudino, E. C., Rinaldi, L., Rotolo, L., Carnaroglio, D., Pirola, C., Cravotto, G., Radoiu, M. and Eynde, J. J. Vanden (2016) Heterogeneous phase microwave-assisted reactions under CO_2 or CO pressure, *Molecules*, 21 (3). DOI:10.3390/molecules21030253.

Ge, Q. (2012) Synthesis and characterization of mesoporous zirconia nanocomposite using self-assembled block copolymer template, pp. 83. *Journal of Organic Chemistry*, 2018 (22), pp. 285-288. DOI:10.1002/ejoc.201800538.

Giraldo, L., Barranco, M. B., Húmpola, P., Carlos, J. and Piraján, M. (2017) the adsorption of phenols derivatives in aqueous solution, 8 (3). pp.8-12. DOI:10.5155/eurjchem.8.3.293-304.1603.

Gong, Q., Luo, H., Cao, D., Zhang, H., Wang, W. and Zhou, X. (2012) Efficient cycloaddition reaction of carbon dioxide with epoxide by Rhodamine based catalyst under 1 atm pressure, *Bulletin of the Korean Chemical Society*, 33 (6), pp. 1945–1948. DOI:10.5012/bkcs.2012.33.6.1945.

Goyal, S., Shaharun, M. S., Kait, C. F. and Abdullah, B. (2018) Effect of monometallic copper on zeolitic imidazolate framework-8 synthesized by hydrothermal method, *Journal of Physics: Conference Series*, 1123 (1), pp. 0–6. DOI:10.1088/1742-6596/1123/1/012062.

Guillerm, V., Weseliński, Ł. J., Belmabkhout, Y., Cairns, A. J., D'Elia, V., Wojtas, Ł., Adil, K. and Eddaoudi, M. (2014) Discovery and introduction of a (3,18)-connected net as an ideal blueprint for the design of metal-organic frameworks, *Nature Chemistry*, 6 (8), pp. 673–680. DOI:10.1038/nchem.1982.

Gurav, S. K., Shirsath, S. E., Kadam, R. H., Patange, S. M., Lohar, K. S. and Mane, D. R. (2013) Less magnetic and larger Zr^{4+}-Zn^{2+} ions co-substituted structural and magnetic properties of ordered Li 0.5Fe2.5O4 nanoparticles, *Materials Research Bulletin*, 48 (9), pp. 3530–3536. DOI:10.1016/j.materresbull.2013.05.047.

Hagen, J., Chorkendorff, I. and Niemantsverdriet, J. W. (2006) *Concepts of Modern Catalysis and Kinetics Catalysis from A to Z Principles and Practice of Heterogeneous Catalysis Catalytic Membranes and Membrane Reactors Spectroscopy in Catalysis*, *Simulation*. 33 (6), pp. 1945–1948. DOI:10.5012/bkcs.2012.33.6.1945.

Han, L., Li, H., Choi, S. J., Park, M. S., Lee, S. M., Kim, Y. J. and Park, D. W. (2012) Ionic liquids grafted on carbon nanotubes as highly efficient heterogeneous catalysts for the synthesis of cyclic carbonates, *Applied Catalysis* 429 (3), pp. 67–72. DOI:10.1016/j.apcata.2012.04.008.

Han, X., Zhu, G., Ding, Y., Miao, Y., Wang, K., Zhang, H., Wang, Y. and Liu, S. Bin (2019) Selective catalytic synthesis of glycerol monolaurate over silica gel-based sulfonic acid functionalized ionic liquid catalysts, *Chemical Engineering Journal*, 359 (11), pp. 733–745. DOI:10.1016/j.cej.2018.11.169.

He, Y., Sun, J., Guo, F. J., Fang, X. and Zhou, M. D. (2017) Efficient synthesis of dibenzyl carbonates from benzyl halides and Cs_2CO_3, *Journal of Saudi Chemical Society*, 21 (5), pp. 583–586. DOI:10.1016/j.jscs.2017.01.003.

Herodotou, S. (2015) Zirconium doped zinc oxide thin films deposited by atomic layer deposition, PhD Thesis, University of Lverpool, uk.

Herodotou, S., Treharne, R. E., Durose, K., Tatlock, G. J. and Potter, R. J. (2015) The effects of Zr doping on the optical, electrical and microstructural properties of thin ZnO films deposited by atomic layer deposition, *Materials*, 8 (10), pp. 7230–7240. DOI:10.3390/ma8105369.

Hong, M., Kim, Y., Kim, H., Cho, H. J., Baik, M. H. and Kim, Y. (2018) Scorpionate Catalysts for Coupling CO_2 and Epoxides to Cyclic Carbonates: A Rational Design Approach for Organocatalysts, *Journal of Organic Chemistry*, 83 (16), pp. 9370–9380. research-article. DOI:10.1021/acs.joc.8b00722.

Huang, X., Chen, Y., Lin, Z., Ren, X., Song, Y., Xu, Z., *et al.* (2014) Zn-BTC MOFs with active metal sites synthesized via a structure-directing approach for highly efficient carbon conversion, *Chemical Communications*, 50 (20), pp. 2624–2627. DOI:10.1039/c3cc49187k.

Hwang, G. Y., Roshan, R., Ryu, H. S., Jeong, H. M., Ravi, S., Kim, M. Il and Park, D. W. (2016) A highly efficient zeolitic imidazolate framework catalyst for the co-catalyst and solvent free synthesis of cyclic carbonates from CO_2, *Journal of CO_2 Utilization*, 15 (1), pp. 123–130. DOI:10.1016/j.jcou.2016.02.005.

Jang, M.-S., Lee, Y.-R. and Ahn, W.-S. (2015) CO_2 Cycloaddition of Epichlorohydrin over NH_2 -Functionalized MIL-101, *Bulletin of the Korean Chemical Society*, 36 (1), pp. 363–366. DOI:10.1002/bkcs.10008.

Jasiak, K., Krawczyk, T., Pawlyta, M., Jakóbik-Kolon, A. and Baj, S. (2016) One-Pot Synthesis of Styrene Carbonate from Styrene and CO_2 over the Nanogold-Ionic Liquid Catalyst, *Catalysis Letters*, 146 (5), pp. 893–901. DOI:10.1007/s10562-016-1703-z.

Jazi, M. E., Al-mohanna, T. and Aghabozorgi, F. (2016) Synthesis and Applications of Isocyanate Free Polyurethane Materials, *Chemical Engineering Journal*, 359 (November 2018), pp. 733–745. DOI:10.1016/j.cej.2018.11.169.

Jeffries, T. (2003) Changing Flux of Xylose Metabolites by Altering Expression of Xylose Reductase and Xylitol Dehydrogenase in Changing Flux of Xylose Metabolites by Altering Expression of Xylose Reductase and Xylitol Dehydrogenase, *Journal of the Food Hygienic Society of Japan*, 1 (2), pp. 78–83. DOI:10.1385/ABAB.

Jeirani, Z., Mohamed Jan, B., Si Ali, B., Mohd. Noor, I., Chun Hwa, S. and Saphanuchart, W. (2012) The optimal mixture design of experiments: Alternative method in optimizing the aqueous phase composition of a microemulsion, *Chemometrics and Intelligent Laboratory Systems*, 112, (4) pp. 1–7. DOI:10.1016/j.chemolab.2011.10.008.

Jeong, H.-M., Roshan, R., Babu, R., Kim, H.-J. and Park, D.-W. (2017) Zirconium-based isoreticular metal-organic frameworks for CO_2 fixation via cyclic carbonate synthesis, *Korean Journal of Chemical Engineering*, 35 (2), pp. 438–444. DOI:10.1007/s11814-017-0294-8.

Jessop, P. G. (2004) Applications of CO_2 in homogeneous catalysis, *Abstracts of Papers of the American Chemical Society*, 227, pp. U1069–U1069. DOI:10.1002/chin.200425269.

Jia, Y. Y., Liu, X. T., Feng, R., Zhang, S. Y., Zhang, P., He, Y. B., Zhang, Y. H. and Bu, X. H. (2017) Improving the Stability and Gas Adsorption Performance of Acylamide Group Functionalized Zinc Metal-Organic Frameworks through Coordination Group Optimization, *Crystal Growth and Design*, 17 (5), pp. 2584–2588. DOI:10.1021/acs.cgd.7b00119.

Jiang, Z. R., Wang, H., Hu, Y., Lu, J. and Jiang, H. L. (2015) Polar Group and Defect Engineering in a Metal-Organic Framework: Synergistic Promotion of Carbon Dioxide Sorption and Conversion, *ChemSusChem*, 8 (5), pp. 878–885. DOI:10.1002/cssc.201403230.

Jin, Z. and Yang, H. (2017) Exploration of Zr–Metal–Organic Framework as Efficient Photocatalyst for Hydrogen Production, *Nanoscale Research Letters*, 12 (4). pp. 4-8. DOI:10.1186/s11671-017-2311-6.

JK, K., MJ, M. and JK, K. (2017) Response Surface Methodology Approach to the Optimization of Potato (Solanum tuberosum) Tuber Yield Using Second-Order Rotatable Design, *Journal of Biometrics & Biostatistics*, 08 (03).pp. 6-9 DOI:10.4172/2155-6180.1000351.

Jose, T., Hwang, Y., Kim, D. W., Kim, M. Il and Park, D. W. (2015) Functionalized zeolitic imidazolate framework F-ZIF-90 as efficient catalyst for the cycloaddition of carbon dioxide to allyl glycidyl ether, *Catalysis Today*, 245, (5), pp. 61–67. DOI:10.1016/j.cattod.2014.05.022.

Jutz, F., Grunwaldt, J. D. and Baiker, A. (2008) Mn(III)(salen)-catalyzed synthesis of cyclic organic carbonates from propylene and styrene oxide in 'supercritical' CO_2, *Journal of Molecular Catalysis A: Chemical*, 279 (1), pp. 94–103. DOI:10.1016/j.molcata.2007.10.010.

Karagiaridi, O., Lalonde, M. B., Bury, W., Sarjeant, A. A., Farha, O. K. and Hupp, J. T. (2012) Opening ZIF-8: A catalytically active zeolitic imidazolate framework of sodalite topology with unsubstituted linkers, *Journal of the American Chemical Society*, 134 (45), pp. 18790–18796. DOI:10.1021/ja308786r.

Kathalikkattil, A. C., Babu, R., Tharun, J., Roshan, R. and Park, D. W. (2015) Advancements in the Conversion of Carbon Dioxide to Cyclic Carbonates Using Metal Organic Frameworks as Catalysts, *Catalysis Surveys from Asia*, 19 (4), pp. 223–235. DOI:10.1007/s10563-015-9196-0.

Kawanami, H., Sasaki, A., Matsui, K. and Ikushima, Y. (2003) A rapid and effective synthesis of propylene carbonate using a supercritical CO_2-ionic liquid system, *Chemical Communications*, 3 (7), pp. 896–897. DOI:10.1039/b212823c.

Kazemi, S. (2013) *Sustainable Ways of Combining Reactions and Separations Using Ionic Liquids and Carbon Dioxide*.

Kellici, S., Gong, K., Lin, T., Brown, S., Clark, R. J. H., Vickers, M., *et al.* (2010) High-throughput continuous hydrothermal flow synthesis of Zn-Ce oxides: unprecedented solubility of Zn in the nanoparticle fluorite lattice., *Philosophical Transactions. Series A, Mathematical, Physical, and Engineering Sciences*, 368 (1927), pp. 4331–49. DOI:10.1098/rsta.2010.0135.

Khan, W., Jia, X., Wu, Z., Choi, J. and Yip, A. C. K. (2019) Incorporating hierarchy into conventional zeolites for catalytic biomass conversions: A review, *Catalysts*, 9 (2). DOI:10.3390/catal9020127.

Khuri, A. I. and Mukhopadhyay, S. (2010) Response surface methodology, *Wiley Interdisciplinary Reviews: Computational Statistics*. 12 (3), pp. 3-6. DOI:10.1002/wics.73.

Kilic, A., Durgun, M., Aytar, E. and Yavuz, R. (2018) Synthesis and characterization of novel positively charged organocobaloximes as catalysts for the fi xation of CO_2 to cyclic carbonates, *Journal of Organometallic Chemistry*, 858, pp. 78–88. DOI:10.1016/j.jorganchem.2018.01.029.

Kim, H. U., Babu, R., Roshan, R. and Park, D. W. (2017) Catalytic performance of metal azolate frameworks in the solventless synthesis of cyclic carbonates from CO_2 and epoxides, *Applied Catalysis A: General*, 538, (1) pp. 59–65. DOI:10.1016/j.apcata.2017.03.028.

Kim, J., Kim, S., Jang, H., Seo, G. and Ahn, W. (2013a) Applied Catalysis A : General CO_2 cycloaddition of styrene oxide over MOF catalysts, *'Applied Catalysis A, General'*, 453 (2), pp. 175–180. DOI:10.1016/j.apcata.2012.12.018.

Kim, J., Kim, S. N., Jang, H. G., Seo, G. and Ahn, W. S. (2013b) CO_2 cycloaddition of styrene oxide over MOF catalysts, *Applied Catalysis A: General*, 453 (5), pp. 175–180. DOI:10.1016/j.apcata.2012.12.018.

Kim, S. H., Babu, R., Kim, D. W., Lee, W. and Park, D. W. (2018) Cycloaddition of CO_2 and propylene oxide by using M(HBTC)(4,4'-bipy)·3DMF (M = Ni, Co, Zn) metal-organic frameworks, *Cuihua Xuebao/Chinese Journal of Catalysis*, 39 (8), pp. 1311–1319. DOI:10.1016/S1872-20671763005-5.

Kleij, A. W. (2014) Catalytic conversion and use of carbon dioxide, *Catalysis Science & Technology*, 4 (6), pp. 1481. DOI:10.1039/c4cy90014f.

Kumar, A., Gupta, M., Mazumder, A., Poluri, K. M. and Rao, V. K. (2017) Use of Box Behnken Design for Development of High Throughput Quantitative Proton Nuclear Magnetic Resonance Experiments for Industrial Applications, *Industrial and Engineering Chemistry Research*, 56 (11), pp. 2873–2882. DOI:10.1021/acs.iecr.6b04697.

Kuruppathparambil, R. R., Babu, R., Jeong, H. M., Hwang, G. Y., Jeong, G. S., Kim, M. Il, Kim, D. W. and Park, D. W. (2016a) A solid solution zeolitic imidazolate framework as a room temperature efficient catalyst for the chemical fixation of CO_2, *Green Chemistry*, 18 (23), pp. 6349–6356. DOI:10.1039/c6gc01614f.

Kuruppathparambil, R. R., Jose, T., Babu, R., Hwang, G. Y., Kathalikkattil, A. C., Kim, D. W. and Park, D. W. (2016b) A room temperature synthesizable and environmental friendly heterogeneous ZIF-67 catalyst for the solvent less and co-catalyst free synthesis of cyclic carbonates, *Applied Catalysis B: Environmental*, 182 (6), pp. 562–569. DOI:10.1016/j.apcatb.2015.10.005.

Kuznetsova, S. A., Rulev, Y. A., Larionov, V. A., Smol'yakov, A. F., Zubavichus, Y. V., Maleev, V. I., *et al.* (2019) Self-Assembled Ionic Composites of Negatively Charged Zn(salen) Complexes and Triphenylmethane Derived Polycations as Recyclable Catalysts for the Addition of Carbon Dioxide to Epoxides, *ChemCatChem*, 11 (1), pp. 511–519. DOI:10.1002/cctc.201800908.

Lai, L. S., Yeong, Y. F., Lau, K. K. and Shariff, A. M. (2016) Effect of Synthesis Parameters on the Formation of ZIF-8 under Microwave-assisted Solvothermal, *Procedia Engineering*, 148 (2), pp. 35–42. DOI:10.1016/j.proeng.2016.06.481.

Lee, D. W., Marasini, N., Poudel, B. K., Kim, J. H., Cho, H. J., Moon, B. K., Choi, H. G., Yong, C. S. and Kim, J. O. (2014) Application of Box-Behnken design in the preparation and optimization of fenofibrate-loaded self-microemulsifying drug delivery system (SMEDDS), *Journal of Microencapsulation*, 31 (1), pp. 31–40. DOI:10.3109/02652048.2013.805837.

Lescouet, T., Chizallet, C. and Farrusseng, D. (2012) The Origin of the Activity of Amine-Functionalized Metal–Organic Frameworks in the Catalytic Synthesis of Cyclic Carbonates from Epoxide and CO_2, *ChemCatChem*, 4 (11), pp. 1725–1728. DOI:10.1002/cctc.201200288.

Li-yan, N. a, Rui-nian, H. U. a, Gui-ling, N. and Xiao-xia, O. U. (2012) Nano/Micro HKUST-1 Fabricated by Coordination Modulation Method at Room Temperature, *Science*, 28 (4), pp. 555–558. DOI:10.3109/02652048.2013.805844.

Li, H. and Niu, Y. (2011) Synthesis of cyclic chloropropylene carbonate from carbon dioxide with epichlorohydrin, *Asian Journal of Chemistry*, 23 (8), pp. 3344–3346. DOI:10.1002/bkcs.10008.

Li, M., Feng, Z., Xiong, G., Ying, P., Xin, Q. and Li, C. (2001) Phase Transformation in the Surface Region of Zirconia Detected by UV Raman Spectroscopy Phase Transformation in the Surface Region of Zirconia Detected by UV Raman Spectroscopy, *Society*, 67 (9), pp. 1–7. DOI:10.1021/jp010526l.

Li, P. Z., Wang, X. J., Liu, J., Lim, J. S., Zou, R. and Zhao, Y. (2016) A Triazole-Containing Metal-Organic Framework as a Highly Effective and Substrate Size-Dependent Catalyst for CO_2 Conversion, *Journal of the American Chemical Society*, 138 (7), pp. 2142–2145. DOI:10.1021/jacs.5b13335.

Li, R., Tong, X., Li, X. and Hu, C. (2012) Chlorine-free catalysts for green synthesis of cyclic carbonates from carbon dioxide, *Pure and Applied Chemistry*, 84 (3), pp. 621–636. DOI:10.1351/PAC-CON-11-06-08.

Liang, J., Chen, R. P., Wang, X. Y., Liu, T. T., Wang, X. S., Huang, Y. B. and Cao, R. (2017) Postsynthetic ionization of an imidazole-containing metal-organic framework for the cycloaddition of carbon dioxide and epoxides, *Chemical Science*, 8 (2), pp. 1570–1575. DOI:10.1039/c6sc04357g.

Liang, J., Huang, Y.-B. and Cao, R. (2019a) Metal–organic frameworks and porous organic polymers for sustainable fixation of carbon dioxide into cyclic carbonates, *Coordination Chemistry Reviews*, 378 (7), pp. 32–65. DOI:10.1016/J.CCR.2017.11.013.

Liang, J., Huang, Y. B. and Cao, R. (2019b) Metal–organic frameworks and porous organic polymers for sustainable fixation of carbon dioxide into cyclic carbonates, *Coordination Chemistry Reviews*, 378 (6), pp. 32–65. DOI:10.1016/j.ccr.2017.11.013.

Liang, J., Huang, Y. B. and Cao, R. (2019c) Metal–organic frameworks and porous organic polymers for sustainable fixation of carbon dioxide into cyclic carbonates, *Coordination Chemistry Reviews*, 378 (1), pp. 32–65. DOI:10.1016/j.ccr.2017.11.013.

Liu, A.-H., Li, Y.-N. and He, L.-N. (2012) Organic synthesis using carbon dioxide as phosgene-free carbonyl reagent, *Pure and Applied Chemistry*, 84 (3), pp. 581–602. DOI:10.1351/PAC-CON-11-05-04.

Liu, B., Liu, M., Liang, L. and Sun, J. (2015a) Guanidine Hydrochloride/ZnI_2 as Heterogeneous Catalyst for Conversion of CO_2 and Epoxides to Cyclic Carbonates under Mild Conditions, *Catalysts*, 5 (1), pp. 119–130. DOI:10.3390/catal5010119.

Liu, D., Li, G. and Liu, H. (2018) Functionalized MIL-101 with imidazolium-based ionic liquids for the cycloaddition of CO_2 and epoxides under mild condition, *Applied Surface Science*, 428 (1), pp. 218–225. DOI:10.1016/j.apsusc.2017.09.040.

Liu, J., He, J., Wang, L., Li, R., Chen, P., Rao, X., Deng, L., Rong, L. and Lei, J. (2016a) NiO-PTA supported on ZIF-8 as a highly effective catalyst for hydrocracking of Jatropha oil, *Scientific Reports*, 6 (6), pp. 1–11. DOI:10.1038/srep23667.

Liu, Q., Wu, L., Jackstell, R. and Beller, M. (2015b) Using carbon dioxide as a building block in organic synthesis, *Nature Communications*, 6 (1), pp. 59-33. DOI:10.1038/ncomms6933.

Liu, Y., Liu, F., Ni, L., Meng, M., Meng, X., Zhong, G. and Qiu, J. (2016b) A modeling study by response surface methodology (RSM) on Sr(II) ion dynamic adsorption optimization using a novel magnetic ion imprinted polymer, *RSC Advances*, 6 (60), pp. 54679–54692. DOI:10.1039/c6ra07270d.

Long, X., Cai, L. and Li, W. (2019) RSM-based assessment of pavement concrete mechanical properties under joint action of corrosion, fatigue, and fiber content, *Construction and Building Materials*, 197, pp. 406–420. DOI:10.1016/j.conbuildmat.2018.11.157.

Luanwuthi, S., Krittayavathananon, A., Srimuk, P. and Sawangphruk, M. (2015) In situ synthesis of permselective zeolitic imidazolate framework-8/graphene oxide composites: rotating disk electrode and Langmuir adsorption isotherm, *RSC Adv.*, 5 (58), pp. 46617–46623. DOI:10.1039/C5RA05950J.

Luo, R. and Zhou, X. (2014) Metal- and solvent-free synthesis of cyclic carbonates from epoxides and CO_2 in the presence of graphite oxide and ionic liquid under mild conditions : A kinetic study, *Carbon*, 82 (3), pp. 1–11. DOI:10.1016/j.carbon.2014.10.004.

Luo, S., Fan, G., Luo, M., Li, J. and Song, G. (2016) Synthesis of styrene carbonate from styrene oxide and CO_2 over $ZnBr_2$ supported on MCM-41 - Coated magnetic Fe3O4, *Journal of CO_2 Utilization*, 14 (4), pp. 23–30. DOI:10.1016/j.jcou.2016.02.001.

Ma, D., Li, B., Liu, K., Zhang, X., Zou, W., Yang, Y., Li, G., Shi, Z. and Feng, S. (2015) Bifunctional MOF heterogeneous catalysts based on the synergy of dual functional sites for efficient conversion of CO_2 under mild and co-catalyst free conditions, *Journal of Materials Chemistry A*, 3 (46), pp. 23136–23142. DOI:10.1039/c5ta07026k.

MacGillivray, L. (2010) *Metal-organic frameworks: design and application*. *Chemical Engineering Journal*, 359 (11), pp. 733–745. DOI:10.1002/9780470606858.

MacIas, E. E., Ratnasamy, P. and Carreon, M. A. (2012a) Catalytic activity of metal organic framework $Cu_3(BTC)_2$ in the cycloaddition of CO_2 to epichlorohydrin reaction, *Catalysis Today*, 198 (1), pp. 215–218. DOI:10.1016/j.cattod.2012.03.034.

MacIas, E. E., Ratnasamy, P. and Carreon, M. A. (2012b) Catalytic activity of metal organic framework $Cu_3(BTC)_2$ in the cycloaddition of CO_2 to epichlorohydrin reaction, *Catalysis Today*, 198 (1), pp. 215–218. DOI:10.1016/j.cattod.2012.03.034.

Maeda, C., Miyazaki, Y. and Ema, T. (2014) Recent progress in catalytic conversions of carbon dioxide, *Catalysis Science & Technology*, 4 (6), pp. 14-82. DOI:10.1039/c3cy00993a.

Mäkelä, M. (2017) Experimental design and response surface methodology in energy applications: A tutorial review, *Energy Conversion and Management*, 151 (8), pp. 630–640. DOI:10.1016/j.enconman.2017.09.021.

Manohar, M., Joseph, J., Selvaraj, T. and Sivakumar, D. (2013) Application of box Behnken design to optimize the parameters for turning inconel 718 using coated carbide tools, *International Journal of Scientific and Engineering Research*, 4 (4), pp. 620–642. DOI:10.4314/tjpr.v11i5.2.

Mao, J., Ge, M., Huang, J., Lai, Y., Lin, C., Zhang, K., Meng, K. and Tang, Y. (2017) Constructing multifunctional MOF@rGO hydro-/aerogels by the self-assembly process for customized water remediation, *J. Mater. Chem. A*, 5 (23), pp. 11873–11881. DOI:10.1039/C7TA01343D.

Marshall, R. J. and Forgan, R. S. (2016) Postsynthetic Modification of Zirconium Metal-Organic Frameworks, *European Journal of Inorganic Chemistry*, 2016 (27), pp. 4310–4331. DOI:10.1002/ejic.201600394.

Mennicken, L., Janz, A. and Roth, S. (2016) The German R&D Program for CO_2 Utilization—Innovations for a Green Economy, *Environmental Science and Pollution Research*, 23 (11), pp. 11386–11392. DOI:10.1007/s11356-016-6641-1.

Miao, C.-X., Wang, J.-Q. and He, L.-N. (2008) Catalytic Processes for Chemical Conversion of Carbon Dioxide into Cyclic Carbonates and Polycarbonates, *The Open Organic Chemistry Journal*, 2, (2), pp. 68–82. DOI:10.2174/1874095200801020068.

Miralda, C. M., MacIas, E. E., Zhu, M., Ratnasamy, P. and Carreon, M. A. (2012a) Zeolitic imidazole framework-8 catalysts in the conversion of CO_2 to chloropropene carbonate, *ACS Catalysis*, 2 (1), pp. 180–183. DOI:10.1021/cs200638h.

Miralda, C. M., MacIas, E. E., Zhu, M., Ratnasamy, P. and Carreon, M. A. (2012b) Zeolitic imidazole framework-8 catalysts in the conversion of CO_2 to chloropropene carbonate, *ACS Catalysis*, 2 (1), pp. 180–183. DOI:10.1021/cs200638h.

Mohammadifard, H. and Amiri, M. C. (2018) On tailored synthesis of nano $CaCO_3$ particles in a colloidal gas aphron system and evaluating their performance with response surface methodology for heavy metals removal from aqueous solutions, *J. Water Environ. Nanotechnol.*, 3 (2), pp. 141–149. DOI:10.22090/jwent.2018.02.005.

Montoya, C. A., Paninho, A. B., Felix, P. M., Zakrzewska, M. E., Vital, J., Najdanovic-Visak, V. and Nunes, A. V. M. (2015) Styrene carbonate synthesis from CO_2 using tetrabutylammonium bromide as a non-supported heterogeneous catalyst phase, *Journal of Supercritical Fluids*, 100, pp. 155–159. DOI:10.1016/j.supflu.2015.01.027.

Mostafaei, M., Ghobadian, B., Barzegar, M. and Banakar, A. (2015) Optimization of ultrasonic assisted continuous production of biodiesel using response surface methodology, *Ultrasonics Sonochemistry*, 27, pp. (1), 54–61. DOI:10.1016/j.ultsonch.2015.04.036.

Mousavi, B., Chaemchuen, S., Phatanasri, S., Chen, C., Zeng, C., Ganguly, R., Zhuiykov, S. and Verpoort, F. (2017) Selective cyclodimerization of epichlorohydrin to dioxane derivatives over MOFs, *Arabian Journal of Chemistry*. 12 (2), pp. 2-8. DOI:10.1016/j.arabjc.2017.09.011.

Muthusamy, S., Manickam, L. P., Murugesan, V., Muthukumaran, C. and Pugazhendhi, A. (2019) Pectin extraction from Helianthus annuus (sunflower) heads using RSM and ANN modelling by a genetic algorithm approach, *International Journal of Biological Macromolecules*, 124 (2), pp. 750–758. DOI:S0141813018318580.

Nabipour, H., Sadr, M. H. and Bardajee, G. R. (2017) Synthesis and characterization of nanoscale zeolitic imidazolate frameworks with ciprofloxacin and their applications as antimicrobial agents, *New Journal of Chemistry*, 41 (15), pp. 7364–7370. DOI:10.1039/c7nj00606c.

Nandiwale, K. Y. and Bokade, V. V. (2014) Process optimization by response surface methodology and kinetic modeling for synthesis of methyl oleate biodiesel over H3PW12O40anchored montmorillonite K10, *Industrial and Engineering Chemistry Research*, 53 (49), pp. 18690–18698. DOI:10.1021/ie500672v.

Nordin, N. A. H. M., Ismail, A. F. and Mustafa, A. (2014) Synthesis and preparation of asymmetric PSf/ZIF-8 mixed matrix membrane for CO2/CH4 separation, *Jurnal Teknologi (Sciences and Engineering)*, 69 (9), pp. 73–76. DOI:10.11113/jt.v69.3400.

North, M. (2012) Synthesis of cyclic carbonates from epoxides and carbon dioxide using bimetallic aluminium (salen) complexes, *Arkivoc*, 2012 (i), pp. 610–628. DOI:10.1016/j.supflu.2015.01.027.

North, M. and Pasquale, R. (2009) Mechanism of cyclic carbonate synthesis from epoxides and CO_2, *Angewandte Chemie - International Edition*, 48 (16), pp. 2946–2948. DOI:10.1002/anie.200805451.

North, M., Pasquale, R. and Young, C. (2010) Synthesis of cyclic carbonates from epoxides and CO_2, *Green Chemistry*, 12 (9), pp. 1514–1539. DOI:10.1039/c0gc00065e.

Nwabueze, T. U. (2010) Basic steps in adapting response surface methodology as mathematical modelling for bioprocess optimisation in the food systems, *International Journal of Food Science and Technology*, 45 (9), pp. 1768–1776. DOI:10.1111/j.1365-2621.2010.02256.x.

Ola, O., Maroto-Valer, M. M. and Mackintosh, S. (2013) Turning CO_2 into valuable chemicals, *Energy Procedia*, 37 (6), pp. 6704–6709. DOI:10.1016/j.egypro.2013.06.603.

Olaniyan, B. Saha, B. (2020) Comparison of catalytic activity of ZIF-8 and Zr/ZIF-8 for greener synthesis of chloromethyl ethylene carbonate by CO_2 utilization'', *Energies*,158 (2), pp. 405 -19. doi:10.3390/j.energies13030521

Olaniyan, B. Saha, B. (2020) Multiobjective optimization for the greener synthesis of chloromethyl ethylene carbonate by CO_2 and epichlorohydrin *via* response surface methodology,'' *Energies*, 162 (4) pp. 408–20. doi:10.1016/j.energies.2067.07.194

Onyenkeadi, V., Aboelazayem, O. and Saha, B. (2019) Systematic multivariate optimisation of butylene carbonate synthesis via CO_2 utilisation using graphene-inorganic nanocomposite catalysts, *Catalysis Today*, (3), pp. 1–13. DOI:10.1016/j.cattod.2019.03.027.

Onyenkeadi, V., Kellici, S. and Saha, B. (2018) Greener synthesis of 1,2-butylene carbonate from CO_2 using graphene-inorganic nanocomposite catalyst, *Energy*, 165 (6), pp. 867–876. DOI:10.1016/j.energy.2018.09.135.

Panchariya, D. K., Rai, R. K., Anil Kumar, E. and Singh, S. K. (2018) Core-Shell Zeolitic Imidazolate Frameworks for Enhanced Hydrogen Storage, *ACS Omega*, 3 (1), pp. 167–175. DOI:10.1021/acsomega.7b01693.

Pang, S. H., Han, C., Sholl, D. S., Jones, C. W. and Lively, R. P. (2016) Facet-specific stability of ZIF-8 in the presence of acid gases dissolved in aqueous solutions, *Chemistry of Materials*, 28 (19), pp. 6960–6967. DOI:10.1021/acs.chemmater.6b02643.

Paquin, F., Rivnay, J., Salleo, A., Stingelin, N. and Silva, C. (2015) Multi-phase semicrystalline microstructures drive exciton dissociation in neat plastic semiconductors, *J. Mater. Chem. C*, 3 (1), pp. 10715–10722. DOI:10.1039/b000000x.

Peng, J., Wang, S., Yang, H., Ban, B., Wei, Z., Wang, L. and Lei, B. (2018) Highly e ffi cient fi xation of carbon dioxide to cyclic carbonates with new multi-hydroxyl bis- (quaternary ammonium) ionic liquids as metal-free catalysts under mild conditions, *Fuel*, 224 (1), pp. 481–488. DOI:10.1016/j.fuel.2018.03.119.

Pérez-Fortes, M., Schöneberger, J. C., Boulamanti, A., Harrison, G. and Tzimas, E. (2016) Formic acid synthesis using CO_2 as raw material: Techno-economic and environmental evaluation and market potential, *International Journal of Hydrogen Energy*, 41 (37), pp. 16444–16462. DOI:10.1016/j.ijhydene.2016.05.199.

Pescarmona, P. P. and Taherimehr, M. (2012) Challenges in the catalytic synthesis of cyclic and polymeric carbonates from epoxides and CO_2, *Catalysis Science & Technology*, 2 (11), pp. 2169. DOI:10.1039/c2cy20365k.

Pham, T. T., Le, L. N., Nguyen, H. N., Luong, T. T. K., Pham, T. N., Nguyen, H. L. and Nguyen, T. K. (2018) Encapsulating gold nanoparticles in zeolitic imidazolate framework crystal for novel optical response, *Polyhedron*, 148, pp. 171–177. DOI:10.1016/j.poly.2018.04.002.

Phillips, C. E. (2012) Cobalt Mof-5: a Novel Catalyst for CO_2 Conversion To Carbonates, PhD *Thesis*, (August).

Qiao, K., Ono, F., Bao, Q., Tomida, D. and Yokoyama, C. (2009) Efficient synthesis of styrene carbonate from CO_2 and styrene oxide using zinc catalysts immobilized on soluble imidazolium-styrene copolymers, *Journal of Molecular Catalysis A: Chemical*, 303 (12), pp. 30–34. DOI:10.1016/j.molcata.2008.12.025.

Rabiee, F. and Mahanpoor, K. (2018) Catalytic oxidation of SO_2 by novel Mn/copper slag nanocatalyst and optimization by Box-Behnken design, *International Journal of Industrial Chemistry*, 9 (1), pp. 27–38. DOI:10.1007/s40090-018-0141-8.

Ramin, M. O. (2006) Heterogeneously Catalyzed Synthesis of Propylene Carbonate Using, (*International Journal of Food Science and Technology*, 45 (9), pp. 1768–1776. DOI:10.1111/j.1365-2621.2010.02256.x.

Ravi, S., Roshan, R., Tharun, J., Kathalikkattil, A. C. and Park, D. W. (2015) Sulfonic acid functionalized mesoporous SBA-15 as catalyst for styrene carbonate synthesis from CO_2 and styrene oxide at moderate reaction conditions, *Journal of CO_2 Utilization*, 10 (3), pp. 88–94. DOI:10.1016/j.jcou.2015.01.003.

Redissi, Y. and Bouallou, C. (2013) Valorization of carbon dioxide by co-electrolysis of CO_2/H_2O at high temperature for syngas production, *Energy Procedia*, 37 (7), pp. 6667–6678. DOI:10.1016/j.egypro.2013.06.599.

Remya, V. R. and Kurian, M. (2019) Synthesis and catalytic applications of metal–organic frameworks: a review on recent literature, *International Nano Letters*, 9 (1), pp. 17–29. DOI:10.1007/s40089-018-0255-1.

Ren, J., Ledwaba, M., Musyoka, N. M., Langmi, H. W., Mathe, M., Liao, S. and Pang, W. (2017) Structural defects in metal–organic frameworks (MOFs): Formation, detection and control towards practices of interests, *Coordination Chemistry Reviews*, 349 (3), pp. 169–197. DOI:10.1016/j.ccr.2017.08.017.

Ren, Y., Cheng, X., Yang, S., Qi, C., Jiang, H. and Mao, Q. (2013a) A chiral mixed metal-organic framework based on a Ni(saldpen) metalloligand: Synthesis, characterization and catalytic performances, *Dalton Transactions*, 42 (27), pp. 9930–9937. DOI:10.1039/c3dt50664a.

Ren, Y., Shi, Y., Chen, J., Yang, S., Qi, C. and Jiang, H. (2013b) Ni(salphen)-based metal-organic framework for the synthesis of cyclic carbonates by cycloaddition of CO2to epoxides, *RSC Advances*, 3 (7), pp. 2167–2170. DOI:10.1039/c2ra22550f.

Riduan, S. N. (2012) Carbon Dioxide Fixation and Utilization, *PhD Thesis*, National University of Singapore, Singapore. DOI:10.1021/ed030p104.2.

Rimoldi, M., Howarth, A. J., Destefano, M. R., Lin, L., Goswami, S., Li, P., Hupp, J. T. and Farha, O. K. (2017) Catalytic Zirconium/Hafnium-Based Metal-Organic Frameworks, *ACS Catalysis*, 7 (2), pp. 997–1014. DOI:10.1021/acscatal.6b02923.

Roshan, R., Jose, T., Babu, R., Hwang, G., Cherian, A., Kim, D. and Park, D. (2016) Applied Catalysis B : Environmental A room temperature synthesizable and environmental friendly heterogeneous ZIF-67 catalyst for the solvent less and co-catalyst free synthesis of cyclic carbonates, *'Applied Catalysis B, Environmental'*, 182, pp. 562–569. DOI:10.1016/j.apcatb.2015.10.005.

Ryan, J. C. and Daly, T. M. (2019) Barriers to innovation and knowledge generation: The challenges of conducting business and social research in an emerging country context, *Journal of Innovation & Knowledge*, 4 (1), pp. 47–54. DOI:10.1016/j.jik.2017.10.004.

Saada, R. (Supervisor-Saha. B) Catalytic Conversion of Carbon Dioxide (CO_2) into Value Added Chemicals. Ph.D. Thesis, *London South Bank University,* London, UK, 2015.

Saada, R., AboElazayem, O., Kellici, S., Heil, T., Morgan, D., Lampronti, G. I. and Saha, B. (2018) Greener synthesis of dimethyl carbonate using a novel tin-zirconia/graphene nanocomposite catalyst, *Applied Catalysis B: Environmental*, 226 (12), pp. 451–462. DOI:10.1016/j.apcatb.2017.12.081.

Sabale, S., Zheng, J., Vemuri, R. S., Yu, X.-Y., Mcgrail, P. and Motkuri, R. K. (2016) Synthesis and Catalysis: Open Access Recent Advances in Metal-Organic Frameworks for Heterogeneous Catalyzed Organic Transformations, 1 (5), pp. 1–8. DOI:10.1016/j.molcata.2008.12.025.

Sadeghi, N., Sharifnia, S. and Do, T. O. (2018) Optimization and modeling of CO2photoconversion using a response surface methodology with porphyrin-based metal organic framework, *Reaction Kinetics, Mechanisms and Catalysis*, 125 (1), pp. 411–431. DOI:10.1007/s11144-018-1407-z.

Sakakura, T. and Kohno, K. (2009) The synthesis of organic carbonates from carbon dioxide, *Chemical Communications*, (11), pp. 1312–1330. DOI:10.1039/b819997c.

Sankaranarayanan, S. and Srinivasan, K. (2012) Carbon dioxide - A potential raw material for the production of fuel, fuel additives and bio-derived chemicals, *Indian Journal of Chemistry - Section A Inorganic, Physical, Theoretical and Analytical Chemistry*, 51 (9–10), pp. 1252–1262. DOI:10.1016/j.molcata.2008.12.025.

Saptal, V. B. and Bhanage, B. M. (2017a) Current advances in heterogeneous catalysts for the synthesis of cyclic carbonates from carbon dioxide, *Current Opinion in Green and Sustainable Chemistry*, 3, pp. 1–10. DOI:10.1016/j.cogsc.2016.10.006.

Saptal, V. B. and Bhanage, B. M. (2017b) Current advances in heterogeneous catalysts for the synthesis of cyclic carbonates from carbon dioxide, *Current Opinion in Green and Sustainable Chemistry*, 3 (November 2016), pp. 1–10. DOI:10.1016/j.cogsc.2016.10.006.

Sarbu, T., Styranec, T. J. and Beckman, E. J. (2000) Design and Synthesis of Low Cost, Sustainable CO_2-philes, *Industrial & Engineering Chemistry Research*, 39 (12), pp. 4678–4683. DOI:10.1021/ie0003077.

Sathe, A. A., Nambiar, A. M. K. and Rioux, R. M. (2017a) Synthesis of cyclic organic carbonates via catalytic oxidative carboxylation of olefins in flow reactors, *Catalysis Science and Technology*, 7 (1), pp. 84–89. DOI:10.1039/c6cy01974a.

Sathe, A. A., Nambiar, A. M., Sturgis, N. and Rioux, M. (2017b) Synthesis of cyclic organic carbonates via catalytic oxidative carboxylation of olefins in flow reactors, *Catalysis Science & Technology*, 7 (2), pp. 2–3. DOI:10.1039/C6CY01974A.

Scha, B., Scha, F. and Bo, A. (2010) Organic Carbonates as Solvents in Synthesis and Catalysis 9 (5), pp. 4554–4581. DOI:10.1016/j.0972008.12.025.

Schäffner, B., Holz, J., Verevkin, S. P. and Börner, A. (2008) Organic carbonates as alternative solvents for palladium-catalyzed substitution reactions, *ChemSusChem*. DOI:10.1002/cssc.200700142.

Schejn, A., Aboulaich, A., Balan, L., Falk, V., Lalevée, J., Medjahdi, G., Aranda, L., Mozet, K. and Schneider, R. (2015) Cu $^{2+}$ -doped zeolitic imidazolate frameworks (ZIF-8): efficient and stable catalysts for cycloadditions and condensation reactions, *Catal. Sci. Technol.*, 5 (3), pp. 1829–1839. DOI:10.1039/C4CY01505C.

Seibert, E. and Tracy, T. S. (2014) Fundamentals of enzyme kinetics, *Methods in Molecular Biology*, 1113, pp. 9–22. DOI:10.1007/978-1-62703-758-7_2.

Senthilkumar, S., Maru, M. S., Somani, R. S., Bajaj, H. C. and Neogi, S. (2018) Unprecedented NH2-MIL-101(Al)/n-Bu4NBr system as solvent-free heterogeneous catalyst for efficient synthesis of cyclic carbonates via CO_2 cycloaddition, *Dalton Transactions*, 47 (2), pp. 418–428. DOI:10.1039/c7dt03754f.

Serrano, J. E., Félix, D., Soria, G.-O. and Serrano, E. (2015) TESIS DOCTORAL Procesos verdes para la producción de carbonato de glicerina y solketal Green processes for the production of glycerol carbonate and solketal MEMORIA PARA OPTAR AL GRADO DE DOCTOR PRESENTADA POR.

Shaikh, A.-A. G. and Sivaram, S. (1996) Organic Carbonates †, *Chemical Reviews*, 96 (3), pp. 951–976. DOI:10.1021/cr950067i.

Shi, F., Deng, Y., SiMa, T., Peng, J., Gu, Y. and Qiao, B. (2003) Alternatives to phosgene and carbon monoxide: Synthesis of symmetric urea derivatives with carbon dioxide in ionic liquids, *Angewandte Chemie - International Edition*, 42 (28), pp. 3257–3260. DOI:10.1002/anie.200351098.

Shi, J., Song, J., Ma, J., Zhang, Z., Fan, H. and Han, B. (2013) Effective synthesis of cyclic carbonates from CO_2 and epoxides catalyzed by KI/cucurbit[6]uril, *Pure and Applied Chemistry*, 85 (8), pp. 1633–1641. DOI:10.1351/PAC-CON-12-10-09.

Shi, L., Qi, W., Liu, W., Yan, P., Li, F., Sun, J. and Su, D. (2018) Carbon nitride modified nanocarbon materials as efficient non-metallic catalysts for alkane dehydrogenation, *Catalysis Today*, 301 (April 2017), pp. 48–54. DOI:10.1016/j.cattod.2017.03.047.

Shui, J., Chen, C., Grabstanowicz, L., Zhao, D. and Liu, D.-J. (2015) Highly efficient nonprecious metal catalyst prepared with metal–organic framework in a continuous carbon nanofibrous network, *Proceedings of the National Academy of Sciences*, 112 (34), pp. 10629–10634. DOI:10.1073/pnas.1507159112.

Shukla, K. and Srivastava, V. C. (2017a) *Synthesis of organic carbonates from alcoholysis of urea : A review*, *Catalysis Reviews*. Routledge. 7 (2), pp. 6-9 .doi.org/10.1080/01614940.2016.1263088

Shukla, K. and Srivastava, V. C. (2017b) Synthesis of organic carbonates from alcoholysis of urea: A review, *Catalysis Reviews - Science and Engineering*, 59 (1), pp. 1–43. DOI:10.1080/01614940.2016.1263088.

Song, C. (2002a) CO_2 Conversion and Utilization: An Overview, *CO_2 Conversion and Utilization*, 809 (September), 4 (4), pp. 1–2. DOI:doi:10.1021/bk-2002-0809.ch001.

Song, C. (2002b) CO_2 Conversion and Utilization: An Overview, *CO_2 Conversion and Utilization*, 809 (1), pp. 1–2. DOI:doi:10.1021/bk-2002-0809.ch001.

Song, J., Zhang, Z., Hu, S., Wu, T., Jiang, T. and Han, B. (2009) MOF-5/n-Bu4NBr: An efficient catalyst system for the synthesis of cyclic carbonates from epoxides and CO_2 under mild conditions, *Green Chemistry*, 11 (7), pp. 1031–1036. DOI:10.1039/b902550b.

Song, Q., Nataraj, S. K., Roussenova, M. V., Tan, J. C., Hughes, D. J., Li, W., *et al.* (2012) Zeolitic imidazolate framework (ZIF-8) based polymer nanocomposite membranes for gas separation, *Energy & Environmental Science*, 5 (8), pp. 835-839. DOI:10.1039/c2ee21996d.

Srivastava, R., Srinivas, D. and Ratnasamy, P. (2005) Zeolite-based organic-inorganic hybrid catalysts for phosgene-free and solvent-free synthesis of cyclic carbonates and carbamates at mild conditions utilizing CO_2, *Applied Catalysis A: General*, 289 (2), pp. 128–134. DOI:10.1016/j.apcata.2005.04.055.

Stewart, J. A. (2015) *Towards Green Cyclic Carbonate Synthesis : Heterogeneous and Homogeneous Catalyst Development Bijdrage aan Groene Cyclische Carbonaten Synthese*.4 (2), pp. 5-9. DOI:10.1039/b902550b.

Styring, P., Jansen, D., de Coninck, H., Reith, H. and Armstrong, K. (2011) *Carbon Capture and Utilisation in the green economy*, *Centre for Low Carbon Futures*. 96 (3), pp. 951–976. DOI:10.1021/cr950067i.

Sun, J., Fujita, S. I., Bhanage, B. M. and Arai, M. (2004) One-pot synthesis of styrene carbonate from styrene in tetrabutylammonium bromide, *Catalysis Today*, 93–95, pp. 383–388. DOI:10.1016/j.cattod.2004.06.105.

Sun, J., Fujita, S. I., Zhao, F., Hasegawa, M. and Arai, M. (2005) A direct synthesis of styrene carbonate from styrene with the Au/SiO 2-ZnBr2/Bu4NBr catalyst system, *Journal of Catalysis*, 230 (2), pp. 398–405. DOI:10.1016/j.jcat.2004.12.015.

Sun, J., Wang, Y., Son, J., Xiang, D., Wang, L. and Xiao, F. S. (2009) A facile, direct synthesis of styrene carbonate from styrene and CO_2 Catalyzed by Au/Fe(OH)3-ZnBr2/Bu 4NBr system, *Catalysis Letters*, 129 (3–4), pp. 437–443. DOI:10.1007/s10562-008-9820-y.

Taherimehr, M., Decortes, A., Al-Amsyar, S. M., Lueangchaichaweng, W., Whiteoak, C. J., Escudero-Adán, E. C., Kleij, A. W. and Pescarmona, P. P. (2012) A highly active Zn(salphen) catalyst for production of organic carbonates in a green CO_2 medium, *Catalysis Science & Technology*, 2 (11), pp. 2231. DOI:10.1039/c2cy20171b.

Tanaka, S., Fujita, K., Miyake, Y., Miyamoto, M., Hasegawa, Y., Makino, T., *et al.* (2015) Adsorption and Diffusion Phenomena in Crystal Size Engineered ZIF-8 MOF, *Journal of Physical Chemistry C*, 119 (51), pp. 28430–28439. DOI:10.1021/acs.jpcc.5b09520.

Tharun, J., Bhin, K. M., Roshan, R., Kim, D. W., Kathalikkattil, A. C., Babu, R., Ahn, H. Y., Won, Y. S. and Park, D. W. (2016) Ionic liquid tethered post functionalized ZIF-90 framework for the cycloaddition of propylene oxide and CO_2, *Green Chemistry*, 18 (8), pp. 2479–2487. DOI:10.1039/c5gc02153g.

Thi Thanh, M., Vinh Thien, T., Thi Thanh Chau, V., Dinh Du, P., Phi Hung, N. and Quang Khieu, D. (2017) Synthesis of Iron Doped Zeolite Imidazolate Framework-8 and Its Remazol Deep Black RGB Dye Adsorption Ability, *Journal of Chemistry*, 2017. DOI:10.1155/2017/5045973.

Unnikrishnan, P. and Darbha, S. (2016) Direct synthesis of dimethyl carbonate from CO2 and methanol over CeO_2 catalysts of different morphologies, *Journal of Chemical Sciences*, 128 (6), pp. 957–965. DOI:10.1007/s12039-016-1094-0.

Upare, P. P., Kinage, A. K., Shingote, S. K. and Gupte, S. P. (2012) Environmentally benign synthesis of β-hydroxy sulfides using cyclic carbonates catalyzed by large-pore zeolites, *Green Chemistry Letters and Reviews*, 5 (1), pp. 19–26. DOI:10.1080/17518253.2011.574295.

Valavanidis, A. (2012) Green Chemistry and New Technological Developments., *New Avenues for the Green Economy and Sustainable Future of Science and Technology.*, 78 (9,)pp. 1–33.DOI:10.1021/cr950067i.

Van Meerendonk, W. J. (2005) *CO_2 as a monomer for the phosgene-free synthesis of new polycarbonates - catalyst development, mechanistic investigations and monomer screening*, *Laboratory of Polymer Chemistry*. 6 (2), pp. 1-2. DOI:10.6100/IR596016.

Vansant, J. (2013) *Carbon dioxide emission and merchant market in the european union*, *Carbon Dioxide Recovery and Utilization*. 9 (9), pp. 2-6. DOI:10.1007/978-94-017-0245-4.

Vermoortele, F., Vimont, A., Serre, C. and De Vos, D. (2011) An amino-modified Zr-terephthalate metal–organic framework as an acid–base catalyst for cross-aldol condensation, *Chemical Communications*, 47 (5), pp. 1521–1523. DOI:10.1039/c0cc03038d.

Wang, B., Lv, X. L., Feng, D., Xie, L. H., Zhang, J., Li, M., Xie, Y., Li, J. R. and Zhou, H. C. (2016) Highly Stable Zr(IV)-Based Metal-Organic Frameworks for the Detection and Removal of Antibiotics and Organic Explosives in Water, *Journal of the American Chemical Society*, 138 (19), pp. 6204–6216. DOI:10.1021/jacs.6b01663.

Wang, J.-Q., Kong, D.-L., Chen, J.-Y., Cai, F. and He, L.-N. (2006) Synthesis of cyclic carbonates from epoxides and carbon dioxide over silica-supported quaternary ammonium salts under supercritical conditions, *Journal of Molecular Catalysis A: Chemical*, 249 (1–2), pp. 143–148. DOI:10.1016/j.molcata.2006.01.008.

Wang, M., She, Y., Zhou, X. and Ji, H. (2011a) Efficient solvent-free synthesis of chloropropene carbonate from the coupling reaction of CO_2 and epichlorohydrin catalyzed by magnesium porphyrins as chlorophyll-like catalysts, *Chinese Journal of Chemical Engineering*, 19 (3), pp. 446–451. DOI:10.1016/S1004-9541(11)60005-0.

Wang, S., Ma, Z., Du, X., Zhang, S. and Chen, Z. (2018) Lanthanum doping of metal-organic frameworks-5 and its effect on thermal stability and CO_2 adsorption property , *Materials Express*, 8 (4), pp. 381–387. DOI:10.1166/mex.2018.1441.

Wang, W., Wang, S., Ma, X. and Gong, J. (2011b) Recent advances in catalytic hydrogenation of carbon dioxide, *Chemical Society Reviews*, 40 (7), pp. 3703. DOI:10.1039/c1cs15008a.

Wang, X., Sun, G. and Chen, P. (2014) Three-Dimensional Porous Architectures of Carbon Nanotubes and Graphene Sheets for Energy Applications, *Frontiers in Energy Research*, 2 (8), pp. 1–8. DOI:10.3389/fenrg.2014.00033.

Wilding, M. A. (2011) Redesigning Racemases : Engineering Novel Biocatalysts for Chiral Carboxylic Acid Production. 96 (3), pp. 951–976. DOI:10.1021/cr950067i.

Wilhelm, M. E., Herrmann, W. A. and Mink, J. (2015) Ionic Catalysts for the Cycloaddition of Carbon Dioxide with Epoxides and the Oxidation of Olefins.

Wu, L. X., Wang, H., He, L., Wu, L., Zhang, A. J., Kajiura, H., Li, Y. M. and Lu, J. X. (2012) Direct electrosynthesis of organic carbonates from CO_2 with alcohols under mild condition, *International Journal of Electrochemical Science*, 7 (6), pp. 5616–5625.

Wu, M., Ye, H., Zhao, F., Zeng, B., Jiang, H. L., Xu, Q., *et al.* (2017) High-Quality Metal–Organic Framework ZIF-8 Membrane Supported on Electrodeposited ZnO/2-methylimidazole Nanocomposite: Efficient Adsorbent for the Enrichment of Acidic Drugs, *Scientific Reports*, 7 (November 2016), pp. 39778–39787. DOI:10.1038/srep39778.

Wu, Y., Song, X., Zhang, J., Xu, S., Xu, N., Yang, H., *et al.* (2018) Zn2(C9H3O6)(C4H5N2)(C4H6N2)3 MOF as a highly efficient catalyst for chemical fixation of CO_2 into cyclic carbonates and kinetic studies, *Chemical Engineering Research and Design*, 140, pp. 273–282. DOI:10.1016/j.cherd.2018.10.034.

Xiang, D., Liu, X., Sun, J., Xiao, F. S. and Sun, J. (2009) A novel route for synthesis of styrene carbonate using styrene and CO_2 as substrates over basic resin R201 supported Au catalyst, *Catalysis Today*, 148 (3–4), pp. 383–388. DOI:10.1016/j.cattod.2009.07.068.

Xiang, W., Sun, Z., Wu, Y., He, L. N. and Liu, C. jun (2019) Enhanced cycloaddition of CO_2 to epichlorohydrin over zeolitic imidazolate frameworks with mixed linkers under solventless and co-catalyst-free condition, *Catalysis Today*, 12 (12), pp. 0–1. DOI:10.1016/j.cattod.2019.01.050.

Xiang, W., Zhang, Y., Lin, H. and Liu, C. J. (2017) Nanoparticle/metal-organic framework composites for catalytic applications: Current status and perspective, *Molecules*, 22 (12). DOI:10.3390/molecules22122103.

Xie, Y., Wang, T.-T., Liu, X.-H., Zou, K. and Deng, W.-Q. (2013) Capture and conversion of CO_2 at ambient conditions by a conjugated microporous polymer, *Nature Communications*, 4 (4), pp. 1960–1967. DOI:10.1038/ncomms2960.

Xu, W., Thapa, K. B., Ju, Q., Fang, Z. and Huang, W. (2018) Heterogeneous catalysts based on mesoporous metal–organic frameworks, *Coordination Chemistry Reviews*, 373 (4), pp. 199–232. DOI:10.1016/j.ccr.2017.10.014.

Xuan, K., Pu, Y., Li, F., Li, A., Luo, J., Li, L., Wang, F. and Zhao, N. (2018) Direct synthesis of dimethyl carbonate from CO_2 and methanol over tri fl uoroacetic acid modulated UiO-66, *Journal of CO_2 Utilization*, 27 (August), pp. 272–282. DOI:10.1016/j.jcou.2018.08.002.

Xuan, Z. H., Zhang, D. S., Chang, Z., Hu, T. L. and Bu, X. H. (2014) Targeted structure modulation of 'pillar-layered' metal-organic frameworks for CO_2 capture, *Inorganic Chemistry*, 53 (17), pp. 8985–8990. DOI:10.1021/ic500905z.

Y. Wen et al. (2015) Direct synthesis of dimethyl carbonate and propylene glycol using potassium bicarbonate as catalyst in supercritical CO_2, (Scheme 1), pp. 16–18.

Yang, D. A., Cho, H. Y., Kim, J., Yang, S. T. and Ahn, W. S. (2012) CO_2 capture and conversion using Mg-MOF-74 prepared by a sonochemical method, *Energy and Environmental Science*, 5 (4), pp. 6465–6473. DOI:10.1039/c1ee02234b.

Yang, L., Yu, L., Diao, G., Sun, M., Cheng, G. and Chen, S. (2014) Zeolitic imidazolate framework-68 as an efficient heterogeneous catalyst for chemical fixation of carbon dioxide, *Journal of Molecular Catalysis A: Chemical*, 392, pp. 278–283. DOI:10.1016/j.molcata.2014.05.033.

Yang, X., Qiu, L. and Luo, X. (2018) ZIF-8 derived Ag-doped ZnO photocatalyst with enhanced photocatalytic activity, *RSC Advances*, 8 (9), pp. 4890–4894. DOI:10.1039/c7ra13351k.

Yao, J., He, M., Wang, K., Chen, R., Zhong, Z. and Wang, H. (2013) High-yield synthesis of zeolitic imidazolate frameworks from stoichiometric metal and ligand precursor aqueous solutions at room temperature, *CrystEngComm*, 15 (18), pp. 3601–3606. DOI:10.1039/c3ce27093a.

Ye, Y., Yin, D., Wang, B., Zhang, Q., Ye, Y., Yin, D., Wang, B. and Zhang, Q. (2015) Synthesis of Three-Dimensional Fe_3O_4 /Graphene Aerogels for the Removal of Arsenic Ions from Water, *Journal of Nanomaterials*, 2015, pp. 1–6. DOI:10.1155/2015/864864.

Yin, H., Kim, H., Choi, J. and Yip, A. C. K. (2015) Thermal stability of ZIF-8 under oxidative and inert environments: A practical perspective on using ZIF-8 as a catalyst support, *Chemical Engineering Journal*, 278, pp. 293–300. DOI:10.1016/j.cej.2014.08.075.

Yu, X. L. and He, Y. (2017) Application of Box-Behnken designs in parameters optimization of differential pulse anodic stripping voltammetry for lead(II) determination in two electrolytes, *Scientific Reports*, 7 (1), pp. 1–8. DOI:10.1038/s41598-017-03030-2.

Yuan, J., Huang, J., Wu, G., Tong, J., Xie, G., Duan, J. ao and Qin, M. (2015) Multiple responses optimization of ultrasonic-assisted extraction by response surface methodology (RSM) for rapid analysis of bioactive compounds in the flower head of Chrysanthemum morifolium Ramat., *Industrial Crops and Products*, 74, pp. 192–199. DOI:10.1016/j.indcrop.2015.04.057.

Yuan, S., Zou, L., Li, H., Chen, Y. P., Qin, J., Zhang, Q., Lu, W., Hall, M. B. and Zhou, H. C. (2016) Flexible Zirconium Metal-Organic Frameworks as Bioinspired Switchable Catalysts, *Angewandte Chemie - International Edition*, 55 (36), pp. 10776–10780. DOI:10.1002/anie.201604313.

Yuan, W., Gu, Y. and Li, L. (2012) Green synthesis of graphene/Ag nanocomposites, *Applied Surface Science*, 261, pp. 753–758. DOI:10.1016/j.apsusc.2012.08.094.

Zalomaeva, O. V., Chibiryaev, A. M., Kovalenko, K. A., Kholdeeva, O. A., Balzhinimaev, B. S. and Fedin, V. P. (2013) Cyclic carbonates synthesis from epoxides and CO_2 over metal-organic framework Cr-MIL-101, *Journal of Catalysis*, 298, pp. 179–185. DOI:10.1016/j.jcat.2012.11.029.

Zanon, A., Chaemchuen, S., Mousavi, B. and Verpoort, F. (2017a) 1 Zn-doped ZIF-67 as catalyst for the CO_2 fixation into cyclic carbonates, *Journal of CO_2 Utilization*, 20 (July), pp. 282–291. DOI:10.1016/j.jcou.2017.05.026.

Zanon, A., Chaemchuen, S., Mousavi, B. and Verpoort, F. (2017b) 1 Zn-doped ZIF-67 as catalyst for the CO_2 fixation into cyclic carbonates, *Journal of CO_2 Utilization*, 20 (May), pp. 282–291. DOI:10.1016/j.jcou.2017.05.026.

Zhang, H., Liu, H. B. and Yue, J. M. (2014) Organic carbonates from natural sources, *Chemical Reviews*, 114 (1), pp. 883–898. DOI:10.1021/cr300430e.

Zhang, X., Zhang, X., Johnson, J. A., Chen, Y. S. and Zhang, J. (2016) Highly Porous Zirconium Metal-Organic Frameworks with β-UH3-like Topology Based on Elongated Tetrahedral Linkers, *Journal of the American Chemical Society*, 138 (27), pp. 8380–8383. DOI:10.1021/jacs.6b04608.

Zhang, Y., Yin, S., Luo, S. and Au, C. T. (2012) Cycloaddition of CO_2 to epoxides catalyzed by carboxyl-functionalized imidazolium-based ionic liquid grafted onto cross-linked polymer, *Industrial and Engineering Chemistry Research*, 51 (10), pp. 3951–3957. DOI:10.1021/ie203001u.

Zhao, X., Liu, S., Tang, Z., Niu, H., Cai, Y., Meng, W., Wu, F. and Giesy, J. P. (2015) Synthesis of magnetic metal-organic framework (MOF) for efficient removal of organic dyes from water, *Scientific Reports*, 5 (1), pp. 11849. DOI:10.1038/srep11849.

Zhao, Y., Song, Z., Li, X., Sun, Q., Cheng, N., Lawes, S. and Sun, X. (2016) Metal organic frameworks for energy storage and conversion, *Energy Storage Materials*, 2, pp. 35–62. DOI:10.1016/j.ensm.2015.11.005.

Zheng, J., Wu, M., Jiang, F., Su, W. and Hong, M. (2015) Stable porphyrin Zr and Hf metal-organic frameworks featuring 2.5 nm cages: High surface areas, SCSC transformations and catalyses, *Chemical Science*, 6 (6), pp. 3466–3470. DOI:10.1039/c5sc00213c.

Zhong, S., Liang, L., Liu, B. and Sun, J. (2014) ZnBr2/DMF as simple and highly active Lewis acid–base catalysts for the cycloaddition of CO_2 to propylene oxide, *Journal of CO_2 Utilization*, 6, pp. 75–79. DOI:10.1016/j.jcou.2014.02.004.

Zhou, K., Mousavi, B., Luo, Z., Phatanasri, S., Chaemchuen, S. and Verpoort, F. (2017) Characterization and properties of Zn/CO zeolitic imidazolate frameworks vs. ZIF-8 and ZIF-67, *J. Mater. Chem. A*, 5 (3), pp. 952–957. DOI:10.1039/C6TA07860E.

Zhou, L., Li, N., Owens, G. and Chen, Z. (2019) Simultaneous removal of mixed contaminants, copper and norfloxacin, from aqueous solution by ZIF-8, *Chemical Engineering Journal*, 362 (November 2018), pp. 628–637. DOI:10.1016/j.cej.2019.01.068.

Zhou, X., Zhang, Y., Yang, X., Zhao, L. and Wang, G. (2012) Functionalized IRMOF-3 as efficient heterogeneous catalyst for the synthesis of cyclic carbonates, *Journal of Molecular Catalysis A: Chemical*, 361–362, pp. 12–16. DOI:10.1016/j.molcata.2012.04.008.

Zhou, Y., Hu, S., Ma, X., Liang, S., Jiang, T. and Han, B. (2008) Synthesis of cyclic carbonates from carbon dioxide and epoxides over betaine-based catalysts, *Journal of Molecular Catalysis A: Chemical*, 284 (1–2), pp. 52–57. DOI:10.1016/j.molcata.2008.01.010.

Zhou, Z., He, C., Xiu, J., Yang, L. and Duan, C. (2015) Metal-Organic Polymers Containing Discrete Single-Walled Nanotube as a Heterogeneous Catalyst for the Cycloaddition of Carbon Dioxide to Epoxides, *Journal of the American Chemical Society*, 137 (48), pp. 15066–15069. DOI:10.1021/jacs.5b07925.

Zhu, M. (2013) Catalytic activity of ZIF-8 in the synthesis of styrene carbonate from CO_2 and styrene oxide (2013), *Catalysis Communications*, 32, pp. 36–40. DOI:10.1016/J.CATCOM.2012.12.003.

Zhu, M., Srinivas, D., Bhogeswararao, S., Ratnasamy, P. and Carreon, M. A. (2013a) Catalytic activity of ZIF-8 in the synthesis of styrene carbonate from CO2 and styrene oxide, *Catalysis Communications*, 32 (3), pp. 36–40. DOI:10.1016/j.catcom.2012.12.003.

Zhu, Z., Rosendahl, L., Toor, S. S. and Chen, G. (2018) Optimizing the conditions for hydrothermal liquefaction of barley straw for bio-crude oil production using response surface methodology, *Science of the Total Environment*, 630 (8), pp. 560–569. DOI:10.1016/j.scitotenv.2018.02.194.